THE ELECTRONIC ABSORPTION SPECTRUM OF THIOFORMALDEHYDE (CH_2S)

THE ELECTRONIC ABSORPTION SPECTRUM OF THIOFORMALDEHYDE (CH_2S)

By

RICHARD HENRY JUDGE, B.Sc.

A Thesis

Submitted to the School of Graduate Studies

in Partial Fulfilment of the Requirement

for the Degree

Doctor of Philosophy

McMaster University

May, 1977

Dedicated

to

Mom and Dad

DOCTOR OF PHILOSOPHY
(Chemistry)

McMASTER UNIVERSITY,
Hamilton, Ontario.

TITLE: The Electronic Absorption Spectrum of Thioformaldehyde (CH_2S)

AUTHOR: Richard Henry Judge, B.Sc. (Loyola of Montreal)

SUPERVISOR: Professor G. W. King

NUMBER OF PAGES: (xi), 238

SCOPE AND CONTENTS:

The $^1A_2 \leftarrow {}^1A_1$ ($\pi^* \leftarrow n$) electronic absorption spectrum of thioformaldehyde vapour has been investigated. The six excited state fundamental frequencies for both CH_2S and CD_2S are determined from the vibrational analysis. The three rotational constants and three symmetric top distortion constants for the 0_0^0, 4_0^1 and $3_0^1 4_0^3$ bands of CH_2S and the 0_0^0, 4_0^1 and 5_0^1 bands of CD_2S are determined from a least squares rotational analysis of these bands. The rotational constants of the 0_0^0 and 4_0^1 bands of CH_2S and CD_2S are used to determine the structure of the molecule in the excited state.

ACKNOWLEDGEMENTS

I wish to thank Professor G. W. King for suggesting the problem, for allowing me complete freedom in my research and for his constructive criticism.

To my wife, Susan, a special thank you, not only for her skillful typing of the thesis but also for giving me the necessary incentive and help to complete the project.

To my colleagues at McMaster: John Bradford, Christina Castro, Mike Danyluk, Frank Greening, Carol Lessard, Bob McFadden, Bob McLean, Bob Meatherall, Dave Paape, Jeff Robins and Antoon Van Putten, thank you for your help, encouragement and friendship. I would like also to extend my appreciation to Dave Moule for many helpful discussions.

Finally, I wish to acknowledge the financial support of the Department of Chemistry of McMaster University for the years 1972 to 1976.

TABLE OF CONTENTS

Table of Contents Page

Table of Contents Page

LIST OF TABLES

LIST OF FIGURES

CHAPTER 1

INTRODUCTION

In October of 1971, the 212-211 rotational transition of thioformaldehyde (CH_2S) was detected in absorption from the direction of the galactic centre radio source $SgrB_2$[1, 2]. With this discovery, thioformaldehyde became the newest member of the select group of molecules known to be present in the interstellar medium.

Only months previous to this discovery, Johnson and Powell[3, 4] obtained the microwave spectrum and structure of CH_2S in its electronic ground state from experiments performed at the National Bureau of Standards Laboratories in Washington, D.C. In obtaining the spectrum, the authors found that thioformaldehyde very readily trimerizes to form the six-membered heterocyclic compound, s-trithiane. Accordingly, thioformaldehyde vapour, prepared by thermally cracking suitable starting materials, was maintained at pressures less than 0.05 torr within the absorption cell of the microwave spectrometer. Analysis of the spectrum resulted in the assignment of 27 rotational transitions and the elucidation of a ground state geometry similar to that of formaldehyde, the oxygen-containing analog of CH_2S. Subsequent microwave studies[1] have confirmed the planar ground state structure of CH_2S and, at present, very accurate values exist for the C=S and C-H bond lengths and HCH angle.

The identification and analysis of the vapour phase infrared spectrum of CH_2S have proved to be more challenging than that experienced for the microwave spectrum. By employing path lengths up to 40 m and a total absorption cell pressure of 0.7 torr, Johns and Olson[5] were able to

identify positively under high resolution three vibrational bands of CH_2S within the C-H stretch region of the spectrum (3000 cm^{-1}). Their method of generating CH_2S resulted in the formation of numerous by-products whose absorption in the lower wavelength region of the infrared obscured the absorption due to CH_2S vapour. Thus, the authors were able to assign only three of the six possible normal modes of vibration of thioformaldehyde. The low temperature Ar matrix study of CH_2S by Jacox and Milligan[6] has added the assignment of two additional normal modes as well as confirming the existing assignments.

Although two independent investigators[7, 8] have suggested that some of the 2000 Å weak, unresolved absorption bands of the pyrolysis products of dimethyl disulfide are due to absorption by CH_2S, the positive identification of the electronic absorption spectrum has remained elusive up to the present investigation. The reason is two-fold. In addition to the problem of working with a transient molecule at very low pressure, the first electronic transition of CH_2S is expected, by analogy with CH_2O, to be forbidden by electronic selection rules (see Chapter 2). These two unfavourable factors have necessitated the use of extremely long path lengths of up to 400 m, ten times that employed by Johns and Olson in order that the weak visible absorption spectrum can be recorded successfully.

In Chapters 2, 3 and 4, a detailed discussion of the analysis of the electronic absorption spectrum of thioformaldehyde and thioformaldehyde-d_2 is presented. The analysis is presented in two sections. The first deals with a discussion of the overall <u>electronic</u> spectrum of CH_2S (Chapter 2) while the remaining section presents the analysis of the <u>vibrational</u> and <u>rotational</u> structure of the first electronic transition of thioformaldehyde.

Basic spectroscopic theory is not presented here; instead the reader is referred to the texts written by Herzberg[9], King[10] and Harmony[11]. In future, these texts will be referenced only when specific information is taken from these sources.

CHAPTER 2

THE ELECTRONIC ABSORPTION SPECTRUM OF CH_2S

2.1 The Electronic States of Thiocarbonyl Compounds

The purely electronic hamiltonian can be shown[12] to commute with the symmetry operators of the molecular point group of the equilibrium configuration of the molecule. The electronic state of the molecule is thus classified according to the behaviour of the electronic wavefunction (ψ_e) on application of the operations of the molecular point group. ψ_e will either be invariant, change sign or, if degenerate, be transformed into a linear combination of the degenerate wavefunctions under these symmetry operators. Hence, ψ_e will transform as one member of the irreducible representation of the molecular point group. For the sake of the symmetry arguments that follow, the molecular electronic wavefunction may be written simply as a product function of molecular orbitals, with each M.O. containing a maximum of two electrons of opposite spin, i.e.,

$$\psi_e = \prod_{i=1}^{n} a_i \phi_i \qquad (2\text{-}1)$$

The symmetry designation of ψ_e is the direct product of the symmetry species of each of the occupied molecular orbitals, ϕ_i. Since the planar ground state configuration of thioformaldehyde is classified under the C_{2v} molecular point group, each molecular orbital is a basis for one of the irreducible representations listed in Table 2-1.

The molecular orbitals may be expressed as linear combinations of atomic orbitals (L.C.A.O.), i.e.,

$$\phi_i = \sum_j c_{ij} \chi_j \qquad (2\text{-}2)$$

TABLE 2-1

The Character Table for the C_{2v} Molecular Point Group

C_{2v}	E	$C_2(z)$	$\sigma_v(xz)$	$\sigma_v'(yz)$		
A_1	1	1	1	1	T_z	
A_2	1	1	-1	-1		R_z
B_1	1	-1	1	-1	T_x	R_y
B_2	1	-1	-1	1	T_y	R_x

The basis set used to form the molecular orbitals of CH_2S are

$(1s_{1H} + 1s_{2H})$; $1s_C$, $2s_C$, $2p_{zC}$; $1s_S$, $2s_S$, $2p_{zS}$, $3s_S$, $3p_{zS}$, all of a_1 symmetry;

$(1s_{1H} - 1s_{2H})$; $2p_{yC}$, $2p_{yS}$, $3p_{yS}$, all of b_2 symmetry; and

$2p_{xC}$, $2p_{xS}$, $3p_{xS}$, of b_1 symmetry.

The energy ordering of the nine a_1, four b_2 and three b_1 molecular orbitals can be estimated qualitatively from correlation diagrams similar to the ones illustrated by Herzberg, or by the more elegant ab initio calculation, which give a quantitative ordering of the orbitals. Several ab initio calculations, involving the use of either gaussian or Slater orbitals to approximate the atomic orbitals, have been performed for carbonyl and thiocarbonyl compounds. The most recent calculation performed for thioformaldehyde is that of Bruna et al[13]. Their self-consistent-field configuration interaction (S.C.F.-C.I.) calculation employed a more expanded basis set than indicated above and has led to the following ordering of the molecular orbitals:

$$1a_1<2a_1<3a_1<4a_1<1b_1<1b_2<5a_1<6a_1<2b_2<7a_1<2b_1<3b_2<3b_1$$

An examination of the M.O. of symmetry $7a_1$ reveals that the orbital is largely localized along the C=S bond axis. If one neglects the hydrogen atoms, the orbital is of cylindrical symmetry and is designated as a σ type bonding orbital. Similar considerations show that the $2b_1$, $3b_2$ and $3b_1$ orbitals are designated as π bonding, n non-bonding and π^* antibonding orbitals, respectively. A sketch of these higher energy molecular orbitals presented in Figure 2-1.

The electronic configuration of the ground state of CH_2S

$$\ldots 7a_1(2)\sigma,\ 2b_1(2)\pi,\ 3b_2(2)n \quad - \quad {}^1A_1$$

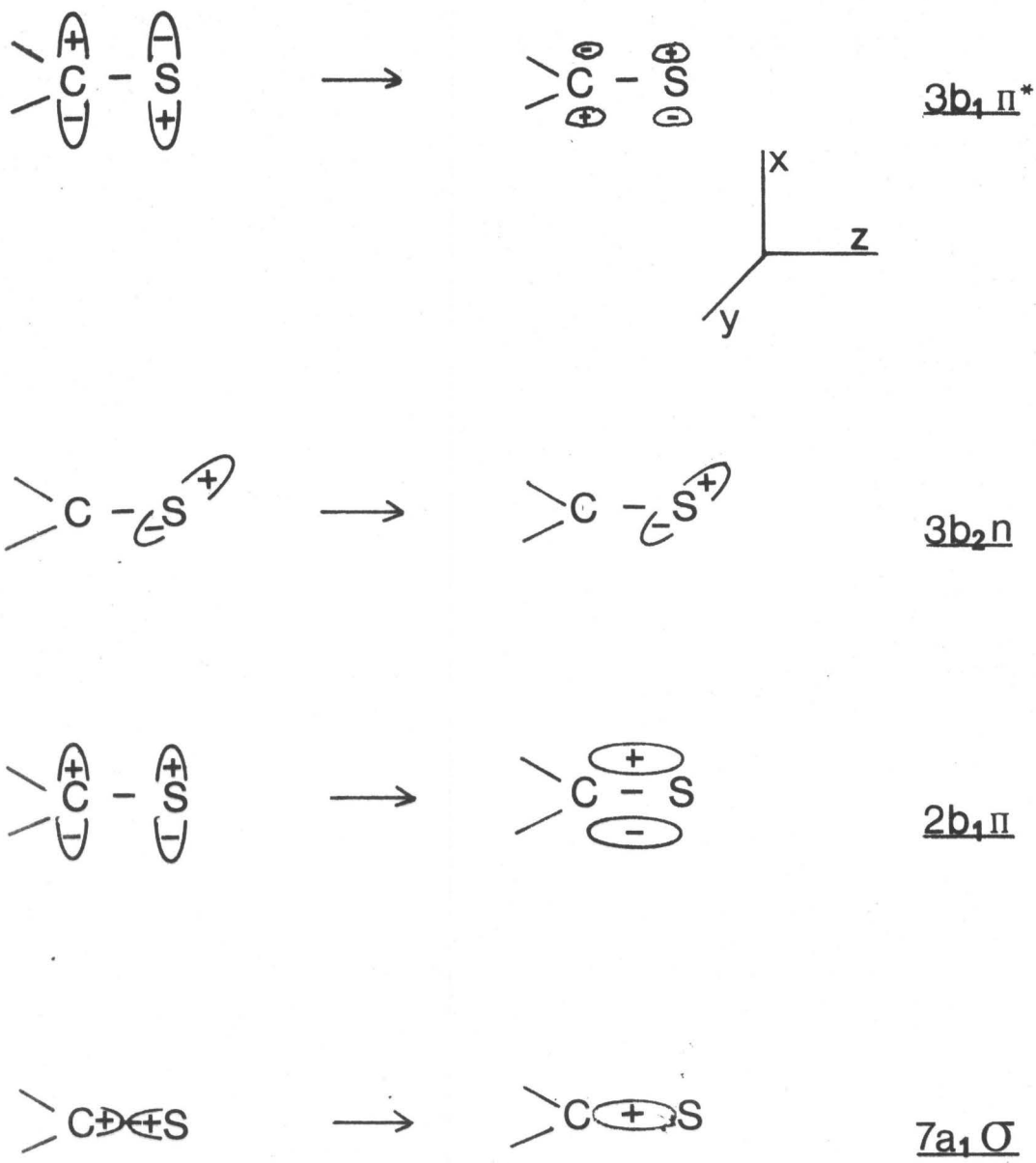

Figure 2-1. The higher energy molecular orbitals of CH_2S.

is therefore of overall $^1A_1$ symmetry. Promotion of a single non-bonding (n) electron to the π^* molecular orbital is calculated to be the transition of lowest energy and results in an excited state of $^{1,3}A_2$ electronic symmetry. Accordingly, the electronic configuration of the first excited state of CH_2S is

$$...7a_1(2)\sigma,\ 2b_1(2)\pi,\ 3b_2(1)n,\ 3b_1(1)\pi^* \quad - \quad {}^{1,3}A_2$$

The triplet state is calculated to be of lower energy than the singlet state, in agreement with Hund's rule.

Although numerous other transitions of higher energy are possible, only the singlet $\pi^* \leftarrow n$ transition will be considered further.

2.2 Variation of Molecular Orbital Energy with Geometry

2.2.1 Walsh Diagrams

Correlation diagrams first developed by Walsh[14] have been used extensively in the literature to show the variation of molecular orbital energy with changes in a selected geometrical parameter. These diagrams are useful in predicting, qualitatively, the geometry of a molecule in its ground and excited states.

The correlation diagrams are developed in accordance with the following rules. Molecular orbitals of the two geometrical extrema are joined if they exhibit identical behaviour with respect to a symmetry element common to both configurations. In correlating orbitals, the conditions of the non-crossing rule must be obeyed. Whether the energy of the M.O. increases or decreases on changing geometry is determined from a set of rules developed by Walsh, the most significant of which states that a M.O. is of lower energy if, on changing the geometrical parameter, the M.O.

experiences an increase in the s orbital contribution from its constituent atomic orbitals.

All molecular orbitals of carbonyl and thiocarbonyl compounds up to and including the non-bonding orbital show a slight increase in energy with an increase in the out-of-plane angle. However, the π^* M.O., which consists of contributions from the p-A.O. exclusively, experiences a marked decrease in energy on correlation to the A' molecular orbital of the non-planar configuration. Accordingly, the molecule is expected to be planar in its ground state and non-planar in its first excited state.

The detailed calculations of Bruna et al[13] support the qualitative arguments of Walsh. Their ab initio calculation shows that the ground state energy curve of CH_2S exhibits a definite minimum at 0^o. However, a very shallow minimum is predicted at approximately 15^o out-of-plane for CH_2S in its first excited state. Thus, thioformaldehyde in its $^1A_2$ state is expected to be less strongly bent out-of-plane than is formaldehyde.

2.2.2 The Consequences of a Non-planar Excited State

Two equivalent pyramidal forms of CH_2S exist. If the molecule is rigidly non-planar, then inversion from one form to the other is impossible. In this case, the barrier to interconversion (inversion) is of infinite energy and the potential energy functions of the two equivalent structures are identical (Figure 2-2(a)). The wavefunctions for the two configurations are degenerate and are designated as $\psi(Q^+)$ and $\psi(Q^-)$.

If we now allow the molecule to become flexible, then the barrier to inversion becomes finite and the molecule will undergo the inversion motion. Classically, inversion will occur only if the potential energy of the molecule is greater than or equal to the barrier energy. Quantum mechanically,

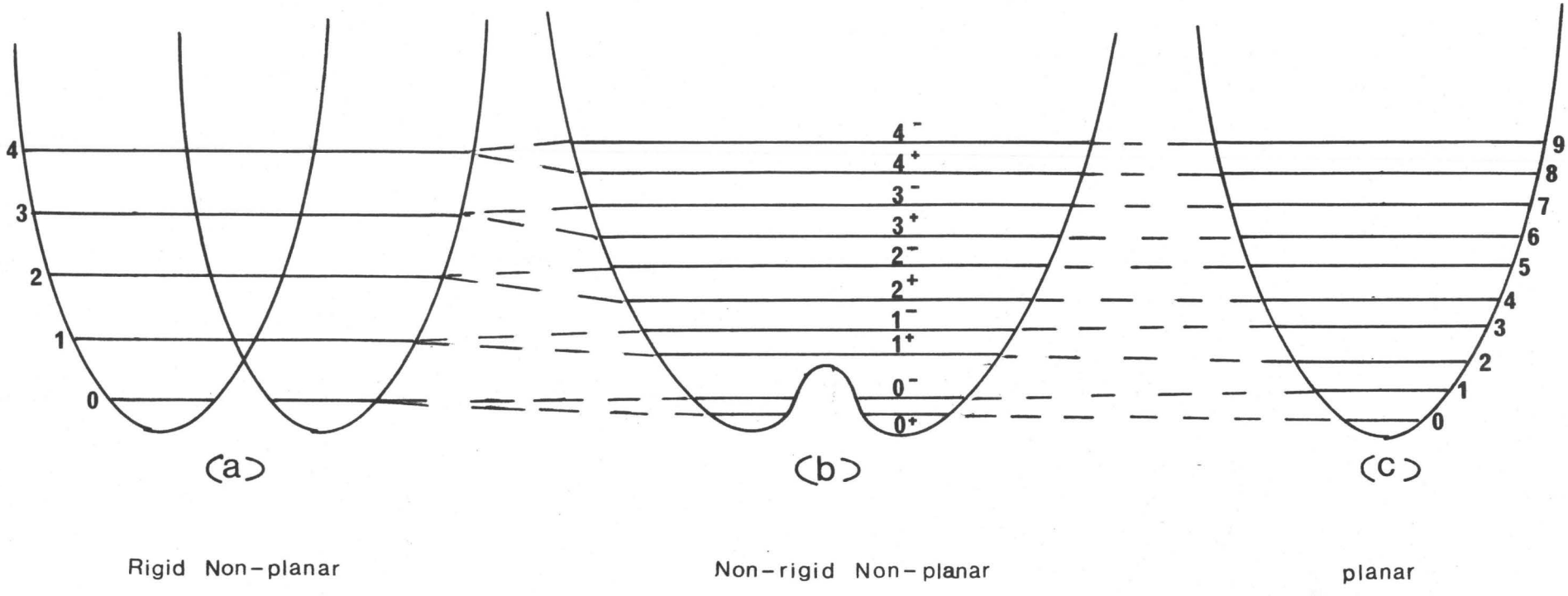

Figure 2-2. The vibrational energy levels of (a) rigid non-planar CH_2S, (b) non-planar non-rigid CH_2S and (c) planar CH_2S.

however, tunnelling can occur through the barrier and, consequently, inversion is possible at all vibrational levels.

The wavefunction for the double minimum oscillator is expressed as a linear combination of the two degenerate rigid molecule wavefunctions $\psi(Q^+)$ and $\psi(Q^-)$, that is,

$$\psi^{\pm} = 1/\sqrt{2}\ (\psi(Q^+) \pm (-1)^n \psi(Q^-)) \qquad (2\text{-}3)$$

where n is the quantum number of the vibrational level of the out-of-plane bending mode of the non-planar molecule to which $\psi^{\pm}$ correlates. For n = 0, the levels are designated as 0^+ and 0^-. For higher n, an analogous numbering scheme is followed. The wavefunction is classified according to the non-rigid molecular symmetry group G(4), isomorphic with the C_{2v} molecular point group (see Chapter 3). In Chapter 3 it is shown that the lower energy ψ^+ levels are of a_1 vibrational symmetry while the higher energy ψ^- levels are given the b_1 symmetry label. The potential energy diagram and symmetry labelling of the vibrational levels of the ν_4' inversion mode are depicted in Figure 2-2(b).

As the barrier to inversion approaches zero, the wavefunctions and energy levels of the double minimum oscillator approach that of the planar harmonic oscillator. The 0^+ and 0^- levels of the non-rigid, non-planar molecule correlate to the $\nu_4' = 0$ and 1 levels of the planar structure. Accordingly, the vibrational energy levels of the non-planar structure may be designated by the vibrational labels of its planar correlation partner.

Since the molecular symmetry group of the non-rigid, non-planar molecule is isomorphic with the C_{2v} point group, the vibronic selection rules

(see next section) for transitions to the $^1A_2$ electronic state are those of a planar to planar transition.

2.3 The $^1A_2(\pi^*) \leftarrow {}^1A_1(n)$ Transition of CH_2S

2.3.1 The Intensity of Electronic Transitions

The probability that an oscillating electromagnetic field induces a transition from vibronic states m to n is given by

$$B_m^n = \frac{2\pi}{3\hbar^2} |M_m^n|^2 \tag{2-4}$$

where B_m^n is the Einstein probability coefficient and M_m^n is the transition moment integral defined as

$$M_m^n = \langle \psi_m^{ev} | \bar{\mu} | \psi_n^{ev} \rangle \tag{2-5}$$

where ψ_m^{ev} is the vibronic wavefunction of state m.

The molecule fixed electric dipole operator, $\bar{\mu}$, defined as

$$\bar{\mu} = \sum_i m_i r_i = \bar{\mu}_N + \bar{\mu}_e \tag{2-6}$$

will transform as the translation operator of the molecular point groups. If the Born-Oppenheimer approximation is valid, the vibronic wavefunction may be written as

$$\psi_{ev} = \psi_e \psi_v \tag{2-7}$$

and the transition integral takes the form

$$M_m^n = \langle \psi_m^v | \psi_m^v \rangle \langle \psi_m^e | \bar{\mu}_e | \psi_n^e \rangle + \langle \psi_m^v | \bar{\mu}_N | \psi_n^v \rangle \langle \psi_m^e | \psi_n^e \rangle \tag{2-8}$$

Since the electronic wavefunctions are orthogonal, equation (2-8) takes the simplified form of

$$M_m^n = \langle\psi_m^v|\psi_n^v\rangle\langle\psi_m^e|\bar{\mu}_e|\psi_n^e\rangle \tag{2-9}$$

Application of this equation to the $^1A_2 \leftarrow {}^1A_1$ transition of CH_2S shows that, in this level of approximation, M_m^n is zero since none of the three components of $\bar{\mu}_e$ transform as the A_2 representation of the C_{2v} point group. The transition may become allowed (of non-zero intensity) if the Born-Oppenheimer approximation is relaxed, that is, if ψ_e is allowed to vary with nuclear motion. If the interaction of electronic and vibrational motion is not too large, then the use of a product function to represent the wavefunction is still a good approximation; however, the electronic hamiltonian takes the form

$$H^e = H_o^e + \sum_i \left(\frac{\partial H}{\partial Q_i}\right)Q_i = H_o^e + H' \tag{2-10}$$

where H_o^e is the zeroth order hamiltonian of the B.O. approximation and H' represents the perturbation of H_o^e. The electronic wavefunction of the perturbed hamiltonian is written as an expansion of the zero order wavefunction, that is,

$$\psi_n^e = \psi_n^o + \sum_{k\neq n} c_{nk}\psi_k^o \tag{2-11}$$

The transition moment integral of equation (2-9) now takes the form

$$M_m^n = \sum_{k\neq n} c_{nk}\langle\psi_m^o|\bar{\mu}_e|\psi_k^o\rangle\cdot\langle\psi_m^v|\psi_n^v\rangle \tag{2-12}$$

where ψ_m^o is the unperturbed ground state electronic wavefunction. The coefficients c_{nk} are given by perturbation theory as

$$c_{nk} = (1/(E_k^o - E_n^o))\cdot\langle\psi_k^o|H'|\psi_n^o\rangle \tag{2-13}$$

The two conditions that must be satisfied before M_m^n is non-zero are:

1) at least one integral within the summation term of equation (2-12) must be non-zero, which implies that the direct product of the irreducible representation of ψ_m^o, $\overline{\mu}_e$ and ψ_k^o contain the totally symmetric representation (A_1); and

2) the coefficients c_{nk} must be non-zero, which implies that the direct product of the irreducible representation of ψ_k^o, H' and ψ_n^o contain the totally symmetric representation. H' may be seen by inspection of equation (2-10) to transform as the vibrational normal coordinates, Q_i.

If these conditions are met, then state n is said to "borrow" intensity from state k.

Application of equation (2-12) to the $^1A_2 \leftarrow {}^1A_1$ transition of CH_2S shows that if the ground vibronic state is totally symmetric, then the $^1A_2$ state may borrow intensity from the $^1B_2$ state provided that the vibrational wavefunction of the excited state transforms as the b_1 representation. Intensity stealing from the $^1B_1$ state is possible if the excited state vibrational wavefunction is of b_2 symmetry. Excited state vibrational combination bands of a_2 symmetry will allow intensity borrowing from the π^* ($^1A_1$) electronic state.

A complete breakdown of the B.O. approximation results in the inability to represent the vibronic wavefunction (ψ_{ev}) as a simple product function of the vibrational and electronic wavefunctions. Nonetheless, ψ_{ev} still retains the symmetry of the direct product of ψ_e and ψ_v and, therefore, the selection rules of the vibronic transition moment integral are identical to those considered above.

2.3.2 Oscillator Strengths

The Einstein probability coefficient, B_n^m, is seldom reported in the literature. Instead, the term oscillator strength, related to M_m^n by[10]

$$f_m^n = \frac{4\pi m_e c\sigma}{3\hbar e^2} |M_m^n|^2 \qquad (2\text{-}14)$$

is often used to give an indication of the intensity of the electronic transition from state m to n. Transitions that are both electronically and spin-allowed characteristically have an oscillator strength of about $0.01 \leftrightarrow 0.4$ while values ranging from 10^{-6} to 10^{-4} are expected for vibronically-allowed or spin-forbidden transitions.

The oscillator strength is related to the experimentally observed absorbance (A_σ) by[15]

$$f_m^n = \frac{4.319 \times 10^{-9}}{bc} \int_{\sigma_1}^{\sigma_2} A_\sigma d\sigma \qquad (2\text{-}15)$$

where b is the path length, c is the concentration, and σ_1 and σ_2 are, respectively, the lower and higher wavenumber limits of the electronic absorption band under consideration. The absorbance (A_σ) is a function of wavenumber and can be estimated from microdensitometer tracings of the spectra.

2.4 Experimental

2.4.1 The Procurement of the Spectrum

Thioformaldehyde can be obtained by decomposing s-trithiane thermally or by decomposing other compounds such as dimethyl disulphide either thermally or in an electric discharge. However, the most advantageous method to prepare both CH_2S and CD_2S for visible spectroscopy is by pyrolysis of thiocyclobutane. The reaction is primarily

$$(CH_2)_3S \xrightarrow{\Delta} CH_2S + CH_2{=}CH_2 \qquad (2\text{-}16)$$

The ethylene that is produced does not absorb in the visible or near U.V. regions. The starting materials, thiocyclobutane and thiocyclobutane-d_6, were obtained from Eastman-Kodak and Merck, Sharpe and Dohme (Canada) Ltd., respectively, and were used without further purification.

These substances were cracked in an electric furnace at approximately 700°C and the products flowed through a 20-ft White type multiple reflection cell. Helium at 1 torr pressure was used as a carrier gas and the total pressure in the cell was 1.3 to 1.5 torr. The mean temperature of the gas in the absorption cell was estimated to be about 100°C from the rotational intensity distribution for the absorption bands.

The absorption spectra recorded on the low-resolution 1.5 m Bosch and Lomb Model II grating spectrograph required path lengths of up to 100 m. The first order resolving power and the dispersion of this instrument are 35,000 and 15 Å/mm respectively. The spectrograms obtained from the Bosch and Lomb were used both in the calculation of the experimental oscillator strength as well as in the assignment of the vibrational spectrum of the electronic transition.

The entire $^1A_2$ electronic absorption band system was photographed in the first order using an Ebert type spectrograph similar to that described by King[16]. Under these conditions, the instrument has a theoretical resolution of approximately 150,000 with a dispersion of ~0.7 Å/mm. The average absorption path length required to observe the visible spectrum was approximately 170 m while very weak bands required path lengths up to 220 m. An optimum slit width of 50 μ was employed. Although the Ebert spectrograms were used primarily in the rotational analysis of selected vibronic bands, the high resolution plates greatly aided in the vibrational

analysis of highly overlapped bands.

A high pressure 450 watt xenon arc lamp obtained from Osram Inc. served as a continuous source of radiation for all experiments.

Exposure times averaged from four to ten minutes; some weak bands required 30 minutes' exposure time.

In the absorption cell, thioformaldehyde rapidly polymerized to fine particles which remained suspended in the light path. Because of these, the cell became almost opaque to radiation after 30 minutes exposure time. In addition, the formation of a polymeric film on the reflection cell mirrors made it necessary to dismantle and clean the cell at frequent intervals. Although the scattering and the build-up of the polymeric film on the mirrors could be kept to a minimum by restricting the pressure to no more than 2 torr, nonetheless, the absorption cell required a thorough cleaning after a total of 30 minutes flow time. If the emission spectrum obtained from a Beckman Instrument Fe-Ne hollow cathode tube contained a sufficient number of lines in the spectral region under consideration and if the exposure times were not unreasonably long, then these lines were placed adjacent to the absorption spectrum. In other cases, the iron lines from a Pfund type iron arc run at 2-4 amps were used for calibration.

In the region between 7600 Å and 6500 Å, Kodak High Speed Infrared film was used to record the spectrum. The visible spectrum below 6500 Å was best recorded on Ilford FP4 (ASA 100) film or on Type IIIf spectroscopic plates manufactured by Kodak.

The inability to vary the temperature of CH_2S within the absorption cell greatly limited the investigation of the "hot" bands of the system (see Chapter 3). Although the temperature of the cracking unit could be

varied from 500-1200°C, the rapid cooling of the gas on contact with the cool walls of the absorption cell made it impossible to significantly change the ultimate average temperature of CH_2S.

2.4.2 Measurement and Calibration of Spectra

A McPherson travelling microscope calibrated to 0.0001 mm was used to measure the position of spectral lines and band heads. Maximum accuracy in the measurement procedure was assured by using high resolution spectrograms recorded on the Ebert spectrograph. The wavelengths of the iron arc emission lines were taken from a list compiled by the Spectroscopy Division of the National Research Council of Canada. In the case of hollow cathode emission lines, the wavelengths were obtained from tables published by Crosswhite[17] (1975). The calibration lines were then fitted to an equation of the form $y = a_0 + a_1x + a_2x^2$ with the aid of a least squares computer programme. Higher order fits were attempted but they resulted in little or no improvement in the overall quality of fit. The average maximum deviation in the fit of the iron arc and hollow cathode lines to the quadratic equation was approximately 0.060 cm^{-1} and 0.030 cm^{-1} respectively. The wavelengths, in air, of the spectral lines were then computed by quadratic interpolation from the above least squares coefficients, converted to vacuum wavenumbers by means of Edlén's Tables[18] and, finally, reported as vacuum wavenumbers. In this manner, the positions of the centre of isolated spectral lines could be estimated to within 0.010 cm^{-1} while the precision of the overlapped lines was approximately 0.040 cm^{-1}.

Profiles of the absorption bands, obtained from a Joyce-Loebel Mk III C double beam microdensitometer were useful not only in comparing these contours with those generated by the computer but also in determining the

polarization of partially analysed bands.

2.5 Some General Comments About the Electronic Absorption Spectrum of CH_2S

The experimental procedure used to produce thioformaldehyde generated a rich absorption spectrum extending from 8000 Å to 2500 Å. Most of the absorption in the ultraviolet can be attributed to strongly absorbing impurity molecules such as H_2S and CS_2; however, the bands extending from 8000 Å $\leftrightarrow$ 4000 Å are due to absorption by CH_2S. The fact that the absorbing species within this region is indeed thioformaldehyde is deduced from both physical and chemical evidence. A rotational analysis of selected bands within this system (Chapter 4) shows that the absorbing molecule is a slightly asymmetric rotor. The 3:1 intensity alternation of the sub-branches of CH_2S coupled with the 3:6 intensity alternation for CD_2S indicates the presence of two equivalent hydrogen nuclei. The rotational constants and geometry obtained from a least squares analysis of selected bands is consistent with the anticipated structure of the excited state. Also, the experimentally determined half-life of approximately 5 min agrees very well with that obtained by Johnson et al[4].

Although the most advantageous method of generating CH_2S was by thermally cracking thiocyclobutane, both s-trithiane and dimethyl disulphide are known to generate CH_2S when vigorously heated. When these compounds were thermally cracked under conditions identical with those used for thiocyclobutane, the visible absorption spectrum attributed to CH_2S was also obtained.

Once the identity of the absorber was established, the assignment of the electronic transition(s) present within the visible region was undertaken. Examination of the visible spectrum reveals that the region is

composed of two distinct systems characterized by different rotational profiles of the bands they contain. A vibrational and rotational analysis (Chapters 3 and 4) of the bands to the higher energy side of 6100 Å reveals that these bands may be attributed to the $^1A_2 \leftarrow {}^1A_1$ electronic transition. The experimental oscillator strength (equation 2-15) of 4×10^{-5} and the very low value of 2.03 ev (16400 cm^{-1}) for the vertical electronic transition energy adds support to this assignment. The observed oscillator strength is that expected of an electronically forbidden electric dipole transition and the observed vertical electronic transition energy is in good agreement with the calculated transition energy (2.17 ev) for the $^1A_2 \leftarrow {}^1A_1$ transition[13].

The region from 8000 Å to 6100 Å is found, under high resolution, to contain red-degraded double-headed bands whose rotational profile is dissimilar to those of the singlet system. This is in contrast to the observed vibrational intervals of this system which are just slightly larger than the corresponding intervals of the singlet system. Since the bands are remarkably similar to those of the $^3A_2$ state of CH_2O[66], the bands of this region are assigned to the spin-forbidden $^3A_2 \leftarrow {}^1A_1$ electronic transition. The observed oscillator strength of 4×10^{-6} and the close agreement between the calculated[13] (1.84 ev) and observed (1.80 ev) vertical electronic transition energy of the $^3\pi^* \leftarrow {}^1n$ transition adds further evidence for the assignment.

CHAPTER 3

THE VIBRATIONAL STRUCTURE OF THE $^1A_2$ STRUCTURE

3.1 The Symmetry Classification of the Vibrational Modes of Non-planar CH_2S

Group theory has long been a useful tool for the classification of the electronic, vibrational and rotational states of rigid polyatomic molecules. The definition of rigid polyatomic molecules is given by Longuet-Higgins[19] as being those molecules that never depart significantly from a unique geometrical configuration. Conversely, a molecule is said to be non-rigid if it is in an electronic state with two or more potential energy minima separated by surmountable energy barriers.

A rigid molecule fulfilling the above definition is thioformaldehyde in its planar ground state whose structure is shown in Figure 3-1(a). The symmetry classification of its normal modes of vibration under the C_{2v} point group is presented in Figure 3-2. This classification is valid only if the nuclear displacements are infinitesimally small. Classification schemes based on symmetry properties enable the vibronic selection rules and band polarizations for the infrared, Raman and visible spectroscopy of rigid polyatomic molecules to be determined.

In this and later chapters, evidence is presented which shows that CH_2S is non-planar in its first excited state which, in turn, implies that the molecule, if rigid, should be classified under the C_s point group (see Figure 3-1(b)). If the barrier to inversion (inversion in the sense that the molecule passes from one non-planar conformation to the other) is insurmountably high, then the symmetry classification under this molecular point group is valid. However, if execution of the inversion motion is possible, as in the case of non-planar CH_2O in its $^1A_2$ excited state, the

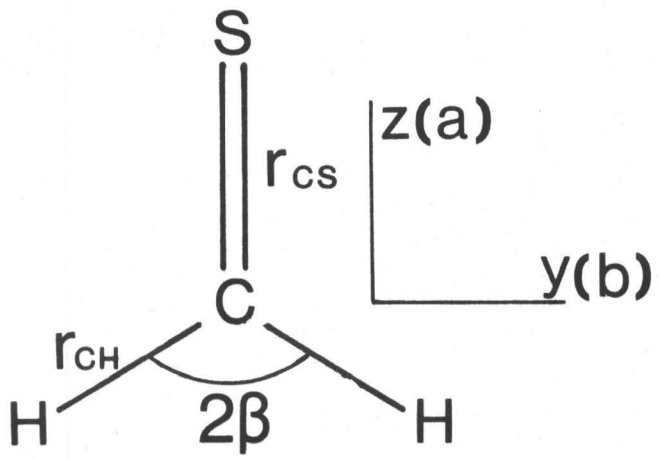

Figure 3-1. (a) The ground state structure of CH_2S. r_{CS} is the C=S bond length (1.6108 Å), r_{CH} is the C-H bond length (1.0925 Å), and 2β is the HCH angle (116.87°)[4].

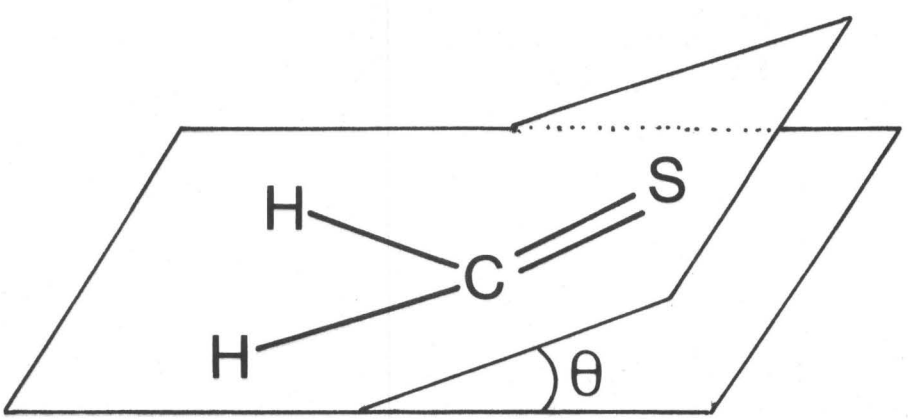

Figure 3-1. (b) The definition of the out-of-plane angle (θ).

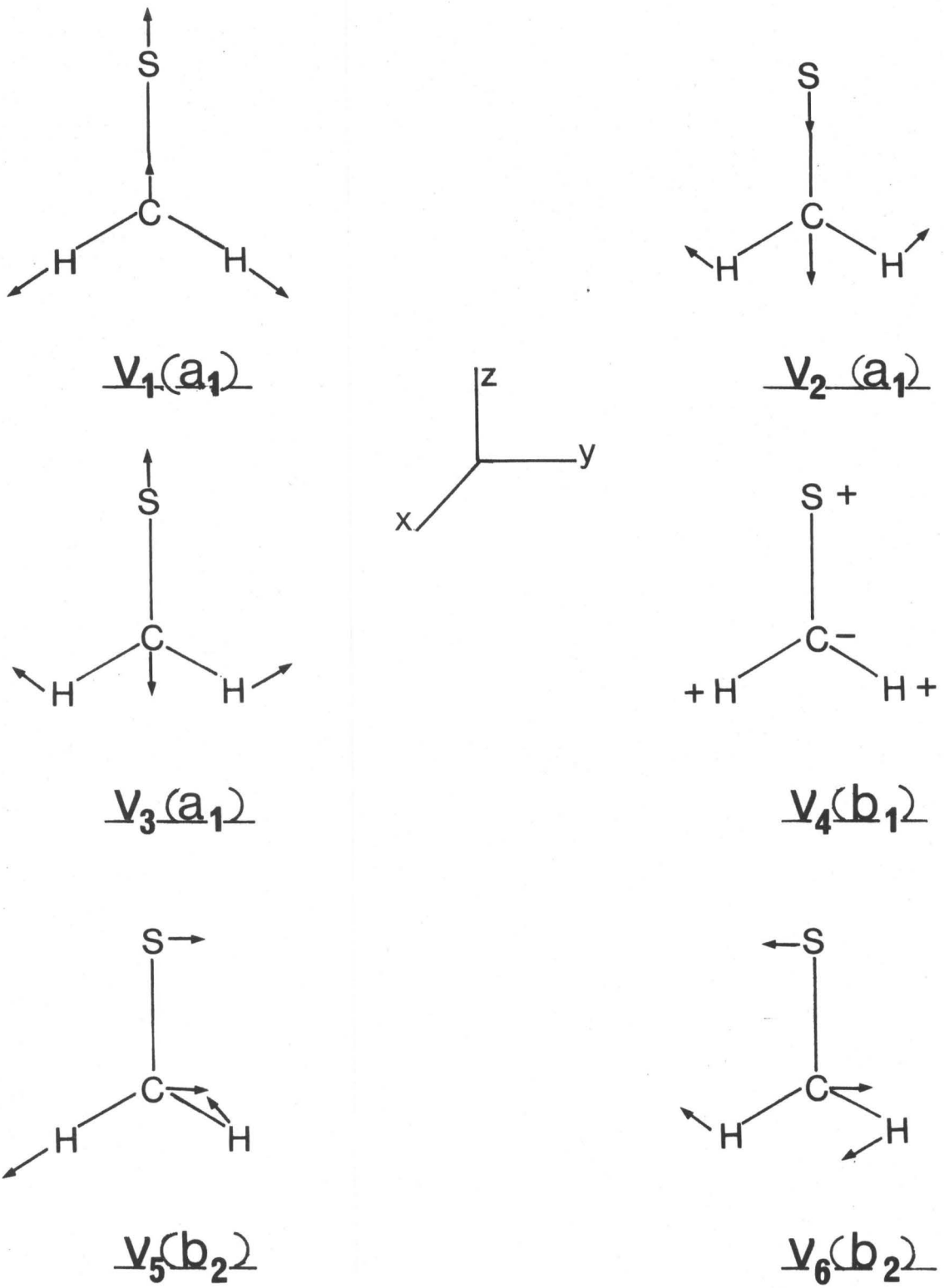

Figure 3-2. The symmetry classification of the normal modes of vibration of CH_2S under the C_{2v} point group. The displacement vectors are not drawn to scale.

molecule is no longer deemed rigid, in accordance with the above definition. Therefore, some uncertainty exists as to which molecular point group the molecule should be classified under, since in exciting the inversion motion, the molecule passes from a non-planar to a planar (C_{2v}) and then back to a non-planar configuration (C_s).

Longuet-Higgins has proposed a classification method for non-rigid molecules based on the symmetry behaviour of the molecule under four basic operations which leave the total molecular hamiltonian invariant. These four operations are classified as feasible or unfeasible according to whether or not the operation can be achieved without passing over an insuperable energy barrier (i.e. the operation may actually occur within the time necessary to record the spectrum). The molecular symmetry group is composed of only the feasible elements.

The operators which leave the molecular hamiltonian invariant are:

a) the identity operator, E;

b) the permutation of positions and spins of identical nuclei, P;

c) the inversion of all particle positions (electron and nuclear), E* (this is not to be confused with the inversion of configuration of non-planar molecules); and

d) the product E*P = PE*, P*.

The molecular symmetry group must contain all feasible P, including E, and all feasible P*, not necessarily including E*. Unlike the molecular point group operations which do not affect the orientation of the molecule-fixed axes, the symmetry group operators involve not only a permutation and/or inversion of nuclei but also a rotation of the molecule-fixed axes.

The feasible elements for thioformaldehyde are E, the permutation of

the two H(D) nuclei, (H_1H_2), the inversion of all particle coordinates, E*, and the permutation-inversion operator (H_1H_2)*, all of which form the molecular symmetry group G_4. The molecular symmetry group G_4 is isomorphic with the molecular point group C_{2v}. Therefore, the symmetry classification of the various states of non-planar CH_2S follows that of the planar ground state molecule.

Since application of the symmetry group operator affects the Eulerian angles, while the molecular point group operators do not, the operations of the two groups are related through the Eulerian angle operators $C_{2(z)}$, $C_{2(y)}$ and $C_{2(x)}$. Specifically, for a type I^{ℓ} representation of CH_2S (see next section),

$$(H_1H_2) = C_{2(a)}C_2;\ E^* = C_{2(c)}\sigma_{yz};\ (H_1H_2)^* = C_{2(b)}\sigma_{xz} \qquad (3\text{-}1)$$

The classification of the double-minimum vibrational wavefunction,

$$\psi^{\pm} = 1/\sqrt{2}\ (\psi(Q_4^{+}) \pm (-1)^n\psi(Q_4^{-})) \qquad (3\text{-}2)$$

is now possible. Since the molecular point group operators C_2 and σ_{yz} change Q_4^{+} to Q_4^{-} and the overall effect of the molecular symmetry operators E* and (H_1H_2) is to invert the configuration of the molecule, then $\psi(Q_4^{+})$ is changed to $(-1)^n\psi(Q^{-})$ under E* and (H_1H_2). Under the operations of E and (H_1H_2)*, the configuration remains unchanged and since E and σ_{xz} also leave Q_4^{+} unchanged, then $\psi(Q_4^{+})$ is unaffected by E and (H_1H_2)*. Similar considerations also apply to $\psi(Q^{-})$. Therefore, the double-minimum vibrational levels designated by ψ^{+} are of a_1 vibrational symmetry while the ψ^{-} levels are given the b_1 symmetry label.

The symmetry classification of the vibrational wavefunctions of the other vibrational modes of CH_2S in the $^1A_2$ excited state follow that of the planar molecule.

3.2 Band Polarizations

Since the vibronic wavefunction for the pyramidal singlet excited state can be classified under the C_{2v} point group, the vibronic selection rules and band polarizations of the $^1A_2 \leftarrow {}^1A_1$ transition are those of a planar to planar transition. The general selection rules for CH_2S, developed for the C_{2v} point group, are given in Chapter 2, while the theory of band polarizations is presented below.

Vibronic transitions of a C_{2v} molecule are said to be polarized along the a, b or c inertial axis, depending on the transformation properties of the component of the molecule fixed electric dipole operator, $\bar{\mu}_e$, which gives the transition moment integral a non-zero value. If a type $I^{\ell(20)}$ representation is used, that is, the a inertial axis is identified with the molecule-fixed z axis, b with the y axis and c with the x axis, then the C_{2v} group character table (depicted in Table 2-1) shows the assignment of the band polarizations. For example, transitions originating from the totally symmetric ground vibronic state to an excited state of B_2 vibronic symmetry are allowed if the electric dipole operator transforms as $T_{y(b)}$. The observed vibronic band is polarized along the b axis, and is classified as a type B vibronic band. Similarly, transitions to excited state vibronic levels of A_1 or B_1 symmetry are polarized along the a or c axis, respectively, and are termed A or C-type bands. The expected polarization of the bands of the $^1A_2 \leftarrow {}^1A_1$ electron transition of CH_2S are summarized in Table 3-1.

Transitions originating from the totally symmetric ground state to vibronic states of A_2 symmetry are forbidden by vibronic electric dipole selection rules. These transitions are allowed by magnetic dipole selec-

TABLE 3-1

A summary of the band polarizations of the $^1A_2 \leftarrow {}^1A_1$ electric dipole transition of CH_2S. A totally symmetric vibronic ground state is assumed.

Vibrational Symmetry No. of Quanta Excited			Band Type	Band Type in Symmetric Top Limit
a_1	b_1	b_2		
Unrestricted	Even	Even	Forbidden	
Unrestricted	Odd	Even	B	$\perp$
Unrestricted	Even	Odd	C	$\perp$
Unrestricted	Odd	Odd	A	$\parallel$

TABLE 3-2

The ground state frequencies of thioformaldehyde.

Vibration	Symmetry	CH_2S (cm^{-1})	CD_2S (cm^{-1})	Source
ν_1	a_1	2971		ab
ν_2	a_1	>1550		a
ν_3	a_1	1063		b
ν_4	b_1	993	783	b
ν_5	b_2	3025		a
ν_6	b_2	1438		ab

a: Johns and Olson[5]

b: Jacox and Milligan[6]

tion rules and may appear in the vibrational electronic spectrum. Their appearance will be that of a type A vibronically allowed band (see Chapter 4).

3.3 The Ground State Fundamental Frequencies of Thioformaldehyde

The identification and assignment of five ground state fundamental frequencies of CH_2S has been completed while the frequency of the remaining fundamental has been estimated by analogy with CH_2O. The high resolution gas phase infrared study of CH_2S by Johns and Olson[5] resulted in the unambiguous assignment of the two ground state fundamentals, ν_1'' and ν_5''. In addition, the authors were able to obtain information about the asymmetric H-C-H wagging mode (ν_6'') from its first overtone band located within the experimentally resolvable CH stretch region of the spectrum. Jacox and Milligan's[6] analysis of the low temperature Ar-N_2 matrix spectrum of CH_2S has confirmed the assignment of ν_6'', in addition to contributing the assignment of both the out-of-plane bending mode (ν_4'') and the symmetric stretching mode (ν_3''). The identification of the symmetric H-C-H bending mode (ν_2'') has remained elusive but its vibrational frequency has been estimated, by analogy with CH_2O, to be greater than 1550 cm^{-1}[5].

Knowledge of the ground state fundamental frequencies of CD_2S is very limited. Since the only vibrational frequency of the deuterated species reported in the literature is that given by Jacox and Milligan for the ν_4'' vibration, the values for the remaining fundamentals must be estimated by analogy with CH_2O and CD_2O.

A summary of the ground state frequencies of CH_2S and CD_2S is presented in Table 3-2.

3.4 The Vibrational Structure of the $^1A_2$ State

The shorthand notation developed by Brand and Watson[21] is used exclusively throughout the remainder of the thesis. Excited state fundamentals are given the same numbering as in the ground state, that is, in order of decreasing frequency within each symmetry class. A given vibrational transition can then be labelled in the form X_m^n, where X is the number of the normal vibration and m and n represent the transition from the m^{th} vibrational level of X in the ground state to the n^{th} vibrational level of X in the excited state. Normal modes that are involved in transitions to and from the zero point ($v_1 = v_2, \ldots = 0$) vibrational levels are omitted, for example, 4_0^0, 5_0^0, etc.

3.4.1 The $^1A_2$ State of CH_2S

Even under low resolution, the vibrational bands of the $\pi^* \leftarrow \underline{n}$ transition of CH_2S showed extensive structure which complicated the identification and assignment of overlapped bands. This problem is particularly acute in the higher energy region of the spectrum. The analysis of the spectrum of the normal isotope is further complicated by the near coincidence of the vibrational frequencies ν_3', $2\nu_4'$ and ν_6' which can give rise to several possible resonance interactions.

The vibrational structure of the $^1A_2 \leftarrow {}^1A_1$ transition of CH_2S is presented in Figure 3-3 along with the assignments of selected vibronic bands. The complete vibrational assignment of the $^1A_2$ state is given in Table 3-3 in which the vacuum wavenumbers reported are for the origins of the vibrational bands. The errors associated with these values are determined as follows.

The most accurate values are those obtained from a complete rotational

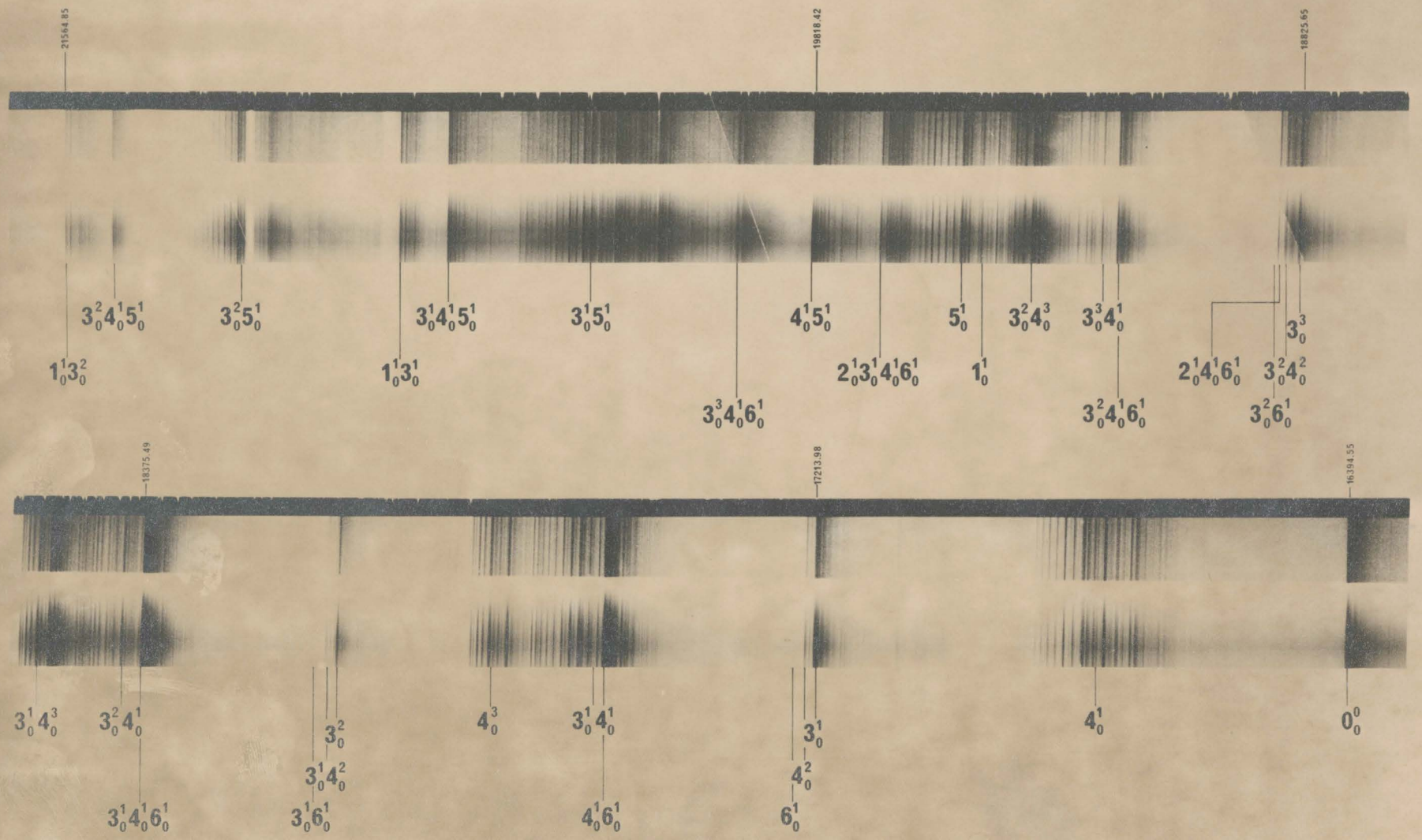

Figure 3.3 Spectrogram of the $\tilde{A}^1A_2 \leftarrow \tilde{X}^1A_1$ transition of Thioformaldehyde (CH_2S)

TABLE 3-3

The vibration frequency and assignments of the $^1A_2$ state of CH_2S.

σ_{vac}		Band Type	Assignment
16394	(*)	A	0_0^0
16765	(*)	B	4_0^1
17213	(x)	A	3_0^1
17220	(x)	C	6_0^1
17229	(†)	A	4_0^2
17563	(x)	A	$6_0^1 4_0^1$
17581	(x)	B	$3_0^1 4_0^1$
17736	(†)	B	4_0^3
18022	(x)	A	3_0^2
18043	(x)	A	$3_0^1 4_0^2$
18047	(x)	C	$3_0^1 6_0^1$
18375	(x)	A	$3_0^1 4_0^1 6_0^1$
18387	(x)	B	$3_0^2 4_0^1$
18548	(*)	B	$3_0^1 4_0^3$
18825	(x)	A	3_0^3
18833	(x)	A	$3_0^2 4_0^2$
18864	(x)	A	$2_0^1 4_0^1 6_0^1$
18862	(x)	C	$3_0^2 6_0^1$
19180	(x)	A	$3_0^2 4_0^1 6_0^1$
19189	(x)	B	$3_0^3 4_0^1$
19356	(x)	B	$3_0^2 4_0^3$
19428	(x)	A	1_0^1
19475	(†)	C	5_0^1
19671	(x)	A	$2_0^1 3_0^1 4_0^1 6_0^1$

Table 3-3 (cont'd.)

σ_{vac}		Band Type	Assignment
19818	(x)	A	$4_0^1 5_0^1$
19982	(x)	A	$3_0^3 4_0^1 6_0^1$
20298	(x)	C	$3_0^1 5_0^1$
20637	(x)	A	$3_0^1 4_0^1 5_0^1$
20749	(x)	A	$1_0^1 2_0^1$
20786	(x)	C	$2_0^1 5_0^1$
20812	(x)	A	$4_0^3 5_0^1$
21112	(x)	C	$3_0^2 5_0^1$
21445	(x)	A	$3_0^2 4_0^1 5_0^1$
21564	(x)	A	$1_0^1 2_0^1 3_0^1$
21608	(x)	C	$2_0^1 3_0^1 5_0^1$
21917	(x)	C	$3_0^3 5_0^1$
22246	(x)	A	$3_0^3 4_0^1 5_0^1$
22371	(x)	A	$1_0^1 2_0^1 3_0^2$
22430	(x)	C	$2_0^1 3_0^2 5_0^1$
22712	(x)	C	$2_0^4 5_0^1$
"Hot" bands			
16170	(x)	A?	3_1^1
16989	(x)	A?	3_1^2

(*): ± 0.01 cm^{-1}

(†): ± 0.5 cm^{-1}

(x): ± 1 cm^{-1}

analysis of the band. An asterisk has been placed beside the values in this table to indicate that the error associated with the determination of the origin of these bands is expected to be less than 10^{-2} cm^{-1}. Bands whose origins are determined to an intermediate level of accuracy fall into the second category. Their values have been estimated from a partial least squares rotational/band contour analysis and are expected to have an accuracy of approximately ± 0.5 cm^{-1}. The least reliable values quoted in the table are those of the totally unanalyzed bands whose origins are estimated by analogy with fully or partially analyzed bands of the same vibronic symmetry. The large errors inherent in this procedure limit the accuracy of the estimated value for the origins to approximately ± 1 cm^{-1}. An (x) is used to indicate the large error associated with these origins.

The remainder of this section is concerned with a detailed discussion of the results of the analysis.

The Origin Band of CH_2S

The absorption band at 16394 cm^{-1} is the lowest frequency strong band of the singlet system. It has been rotationally analyzed and found to be polarized about the a axis. Although the origin band of the $^1A_2 \leftarrow {}^1A_1$ electronic transition of CH_2S is predicted to be absent by electric-dipole vibronic selection rules since the excited state is of A_2 vibronic symmetry, the origin band can appear as the result of the interaction of the molecule's magnetic dipole with the magnetic field of light. As shown in Chapter 4, transitions from the A_1 vibronic ground state to excited states of A_2 vibronic symmetry are allowed by magnetic dipole selection rules. These bands will be polarized about the a axis and will be of identical appearance as ordinary type A electric dipole vibronically-allowed bands. Indeed, the

type A origin band of the $^1A_2 \leftarrow {}^1A_1$ transition of formaldehyde (CH_2O) was the first conclusively assigned magnetic dipole allowed band of a polyatomic molecule observed in electronic spectroscopy[22].

The strong type A band at 16394 cm^{-1} is assigned as the origin band of the $^1A_2 \leftarrow {}^1A_1$ transition of CH_2S. If the isotopic splitting ($\Delta\sigma_0$) for subsequent bands is plotted against the number of quanta excited in the upper state, straight lines are obtained (see Figure 3-4), which adds further weight to the assignment.

The oscillator strength (f) of all magnetic dipole allowed type A bands of the $^1A_2 \leftarrow {}^1A_1$ system of CH_2S is approximately 7×10^{-6}, in contrast to an oscillator strength of $\sim 3 \times 10^{-6}$ for the type A bands of CH_2O. Although the contribution to the overall oscillator strength by the type A bands is of the same order of magnitude for CH_2S and CH_2O, the contribution by the perpendicular type bands of CH_2O is $\sim 1 \times 10^{-4}$ in contrast to $\sim 3 \times 10^{-5}$ for CH_2S. Thus, the relative strength of the type A bands with respect to the perpendicular type bands of the system is greater for CH_2S than for CH_2O.

The Inversion Mode, ν_4'

The strong perpendicularly polarized band at 16795 cm^{-1} is the first intense band to the blue of the origin. Since a complete rotational analysis (Chapter 4) of the band has revealed that it is definitely polarized along the b axis and since no other vibrations of b_1 symmetry exist for CH_2S, the band is assigned as the 4_0^1 transition. The small energy separation (371 cm^{-1}) between it and the origin band represents a large percentage decrease from the ground state ν_4'' frequency of 993 cm^{-1}. A similar behaviour has been observed in the electronic spectra of other non-planar molecules able to undergo the inversion motion and, therefore, this is the first in-

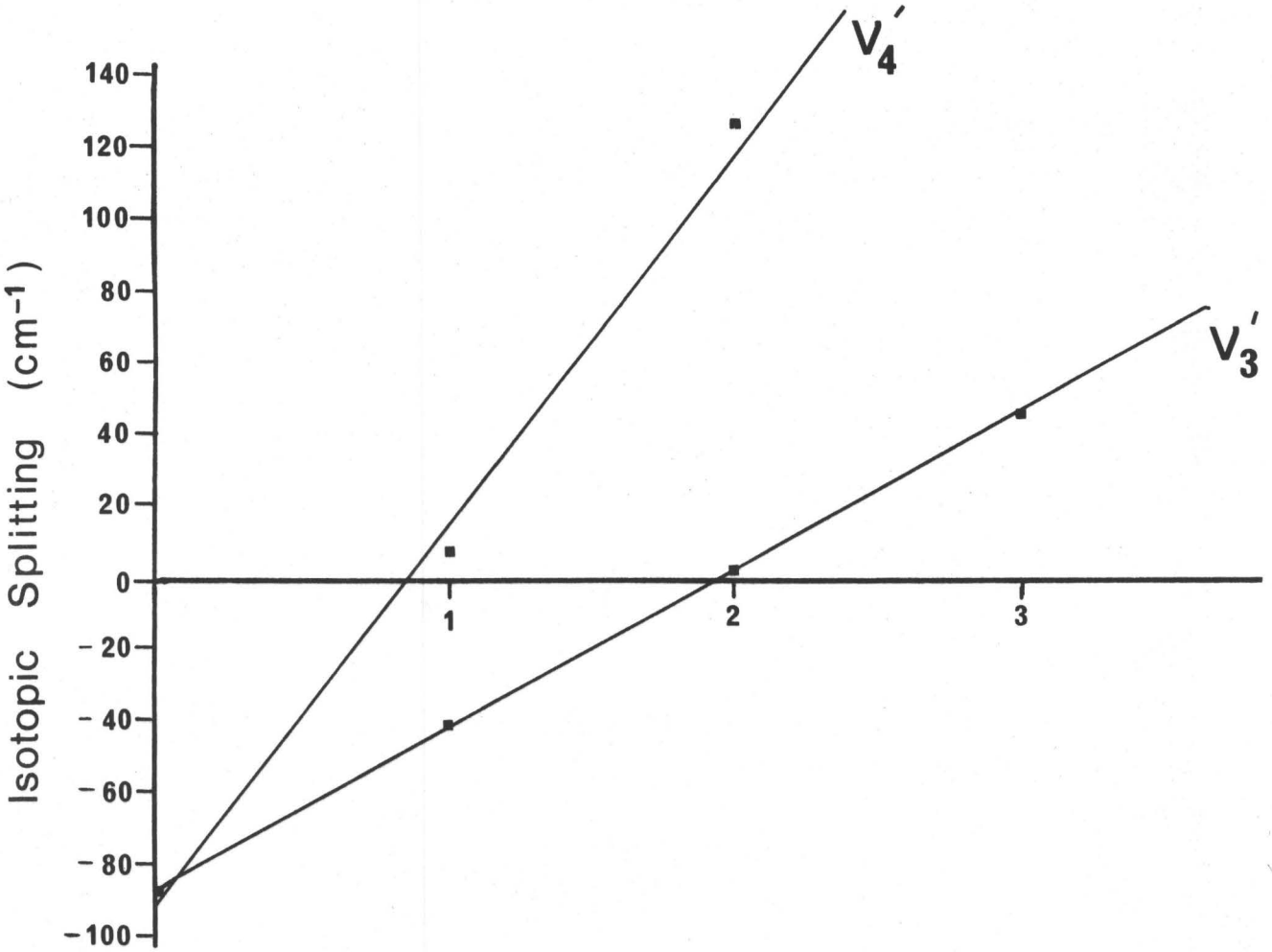

Figure 3-4. Isotopic splitting per quanta of normal frequency of vibration. Splitting refers to the quantity $\Delta\sigma = \sigma(CH_2S) - \sigma(CD_2S)$.

dication that the ν_4' vibrational potential of CH_2S could be described by a double minimum potential function.

The 4_0^2 band is identified as one of the three vibronic bands occurring approximately 460 cm^{-1} to the blue of the 4_0^1 band. Under high resolution, the three bands within this region are resolved into two strong A-type bands and a very weak perpendicular type bands of unknown polarization. A partial rotational analysis of the two type A bands, the results of which are detailed in Chapter 4, supports the assignment of the higher energy type A band at 17229 cm^{-1} to the 4_0^2 transition.

The strong absorption band at 17736 cm^{-1}, 507 cm^{-1} to the blue of 4_0^2 is assigned as the 4_0^3 band of the $^1A_2 \leftarrow {}^1A_1$ system. A rotational analysis of a band of similar appearance ($3_0^1 4_0^3$) has established that the 4_0^3 band has a polarization compatible with the above assignment, that is, it is shown to be polarized about the b axis.

As established from the above assignments, the energy separations between the first four quanta of the ν_4' vibrational potential (371 cm^{-1}, 460 cm^{-1} and 507 cm^{-1}) are highly anharmonic. Thus, a potential energy function other than the usual harmonic oscillator potential or an harmonic oscillator potential containing small corrections for anharmonicity, must be employed in any attempts to describe the observed energy separation (see Section 3-6). The highly anharmonic spacing of the ν_4' vibrational levels is not unexpected for transitions to an excited state of a non-planar molecule able to undergo the inversion motion, since CH_2O[23] in its $^1A_2$ (non-planar) state also exhibits this anomalous behaviour of the ν_4' levels as do other non-planar molecules able to undergo the inversion motion.

Attempts to locate the weaker bands involving higher quanta of the ν_4'

vibration have been unsuccessful. The increased complexity of the spectrum due to the overlap of the bands in the higher energy region of the system is the main cause of the failure.

The C=S Stretch, ν_3'

Results obtained from the rotational analysis indicate that the molecule experiences a large change in the C=S bond length on electronic excitation. In accordance with the Franck-Condon principle, ν_3' is expected to be quite active throughout the visible region in forming the main progression of the band system. Observations support this assumption. The strongest bands form a fairly long progression in a frequency of 820 cm^{-1} which can be interpreted as the C=S stretching vibration in the excited state. Consequently, the type A band at 17213 cm^{-1} is assigned as 3_0^1. The energy separation between it and the 0_0^0 band is 819 cm^{-1}. The 3_0^2 and 3_0^3 bands are then identified as the bands located at 18022 cm^{-1} and at 18825 cm^{-1} respectively.

The Asymmetric C-H Stretch, ν_5'

The strong C-type band located 3034 cm^{-1} to the blue of the origin band is assigned as 5_0^1. This band is the lowest frequency strong C-type band of the system and has built upon it progressions in the ν_3' and ν_4' vibrations. These prominent bands have polarizations consistent with their assignments.

The excited state C-H bond length is calculated (Chapter 4) to be slightly less than its ground state value of 1.093 Å. Since the ν_5' vibration involves primarily C-H stretching motion, the vibrational frequency of this mode should increase slightly on electronic excitation, if Badger's rule applies[24]. This is in agreement with the observed frequency

interval calculated from the above assignments.

The Asymmetric H-C-H Wag, ν_6'

The identification of the 6_0^1 band of CH_2S proved to be difficult without the aid of the CD_2S spectrum. Since the vibrational frequencies of ν_5' and ν_6' of the deuterated species, and ν_5' of the normal species are known, then the Redlich-Teller product ratio rule[25] can be applied to the b_2 vibrations to yield a value of 800 cm^{-1} as the predicted frequency of $\nu_6'(H)$. Accordingly, the very weak perpendicular type band situated at 826 cm^{-1} to the blue of the origin is assigned as 6_0^1. Although the possibility exists that the weak band is indeed a "hot" band, any attempts to assign it as such fail. Furthermore, combination bands of the form $3_0^x 4_0^1 6_0^1$ (x = 1, 2 or 3) appear strongly and with polarization consistent with their assignment (type A).

The Symmetric H-C-H Bend, ν_2'

The 2_0^1 band is not observed, but combination bands involving ν_2', and $\nu_4'\nu_6'$, ν_5' or ν_1' fix its vibrational frequency at approximately 1320 cm^{-1}. The 2_0^1 band may be present in the spectrum but overlap by the $3_0^1 4_0^1$ and 4_0^3 bands prevents its observation.

The Symmetric C-H Stretch, ν_1'

Like the ν_5' vibration, the normal mode ν_1' primarily involves stretching of the C-H bond and, therefore, if Badger's rule is applied once more, the predicted frequency of the excited state vibration ν_1' is anticipated to be slightly larger than its ground state value of 2971 cm^{-1} since the C-H bond length decreases on electronic excitation to the $^1A_2$ state. Under high resolution, the 5140 Å region of CH_2S contains a medium intensity A-type band which is highly overlapped by the strong 5_0^1 band. Accordingly,

the band, separated 3034 cm^{-1} from the origin band, is assigned to the 1_0^1 transition. Combination bands of the form $1_0^1 2_0^1 3_0^x$ (x = 1, 2 or 3) are also observed in the higher energy region of the spectrum.

"Hot" Bands

The extensive overlap of the origin region by the strong singlet-triplet bands of the $A_2 \leftarrow A_1$ electronic transitions prevents the observation of all but two "hot" bands, i.e. bands which result from transitions which originate from excited vibrational levels of the ground state. As indicated in Chapter 2, attempts to increase their intensity by increasing the temperature of the absorbing gas were not successful. The two observed "hot" bands are assigned as 3_1^1 and 3_1^2.

3.4.2 The $^1A_2 \leftarrow {}^1A_1$ System of CD_2S

The electronic spectrum of CD_2S is less overlapped and, therefore, easier to analyse than the heavily overlapped spectrum of CH_2S. Like the spectrum of CH_2S, strong type A bands are observed throughout the spectrum of CD_2S, most of which are also ascribed to magnetic dipole allowed transitions. A listing of the assignments of the spectral bands of CD_2S is presented in Table 3-4. The error associated with the calculation of the band origins is determined by the same procedure used for CH_2S.

A reproduction of the spectrogram of the $^1A_2 \leftarrow {}^1A_1$ transition is presented in Figure 3-5.

The Origin Band

The lowest frequency strong band observed in the spectrum of the $^1A_2 \leftarrow {}^1A_1$ transition of CD_2S is at 16483 cm^{-1} and is shifted 89 cm^{-1} to the blue of the origin band of CH_2S. A complete rotational analysis performed on this band has shown that its polarization, like that of the

TABLE 3-4

The vibrational frequency and assignment of the $^1A_2$ state of CD_2S.

σ_{vac}		Band Type	Assignment
16483	(*)	A	0_0^0
16758	(*)	B	4_0^1
17082	(x)	C	6_0^1
17102	(x)	A	4_0^2
17254	(x)	A	3_0^1
17362	(x)	A	$4_0^1 6_0^1$
17469	(x)	A	2_0^1
17540	(†)	B	$3_0^1 4_0^1$
17771	(†)	B	$2_0^1 4_0^1$
17857	(x)	C	$3_0^1 6_0^1$
17914	(x)	A	4_0^4
18020	(x)	A	3_0^2
18144	(x)	A	$3_0^1 4_0^1 6_0^1$
18344	(†)	B	4_0^5
18550	(x)	B	$2_0^1 3_0^1 4_0^1$
18808	(*)	C	5_0^1
18901	(x)	A	$3_0^2 4_0^1 6_0^1$
18955	(x)	A	$4_0^5 6_0^1$
19065	(x)	A	$4_0^1 5_0^1$
19104	(x)	B	$3_0^1 4_0^5$
19240	(x)	A	$1_0^1 4_0^2$
19306	(x)	B	$2_0^1 3_0^2 4_0^1$
19397	(x)	A	$5_0^1 6_0^1$
19401	(x)	C	$4_0^2 5_0^1$

Table 3-4 (cont'd.)

σ_{vac}		Band Type	Assignment
19579	(x)	C	$3_0^1 5_0^1$
19710	(x)	B	$4_0^1 5_0^1 6_0^1$
19844	(x)	A	$3_0^1 4_0^1 5_0^1$
19860	(x)	B	$3_0^2 4_0^5$
20002	(x)	A	$1_0^1 3_0^1 4_0^2$
20064	(x)	A	$2_0^1 4_0^1 5_0^1$
20163	(x)	A	$3_0^1 5_0^1 6_0^1$
20345	(x)	C	$3_0^2 5_0^1$
20570	(x)	C	$2_0^1 3_0^1 5_0^1$
20628	(x)	A	$3_0^2 4_0^1 5_0^1$
20762	(x)	A	$1_0^1 3_0^2 4_0^2$
20840	(x)	A	$2_0^1 3_0^1 4_0^1 5_0^1$
20914	(x)	A	$3_0^2 5_0^1 6_0^1$
21104	(x)	C	$3_0^3 5_0^1$
21339	(x)	C	$2_0^1 3_0^2 5_0^1$
21865	(x)	C	$3_0^4 5_0^1$
"Hot" bands			
15697	(x)	B?	4_1^0
16469	(x)	B?	$3_0^1 4_1^0$

(*): ± 0.01 cm^{-1}

(†): ± 0.5 cm^{-1}

(x): ± 1 cm^{-1}

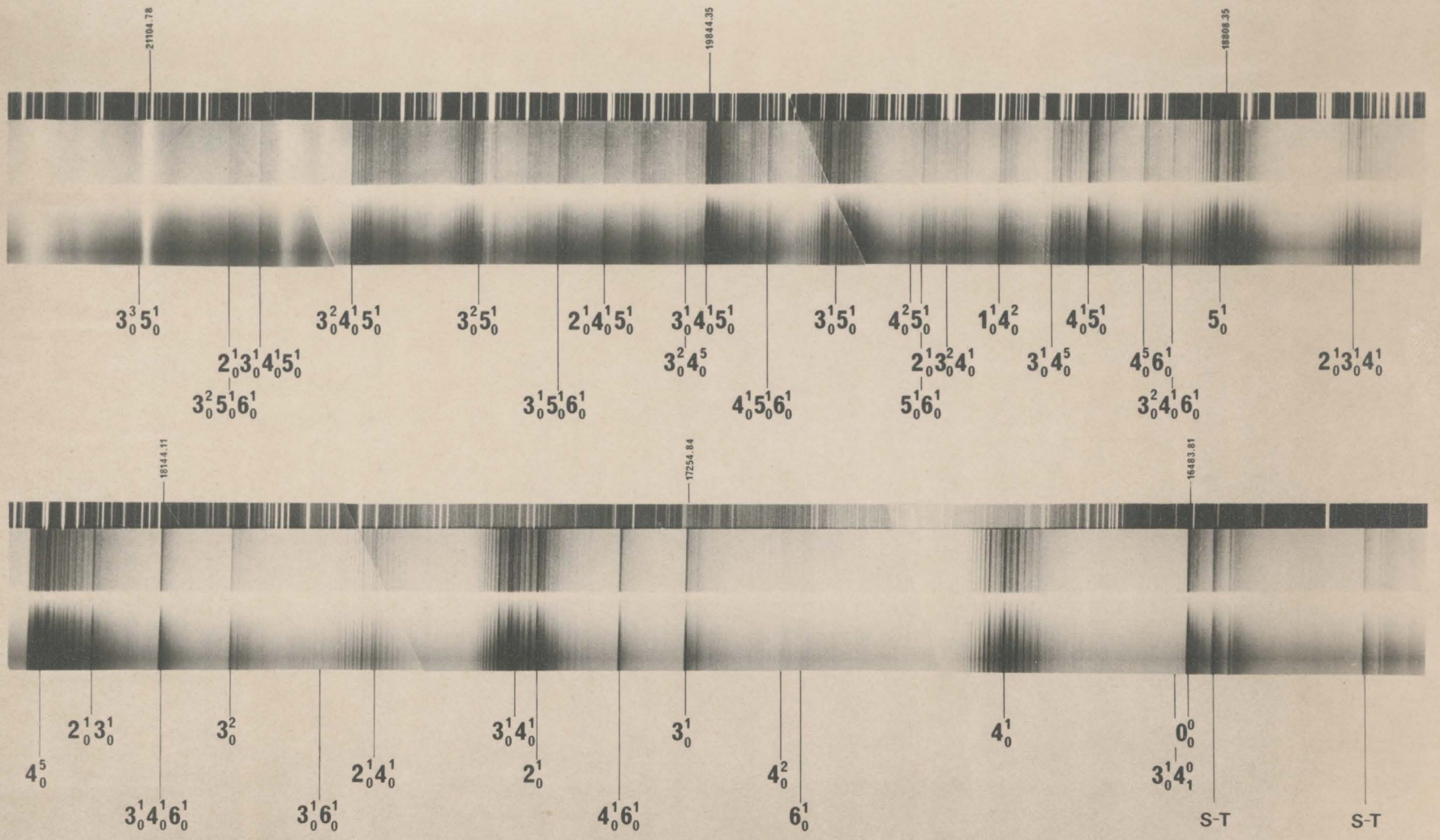

Figure 3.5 Spectrogram of the $\overset{s}{A} \leftarrow \overset{s}{X}$ ($\pi^* \leftarrow n$) system of CD_2S.

origin band of CH_2S, is along the a axis. Consequently, the band is assigned as the origin of the $^1\pi^* \leftarrow {}^1n$ transition of CD_2S. The 4_1^0 "hot" band located 786 cm^{-1} to the red of the origin and the $3_0^1 4_0^1$ "hot" band at 16469 cm^{-1} confirm the assignment.

The large negative value for the isotopic shift of the origin band, defined as $\Delta\sigma_0 = \sigma_0^H - \sigma_0^D$, is consistent with that predicted by theory. Upon electronic excitation, a marked decrease is observed in the frequency of vibration of four of the six normal modes of oscillation of thioformaldehyde. Thus, not only are the excited state vibrational energy levels more closely spaced and the multidimensional excited state potential energy well shallower than in the ground state, but the zero point energy (the level with all $v_i = 0$) of the excited state is less than that of the ground state. Since for two isotopic molecules the energy separation between levels of the same vibrational quantum numbers is proportional to the position of the levels within the well, the isotopic splitting of the excited state vibrationaless levels is less than that of the ground state. Therefore, $\Delta\sigma_0$ is negative as observed.

The Inversion Mode, $\nu_4'(D)$

The first strong band to the blue of the origin has been rotationally analysed and shown to be polarized about the b axis. The only possible assignment compatible with the observed polarization and small energy separation between it and the origin band (275 cm^{-1}) is to the 4_0^1 transition of CD_2S.

The 4_0^2 transition is assigned to the weak A-type band at 17102 cm^{-1}.

The band located 1242 cm^{-1} to the blue of 4_0^2 is very similar in appearance to the 4_0^3 band of CH_2S. A partial rotational/band contour

analysis of the band has revealed that it is polarized along the b axis. Since the large separation between it and 4_0^2 makes the assignment 4_0^3 unlikely, a possible assignment for this band would be $3_0^1 4_0^3$, which places the third quanta of the out-of-plane bending vibration 472 cm^{-1} above that of the second. However, the isotopic splitting of 35 cm^{-1} per quanta of ν_4' excited, as calculated from this assignment, is in very poor agreement with that calculated from the assignments of the 4_0^1 and 4_0^2 bands, namely 96 and 120 cm^{-1} respectively. Furthermore, other possible assignments which involve combinations with 4_0^3 also result in unacceptable isotopic splitting for the $3\nu_4'$ vibration. The band is, therefore, tentatively assigned as 4_0^5. Unfortunately, the isotopic splitting cannot be calculated for this assignment since 4_0^5 is not observed in the spectrum of CH_2S.

The energy of the vibrational levels calculated from these assignments may be fitted to the energy levels of either a simple double-minimum or a more general quadratic-quartic oscillator to yield vibrational constants which are in qualitative agreement with those predicted when the isotopic invariance rule is applied to the vibrational constants of CH_2S (see following section). Furthermore, the constants for CD_2S predict that the 4_0^4 transition will appear at approximately 17900 cm^{-1}. Indeed, a very weak band, similar in appearance to that of the 4_0^2 band, is observed at 17914 cm^{-1} and is assigned as 4_0^4. All 4_0^x (x = 1, 2, 4, 5) assignments are then used to calculate an improved potential energy function for the ν_4' inversion mode of CD_2S.

The C=S Stretch, ν_3'

The main progression, in 770 cm^{-1}, is identified as a progression in

the excited state symmetric C=S stretching mode of CD_2S. Since the ν_3' vibrational mode does not involve a large displacement of the H(D) nuclei, the small (50 cm^{-1}) decrease observed in the vibrational frequency on isotopic substitution is acceptable. The 3_0^1 transition is assigned as the strong type A band located at 17255 cm^{-1}. Combination bands involving ν_3' are observed throughout the spectrum.

The Asymmetric C-D Stretch, ν_5

A complete rotational analysis performed on the perpendicular band assigned as 5_0^1 has shown that the band is the lowest frequency strong C-type band of the system. Combination bands of 5_0^1 with 4_0^1, 4_0^2, 6_0^1 and 3_0^x (x = 1 to 3), whose polarizations are in agreement with those demanded by the assignments, confirm the value of 2325 cm^{-1} for the ν_5' excited state CD_2S vibrational frequency.

The Symmetric D-C-D Bend, ν_2'

The 2_0^1 transition of CD_2S was originally assigned to the strong type A band at 17362 cm^{-1}; however, several difficulties arose with this assignment. In particular, the medium strong band at 17771 cm^{-1}, whose b axis polarization had been definitely established by band contour analysis, could not be given an assignment compatible with its position and polarization if the above assignment of 2_0^1 was correct.

Instead, the highly overlapped type A band, located amongst the strong perpendicularly polarized $3_0^1 4_0^1$ band of CD_2S, is assigned as the 2_0^1 band. Consequently, the previously unassigned type B band at 17771 cm^{-1}, located 275 cm^{-1} to the blue of the 2_0^1 band, is given the unequivocal designation $2_0^1 4_0^1$.

The key to the identification of the unassigned type A band at 17362

cm^{-1} lies with the ν_6' fundamental frequency.

The Asymmetric D-C-D Wag, ν_6'

Of the two possible assignments, 4_0^2 and $4_0^1 6_0^1$, that are consistent with the observed polarization of the 17362 cm^{-1} band, the choice of $4_0^1 6_0^1$ is clearly the best since the other designation, 4_0^2, would necessitate that the $2\nu_4'$ level of CD_2S lie 43 cm^{-1} above that of the corresponding level of CH_2S.

Since the $4_0^1 6_0^1$ assignment implies that the 6_0^1 band should appear approximately 604 cm^{-1} to the blue of the origin, the weak perpendicular type band, observed at approximately +591 cm^{-1} from the origin, is assigned as 6_0^1. The identification of the type A combination bands $3_0^x 5_0^1 6_0^1$ (x = 1 to 3) in the higher energy region of the spectrum adds further support to the value of 591 cm^{-1} as the fundamental frequency of the ν_6' vibration.

The Symmetric C-D Stretch, ν_1'

Information about the ν_1' fundamental frequency of CD_2S is obtained from combination bands of the form $1_0^1 3_0^x 4_0^2$ (x = 1 to 3) and fixes the symmetric C-D stretching mode at a frequency of 2138 cm^{-1}.

"Hot" Bands

As is also the case for CH_2S, overlap of the origin band region by the extensive singlet-triplet system prevents the identification of all but two "hot" bands. Their assignments, mentioned briefly in the discussion of the origin band of CD_2S, are listed in Table 3-4.

A summary of the excited state vibrational frequencies of thioformaldehyde is presented in Table 3-5.

3.5 Isotopic Shifts and the Redlich-Teller Product Ratios

The potential energy for nuclear motion is the sum of the electronic

TABLE 3-5

A summary of the excited state vibrational frequencies.

Vibration	Symmetry	Frequencies (cm^{-1})	
		CH_2S	CD_2S
ν_1	a_1	3034	2138
ν_2	a_1	1320	986
ν_3	a_1	819	771
ν_4	b_1	371	275
ν_5	b_2	3081	2325
ν_6	b_2	826	599

TABLE 3-6

The product rule ratios for the $^1A_2$ state.

CH_2S/CD_2S	Obs.	Cal.	% Difference
a_1 fundamentals	1.93	1.96	-1
b_1 fundamentals	1.35	1.28	5
b_2 fundamentals	1.83	1.77	3

energy and coulombic interaction energy, both of which are independent of mass to a very high degree of approximation. Although the shape of the potential energy well for both the normal and isotopic molecules is nearly identical, the mass-dependent vibrational frequencies are not. Redlich[26] and Teller[27] have derived equations relating the ratio of the vibrational frequencies (ν_i) to the product ratio of the masses (m_i) and moments of inertia (I_α) of the normal and isotopic molecules. The general equation derived under the assumption of an harmonic force field,

$$\prod_{j=1}^{3N-6} \frac{\nu_j(i)}{\nu_j} = \prod_{j=1}^{3N} \left(\frac{m_j}{m_j(i)}\right)^{1/2} \left(\frac{M(i)}{M}\right)^{3/2} \left(\frac{I_x(i) I_y(i) I_z(i)}{I_x I_y I_z}\right)^{1/2} \qquad (3\text{-}3)$$

factors into a more simplified form which involves only vibrations of the same symmetry species[25]. Since the effective geometry (see reference 9 p. 170) of the ground and excited states of CH_2S is of C_{2v} symmetry, the following equations are derived from the six vibrations belonging to the three symmetry classifications of the vibrational modes of CH_2S;

$$a_1: \quad \frac{\nu_1(D)\nu_2(D)\nu_3(D)}{\nu_1(H)\nu_2(H)\nu_3(H)} = \left[\left(\frac{m_H}{m_D}\right)^2 \left(\frac{M_D}{M_H}\right)\right]^{1/2} \qquad (3\text{-}4)$$

$$b_1: \quad \frac{\nu_4(D)}{\nu_4(H)} = \left[\left(\frac{m_H}{m_D}\right)^2 \left(\frac{M_D}{M_H}\right) \left(\frac{I_b(D)}{I_b(H)}\right)\right]^{1/2} \qquad (3\text{-}5)$$

$$b_2: \quad \frac{\nu_5(D)\nu_6(D)}{\nu_5(H)\nu_6(H)} = \left[\left(\frac{m_H}{m_D}\right)^2 \left(\frac{M_D}{M_H}\right) \left(\frac{I_c(D)}{I_c(H)}\right)\right]^{1/2} \qquad (3\text{-}6)$$

A complete listing of the observed and calculated ratios is given in Table 3-6. The moments of inertia used in the calculation for the b_1 and b_2 vibrations were obtained from the 4_0^1 and 0_0^0 bands, respectively, of the normal and deuterated compounds.

The agreement between the observed and calculated ratios is quite

satisfactory, especially since the ν_4' vibration is known to be highly anharmonic. The very good agreement shown for the b_2 vibrations is especially pleasing since it adds further evidence for the assignment of the very weak 6_0^1 bands of both isotopes.

3.6 Potential Energy Functions for the Inversion Mode

Although several potential energy functions for the inversion mode are described in the literature[28], only two potential energy functions are used to attempt a fit to the observed vibrational levels of CH_2S and CD_2S. The first is of the form suggested by Coon et al[29] and is chosen because it had adequately predicted the energy separation between levels of the ν_4' vibrational potential of CH_2O. The second is of the form suggested by Chan[30]. It is chosen since this potential had adequately described the ground state vibrational potential of slightly non-planar and "floppy" planar molecules, for example, the potential energy function of trimethylene oxide[31] and silacyclopent-3-ene[32], respectively. As the energy separation between successive quanta within the vibrational potential of these molecules was observed to increase as v increased, as is also observed for the lower vibrational levels of CH_2S, this function is also used in an attempt to describe the ν_4' vibrational potential of CH_2S.

The form of the two potentials is, respectively,

$$V(Q) = \tfrac{1}{2} \lambda Q^2 + \delta e^{\rho} \text{ EXP}(-\lambda Q^2/2\delta) \qquad (3\text{-}7)$$

and

$$V(Q) = aQ^4 - bQ^2 \qquad (3\text{-}8)$$

where

$$\lambda = (2\pi c \nu_o)^2, \quad \delta = Bhc\nu_o/(e^{\rho} - \rho - 1) \qquad (3\text{-}9, 3\text{-}10)$$

Equation (3-7) represents an harmonic oscillator potential perturbed by a gaussian barrier while the second of the two functions is described as a

quartic potential perturbed by a quadratic potential.

3.6.1 The Gaussian Barrier Double Minimum Potential

The Coon double minimum potential energy function of equation (3-7) is dependent on three fitting parameters, ν_o, B and ρ. ν_o is the frequency of the parabolic part of the potential, B is related to the height of the perturbing gaussian barrier and ρ is a parameter determining the shape of the potential. Small values of ρ will result in a potential where outer walls are steeper than the barrier walls while the reverse effect is true of larger values of ρ.

The vibrational hamiltonian for the inversion mode is written as

$$H = -h/8\pi^2 \frac{d^2}{dQ^2} + \frac{\lambda}{2} Q^2 + \delta\, e^{\rho}\, \mathrm{EXP}(-\lambda\, Q^2/2\delta) \qquad (3\text{-}11)$$

or simply as

$$H = H_0 + H_1 \qquad (3\text{-}12)$$

with H_0 representing the hamiltonian of the harmonic oscillator and H_1 a perturbing term.

The eigenvalues and eigenvectors of the gaussian barrier-harmonic oscillator hamiltonian of equation (3-12) are obtained by the methods of perturbation theory, namely, the direct diagonalization of the hamiltonian matrix whose matric elements are given by

$$H_{ij} = \langle X_i | H | X_j \rangle \qquad (3\text{-}13)$$

If the double minimum wavefunctions are expressed as

$$\Phi_i = \sum_{n=0}^{n'} a_{in} X_n \qquad (3\text{-}14)$$

then the coefficients of the harmonic oscillator wavefunction, X_n, are obtained directly from the matrix diagonalization procedure. In practice,

a basis set which consisted of 20 harmonic oscillator wavefunctions is used (larger basis sets were used (n = 40) but resulted in little improvement in the quality of the fit (see below)).

Since the hamiltonian of equation (3-7) is dependent on the constants ρ, ν_o and B, the eigenvalues obtained from the diagonalization procedure are also dependent on the numerical values chosen for these constants. Thus, ρ, ν_o and B are varied so as to obtain agreement between the predicted energy of the ν_4' vibrational levels and the observed energy calculated from the visible electronic spectrum.

The fitting procedure for both CH_2S and CD_2S involve choosing fixed values of ρ, which are usually chosen to lie in the range of 0.9 to 0.3 and allowing the computer programme to vary both ν_o and B, in a least squares routine, until the best fit is obtained for the particular chosen value of ρ. The least squares computer programme used in the analysis is similar in structure to that discussed in Chapter 4. The subroutine used to calculate the Coon double minimum wavefunction and eigenvalue was obtained from Dr. D. Moule of Brock University.

The results obtained for thioformaldehyde, presented in Table 3-7, indicate that progressively better fits are obtained as smaller values of ρ are chosen. However, as ρ approaches zero, δ of equation (3-10) tends to infinity with the result that the fitting procedure becomes very unstable. The lowest value of ρ attainable, without the failure of the least squares procedure, is found to be 0.3. Unfortunately, the residuals calculated from the analysis are still disappointingly high.

Several quantities of spectroscopic interest can be calculated from the values of the fitting parameters obtained from the least squares anal-

TABLE 3-7

The inversion levels and zero point energy of thioformaldehyde.

CH_2S

		ρ = 0.9		ρ = 0.6		ρ = 0.3	
v	Obs. (cm^{-1})	Cal.	Resid.	Cal.	Resid.	Cal.	Resid.
0	0	0	-	0	-	0	-
1	371.2	366.9	4.3	367.3	3.9	368.4	2.8
2	834.9	864.4	-29.5	856.5	-21.6	848.0	-13.1
3	1342.4	1338.6	3.8	1339.9	2.4	1341.1	1.3
$G(0^+)$		176.2		161.0		148.5	

CD_2S

ρ = 0.3

v	Obs.	Cal.	Resid.
0	0	0	0
1	275.3	268.4	6.9
2	618.5	640.1	-21.6
4	1430.	1442.4	-12.4
5	1860.9	1860.0	0.9
$G(0^+)$		110.7	

ysis. In particular, an equation for the position of the potential energy minima may be derived by simply differentiating equation (3-7) to yield

$$Q_m = \mathrm{SQRT}(2\rho/(e^{\rho} - \rho - 1)\cdot h/(4\pi^2 c)\cdot B/\nu_0) \qquad (3\text{-}15)$$

The position of the minima may then be calculated by substituting the values of ρ, ν_o and B into equation (3-15). The out-of-plane angle (θ_m) at the position of the potential energy minima (Q_m) is calculated from

$$Q_m = \int_0^{\theta_{min}} \mu^{\frac{1}{2}} r d\theta \qquad (3\text{-}16)$$

where the numerical integration procedure is continued until the value of Q_m is reached and, where r is the C=S bond length and μ is the reduced mass defined in Chapter 4 (equation 4-95).

The values of Q_{min} and θ_{min} are listed in Table 3-8 along with ρ and the best least squares vibrational potential constants used to calculate their values.

Since ρ, the barrier height ($B\nu_o$) and the value of the out-of-plane angle (θ_{min}) are isotopically invariant, then the relationship[29]

$$\left(\frac{\mu(D)}{\mu(H)}\right)^{\frac{1}{2}} = \left(\frac{\nu_0(H)}{\nu_0(D)}\right) = \left(\frac{B(D)}{B(H)}\right) \qquad (3\text{-}18)$$

should hold between the two isotopic molecules. The value of the reduced mass ratio is calculated to be 1.13 which fixes the values of ν_o and B for CD_2S at 461 cm^{-1} and 0.0383 respectively. The poor agreement with the calculated values reported in Table 3-8 may be partially attributed to the presence of vibration-rotation interaction amongst the rovibronic levels of the $^1A_2$ state of thioformaldehyde. This type of interaction is similar to that proposed by Moule and Rao[33] to explain the deviation observed between the theoretical isotopic ratio and the ratio calculated

TABLE 3-8

The potential energy constants for the double minimum potential energy function of thioformaldehyde.

	CH_2S	CD_2S
ρ	0.3	0.3
ν_o	521 cm^{-1}	437.5 cm^{-1}
B	0.0339	0.0528
$B\nu_o$ (barrier height)	17.7 cm^{-1} (±1)	23.1 cm^{-1} (±1)
Q_{min}	0.209 x10^{-20} $g^{\frac{1}{2}}$cm (±0.06)	0.285x10^{-20} $g^{\frac{1}{2}}$cm (±0.06)
θ_{min}	13.8° (±5°)	20.7° (±5°)

TABLE 3-9

A comparison of the observed ν_4' vibrational levels of thioformaldehyde with those calculated using the quadratic-quartic potential of equation 3-26.

	CH_2S			CD_2S		
Level	Obs.	Cal.	Resid.	Obs.	Cal.	Resid.
0	0	0		0	0	
1	371.2	371.17	0.03	275.3	276.3	-1.0
2	834.9	828.4	6.47	618.5	616.7	1.8
3	1342.4	1342.5	0.1	-	-	-
4				1430.	1416.	14
5				1860.9	1861.6	-0.7

from the CH_2O-CD_2O vibrational double minimum constants. The 4_0^2 band of CH_2S is particularly suspect since Coriolis and Fermi resonances between the $2\nu_4'$ vibrational level and the ν_6' and ν_2' levels are expected to be prevalent. Similarly, the $3\nu_4'$ level of CH_2S can interact with the nearby $\nu_3'\nu_4'$ and ν_2' rovibronic levels, thereby adding further uncertainty to the analysis.

Although the poor agreement between the observed and calculated energy of the ν_4' vibrational levels can be partially explained by resonance interaction, it is felt that the gaussian barrier-harmonic oscillator potential energy function of equation (3-7) is inadequate to fully describe the ν_4' vibrational potential of thioformaldehyde, since the large amplitude vibrational motion associated with the inversion mode is expected to be highly anharmonic. Accordingly, a potential energy function which involves a dominant anharmonic term is used in an attempt to improve the overall fit.

3.6.2 The Quartic Oscillator

A potential energy function of the form

$$V(Q) = aQ^4 - bQ^2 \qquad \text{(ergs)} \qquad (3\text{-}18)$$

has been applied successfully to interpret the infrared spectrum of several non-planar molecules that are known to undergo the inversion motion[31,34]. Inspection of equation (3-18) reveals that if b is greater than zero, then the potential function will exhibit a double minimum at $\pm Q_m$ and the molecule may then be said to be non-planar. A negative value of b indicates that a barrier to inversion is not present and, therefore, the equilibrium structure of the molecule may be described as "floppy" planar.

The vibrational hamiltonian, whose potential energy is that of equation (3-18), can be reduced to the dimensionless form[30]

$$H = A(P^2 + X^4 - BX^2) \tag{3-19}$$

if the following transformations are used:

$$X = (8a/\hbar^2)^{1/6} Q \tag{3-20}$$

and $$P = (8/a\hbar^4)^{1/6} p \tag{3-21}$$

The fitting parameters A and B of equation (3-19) are related to a and b of equation (3-18) by

$$A = (a\hbar^4/64)^{1/3} \times 1.9863 \times 10^{-16} \quad (cm^{-1}) \tag{3-22}$$

and $$B = (8b^3/a^2\hbar^2)^{1/3} \times 1.9863 \times 10^{-16} \quad (cm^{-1}) \tag{3-23}$$

By expressing the matrix elements of P^2, X^4 and X^2 in terms of the quadratic oscillator wavefunctions[30] as opposed to the harmonic oscillator wavefunctions, the diagonalization of the hamiltonian matrix is very rapid. The basis set of 20 quartic oscillator wavefunctions, which are in turn expressed as linear combinations of the H.O. wavefunction[30], is used in the diagonalization procedure.

The results of a least squares fit of A and B to the observed energy levels of both CH_2S and CD_2S is presented in Table 3-9.

The theoretical values of A and B for the deuterated species can be calculated from the constants derived from the least squares analysis of the normal isotope, if the isotopic invariance rule is applied. Specifically, the equations

$$(\mu_{(D)}/\mu_{(H)})^{1/3} = B_{(D)}/B_{(H)} \tag{3-24}$$

and $$(\mu_{(D)}/\mu_{(H)})^{2/3} = (A_{(H)}/A_{(D)})^{1/3} \tag{3-25}$$

were derived by Chan[31] for the quadratic-quartic oscillator. Since the potential energy function of CH_2S, as calculated from the least squares vibrational analysis, takes the form

$$V(X)_H = 45.59(X^4 + 1.423\ X^2) \qquad (3\text{-}26)$$

then the predicted values of A and B for CD_2S are 38.36 cm^{-1} and -1.69 cm^{-1}, respectively. However, a least squares fit to the observed ν_4' vibrational levels of CD_2S yields a potential energy function of the form

$$V(X)_D = 33.88(X^4 + 1.557\ X^2) \qquad (3\text{-}27)$$

which is in relatively poor agreement with the theoretically expected potential. This discrepancy, as stated in the previous section, may be attributed partially to resonance interactions in the CH_2S spectrum.

The negative value calculated for the fitting parameter B for both CH_2S and CD_2S is somewhat unexpected since its sign is an indication that the barrier to inversion for thioformaldehyde is zero. This, in turn, implies that the molecule is planar in its first excited state. Since the least squares analysis is based on a two-parameter fit to only three or four observed vibrational levels, some of which are expected to be perturbed by resonance interactions, the conclusion is suspect. In fact, the relatively large residuals may indicate that a simple quadratic-quartic potential is inadequate to describe fully the potential energy function of the ν_4' vibration. Instead, a potential of the form

$$V(Q) = \tfrac{1}{2}\ \lambda\ Q^2 + \delta\ e^{\rho}\ EXP(-\lambda\ Q^2/2\delta) + bQ^4 \qquad (3\text{-}28)$$

that is, a quadratic-quartic potential perturbed by a gaussian barrier may have the correct form. As an insufficient number of transitions to higher excited state ν_4' vibrational levels have been observed for a

reliable least squares fit to the potential described by equation (3-28), the adequacy of this function to describe accurately the inversion doubling of thioformaldehyde remains a matter of conjecture.

A diagram of the potential energy function of the ν_4' inversion mode of the ground and excited states of CH_2S is presented in Figure 3-6. The excited state potential is represented by both the Coon double minimum potential and the quadratic-quartic potential of Chan, both of which are constructed from the least squares potential energy constants of Table 3-8 and equation (3-26). The ground state harmonic oscillator potential energy diagram is constructed from the value of the ν_4'' vibrational frequency reported by Jacox and Mulligan[6]. Except for the existence of a very shallow barrier in the Coon potential, the two excited state functions show a remarkably similar appearance. The marked dissimilarity between the ground and excited state potentials qualitatively explains the strong Franck-Condon activity observed for transition to the ν_4' vibrational levels of thioformaldehyde.

Since the model potential energy functions are inadequate to describe accurately the actual molecular potential, considerable doubt exists about the geometry of the excited state, as calculated from the vibrational data alone. However, the models presented above are estimates of the actual potentials and therefore estimates to the geometry, as obtained from the vibrational analysis, may be obtained. The excited state geometry (as obtained from vibrations analysed) may be said to be either very slightly non-planar (approximately 15^{o} out of plane) or "floppy" planar. The barrier to inversion is, certainly, very low, and can be fixed at a value of less than 20 cm^{-1}.

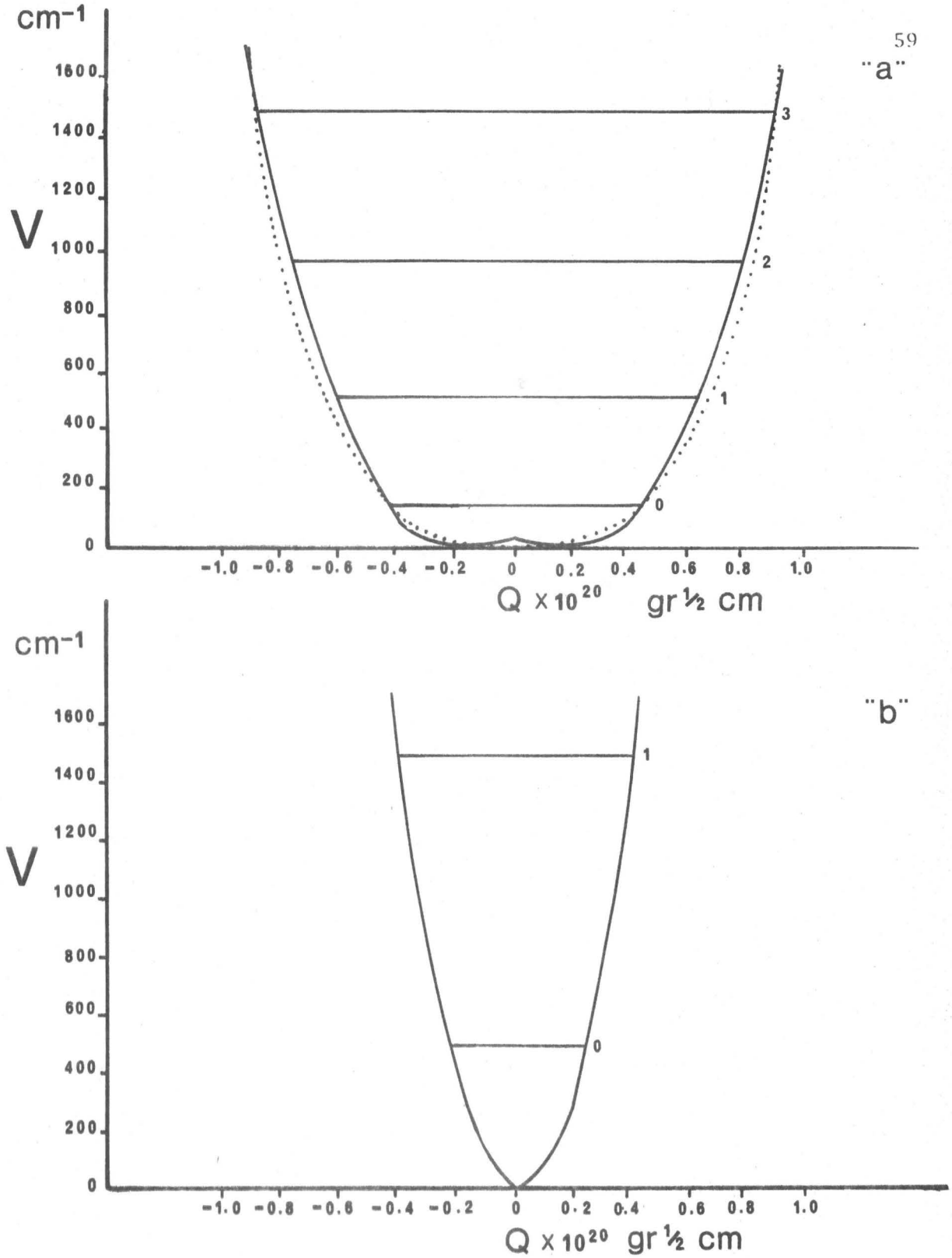

Figure 3-6. The potential energy function of the ν_4' inversion ("a") and out-of-plane binding ("b") mode of CH_2S. The excited state potential ("a") is represented by the Coon double-minimum potential (-) and the Chan quadratic-quartic potential (....).

CHAPTER 4

ROTATIONAL ANALYSIS OF THE $^1A_2$ SYSTEM OF THIOFORMALDEHYDE

4.1 The Molecular Hamiltonian

Wilson[35] has shown that the molecular hamiltonian of a semi-rigid vibrating molecule consists of a purely rotational part, a purely vibrational part, plus terms due to the interaction between vibration and rotation. The model chosen is that of N point masses (the nuclei) held together by semi-rigid springs vibrating in the average field of the electrons. The hamiltonian for such a system is within the limitations of the Born-Oppenheimer approximation,

$$H_N = T_N + V_N \tag{4-1}$$

where T_N is the translational energy of the molecule and V_N is the potential energy. The coordinates for the model are the space-fixed cartesian coordinates (X, Y, Z) of the centre of mass, the molecule-fixed coordinates (x, y, z), and the normal coordinates of vibration. The space- and molecule-fixed cartesian coordinates are related by the Eulerian angles (θ, ϕ, χ) defined in Figure 4-1.

After a lengthy development, which is chronicled in several texts[36,37], the classical hamiltonian is expressed as

$$\begin{aligned} H = {} & \tfrac{1}{2}\{\mu_{xx}(P_x-p_x)^2 + \mu_{yy}(P_y-p_y)^2 + \mu_{zz}(P_z-p_z)^2\} \\ & + \mu_{xy}(P_x-p_x)(P_y-p_y) + \mu_{yz}(P_y-p_y)(P_z-p_z) \\ & + \mu_{zx}(P_z-p_z)(P_x-p_x) + \tfrac{1}{2}\sum_k p_k^2 + V \end{aligned} \tag{4-2}$$

where

$$\mu_{xx} = (I'_{yy}\, I'_{zz} - I'^2_{yz})/\Delta \tag{4-3}$$

$$\mu_{xy} = (I'_{zz}\, I'_{xy} + I'_{yz}\, I'_{xz})/\Delta \tag{4-4}$$

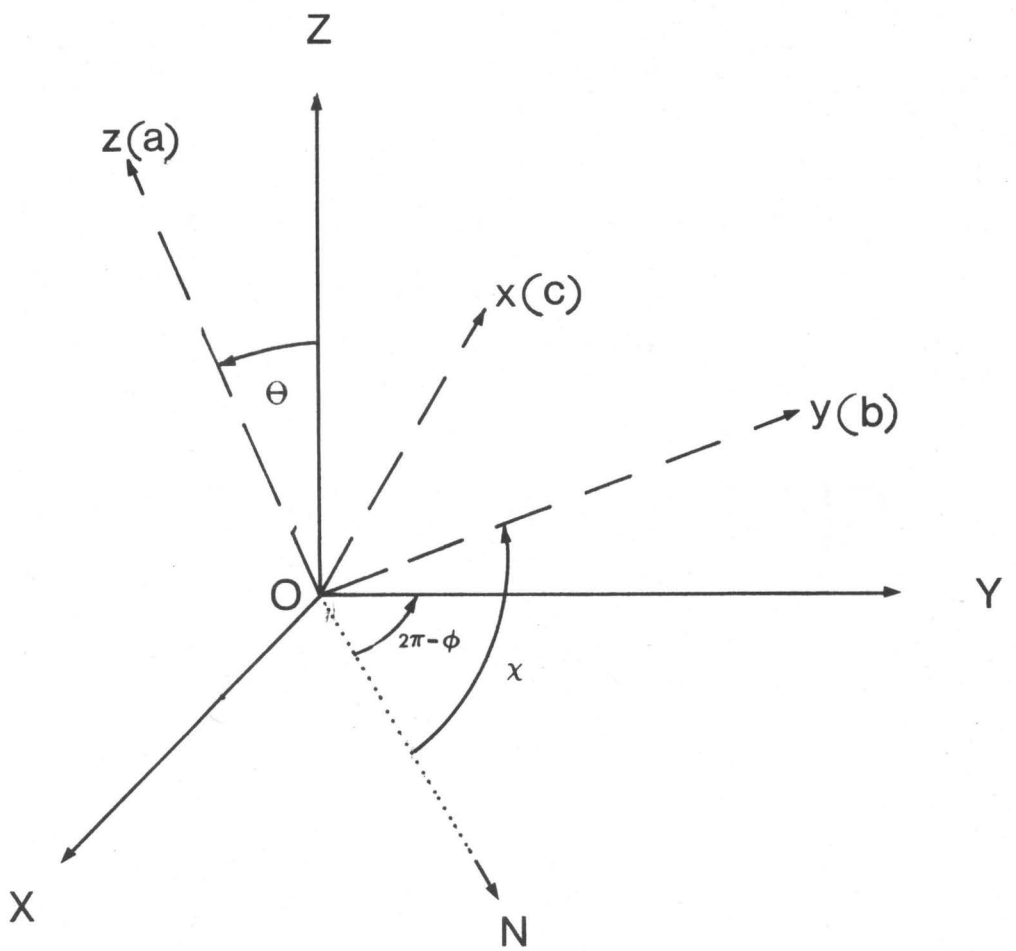

Figure 4-1. The relationship between the space-fixed cartesian coordinates (X, Y, Z) and the molecule-fixed cartesian coordinates (x, y, z).

ON = the intersection of the XY and xy planes.

θ = angle from OZ to Oz ($0 \leq \theta \leq \pi$).

ϕ = angle in XY plane from OX to the projection of Oz on the XY plane. Also, angle from OY to ON ($0 \leq \phi \leq 2\pi$).

χ = angle in xy plane from ON to Oy ($0 \leq \chi \leq 2\pi$).

and where

$$\Delta = \begin{vmatrix} I'_{xx} & -I'_{xy} & -I'_{xz} \\ -I'_{xy} & I'_{yy} & -I'_{yz} \\ -I'_{xz} & -I'_{yz} & I'_{zz} \end{vmatrix} \tag{4-5}$$

is the inertial tensor. P_g (g = x, y or z) is the angular momentum vector, defined in terms of the angular velocity; p_g is one of the components of the vibrational angular momentum, expressed in terms of p_k, which is the angular momentum conjugate to Q_k. Since I'_{gg} is defined in terms of the instantaneous moment of inertia (I) and as a function dependent on the square of the normal coordinates, the coefficients μ_{gg} of equation (4-2) are also dependent on the normal coordinates. The transformation of equation (4-2) to its quantum mechanical equivalent is not straightforward since the momenta, P_x, P_y and P_z, are not conjugate to any coordinates. However, Wilson[37] was able to show that the classical hamiltonian of equation (4-2) reduces to

$$H = \tfrac{1}{2}\,\mu^{\frac{1}{4}} \sum_{gg'} (P_g - p_g)\,\mu_{gg'}\,\mu^{-\frac{1}{2}}\,(P_{g'} - p_{g'})\,\mu^{\frac{1}{4}} + \tfrac{1}{2}\,\mu^{\frac{1}{4}} \sum_{k} p_k\,\mu^{-\frac{1}{2}}\,p_k\,\mu^{\frac{1}{4}} + V \tag{4-6}$$

or, equivalently,

$$H = \tfrac{1}{2} \sum_{gg'} \mu_{gg'}\,P_g P_{g'} - \sum_{g} h_g P_g + \tfrac{1}{2} \sum_{gg'} \mu^{\frac{1}{4}}\,p_g \mu_{gg'} \mu^{-\frac{1}{2}} p_{g'} \mu^{\frac{1}{4}} + \tfrac{1}{2} \sum_{k} \mu^{\frac{1}{4}}\,p_k\,\mu^{-\frac{1}{2}}\,p_k\,\mu^{\frac{1}{4}} + V \tag{4-7}$$

where

$$h_g = \tfrac{1}{2} \sum_{g'} (\mu^{-\frac{1}{4}} \mu_{gg'} p_{g'} \mu^{\frac{1}{4}} + \mu^{\frac{1}{4}} p_{g'} \mu_{gg'} \mu^{-\frac{1}{4}}) \tag{4-8}$$

and where μ is defined as the determinant of the coefficients $\mu_{gg'}$.

The quantum mechanical hamiltonian represented by equations (4-6) and (4-7) is exact, in the sense that no approximation other than the Born-Oppenheimer has been used in its derivation.

4.2 The Rigid Rotor

The general hamiltonian is, to say the least, formidable. Fortunately, a great degree of simplification results if we, for the moment,

1) ignore the dependence of μ and $\mu_{gg'}$ on the normal coordinates;
2) allow the x, y and z axis to coincide with the principle axis of inertia;
3) neglect all terms dependent on the square of the normal coordinates; and, finally,
4) set the internal (vibrational) angular momentum, p_g, equal to zero.

Equation (4-6) then reduces to

$$H = \tfrac{1}{2}\left[\frac{P_x^2}{I_x^e} + \frac{P_y^2}{I_y^e} + \frac{P_z^2}{I_z^e}\right] + \tfrac{1}{2}\sum_k p_k^2 + V \qquad (4\text{-}9)$$

where I_g^e are the equilibrium moments of inertia.

Since the total squared angular momentum operator, defined as

$$P^2 = P_x^2 + P_y^2 + P_z^2 = P_X^2 + P_Y^2 + P_Z^2 \qquad (4\text{-}10)$$

commutes with the operators, P_z and P_Z[11], then the three operators share a common set of wavefunctions which are simultaneously eigenfunctions of each of the operators. If the wavefunction is designated as

$$\psi_r = \langle J, K, M| \qquad (4\text{-}11)$$

then the only non-zero matrix elements of the above operators are diagonal

and have the form

$$\langle J,K,M|P^2|J,K,M\rangle = J(J+1)\hbar^2 \tag{4-12}$$

$$\langle J,K,M|P_z|J,K,M\rangle = K\hbar \tag{4-13}$$

and

$$\langle J,K,M|P_Z|J,K,M\rangle = M\hbar \tag{4-14}$$

The non-commuting operators, P_y^2 and P_z^2, have both non-diagonal and diagonal matrix elements, of the form

$$\langle J,K,M|P_y^2|J,K,M\rangle = \langle J,K,M|P_x^2|J,K,M\rangle = \frac{\hbar^2}{2}\,(J(J+1) - K^2) \tag{4-15}$$

and

$$\langle J,K\pm2,M|P_y^2|J,K,M\rangle = -\langle J,K\pm2,M|P_x^2|J,K,M\rangle$$

$$= \frac{\hbar^2}{4}\left[(J\mp K)(J\pm K+1)(J\mp K-1)(J\pm K+2)\right]^{\frac{1}{2}} \tag{4-16}$$

The energy matrix, H, can be readily obtained from the rigid rotor hamiltonian and has matrix elements of the form

$$\langle J,K,M|H|J,K,M\rangle = \frac{\hbar^2}{4}\left\{\left(\frac{1}{I_x} + \frac{1}{I_y}\right)\left[J(J+1)-K^2\right] + \frac{2K^2}{I_z}\right\} \tag{4-17}$$

and

$$\langle J,K+2,M|H|J,K,M\rangle = \langle J,K,M|H|J,K+2,M\rangle$$

$$= \frac{\hbar^2}{8}\left\{\left(\frac{1}{I_y} - \frac{1}{I_x}\right)\left[(J-K)(J-K-1)(J+K+1)(J+K+2)\right]^{\frac{1}{2}}\right\} \tag{4-18}$$

If the rotation constants, defined as

$$A = \hbar^2/2I_a;\ B = \hbar^2/2I_b;\ C = \hbar^2/2I_c \tag{4-19}$$

with $A > B > C$, are identified with the z, y and x axes respectively, then in the case of the prolate symmetric rotor ($B = C$), the energy matrix is diagonal in J and K and the familiar relationship

$$F(J,K) = (A - B)K^2 + B(J)(J + 1) \tag{4-20}$$

is obtained. For $K \neq 0$, the energy levels represented by F(J,K) are doubly degenerate.

In the case of the asymmetric top ($I_a \neq I_b \neq I_c$), the energy matrix is no longer diagonal in K. Thus, the energy expressions of the asymmetric top are no longer in closed-form. The energies are obtained by diagonalization of the energy matrix. Before the advent of high speed digital computers several simplifying procedures were introduced in order to ease the task of matrix diagonalization. One of these procedures involved the calculation of Ray's asymmetry parameter, κ, defined as

$$\kappa = (2B - A - C)/(A - C) \tag{4-21}$$

in order that the energy expressions could be placed in a more manageable form. Since κ has the values of -1 and +1 for the prolate (B = C) and oblate (A = B) symmetric top limits respectively, this useful parameter is still extensively used to indicate the degree of asymmetry of the molecule.

With present-day computers, this procedure is no longer necessary, although the hamiltonian energy matrix for each value of J is usually put in block diagonal form by applying the Wang transformation[36]

$$X^{-1}EX = E^{+} + E^{-} + O^{-} + O^{+} \tag{4-22}$$

where E and O refer to the even and odd values of K and the plus and minus represent the even or oddness of a parameter γ (see reference 36). Each of the matrices is diagonalized by standard numerical techniques to yield the energy levels of an asymmetric rotor.

A diagram correlating the asymmetric top energy levels to the oblate and prolate symmetric top limits is presented in Figure 4-2. Each of the

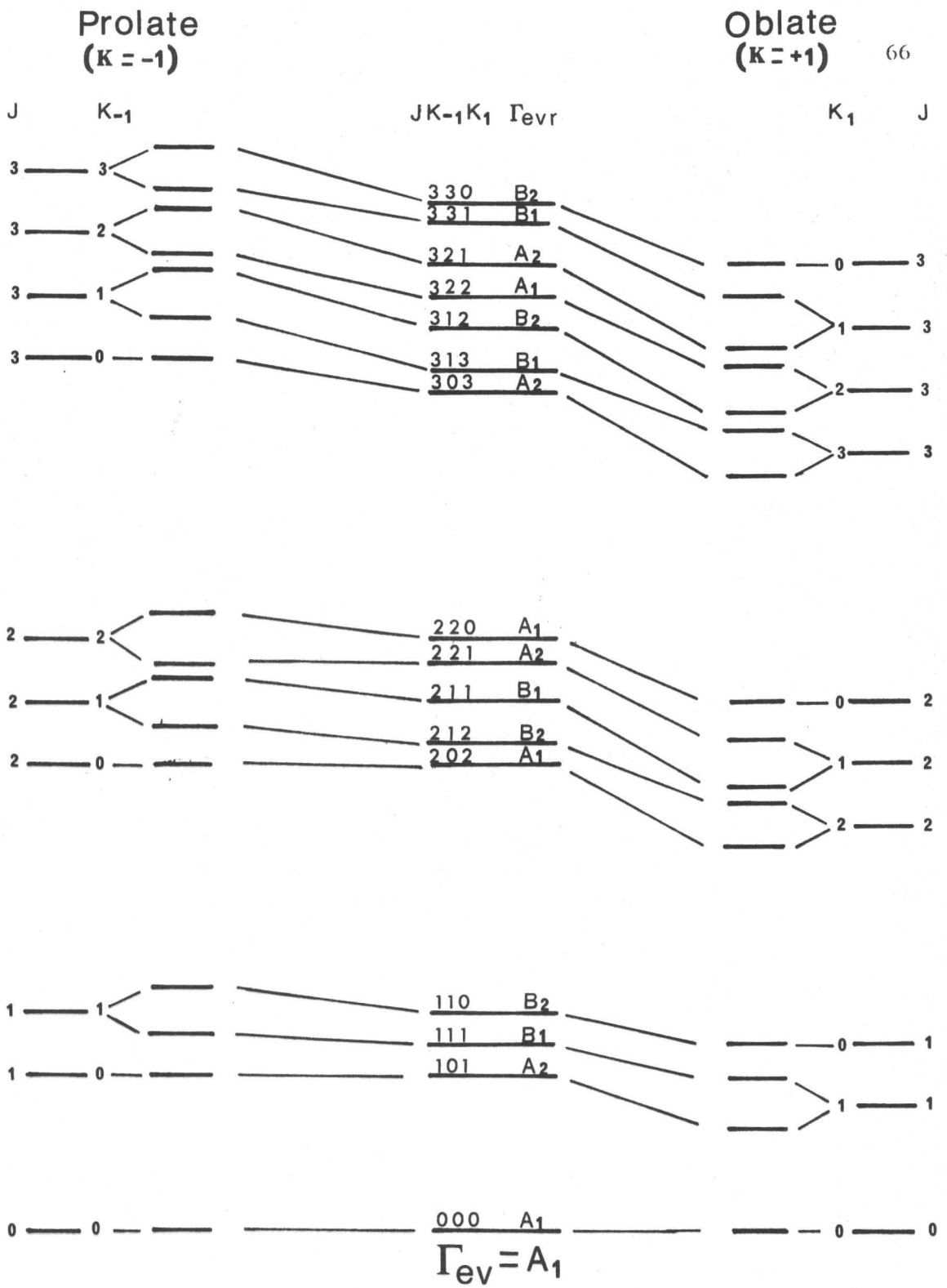

Figure 4-2. A diagram correlating the asymmetric top energy levels to the oblate and prolate symmetric top limits. The symmetry classification of the asymmetric top rovibronic levels under the C_{2v} point group is also shown. Γ_{ev} is assumed to be totally symmetric.

levels of the asymmetric top is designated by its numerical value of J and the values of K_{-1} and K_{+1} to which the levels correlate. In the correlation procedure, J remains a "good" quantum number for all degrees of asymmetry while both K_{-1} and K_{+1} are valid quantum numbers (i.e. denoting the conserved component of angular momentum about a top axis) only at the limits.

4.2.1 The Symmetry Species of the Asymmetric Rotor Energy Levels

The symmetry behaviour of the asymmetric rotor wavefunctions with respect to a rotation of 180^{o} about each of the principle inertial axes is used to determine their rotational symmetry classification. The wavefunction will either remain unchanged (transform as (+1)) or change sign (transform as (-1)) under each of the operations of the D_2 point group. Dennison[38] has shown that the symmetry of the wavefunction can be completely described by the shorthand notation (++), (+-), (-+) or (--) where the + and - signs within the brackets indicate the behaviour of the wavefunction on rotation about the $C_{2(c)}$ and $C_{2(a)}$ axis respectively. The behaviour of the wavefunction with respect to the $C_{2(b)}$ operation is not included in the designation as its symmetry behaviour is determined by the product of $C_{2(a)}$ and $C_{2(c)}$.

A knowledge of the symmetry behaviour of the rotational wavefunction with respect to the full molecular symmetry group is necessary if the overall rovibronic symmetry designation is required. Since the operations of the molecular symmetry groups of Longuet-Higgins involve rotation about the inertial axes, the rotational wavefunctions are readily classified under these symmetry groups. Therefore, the symmetry designation of the rotational wavefunctions of both planar and non-rigid non-planar thioform-

aldehyde can be deduced from equation (3-1) and Table 4-1. The (++), (+-), (-+) and (--) rotational levels transform, respectively, as the A_1, B_2, A_2 and B_1 representations of the G_4 molecular symmetry group. The overall symmetry designation of the rovibronic levels of CH_2S, which is simply the direct product of the symmetry species of ψ_e, ψ_v and ψ_r, is illustrated in Figure 4-2.

4.2.2 Rotational Selection Rules

Selection rules for electric dipole transitions that are based on the full rovibronic wavefunction depend on the space-fixed electric dipole operator, μ. Hougen[39] has pointed out that since free space is isotropic, then only the Z component of the space-fixed electric dipole moment operator need be considered in the derivation of the selection rules. Further, since μ_Z can be expressed in terms of the components of the dipole moment operator along the molecule-fixed axis system, together with the appropriate directional cosines, thus μ_Z transforms as $\Gamma_{T_z} \times \Gamma_{R_z}$. An electric dipole transition between two rovibronic states is allowed if and only if the direct product of the overall species of upper and lower states contains the species of the direct product of $\Gamma_{T_z} \times \Gamma_{R_z}$. For the vibronically-allowed transitions of CH_2S, the following rotational selection rules are derived.

For bands polarized about the molecule-fixed z axis, whose direct product of the symmetry species of the upper and lower state vibronic wavefunction is necessarily A_1, then the selection rules

$$A_1 \leftrightarrow A_2 \qquad \text{and} \qquad B_1 \leftrightarrow B_2 \qquad (4\text{-}23)$$

or, equivalently,

$$(++) \leftrightarrow (-+) \qquad \text{and} \qquad (--) \leftrightarrow (+-) \qquad (4\text{-}24)$$

TABLE 4-1

The G_4 Molecular Symmetry Group

G_4	E	(H_1H_2)	$(H_1H_2)^*$	E*	
$C_{2v}C_2(g)$	E	$C_2C_2(a)$	$\sigma_{ac}C_2(b)$	$\sigma_{ab}C_2(c)$	z=a; y=b; x=c
A_1	1	1	1	1	(++)
A_2	1	1	-1	-1	(-+)
B_1	1	-1	1	-1	(--)
B_2	1	-1	-1	1	(+-)

apply to transitions between the rotational energy levels. As each level of the asymmetric rotor is completely described by the $JK_{-1}K_{+1}$ designation, then an alternate and equivalent set of selection rules for A-type bands is

$$\Delta K_{-1} = 0, \pm 2, \ldots \qquad \Delta K_{+1} = \pm 1, \pm 3, \ldots \tag{4-25}$$

Similarly, B-type bands follow the selection rules

$$A_1 \leftrightarrow B_1 \quad \text{and} \quad B_2 \leftrightarrow B_1 \tag{4-26}$$

$$(++) \leftrightarrow (--) \quad \text{and} \quad (+-) \leftrightarrow (--) \tag{4-27}$$

or $$\Delta K_{-1} = \pm 1, \pm 3, \ldots \quad \text{and} \quad \Delta K_{+1} = \pm 1, \pm 3, \ldots \tag{4-28}$$

while bands polarized along the molecule-fixed c axis follow

$$A_1 \leftrightarrow B_2 \quad \text{and} \quad A_2 \leftrightarrow B_1 \tag{4-29}$$

$$(++) \leftrightarrow (+-) \quad \text{and} \quad (-+) \leftrightarrow (--) \tag{4-30}$$

or $$\Delta K_{-1} = \pm 1, \pm 3, \ldots \quad \text{and} \quad \Delta K_{+1} = 0, \pm 2, \ldots \tag{4-31}$$

The general selection rule which limits the change in total angular momentum

$$\Delta J = 0 \pm 1 \tag{4-32}$$

places further restrictions on the total number of rotational transitions possible.

4.2.3 Nuclear Statistical Weights

On exchange of identical nuclei, the total wavefunction, written as

$$\psi_T = \psi_{evr} \cdot \psi_N \tag{4-33}$$

must either be symmetric or asymmetric according to whether the "resultant" statistics are bose or fermi, respectively. If the nuclear wavefunction is written as a product function of single particle spin states of identical nuclei, then in the case of CH_2S, four possible nuclear wavefunctions exist. The four functions form a basis set whose symmetry behaviour under the four

operations of the G_4 symmetry group is used to determine the number of nuclear wavefunctions that belong to each symmetry classification. Since the spin functions are invarient under E* and, thus, the effect of $(H_1H_2)^*$ is equivalent to (H_1H_2) for CH_2S, then it is easy to show that of the four nuclear wavefunctions, three transform as A_1 and the remaining one as B_1. The total wavefunction must be of B_1 or B_2 symmetry (asymmetric with respect to (H_1H_2)). Then, for the totally symmetric vibronic ground state of CH_2S, the rovibronic levels of A_1 or A_2 symmetry have a statistical weight of 1 while levels of B_1 or B_2 rovibronic symmetry have a weight of 3. This means that levels of odd K''_{-1} have a statistical weight three times greater than levels of even K''_{-1}.

In the case of CD_2S, the presence of two equivalent deuterium nuclei requires that the total wavefunction be symmetric to nuclear permutation, that is, it must transform as either the A_1 or A_2 representation. Of the nine possible nuclear wavefunctions, six belong to the A_1 representation and three to the B_1 representation. If, as before, the ground state is of A_1 vibronic symmetry, then the statistical weight of the (A_1A_2) pair of rovibronic levels and the (B_1B_2) pair are 6 and 3, respectively. Therefore, in the case of CD_2S, transitions originating from the vibronic $^1A_1$ ground state levels of even K''_{-1} are expected to be twice as strong as transitions from levels of odd K''_{-1}.

4.3 Centrifugal Distortion

Only in those regions where the values of J and K are fairly small is there a close agreement between the observed transition energies and those calculated from the rigid rotor hamiltonian of equation (4-9). For non-rigid molecules, the effects of centrifugal distortion, that is, a

stretching of the bonds between atoms as the (classical) angular velocity increases, becomes quite pronounced at high J and K values. The general hamiltonian of equation (4-7) is rewritten as the perturbation expansion

$$H = H_r^0 + \lambda H' \tag{4-34}$$

where H_r^0 represents those members of the first summation term of equation (4-7) that are diagonal in the vibrational quantum number v. H' represents the perturbation terms and contains the remaining members of the first sum not included in H_r^0 plus all the members of the second summation. Since the remaining terms of equation (4-7) are functions only of the vibrational coordinates, these terms may be neglected by including them with the vibrational potential V. The off-diagonal elements of the matrix formed from equation (4-34) are of the order λ; however, if a Van Vleck transformation[40] is performed on equation (4-34) to yield

$$H = H_r^0 + \lambda H_1 + \lambda^2 H_2 \tag{4-35}$$

the off-diagonal elements (in v) are of the order λ^2. If the higher order off-diagonal (λ^2) terms are neglected, the matrix factors into block diagonal form with each block describing a particular vibrational state. The energy may now be calculated correctly to fourth order by using the diagonal elements of H given by

$$H_v = \langle v;JKM|H|v;JK'M\rangle = \langle v;JKM|H_r^0 + H'|v;JK'M\rangle$$

$$+ \sum_{J,K'',M,v''} \frac{\langle v;JKM|H'|v'';JK''M\rangle\langle v'';JK''M|H'|v;JK'M\rangle}{E_v^0 - E_{v''}^0} \tag{4-36}$$

An evaluation of the matrix elements[36] reveals that the coefficients of P_g and P_g^3 are zero while other cubic terms of the form

$P_g^2 P_{g'} - P_g P_{g'}^2$ reduce to quadratic terms. Thus the energy of a non-rigid rotating molecule of orthorhombic symmetry takes the simplified form

$$H_v = Ev + 1/\hbar^2(A_o P_z^2 + B_o P_y^2 + C_o P_x^2) + \tfrac{1}{4} \sum_{gg'jj'} \tau_{gg'jj'} P_g P_{g'} P_j P_{j'} \qquad (4\text{-}37)$$

where A_o, B_o and C_o are proportional to the effective moments of inertia, I_o, and are functions of the particular vibrational state of the molecule, as are the coefficients, $\tau_{gg'jj'}$. The relation between these coefficients ($\tau_{gg'jj'}$) and the centrifugal distortion constants of equations (4-40) - (4-42) is shown in Table 4-2.

If, for the moment, the quadratic terms of equation (4-37) are ignored, then the energy of orthorhombic molecules is given by

$$H_v = Ev + 1/\hbar^2(A_o P_z^2 + B_o P_y^2 + C_o P_x^2) \qquad (4\text{-}38)$$

Although equation (4-38) is very similar to the energy expression of the rigid rotor, it has the important difference that the effective moment of inertia (I_o) is not related simply to either the instantaneous moment of inertia (I) or the equilibrium moment of inertia (I_e).

The evaluation of the matrix elements of equation (4-37) can be simplified if the hamiltonian is rewritten in the form[36]

$$H_v = E_v + 1/\hbar^2(AP_z^2\ BP_y^2 + CP_x^2) + 1/4\hbar^4 \sum_{gg'} \tau'_{ggg'g'} P_g^2 P_{g'}^2 \qquad (4\text{-}39)$$

where the rotational constants A, B and C are no longer distortion free in that they now contain small contributions from the distortion constants τ_{gjgj}. The relationship between the rotational constants of equation (4-39) and the distortion free constants A_o, B_o and C_o of equation (4-37), along with the relationship between the unprimed and primed distortion

TABLE 4-2

The Relationship Between the Centrifugal Distortion Constants and the Primed and Unprimed Molecular Constants

$$D_J = -(1/32)(3\tau_{bbbb} + 3\tau_{cccc} + 2\tau_{bbcc} + 4\tau_{bcbc})\hbar^4$$

$$D_K = D_J - (1/4)(\tau_{aaaa} - \tau_{aabb} - \tau_{aacc} - 2\tau_{abab} - 2\tau_{acac})\hbar^4$$

$$D_{JK} = -D_J - D_K - (1/4)(\tau_{aaaa})\hbar^4$$

$$R_5 = -(1/32)\{\tau_{bbbb} - \tau_{cccc} - 2(\tau_{aabb} + 2\tau_{abab}) + 2(\tau_{aacc} + 2\tau_{acac})\}\hbar^4$$

$$R_6 = (1/64)\{\tau_{bbbb} + \tau_{cccc} - 2(\tau_{bbcc} + 2\tau_{bcbc})\}\hbar^4$$

$$\delta_J = -(1/16)(\tau_{bbbb} - \tau_{cccc})\hbar^4$$

$$A_o = A + (3\tau_{bcbc} - 2\tau_{abab} - 2\tau_{acac})\hbar^4/4$$

$$B_o = B + (3\tau_{acac} - 2\tau_{abab} - 2\tau_{bcbc})\hbar^4/4$$

$$C_o = C + (3\tau_{abab} - 2\tau_{bcbc} - 2\tau_{acac})\hbar^4/4$$

$$\tau'_{\alpha\alpha\beta\beta} = (\tau_{\alpha\alpha\beta\beta} + 2\tau_{\alpha\beta\alpha\beta})\hbar^4 \qquad \alpha \neq \beta$$

$$\tau'_{\alpha\alpha\alpha\alpha} = \tau_{\alpha\alpha\alpha\alpha}\hbar^4$$

constants is given in Table 4-2.

The hamiltonian of equation (4-39) is diagonal in both J and M but contains off-diagonal contributions from both K±2 and K±4. The form of these matrix elements is given by[41]

$$\langle J,K,M|H_v|J,K,M\rangle = AK^2 + \tfrac{1}{2}(B+C)\left[J(J+1) - K^2\right] - J^2(J+1)^2D_J - K^4D_K - J(J+1)K^2D_{JK} - \left[4J(J+1) - 10K^2\right]R_6 \quad (4\text{-}40)$$

$$\langle J,K,M|H_v|J,K\pm2,M\rangle = \{\tfrac{1}{4}(C-B) + \delta_J J(J+1) - R_J\left[K^2 + (K\pm2)^2\right]\} \cdot \{\left[J(J+1)-K(K\pm1)\right]\left[J(J+1)-(K\pm1)(K\pm2)\right]\}^{\frac{1}{2}} \quad (4\text{-}41)$$

$$\langle J,K,M|H_v|J,K\pm4,M\rangle = R_6\{\left[J(J+1) - K(K\pm1)\right]\left[J(J+1) - (K\pm1)(K\pm2)\right]\}^{\frac{1}{2}} \cdot \{\left[J(J+1)-(K\pm2)(K\pm3)\right]\left[J(J+1)-(K\pm3)(K\pm4)\right]\}^{\frac{1}{2}} \quad (4\text{-}42)$$

The three symmetric top distortion constants, D_K, D_J and D_{JK}, along with the three asymmetric top distortion constants, δ_J, R_5 and R_6, are defined in Table 4-2.

The transition energies for non-rigid asymmetric tops calculated using the hamiltonian of equation (4-39) are in excellent agreement with the observed infrared and visible transition energies. However, the very precise measurements possible within the microwave region necessitate that the hamiltonian of equation (4-37) be extended to include sextet terms[42,43] in order that satisfactory agreement with theory and observation is reached.

4.4 The Determination of the Rotational Constants

Once the rotational structure of the visible, or IR, spectrum has been correctly assigned, the rotational constants of both the upper and lower states may be determined by methods derived from the non-rigid asymmetric rotor energy expressions presented in the previous section.

Graphical methods such as those given by Allen and Olson[36] or methods based on the so-called Mecke sum rules[44] are particularly valuable if a rapid, rough estimate of the rotational constants is desired. In fact, with present day digital computers, a complete rotational assignment is no longer necessary since the rotational constants may be estimated from a comparison of the calculated and observed band contours[45,46]. This method is particularly valuable for larger molecules whose rotational structure is only partially resolved.

However, the most elegant, efficient and accurate method is that of a complete analysis of the data by the method of least squares. Since this method is particularly valuable for well resolved spectra, it has been used extensively in the rotational analysis of thioformaldehyde. A brief discussion of the methods and limitations is presented below. Much of this discussion is based on the review article by Lees[47] and the paper by Kirchhoff[43].

4.4.1 The Least Squares Procedure

The rotational energy levels of an asymmetric rotor are functions of the three rotational and the six centrifugal distortion constants of the molecule. The energies of the rovibronic levels of the excited state depend on an additional parameter, ν_o, describing the vibrational or vibronic frequency. ν_o represents the energy separation between the J'' = K'' = 0 level of the ground state and the J' = K' = 0 level of the excited state, i.e., the wavenumber of the band origin. Let the rovibronic energy function be represented by

$$E_i = f_i(A,B,\ldots,\nu_o) \qquad (4\text{-}43)$$

Since the best values of the rotational constants are, as yet, unknown, they may be expressed as

$$A = A' + \Delta a \quad \text{(etc.)} \tag{4-44}$$

where A' is an estimate of the value of the constant and Δa is the correction to A' necessary to give the correct value of A. Equation (4-43) is now written as

$$E_i = f_i(A' + \Delta a,\ B' + \Delta b, \ldots, \nu_o' + \Delta\nu_o) \tag{4-45}$$

or, if a Taylor expansion is performed, as

$$E_i = f_i(A', B', \ldots, \nu_o') + \Delta a \frac{\partial f_i}{\partial A'} + \Delta b \frac{\partial f_i}{\partial B'} + \ldots + \Delta\nu_o \frac{\partial f_i}{\partial \nu_{oi}} \tag{4-46}$$

where E_i is the observed energy and $f(A', B', \ldots, \nu_o')$ is the energy calculated from the trial constants. Equation (4-46) may be rearranged and put into matrix form as

$$\Delta Y = J\Delta A \tag{4-47}$$

where ΔY is a column vector of residuals defined as

$$y_i = (E_i - f_i), \tag{4-48}$$

ΔA is a column vector containing the corrections to the rotational constants and is given by

$$\Delta A = (\Delta a, \Delta b, \Delta c, \ldots, \Delta\nu_o), \tag{4-49}$$

and J is the matrix form by the derivatives $(\frac{\partial f_i}{\partial A'})$ and is termed the Jacobian. Since J is not, in general, a square matrix, both sides of equation (4-47) are left multiplied by the transpose of J. After some matrix manipulation, equation (4-47) reduces to

$$(J^t J)^{-1} J^t \Delta Y = \Delta A \tag{4-50}$$

which gives directly the corrections to the constants. If these corrections are added to the trial rotational constants, an improved set is obtained which is used in the calculation of further improvements to the new trial set. The procedure is continued until the correction to all the rotational constants is less than their standard deviations (defined in equation 4-56), in which case convergence is assumed.

The procedure of weighting each of the observables can be used to increase the stability and the rate of convergence of the least squares procedure. A diagonal matrix W is defined whose elements are

$$w_i = (1/P_i^2) \tag{4-51}$$

where P_i is an estimate of the precision of each of the observables, E_i. If two new matrices, X and Y, defined as

$$X = (J^t W J) \tag{4-52}$$

and

$$Y = (J^t W \Delta Y) \tag{4-53}$$

are introduced, then ΔA is given by

$$\Delta A = X^{-1} Y \tag{4-54}$$

A further advantage of weighting is that the overall standard deviation is defined as

$$\sigma = \mathrm{SQRT}\left(\sum_i^n w_i y_i^2/(n - m)\right) \tag{4-55}$$

where y_i, as before, is the value of the individual residuals, n is the number of observations and m is the number of fitting parameters. The numerical value of σ is an indication of the quality of the analysis. If model errors are small and if the estimate of the precision of the

observables is realistic, then σ will be approximately equal to 1. If the least squares analysis yields residuals that are consistently larger than the estimates of precision, then the value of σ will be greater than 1. The presence of unrealistic precision estimates or model errors, or both, is indicated. Values of σ which are less than 1 usually indicate that the precision estimates are too large.

Along with the overall standard deviation, a quantity δc_i, termed the standard deviation of the fitting constant c_i, is defined as

$$\delta c_i = \sigma \, \mathrm{SQRT}(X^{-1}_{ii}) \tag{4-56}$$

As stated previously, δc_i is the criterion of convergence.

An estimate of the degree of correlation between the constants c_i and c_j is obtained from the value of the correlation coefficients defined as

$$r_{ij} = (X^{-1})_{ij}/\mathrm{SQRT}((X^{-1})_{ii}(X^{-1})_{jj}) \tag{4-57}$$

If there is a near linear dependence of the fitting parameters, r_{ij} approaches ± 1.

A corrected and modified version of a prototype least squares programme obtained from Dr. D. Moule of Brock University was used to calculate both the ground state and excited state rotational constants of thioformaldehyde.

4.5 Some General Remarks Concerning the Rotational Levels of CH_2S

From the ground state rotational constants of CH_2S[4], a value of -0.992 is calculated for the asymmetry parameter κ. This value is close to that for a pure prolate symmetric top. If the upper state value of κ is also close to -1, then both B and C type bands of thioformaldehyde will

closely resemble perpendicular type bands ($\Delta K_{-1} = \pm 1$) of a prolate symmetric top. Type A bands are expected to be very similar to parallel type bands; they follow the selection rule $\Delta K_{-1} = 0$.

Since CH_2S is a near prolate symmetric top, the following shorthand notation has been adopted. Transitions with a constant value of K_{-1} in both excited and ground states form a group that is termed a sub-band. Each sub-band within the spectrum is designated by both a superscript P, Q or R designation, depending on whether $\Delta K_{-1} = -1$, 0 or +1, respectively, and a subscript designating the value of K_{-1} in the ground state. Since ΔJ may take the values of -1, 0 and +1, each sub-band will consist of a P, Q and R branch. Therefore, the total sub-band notation takes the form $^{\Delta K_{-1}}\Delta J_{K''_{-1}}(J'')$. For example, the designation $^{R}Q_7(8)$ would represent the following transition of a type B band:

Upper State			Lower State		
J	K_{-1}	K_{+1}	J	K_{-1}	K_{+1}
8	8	0	8	7	1
8	8	1	8	7	2

or, in a shorthand notation, 880 ← 871 and 881 ← 872. When the symmetric top designation is used for near prolate asymmetric tops, it always describes two possible transitions if K_{-1} is greater than zero. Although the use of these two systems of representation may seem redundant, the shorthand symmetric top notation is very convenient for describing the general features of the band.

4.6 The Ground State Rotational Constants of CH_2S

The rotational spectrum of CH_2S has been investigated in the microwave and millimeterwave region[1, 4]. As a consequence of the correlation be-

tween the rotational constant A and the distortion constant τ_{aaaa} ($\underline{a}$ = z), only their sum could be determined satisfactorily. However, very accurate values were calculated for the B and C rotational constants and the remaining determinable distortion constants. Johns and Olson found that by combining data collected from the high resolution infrared spectrum with that of the microwave spectrum, the correlation between these two constants was greatly reduced. Thus a complete rotational analysis of the ground state was obtained. However, the error associated with A and τ_{aaaa} still remained high since the determination of these constants depended on the relatively inaccurate data collected from the infrared spectrum.

When the ground state constants reported by Johns and Olson were used in the rotational analysis of the 4_0^1 band of CH_2S, several difficulties arose. Although the least squares fit was excellent for those transitions which involve values of K''_{-1} less than 4, the fit to transitions of higher K''_{-1} values was progressively poorer. In fact, the residuals of the individual lines of the R sub-bands in this region were all positive and ranged from 0.1 to 0.3 cm^{-1}. Attempts to fit those P sub-bands described by the same upper state K''_{-1} numbers as the previously-mentioned R sub-bands yielded consistently negative residuals. This type of behaviour of the residuals is not consistent with any type of excited state rotational level perturbations but could indicate the presence of a large systematic measurement error. In an attempt to reduce this, the high resolution visible electronic spectrum was rephotographed on Kodak type III F spectroscopic plates. These plates show a higher degree of tolerance to changes in humidity and temperature than does photographic film. In an effort to ensure the maximum possible accuracy of the calibration of the spectrum,

hollow cathode Fe-Ne emission lines were used exclusively in the calibration procedure. Even with these precautions, the least squares rotational analysis showed little change in the anomalous behaviour of the residuals. Since the travelling microscope was used extensively in the measurement of the spectrum, it was tested to ensure that the error associated with measurements obtained from this instrument was not larger than what is considered normal[48]. The results of the test indicated that the measurement error was random and sufficiently small and could not account for the large residuals of the least squares analysis.

Finally, the rotational assignment themselves were thought to be in error and consequently they were checked by forming combination differences of the form[25]

$$^{R}R_{K''_{-1}}(J) - {}^{R}Q_{K''_{-1}}(J) = {}^{P}Q_{K''_{-1}+2}(J+1) - {}^{P}P_{K''_{-1}+2}(J+1) \qquad (4\text{-}58)$$

When asymmetry splitting (see page 93) was observed, equation (4-58) was modified slightly through the adherence to type B selection rules to include the asymmetry split levels. It was found that for all assignments, except for those that included some badly overlapped lines, the equality held to within experimental measurement error.

The assignments were correct, which implied that the ground state rotational constants which were used in the analysis were slightly in error.

Improved values of the ground state rotational constants were therefore obtained by the method of "combination differences". Those transitions which share a common upper state rovibronic level are selected from the assigned transitions of the 4_0^1 band. The energy difference between the two transitions is calculated to yield a value that is essentially that

of a microwave transition from the ground state rotational level of the first transition to the ground state rotational level of the second. This procedure is illustrated in Figure 4-3(a) for the $^{R}R_{5}(5)$ and $^{P}P_{7}(7)$ pair of transitions. Since combination differences of this type involve the selection rule $\Delta K''_{-1} = 2$, these differences are very useful in reducing the correlation between A'' and τ''_{aaaa}.

The microwave transition frequencies were supplemented with transition frequencies obtained from combination differences which involve the selection rules $\Delta K''_{-1} = 0$ and $\Delta K''_{-1} = 2$, as described above. This yielded a comprehensive set of transition frequencies which were entered into the least squares programme to obtain accurate rotational constants for the ground state. The least squares computer programme is so structured, through the use of the weighting factors, so as to allow the mixing of the relative inaccurate combination differences with the highly accurate microwave data without the loss in accuracy of those rotational constants that can be determined from the microwave spectrum alone. The correlation between τ''_{aaaa} and A'' is significantly reduced by this procedure although the accuracy of these constants is still relatively low. A listing of the microwave transitions and combination differences used in the least squares determination of the ground state rotational constants of CH_2S is included in Appendix 1. Most of the differences used in the analysis are assigned a precision of ± 0.050 cm^{-1} while the precision of the microwave transitions is that reported by Beers *et al*[1].

A comparison of the ground state constants calculated by Johns and Olson with those obtained from the present least squares analysis is presented in Table 4-3. The new values of A'' and τ''_{aaaa} calculated using the

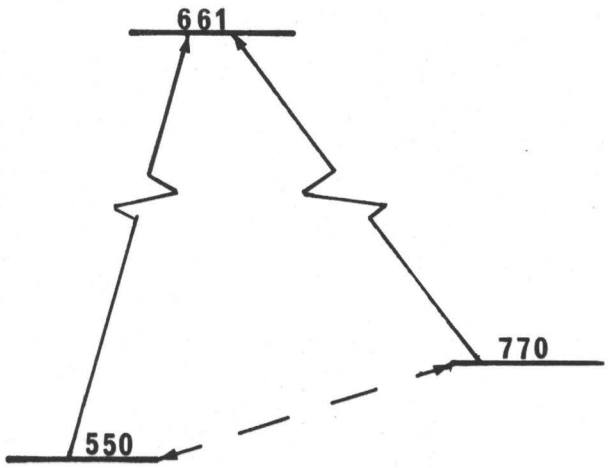

Figure 4-3(a). An illustration of the method used to calculate the ground state combination differences from U.V. data.

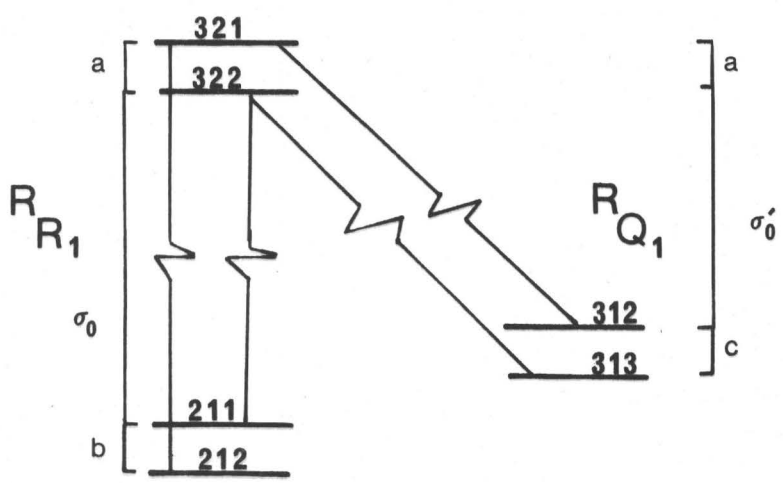

$$\delta = (\sigma(321 \leftarrow 212) - \sigma(322 \leftarrow 211)) + (\sigma(322 \leftarrow 313) - \sigma(321 \leftarrow 312))$$
$$= ((a + b + \sigma_0) - (\sigma_0)) + ((\sigma_0' + c) - (\sigma_0' + a))$$
$$= b + c$$

Figure 4-3(b). A graphical illustration of the combination differences defined in equation (4-63).

TABLE 4-3

A Comparison of the Ground State Rotational Constants of CH_2S

	Present Work		Johns and Olson[5]		
A	9.7302	± 0.00025	9.7311	± 0.0014	cm^{-1}
B	0.5903915	± 0.0000021	0.5903919	± 0.0000011	cm^{-1}
C	0.5554507	± 0.0000032	0.5554514	± 0.0000011	cm^{-1}
τ_{aaaa}	-333.	± 1.9	-480.	±59	$x10^{-5}$ cm^{-1}
τ_{bbbb}	-0.2942	± 0.0013	-0.2961	± 0.0022	$x10^{-5}$ cm^{-1}
τ_{cccc}	-0.2295	± 0.0013	-0.2311	± 0.0023	$x10^{-5}$ cm^{-1}
τ_1	-2.228	± 0.13	-7.927	± 0.089	$x10^{-5}$ cm^{-1}
τ_2	-0.2874	± 0.0076	-0.6250	± 0.0043	$x10^{-5}$ cm^{-1}
τ_3	83.42	± 0.001	88.57	± 0.70	$x10^{-5}$ cm^{-1}

$\sigma = 0.84$

data from the high resolution visible electronic spectrum are just outside the error limits of the values quoted by Johns and Olson. The distortion constants are reported as the "Watson determinable" constants, τ_{aaaa}, τ_{bbbb}, τ_{cccc}, τ_1, τ_2 and τ_3[43]. The relationship between these distortion constants and those of equations (4-37) and (4-39) for planar CH_2S is given in Table 4-4. If the equations of Table 4-2 are used in conjunction with those of Table 4-4, the ground state distortion constants may be given in terms of the symmetric top and asymmetric top distortion constants. The results are presented in Table 4-5. When these constants are used as the ground state rotational parameters in the analysis of the 4_0^1 band, the anomalous behaviour of the residuals is eliminated.

4.7 The Ground State Rotational Constants of CD_2S

The determination of the ground state rotational constants of CD_2S presents a slightly different problem than that encountered for CH_2S. Whereas all but two of the rotational constants of CH_2S were well determined from the microwave spectrum, only rough estimates of A", B" and C" existed for CD_2S[4]. However, a partial assignment of the 4_0^1 band of CD_2S is possible with the aid of these constants (see Section 4.8.2). From the assignments of the partially analysed band, the ground state combination differences are calculated. These values are combined with the accurate values of the four microwave transitions reported in the literature in a least squares analysis to yield initial values of the three ground state symmetric top distortion constants. All constants are then used as a guide to the complete assignment of the 4_0^1 band. Finally, combination differences calculated from the completely analysed band are combined with the microwave data, and a refined set of rotational and centrifugal distortion constants is then

TABLE 4-4

The Relationship Between τ_1, τ_2 and τ_3 and the Distortion Constants of Equation (4-39)

$$\tau_1 = \tau'_{aabb} + \tau'_{bbcc} + \tau'_{aacc}$$

$$\tau_2 = (C/S)\tau'_{aabb} - (A/S)\tau'_{bbcc} + (B/S)\tau'_{aacc}$$

$$\tau_3 = (S/B-A)\tau'_{aabb} + (S/C-B)\tau'_{bbcc} + (S/A-C)\tau'_{aacc}$$

$$S = A + B + C$$

For a planar ground state:

$$\tau_{bcbc} = 0.0$$

$$\tau_{acac} = 0.0$$

$$\tau_{abab} = \frac{B(B-C)}{2(A+B)(A-C)}\tau'_{aaaa} + \frac{A(A-C)}{2(A+B)(B-C)}\tau'_{bbbb} + \frac{AB}{2(A-C)(B-C)}\tau_1 - \frac{(A+B-C)S}{2(A-C)(B-C)}\tau_2$$

TABLE 4-5

The Ground State Rotational Constants of CH_2S Expressed in Terms of the Symmetric Top-Asymmetric Top Distortion Constants

$A = 9.7302\ cm^{-1}$	$D_K = 8.285 \times 10^{-4}\ cm^{-1}$	$R_5 = 1.27 \times 10^{-6}\ cm^{-1}$
$B = 0.59039\ cm^{-1}$	$D_{JK} = 3.87 \times 10^{-6}\ cm^{-1}$	$R_6 = -1.2 \times 10^{-8}\ cm^{-1}$
$C = 0.55545\ cm^{-1}$	$D_J = 6.295 \times 10^{-7}\ cm^{-1}$	$\delta_J = 3.8 \times 10^{-8}\ cm^{-1}$

obtained.

In order that the best set of ground state rotational constants is calculated for CD_2S, combination differences calculated from both the 4_0^1 and 5_0^1 bands are used in the least squares fit. The constants and overall standard deviation of 2.69 remain virtually unchanged over that derived from a least squares fit of differences calculated from the 4_0^1 band alone. The ground state rotational constants of CD_2S are listed in Table 4-6. A representative sample of the 1000 combination differences used in the analysis is presented in Appendix 1.

TABLE 4-6

The Ground State Constants of CD_2S

$A = 4.8821 \pm 0.00027\ cm^{-1}$	$D_K = 1.68 \times 10^{-4} \pm 2.0 \times 10^{-6}\ cm^{-1}$
$B = 0.48715 \pm 0.0000044\ cm^{-1}$	$D_{JK} = 1.02 \times 10^{-5} \pm 6.3 \times 10^{-7}\ cm^{-1}$
$C = 0.45017 \pm 0.0000044\ cm^{-1}$	$D_J = 7.2 \times 10^{-8} \pm 7.9 \times 10^{-8}\ cm^{-1}$

Only three of the six distortion constants are reported for CD_2S. It is felt that because the accuracy of the combination differences calculated from the rovibronic transitions is low and since so few microwave transitions could be included in the fitting procedure, only six constants can be reliably varied. The omission of the three asymmetric rotor distortion constants, whose magnitude is expected to be quite small, will not seriously affect the rotational analysis of the vibronic bands of CD_2S.

4.8 The Perpendicular Bands of Thioformaldehyde

4.8.1 The 4_0^1 Band of CH_2S

The band centered at approximately 5965 Å and which extends some 150 cm^{-1} to either side of the origin region is assigned to the 4_0^1 transition

of CH_2S. The overall appearance of the band is that of a perpendicular type band of a prolate symmetric rotor (see Figure 4-4). The band is composed of a P sub-band region ($\Delta K_{-1} = -1$) and an R sub-band region ($\Delta K_{-1} = +1$) which extend to the red and to the blue, respectively, of the origin. Although each sub-band is composed of a P, Q and R branch, theoretical intensity calculations indicate that the P branch of the R sub-bands and the R branch of the P sub-bands with $K''_{-1} \geq 3$ are of very low intensity. These branches are not experimentally observed. The most prominent feature of the band is the very intense lines which appear to the blue of the origin and which are positioned at roughly equal intervals from each other. These lines are due to the formation band heads within the R branch ($\Delta J = +1$) of each R sub-band. Consequently, the R branches of each sub-band are easily identified.

If, for the moment, the molecule is assumed to be a rigid symmetric top, then an estimate of the value of the excited state rotational constants A' and $\overline{B}'$, is possible. Application of equation (4-20) to the excited and ground states of CH_2S yields as the energy expressions for the sub-band origins

$$\sigma_o^{sub} = \sigma_o' + (A'-\overline{B}') \pm 2(A'-\overline{B}')K''_{-1} + \{(A'-\overline{B}') - (A''-\overline{B}'')\}K''^{2}_{-1} \quad (4\text{-}59)$$

where the plus sign refers to the R sub-bands and the minus sign to the P sub-bands. $\overline{B}$ is defined as

$$\overline{B} = (B + C)/2 \quad (4\text{-}60)$$

By forming the second differences between the frequencies of successive R branch band heads of the R sub-bands a value for the parameter $\{(A'-\overline{B}') - (A''-\overline{B}'')\}$ or $\Delta(A-\overline{B})$ is obtained.

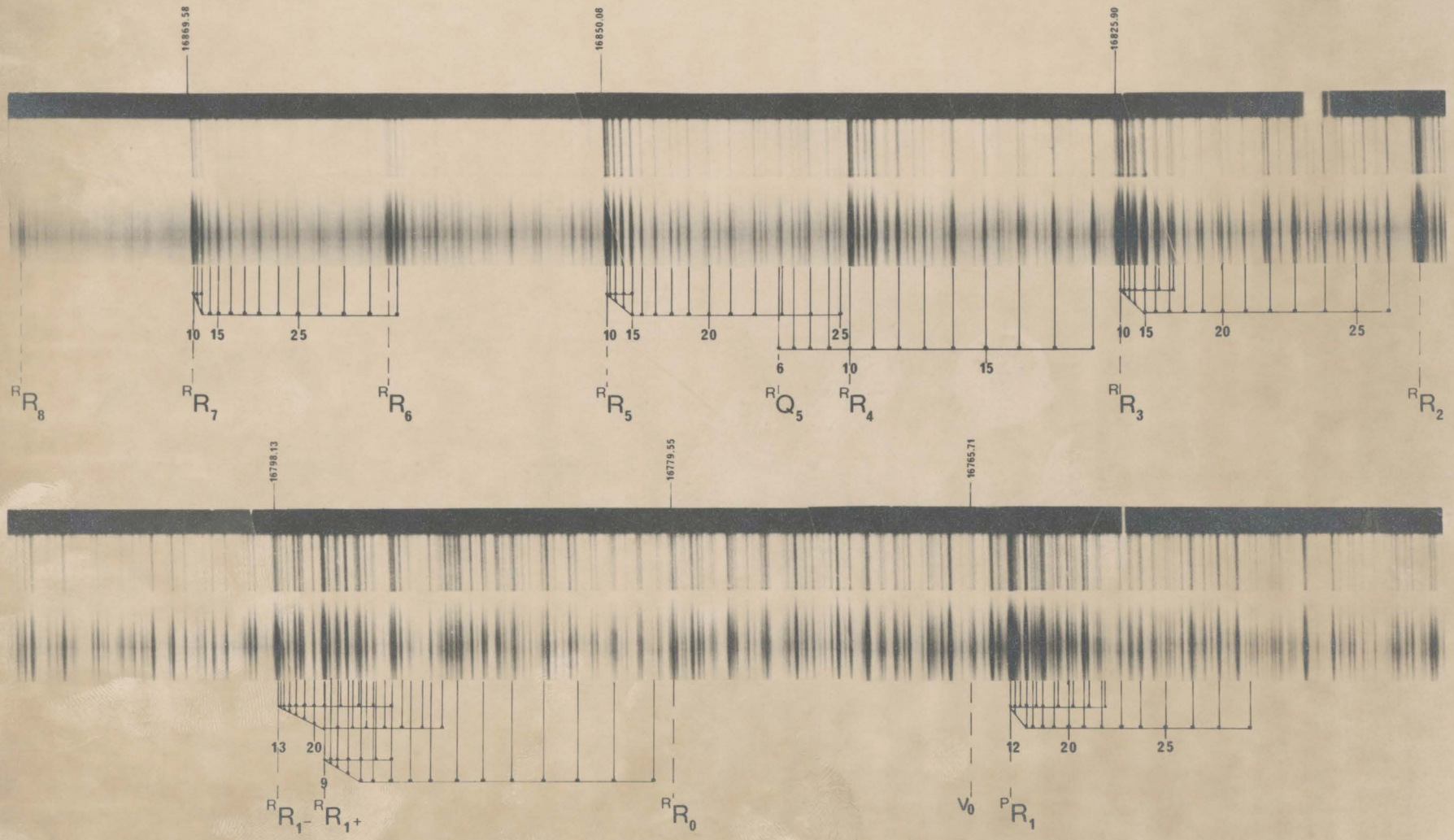

Figure 4.4 The R sub-bands of the 4_0^1 band of CH_2S

Since the values of K''_{-1} and K'_{-1} are constant within any one sub-band, the energy expressions for the R branches can be written as

$$\sigma_R = \sigma_o^{sub} + 2\bar{B}' + (3\bar{B}' - \bar{B}'')J'' + (\bar{B}' - \bar{B}'')J''^2 \qquad (4\text{-}61)$$

As the coefficient of J^2 in the energy expression for the P and Q branches is identical to that of equation (4-61), values of $\Delta\bar{B}$ are obtained by calculating the second differences for the J structure of any branch in the band excluding those branches which originate from the central region of the band ($\Delta K_{-1} < 3$). In the case of CH_2S, a reliable estimate of $\bar{B}'$ is obtained by averaging the $\Delta\bar{B}$ values and by adding this quantity to that of $\bar{B}$ of the ground state. Since values for A'', $\bar{B}''$ and $\bar{B}'$ are known, A' is also calculable.

The value of J corresponding to the band head of R branches (J_{rev}) can be calculated if the magnitude of both the upper and lower state $\bar{B}$'s is known. The expression for J_{rev} is derived by differentiating equation (4-61) with respect to J and setting the derivative equal to zero, i.e.,

$$J''_{rev} = (\bar{B}'' - 2\bar{B}')/2\Delta\bar{B} \qquad (4\text{-}62)$$

For the 4_0^1 band of thioformaldehyde, J_{rev} is calculated to occur at J'' = 10.

The values of $\bar{B}'$ and $\bar{B}''$ may also be used to give an initial estimate of the number of transitions that comprise the R branch band heads. If these values are substituted into equation (4-61), then the transitions which originate from the J'' = 9, 10 and 11 levels are calculated to occur within the observed linewidth of the heads. The same conclusion is also reached by comparing the relative intensity of the head with respect to

the R branch line nearest to the head. Calculations indicate that if K is not too large (≤ 8 for the 4_0^1 band), then this line contains only two R branch transitions. In general, these two transitions give this line a slightly narrower linewidth and slightly weaker intensity than that of the band head. Final confirmation of the number of transitions that comprise the band heads is obtained from the combination differences (see below) calculated for the band. Once the J'' numbering within the R heads is established, the J assignments of the remaining members of the branch is straightforward.

The K''_{-1} numbering of the R branches of the R sub-band region is assigned by noting that the first member of the R branch of the sub-band must always correspond to $J'' = K''_{-1}$, and that the ground state nuclear statistics of CH_2S necessitate that the sub-bands of odd K''_{-1} be three times more intense than those of even K''_{-1}. Consequently, the ${}^{R}R_{K''_{-1}}(J)$ assignment of that portion of the spectrum that can be adequately fitted to the symmetric rotor energy expression is established (i.e., the symmetric rotor portion of the band).

The preliminary assignments obtained above are then used to calculate an improved set of symmetric top rotational constants for the band. The assignments along with the approximate values for A' and $\overline{B}'$ calculated previously together with initial estimates for the distortion constants (D_K, D_{JK} and D_J) and ν_o are entered as data into the least squares programme. The assignments of the ${}^{R}R_{K''_{-1}}$ branches of the 4_0^1 band of CH_2S yields an acceptable set of symmetric top rotational constants, and an overall standard deviation (σ) of approximately 2 to 3. The improved constants are then used as a guide in assigning the ${}^{P}P_{K''_{-1}}$, ${}^{P}Q_{K''_{-1}}$, ${}^{R}Q_{K''_{-1}}$

($K''_{-1} \geq 3$) branches of the symmetric rotor portion of the absorption band. All the assignments are verified by constructing combination differences of the form of equation (4-58). Finally, the new assignments are included in the least squares programme in order to calculate the best set of symmetric top rotational and distortion constants.

A decision must be made as to whether the perpendicular type band is polarized about the b or c axis before an attempt can be made to assign that portion of the band that can only be accurately described by the energy expressions of the asymmetric rotor. The asymmetric rotor portion of the band comprises those transitions of low K''_{-1} values for which the asymmetry splitting of the upper and lower states is sufficiently large that the two transitions of equal J'' and K''_{-1} numbers form two resolved lines in the spectrum.

The band polarizations are determined by a partial band contour analysis. The method involves the use of the ground state values of A, B and C and the excited state value of the A rotational constant, as calculated from the least squares analysis, together with arbitrary values of B' and C'. The values of B and C are restricted in that their sum ($\overline{B}$ x 2) must be equal to that obtained from the least squares analysis. Type B and C band contours are then generated by the computer for each of the chosen sets of excited state rotational constants. It is found that the two types of perpendicular band contours are very nearly identical to each other except in the region about the origin, where C-type bands show a marked decrease in intensity while B-type bands maintain a strong intensity throughout the entire region. A similar conclusion has also been reached by Callomon and Innes[22] for the perpendicular type bands

of CH_2O. By comparing the experimental contours of the 4_0^1 band of CH_2S to those generated by the computer, the transition is shown to be polarized about the b axis.

The identification and assignment of the asymmetry split transitions depends on the fact that the asymmetry splitting increases as J increases (for constant K_{-1}). A sub-band is chosen whose members of low J are adequately described by the energy expressions of a prolate symmetric top but whose members of higher J quantum numbers can only be described in terms of the asymmetric top energy expressions. The lines of low J can be easily identified; as J increases, the lines within these bands become progressively broader until they are split into two components. By keeping track of the J quantum number throughout this procedure, the assignment of this quantum number for the asymmetry split lines is possible. The higher energy asymmetry split line must correspond to the $\Delta K_{+1} = -1$ transition regardless of the degree of asymmetry splitting in the ground state (as illustrated in Figure 4-3(b) for the ${}^{R}R_1(2)$ transitions).

With these preliminary assignments, values for all the rotational constants are then calculated. The new set of asymmetric rotor constants is used as an aid in assigning the remaining portions of the spectrum. At this point, the assignments of the asymmetry split lines may be verified by calculating the combination differences,

$$\delta^{R}R_{K''_{-1}}(J) + \delta^{R}Q_{K''_{-1}}(J+1) \quad \text{or} \quad \delta^{P}P_{K''_{-1}}(J) - \delta^{P}Q_{K''_{-1}}(J-1) \qquad (4\text{-}63)$$

where δ is the asymmetry splitting of the two lines and is defined as the difference between the energy of the higher frequency line and the lower frequency line of the asymmetry split pair of transitions. In calculating

the combination differences listed above, the sum of the asymmetry splittings between the two ground state levels is calculated (see Figure 4-3(b)). These differences must agree, to within experimental error, with the sum of the asymmetry splitting calculated from the microwave data. Inspection of Table 4-7, in which the differences calculated from the 4_0^1 band are contrasted with the values of the asymmetry splitting from the microwave data[1], shows that the agreement is satisfactory.

The assignments may also be checked without the aid of the microwave data by calculating the combination differences of equation (4-58) for each of the asymmetry doublets. The agreement for all but a few heavily overlapped lines is well within experimental error.

A listing of the results of the least squares rotational analysis of the 4_0^1 band of CH_2S is presented in Appendix 1. Values of the rotational constants, band origin and overall standard deviation (σ) calculated from the analysis are given in Table 4-8. As in the case of the determination of the ground state constants of CD_2S, only three of the six distortion constants are reported, for reasons identical to those stated previously.

A final check of the assignments is possible by comparing the observed band contour with that generated by the computer using the excited state rotational constants calculated from the least squares analysis. To this end, a band contour computer programme, originally written by Parkin[49], was modified to include the three symmetric top distortion constants in its calculations. The region about the origin of the calculated and observed spectrum is contrasted in Figure 4-5. The agreement is excellent.

4.8.2 <u>The 4_0^1 Band of CD_2S</u>

The procedure for assigning the perpendicular type 4_0^1 band of CD_2S

TABLE 4-7

The Asymmetry Doubling Sums Obtained from the Visible and Microwave Data of CH_2S

Ground State Levels					4_0^1	Microwave
J	K_{-1}		J	K_{-1}	(cm^{-1})	(cm^{-1})
4	1	+	3	1	0.63	0.56
5	1	+	4	1	0.80	0.87
6	1	+	5	1	1.32	1.26
7	1	+	6	1	1.72	1.71
8	1	+	7	1	2.19	2.23
9	1	+	8	1	2.89	2.83
10	1	+	9	1	3.55	3.49
11	1	+	10	1	4.24	4.22
16	2	+	15	2	0.54	0.48
17	2	+	16	2	0.60	0.68
18	2	+	17	2	0.76	0.86
19	2	+	18	2	1.08	1.10

TABLE 4-8

The Excited State Rotational Constants of the 4_0^1 Band of CH_2S

$A = 9.0601 \pm 0.00026\ cm^{-1}$ $\quad D_K = 4.37 \times 10^{-4} \pm 2.7 \times 10^{-6}\ cm^{-1}$

$B = 0.53763 \pm 0.000053\ cm^{-1}$ $\quad D_{JK} = 1.14 \times 10^{-5} \pm 5.8 \times 10^{-7}\ cm^{-1}$

$C = 0.51026 \pm 0.000053\ cm^{-1}$ $\quad D_J = 6.65 \times 10^{-7} \pm 6.5 \times 10^{-8}\ cm^{-1}$

$\nu_o = 16765.71 \pm 0.01\ cm^{-1}$

$\sigma = 2.25$

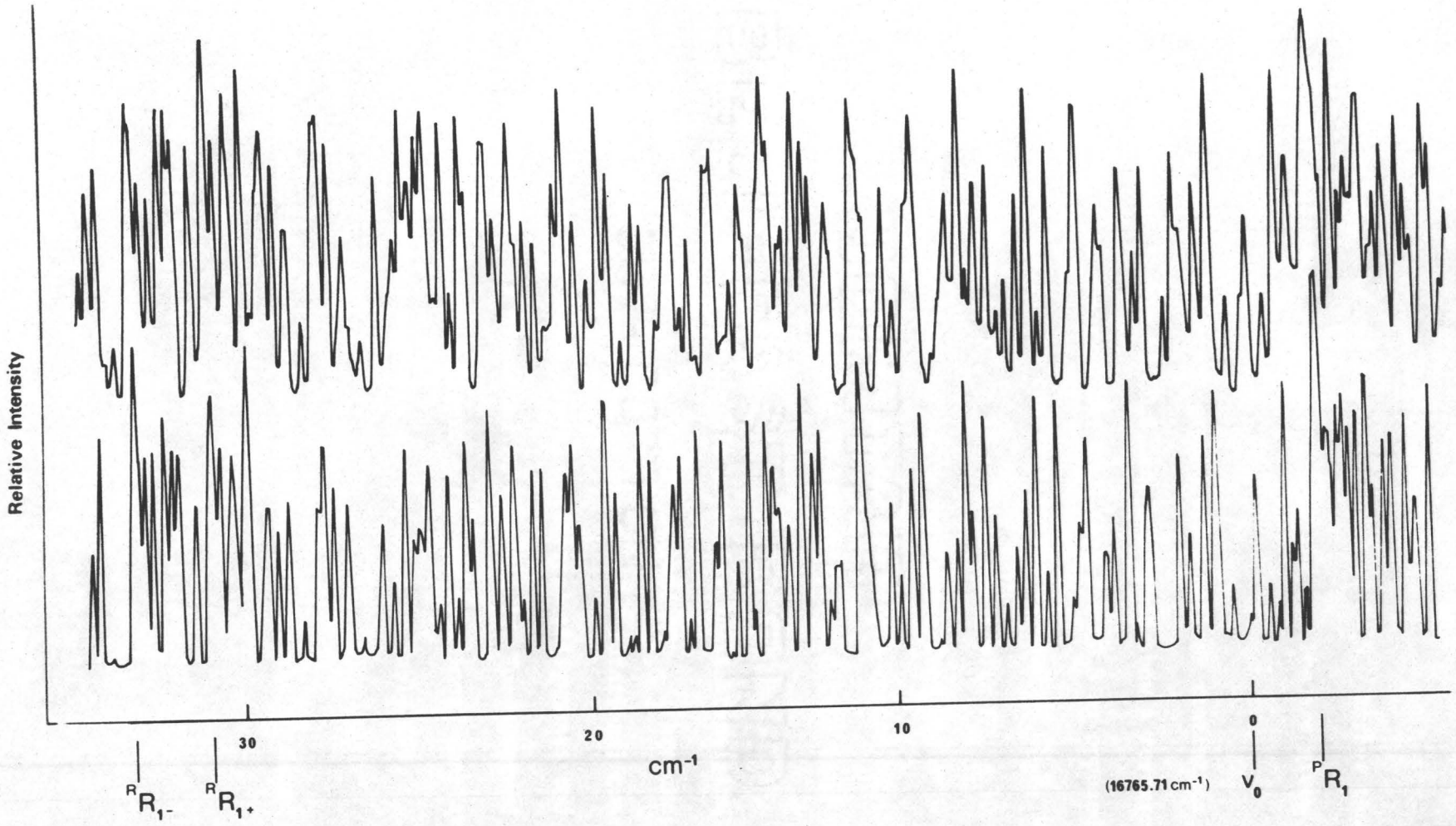

Figure 4.5 The observed (upper) and calculated contours of the 4_0^1 band of CH_2S.

parallels that for the corresponding band of CH_2S. Rather than reiterating the general assignment procedures, only the results are given in the following.

Because of the different ground state nuclear statistics of the (A_1A_2), (B_1B_2) rovibronic levels of CD_2S, the sub-bands show a reversed intensity alternation to that observed for CH_2S (6:3 for CD_2S as opposed to 1:3 for CH_2S (see Figure 4-6)). In contrast to the 4_0^1 band of CH_2S, the $^RR_{K''_{-1}}$ band heads are observed up to $K''_{-1} = 12$. Those heads with $K''_{-1} \leq 10$ consist of four transitions, the first of which originates from the J" = 10 level. The band is identified as type B since the origin region of the experimental contour shows no large decrease in intensity. A C-type band contour shows a marked intensity decrease.

The experimentally resolvable asymmetry split transition are observed and assigned in the $^RR_{2,1}$, $^RQ_{2,1}$, $^PP_{4,3,2}$ and $^PQ_{4,3,2}$ branches. This allows a separate determination of the B and C rotational constants. A listing of the vacuum wavenumbers, rotational assignments and residuals of the 4_0^1 band of CD_2S is presented in Appendix 1. The observed and calculated contours are contrasted in Figure 4-7. The rotational constants calculated from the least squares analysis are reported in Table 4-9.

TABLE 4-9

The Excited State Rotational Constants of the 4_0^1 Band of CD_2S

$A = 4.6197 \pm 0.000093\ cm^{-1}$	$D_K = 1.13 \times 10^{-4} \pm 1.7 \times 10^{-6}\ cm^{-1}$
$B = 0.45777 \pm 0.000023\ cm^{-1}$	$D_{JK} = 1.36 \times 10^{-5} \pm 1.7 \times 10^{-7}\ cm^{-1}$
$C = 0.41872 \pm 0.000023\ cm^{-1}$	$D_J = 1.75 \times 10^{-7} \pm 2.2 \times 10^{-8}\ cm^{-1}$

$$\nu_o = 16758.83 \pm 0.01\ cm^{-1}$$

$$\sigma = 1.8$$

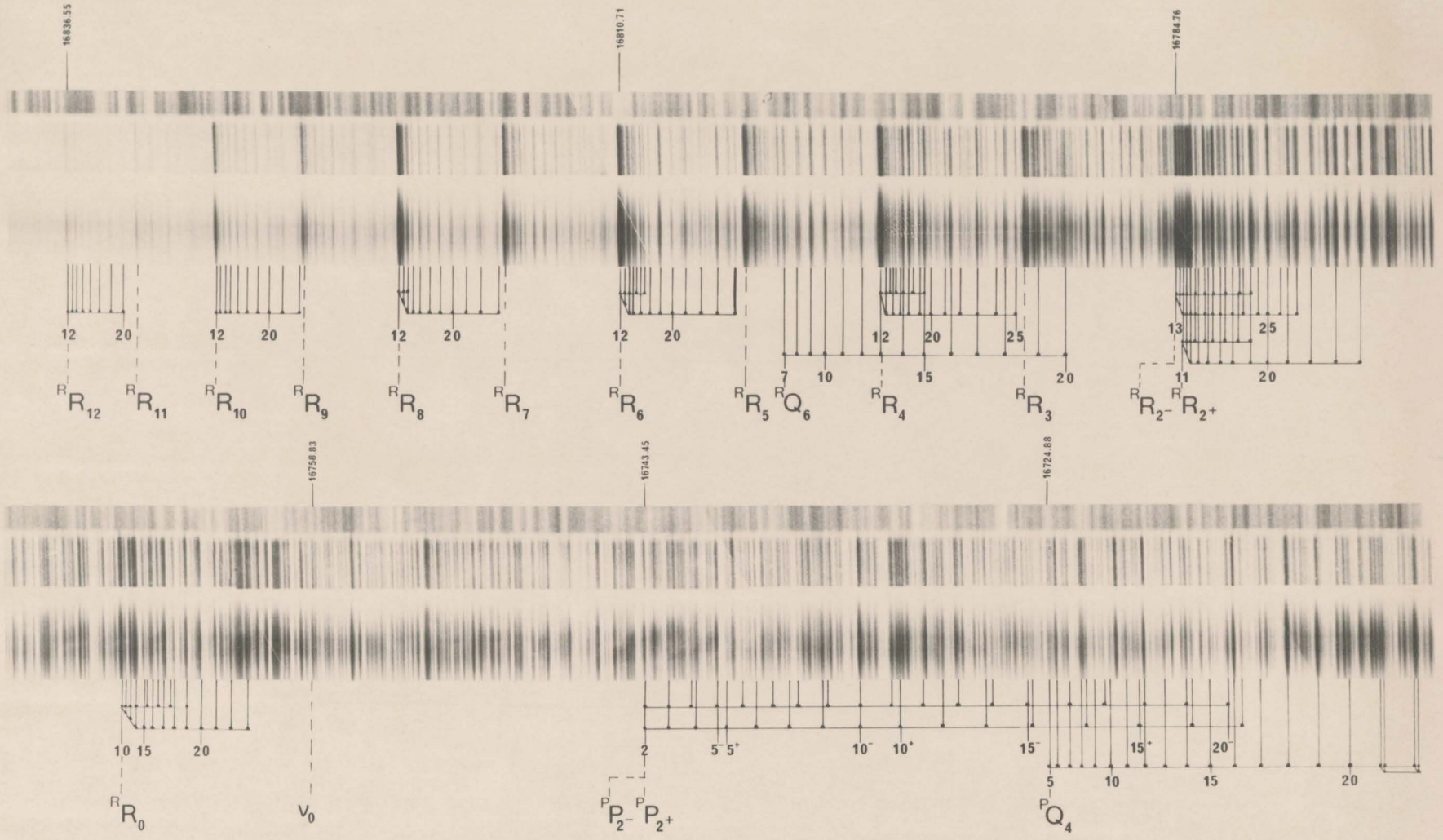

Figure 4.6 The major portion of the 4_0^1 band of CD_2S

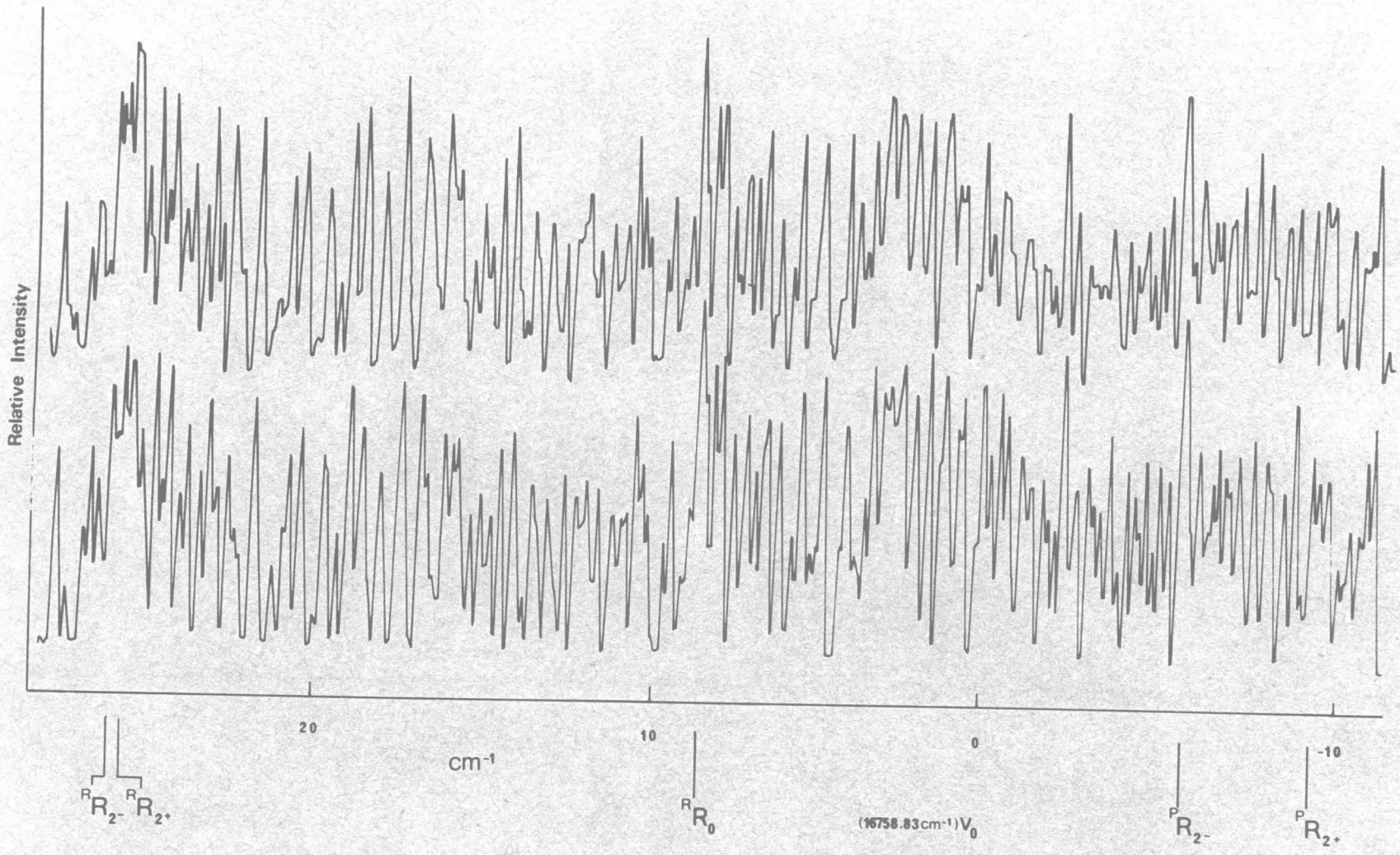

Figure 4.7 Comparison of the observed (upper) and calculated contours of the 4_0^1 band of CD_2S.

4.8.3 The 5_0^1 (Type C) Band of CD_2S

The main feature of the 5_0^1 (type C) band, reproduced in Figure 4-8, which distinguishes it from the two previously analysed perpendicular bands, is the marked decrease in intensity observed about the central region. This is illustrated by Figure 4-9, which shows the origin region of the 4_0^1 (type B) and the 5_0^1 (type C) bands of CD_2S.

Sub-bands with $K''_{-1} \geq 3$ are adequately described by the energy expressions for a perpendicular type band of a prolate symmetric top. Thus the procedure used to determine the assignments of the sub-bands in this region parallels that used in the assignment of the 4_0^1 band of CD_2S. However, because of the different value of $\overline{B}$, the R branch band heads consist of three transitions which originate from the J'' = 10, 11 and 12 levels.

The assignment of the asymmetry split transitions in the P and R sub-bands is straightforward. After the assignments are verified in the usual manner, a least squares analysis is performed (Appendix 1). As a final check, the rotational constants of the 5_0^1 band, listed in Table 4-10, are used to construct a theoretical band contour which is then compared to the experimentally observed contour (Figure 4-10).

TABLE 4-10

The Excited State Rotational Constants of the 5_0^1 Band of CD_2S

$A = 4.6886 \pm 0.00020\ cm^{-1}$ $\quad D_K = 1.70 \times 10^{-4} \pm 2.3 \times 10^{-6}\ cm^{-1}$

$B = 0.45743 \pm 0.000029\ cm^{-1}$ $\quad D_{IJ} = 1.39 \times 10^{-5} \pm 3.1 \times 10^{-7}\ cm^{-1}$

$C = 0.41642 \pm 0.000027\ cm^{-1}$ $\quad D_J = 2.67 \times 10^{-7} \pm 2.8 \times 10^{-8}\ cm^{-1}$

$\nu_o = 18808.35 \pm 0.01\ cm^{-1}$

$\sigma = 2.2$

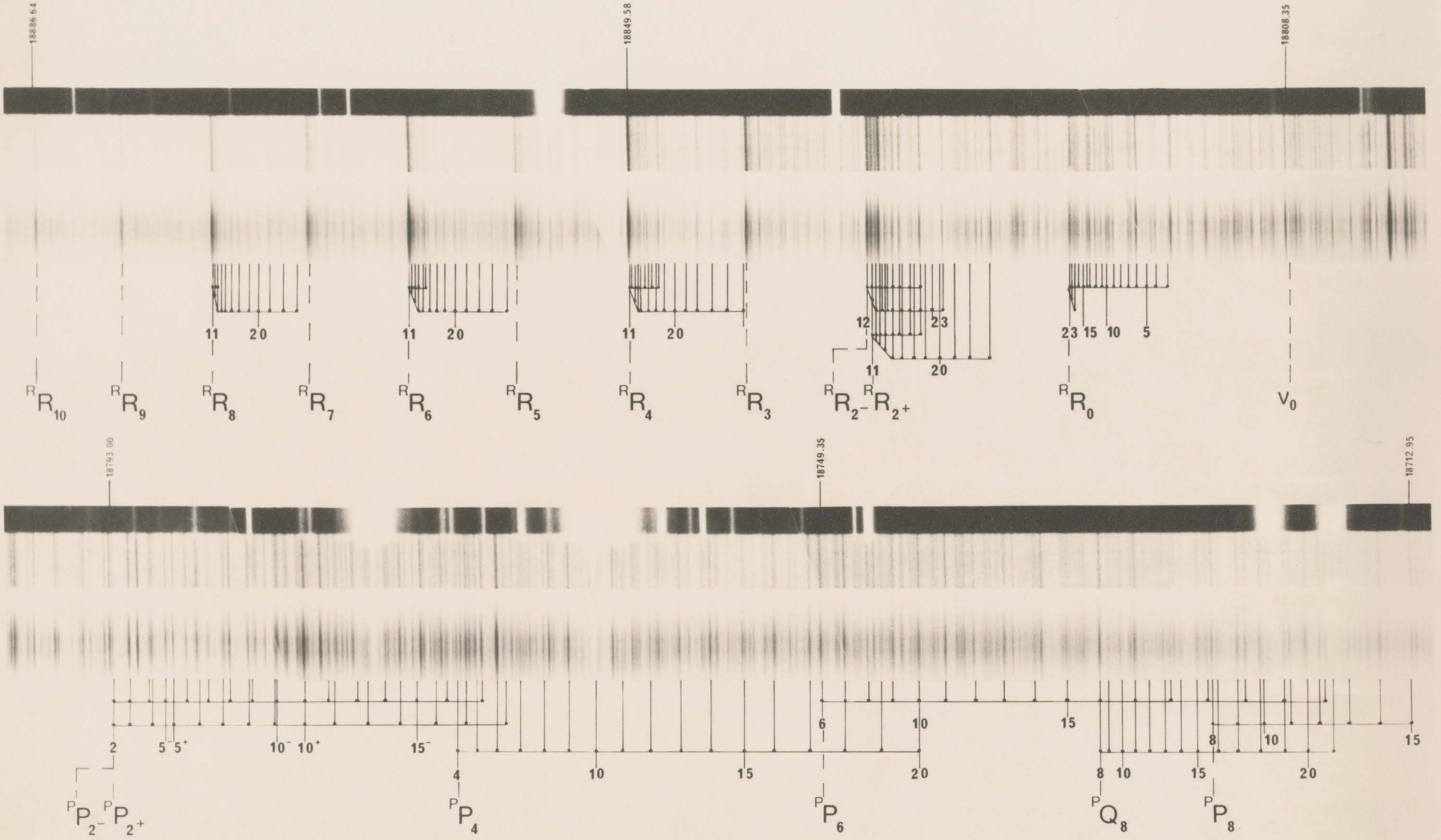

Figure 4.8 The 5_0^1 (C−type) band of CD_2S

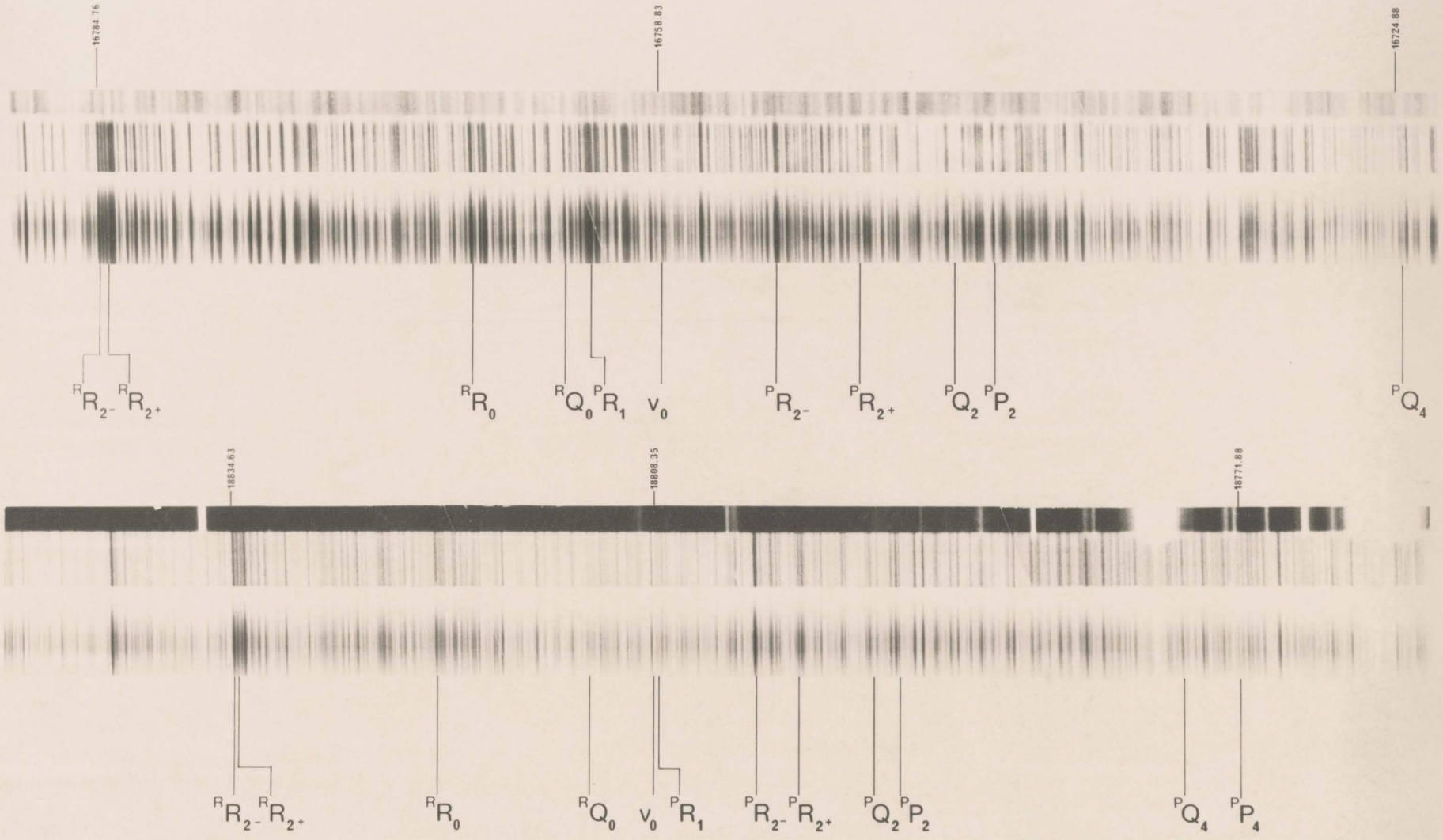

Figure 4.9 Comparison of the central regions of the 4_0^1, B–Type (upper) and 5_0^1, C–Type (lower) bands of CD_2S.

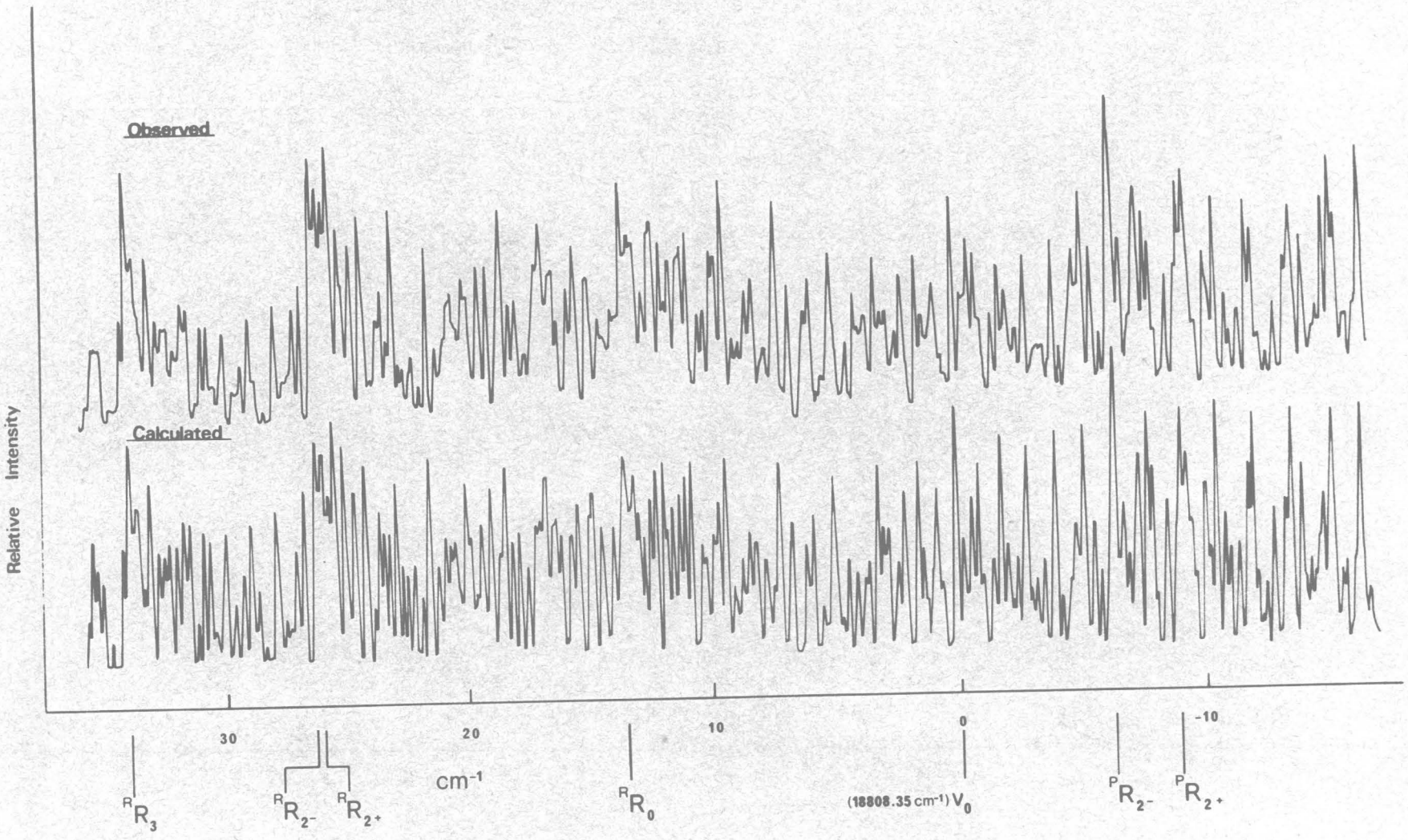

Figure 4.10 C–Type band contours of the 5_0^1 band of CD_2S.

The 5_0^1 band of the normal isotope (CH_2S) is overlapped in its lower energy region and attempts at a complete rotational analysis have been unsuccessful. The results of a partial rotational analysis indicate that the band is slightly perturbed in both the K and J structure. The only information that is readily obtained from the band is the direction of polarization (type C), as established by band contour methods.

4.8.4 The $3_0^1 4_0^3$ Band of CH_2S

Under low resolution, the $3_0^1 4_0^3$ band has the appearance of a strong A-type band. When photographed on the Ebert spectrograph, the band still retains its parallel-like appearance with a sharp head at 18608.89 cm^{-1} (see Figure 4-11). This type of head formation at the highest frequency of the band has been observed in the previously analysed A-type bands of the system (see Section 4-9). Therefore, the band was originally thought to be polarized about the a axis. However, attempts to confirm this hypothesis by either least squares or band contour methods ended in failure. Consequently, the band must be assigned as either a B or C type band. The anomalous appearance may be explained as follows.

Just as the R branches of the spectral bands of CH_2S form a head at a particular value of J, the R sub-bands of a perpendicular type band may themselves form a head at a particular value of K''_{-1}. The ground state value of K''_{-1} at which the head of heads forms is given by the expression

$$K''_{rev} = -(A' - \bar{B}')/\Delta(A - \bar{B}) \simeq -A'/\Delta A \qquad (4\text{-}64)$$

which can be obtained by differentiating equation (4-59) with respect to K''_{-1}. For light molecules such as CH_2S, K reversal is expected to be observable only if $\Delta(A - \bar{B})$ is very large or, since ΔB is small, if ΔA is

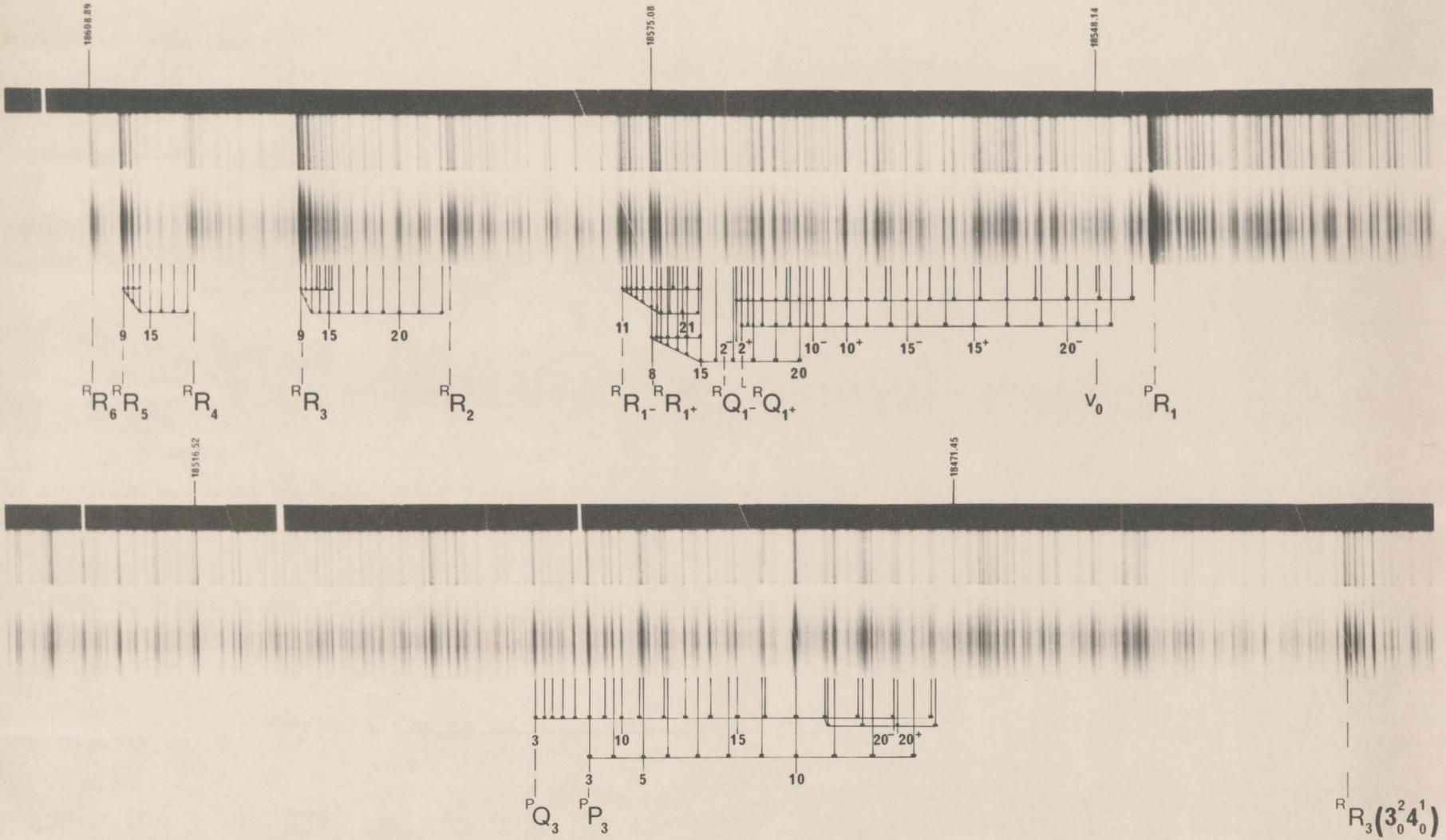

Figure 4.11 The $3_0^1 4_0^3$ (Type B) band of CH_2S. Due to the large value of ΔA, K reversal is observed at $K''_{-1} = 6$.

very large. Since the previously analysed perpendicular type band showed a small change in A, the head of heads is not experimentally observable because the intensities of transitions to these high energy rotational levels are extremely low. However, if the second differences of the R branch band heads are calculated for the $3_0^1 4_0^3$ band of CH_2S, a value of $\sim$1.30 cm^{-1} is calculated for ΔA. Thus, K_{rev} is calculated to occur between K''_{-1} = 6 and 7 and is expected to be experimentally observable. Analysis of the band has verified that the head of heads at 18608.89 cm^{-1} can be assigned to the $^RR_6$ transition.

The assignment of the spectrum proceeds in the usual fashion for those transitions whose upper state K'_{-1} designation is equal to or greater than two. In analysing the $3_0^1 4_0^3$ band instead of the overlapped 4_0^3 band, whose R sub-band region is of almost identical appearance, higher J'' and K''_{-1} assignments within the P sub-band region of the $3_0^1 4_0^3$ band were possible. Nonetheless, assignments within the P sub-bands of the $3_0^1 4_0^3$ band are limited to transitions which originate from levels with $K''_{-1} \leq 3$.

As with other perpendicular bands, the band type is established by contour methods. These predict a type B band should have a distinct, high intensity $^PR_1$ band head at 18545 cm^{-1}, and this is indeed observed. The intensity of this head in a calculated type C band contour is considerably less and this settles the assignment of the band as type B.

The experimentally resolvable symmetry split transition can be observed and assigned in the $^RR_1$, $^RQ_1$, $^RP_1$, $^PP_3$ and $^PQ_3$ branches. Thus a separate determination of the B and C rotational constants is possible. Even with the limitations arising from overlap of the P sub-band region, the assignments reported in Appendix 1 for the $3_0^1 4_0^3$ band yield reliable

values for the three rotational and three distortion constants listed in Table 4-11.

Inclusion of transitions to levels with K'_{-1} = 0, 1 and 7 in the least squares analysis resulted in a substantial increase in the overall standard deviation (σ) of the fit. Indeed, the residuals of these lines are found to increase dramatically as J increased. Thus, the presence of a perturbation in the band is indicated. If the more severely perturbed lines are omitted in the analysis, the rotational constants listed in Table 4-11 are obtained. The presence of a perturbation within this band is further indicated by the negative value of the D'_K distortion constant, as calculated from the fit to the slightly perturbed levels ($2 \leq K'_{-1} \leq 6$). This anomalous behaviour of the distortion constant has also been observed for those bands of CH_2O that are known to be perturbed[50]. A discussion of the nature of the perturbation present in the $3_0^1 4_0^3$ band of CH_2S is given in a subsequent section. However, even though the perturbation is present, it is felt that the rotational constants are well determined, as indicated by the satisfactory agreement between the observed and calculated contours of Figure 4-12.

TABLE 4-11

The Excited State Rotational Constants of the $3_0^1 4_0^3$ Band of CH_2S

$A = 8.309 \pm 0.0014\ cm^{-1}$	$D_K = -1.02 \times 10^{-3} \pm 3.5 \times 10^{-5}\ cm^{-1}$
$B = 0.5294 \pm 0.00025\ cm^{-1}$	$D_{JK} = 8.7 \times 10^{-6} \pm 1.7 \times 10^{-6}\ cm^{-1}$
$C = 0.5112 \pm 0.00027\ cm^{-1}$	$D_J = 7.2 \times 10^{-7} \pm 7.8 \times 10^{-8}\ cm^{-1}$

$\nu_o = 18548.17 \pm 0.01\ cm^{-1}$

$\sigma = 2.58$

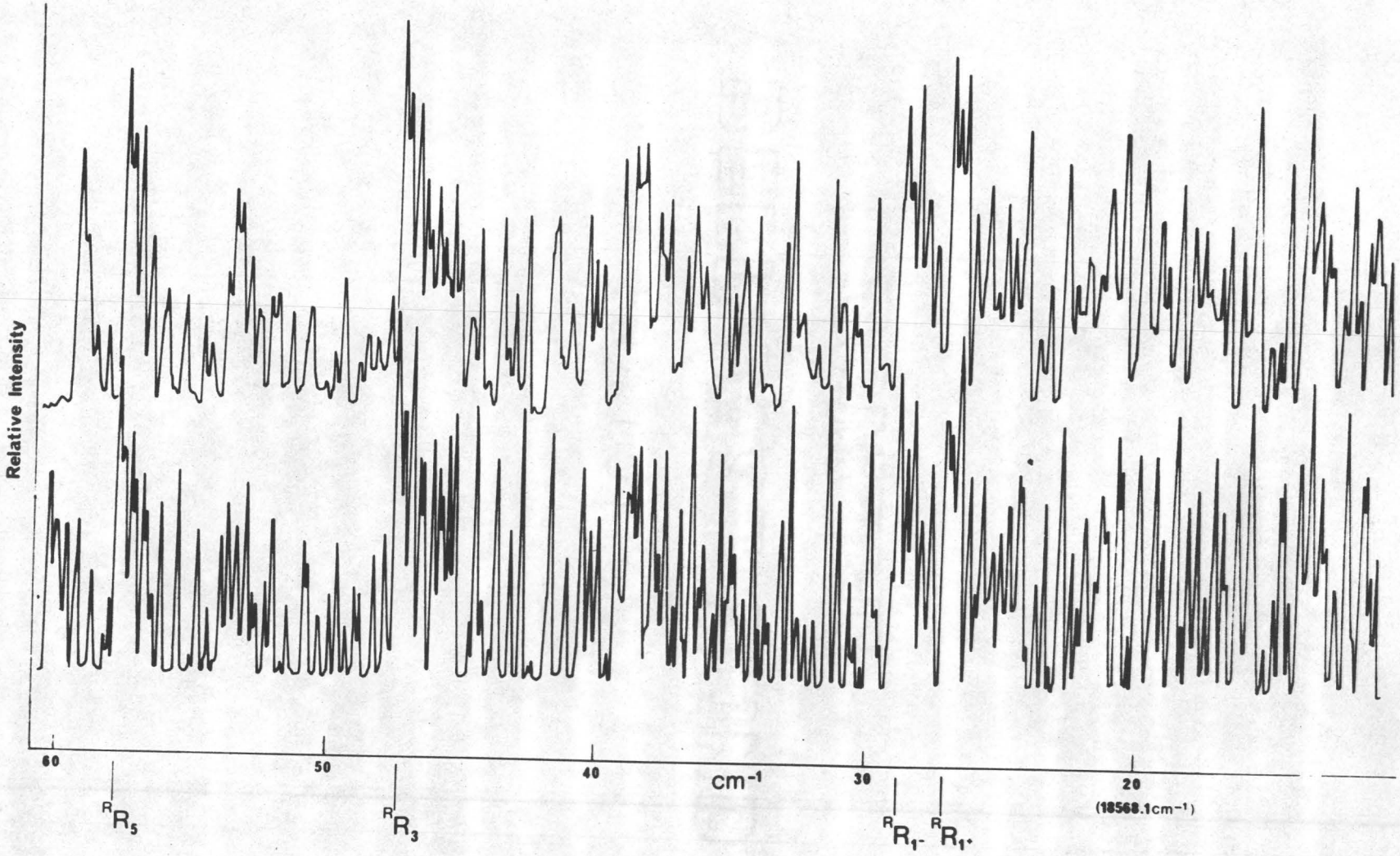

Figure 4.12 The observed (upper) and calculated contours of the $3_0^1 4_0^3$ band of CH_2S.

4.9 The Parallel Bands of Thioformaldehyde

4.9.1 Coriolis-induced Transitions vs Magnetic Dipole Allowed Transitions

In Chapter 2, it was shown that electric dipole transitions, forbidden by electronic selection rules, may acquire a non-zero intensity via the mechanism of vibronic coupling. Further, it was shown that the origin band of the $^1A_2 \leftarrow {}^1A_1$ electronic transition, as well as transitions of the type 2_0^1, 4_0^2, etc., would have zero intensity even if this mechanism could occur. But such bands are observed in the spectrum and the question arises as to how they acquire intensity.

Herzberg has shown that vibronically forbidden transitions may also acquire intensity through electronic-rotational interactions, which for H_2CS would couple the $^1A_2$ state with higher energy states that can electronically combine with the $^1A_1$ ground state in electric dipole transitions. The restrictions are that interactions can occur only between levels of the same J values and the same overall rovibronic species. The derivation of these selection rules for electronic-rotational interaction parallels the development of the selection rules for vibrational-rotational interaction presented in Section 4.11.1. Only the general results are presented here.

If the interacting state is of A_1 electronic symmetry, then rotation about the z axis can cause mixing with a $^1A_2$ state. This type of interaction follows the selection rule $\Delta K_{-1}^{INT} = 0$. Since the J^{th} rotational levels of the two $K_{-1} = 0$ interacting levels are of different rovibronic symmetry, interaction between the $K_{-1} = 0$ levels of A_1 and A_2 vibronic states is forbidden. Thus, vibronically forbidden transitions made allowed by this mechanism result in bands whose overall appearance is that of a vibronically allowed type A band but with the $K' = 0 \leftrightarrow K'' = 0$ transition absent. Fur-

ther, an anomalous intensity distribution in the K structure is also expected[51].

Interactions of the $^1A_2$ state with higher excited states of either B_1 or B_2 electronic symmetry will follow the selection rule $\Delta K_{-1}^{INT} = \pm 1$. This mechanism will allow interactions with the K' = 0 level of the $^1A_2$ state. The selection rules for transition from the $^1A_1$ ground state will follow $\Delta K_{-1} = 0, \pm 2$ with the further restriction that the $^PP_0$ and $^QR_0$ branches are absent. The band is also expected to show an anomalous intensity distribution in the J structure.

Classically, an oscillating magnetic dipole moment also leads to the absorption of radiation. In quantum theory, the transition probability produced by magnetic dipole radiation is obtained if the magnetic dipole moment (μ_m) is substituted in place of the electric dipole moment in the transition moment integral of equation (2-5). The components of μ_m transform as the three rotations R_x, R_y and R_z about the molecule fixed axis. Thus, for CH_2S, transitions originating from the totally symmetric ground state to upper vibronic states of A_2 symmetry are magnetic dipole allowed and are polarized about the a (z) axis.

The derivation of the overall rovibronic selection rules that are based on the space-fixed magnetic dipole operator parallels the development presented in Section 4.2.2 for electric dipole selection rules. The space-fixed magnetic dipole operator (μ_{mZ}) is expressed in terms of the components of μ_m about the molecule-fixed axes together with the appropriate directional cosines. Both the component of μ_m and its directional cosine transform as a rotation about the same axis. Therefore, the rovibronic magnetic dipole selection rule necessitates that the product

of the overall symmetry species of the upper and lower state rovibronic wavefunctions transform as A_1. Consequently, the vibronic $^1A_2 \leftarrow {}^1A_1$ transition is magnetic dipole allowed with the rotational selection rules

$$A_1 \leftrightarrow A_2 \qquad \text{and} \qquad B_1 \leftrightarrow B_2 \tag{4-65}$$

or, equivalently,

$$(++) \leftrightarrow (-+) \qquad \text{and} \qquad (--) \leftrightarrow (+-) \tag{4-66}$$

The structure of these bands is the same as ordinary type A vibronically allowed bands. Sidman[52] was the first to suggest this mechanism for the $^1A_2 \leftarrow {}^1A_1$ transition of formaldehyde, while Callomon and Innes[22] showed conclusively that the mechanism is responsible for the appearance of most type A bands of CH_2O.

4.9.2 The 0_0^0 Band of CH_2S

Unlike the origin band of the formaldehyde spectrum, which is weak and heavily overlapped by "hot" bands, the type A origin band at 16394.55 cm^{-1} is free from any noticeable overlap (see Figure 4-13). The strong, sharp red-degraded parallel-type band is ideal for a rotational analysis.

A parallel type band follows the selection rules $\Delta K_{-1} = 0$ and $\Delta J = 0, \pm 1$. Thus, this band exhibits only Q sub-bands. Within each sub-band, P, Q and R branches are observed. However, for molecules such as CH_2S, only the first few members of the Q branches are observed due to unfavourable intensity factors, as verified from the band contour programme.

Early in the analysis, a perturbation of the excited state rotational levels was detected. The perturbation is most clearly manifested by a break in the regular progression of lines in the strong $^QP_3(J)$ branch. Similar breaks are also observed in the $^QR_3(J)$ and in the asymmetry split

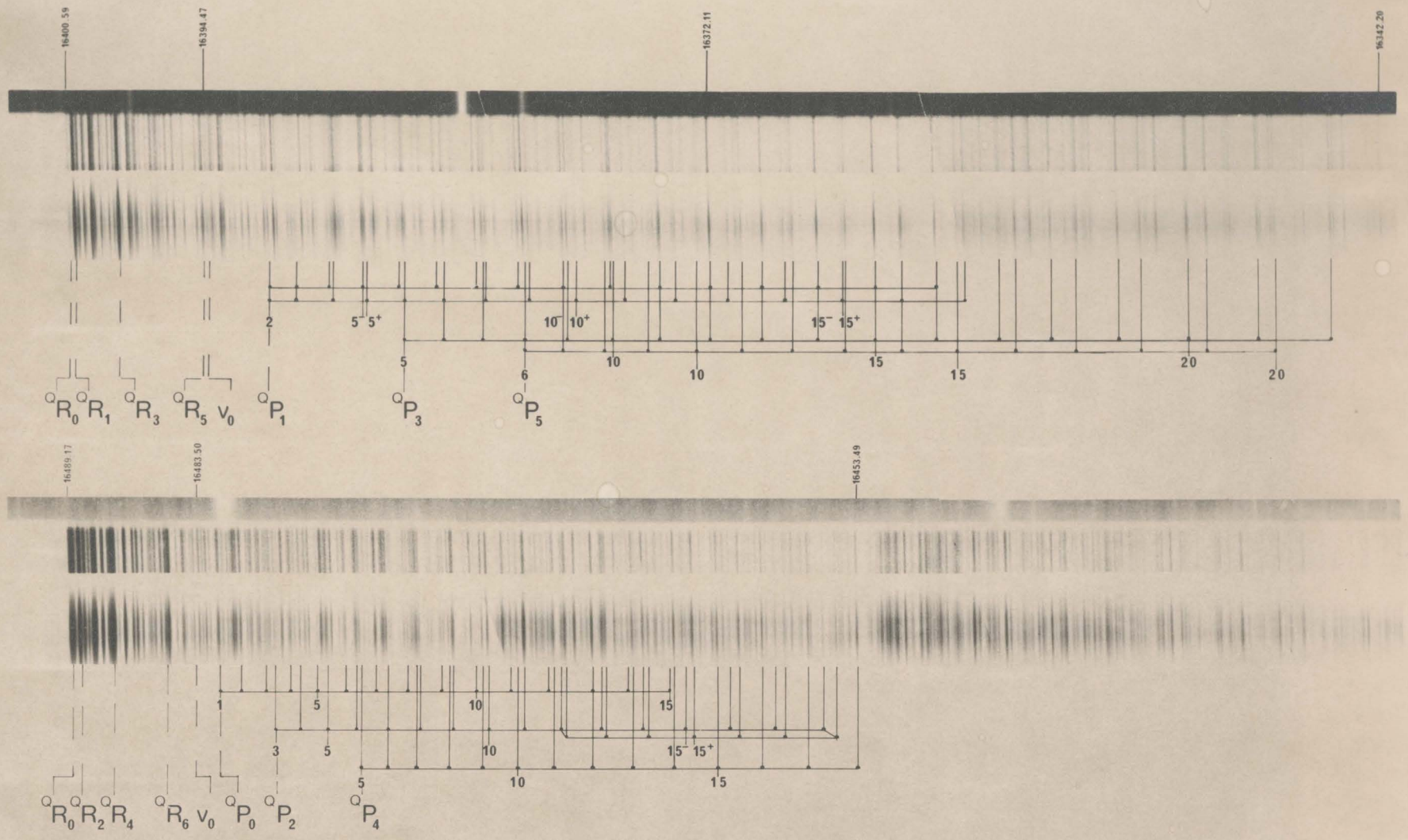

Figure 4.13 The Type A Origin bands of CH_2S (upper) and CD_2S (lower)

$^{Q}P_1(J)$ and $^{Q}R_1(J)$ branches. Fortunately, the effects of the perturbation are detectable only over a very limited range in J for each of the branches. Thus, a complete determination of the rotational constants is possible from assignments of transitions to the unperturbed levels. A discussion of the type of perturbations expected for the $^1A_2$ state of CH_2S is given in a subsequent section, while the remainder of this section is concerned with the analysis of the origin band. Since the perturbation is very localized, the assignment procedure for the band proceeds normally. Lines that are found to be displaced from their anticipated position are not included in the analysis.

Within the lower energy region of the origin band, several $^{Q}P_{K''_{-1}}(J)$ progressions are observed whose K''_{-1} numbering is established as follows. The $^{Q}P_3$ branch is easily identified from amongst the other progressions since a theoretical intensity calculation, as obtained from the band contour programme, predicts that the $^{Q}P_3$ branch forms the strongest branch in this region. The remaining branches are assigned as follows. The first differences in J of each of the lines of the branches are calculated. Within the rigid rotor approximation, lines of each $^{Q}P_{K''_{-1}}(J)$ branch with the same J'' quantum number have identical values for their first differences. However, the lines with the same J values are of different energies since each of the values for their sub-band origins are different. The higher energy lines are described by the lower K''_{-1} values while the lower energy lines are of higher K''_{-1} values. Thus, once the $^{Q}P_3$ progression is identified, the K''_{-1} numbering of the remaining progressions is established with the aid of the theoretically predicted intensity alternation.

As determined from the band contour programme, the strongest line in

the spectrum is expected to be the $^{Q}R_3$ band head. It is easily identified and assigned as the band head at 16398.40 cm^{-1}. From the average value of $\Delta\bar{B}$ obtained from the $^{Q}P_{K''_{-1}}$ branches, J_{rev} is estimated to occur at J'' = 10. $\Delta\bar{B}$ is close to that calculated for the 4^1_0 band of CH_2S, and by analogy with this band, the $^{Q}R_{K''_{-1}}$ band heads also contain transitions which originate from the J'' = 9, 10 and 11 levels. The assignment of the remaining band heads is established by using the $^{Q}R_3$ assignment, the value of ΔA calculated from the $^{Q}R_{K''_{-1}}$ branches, and the observed intensity alternation. The J'' assignments of the $^{Q}P_{K''_{-1}}$ ($K''_{-1} \geq 3$) branches is established with the aid of the improved value of A', and the value of ν_o, both of which are obtained from a least squares fit to the band head assignments. Finally, the weaker lines of the symmetric rotor portion of the band are assigned and used to calculate the best set of symmetric rotor constants for the band.

The ground state nuclear statistics of the odd K''_{-1} levels is three times that of the even levels. Assignment of the asymmetry split doublets of the band is first made in the $^{Q}R_1$ and $^{Q}P_1$ branches. A complete set of asymmetric top rotational constants is then calculated from a least squares analysis of these assignments. These constants are then used as a guide in assigning the weaker $^{Q}R_{0,2}$, $^{Q}P_2$ branches of the band. All of the assignments that are listed in Appendix 1 are then used to obtain the rotational constants reported in Table 4-12.

TABLE 4-12

The CH_2S Origin Band Excited State Constants

$A = 9.447 \pm 0.0014\ cm^{-1}$	$D_K = 8.10 \times 10^{-4} \pm 5.3 \times 10^{-5}$
$B = 0.53891 \pm 0.000056\ cm^{-1}$	$D_{JK} = 2.25 \times 10^{-5} \pm 1.5 \times 10^{-6}$
$C = 0.50910 \pm 0.000056\ cm^{-1}$	$D_J = 8.81 \times 10^{-7} \pm 6.0 \times 10^{-8}$
$\nu_o = 16394.47 \pm 0.01\ cm^{-1}$	$\sigma = 2.69$

The results of the analysis indicate that the band is magnetic dipole allowed. The intensity distribution of the band is that expected of a type A band. Furthermore, the identification of the $^{Q}R_{0}$ band head eliminates the possibility of the band appearing through any a, b or c axis coriolis-coupling mechanisms. Even though a perturbation of the excited state rotational levels is present, the least squares analysis has satisfactorily determined the rotational constants since the overall standard deviation (σ) is low. Apart from the severely perturbed lines of the spectrum, the agreement between the observed and calculated contours of Figure 4-14 is quite satisfactory.

4.9.3 The Origin Band of CD_2S

Because of the greater density of rotational lines, the origin band of CD_2S could only be partially resolved by the Ebert spectrograph. Consequently, assignment of the rotational lines in this band is primarily limited to the P sub-band region.

The key to the analysis is the assignment of the intense $^{Q}P_{4}$ branch (see Figure 4-13). From this assignment, the K''_{-1} numbering of the other P branches is established by methods similar to that described for the assignment of the P branches of the origin band of CH_2S.

Since the value of ΔA (0.15 cm^{-1}), estimated from the second differences in K_{-1} of the P branches, is small, overlap of the R branch region is expected to be extensive. Thus, preliminary assignments in this area are limited to the $^{Q}R_{K''_{-1}}$ ($K''_{-1} \geq 3$) band heads. Since the $^{Q}R_{4}$ band head is the strongest line in the band (as established from the band contour programme), it is easily identified as the line at 16487.27 cm^{-1}. The K_{-1} numbering of the remaining band heads is established with the aid of the

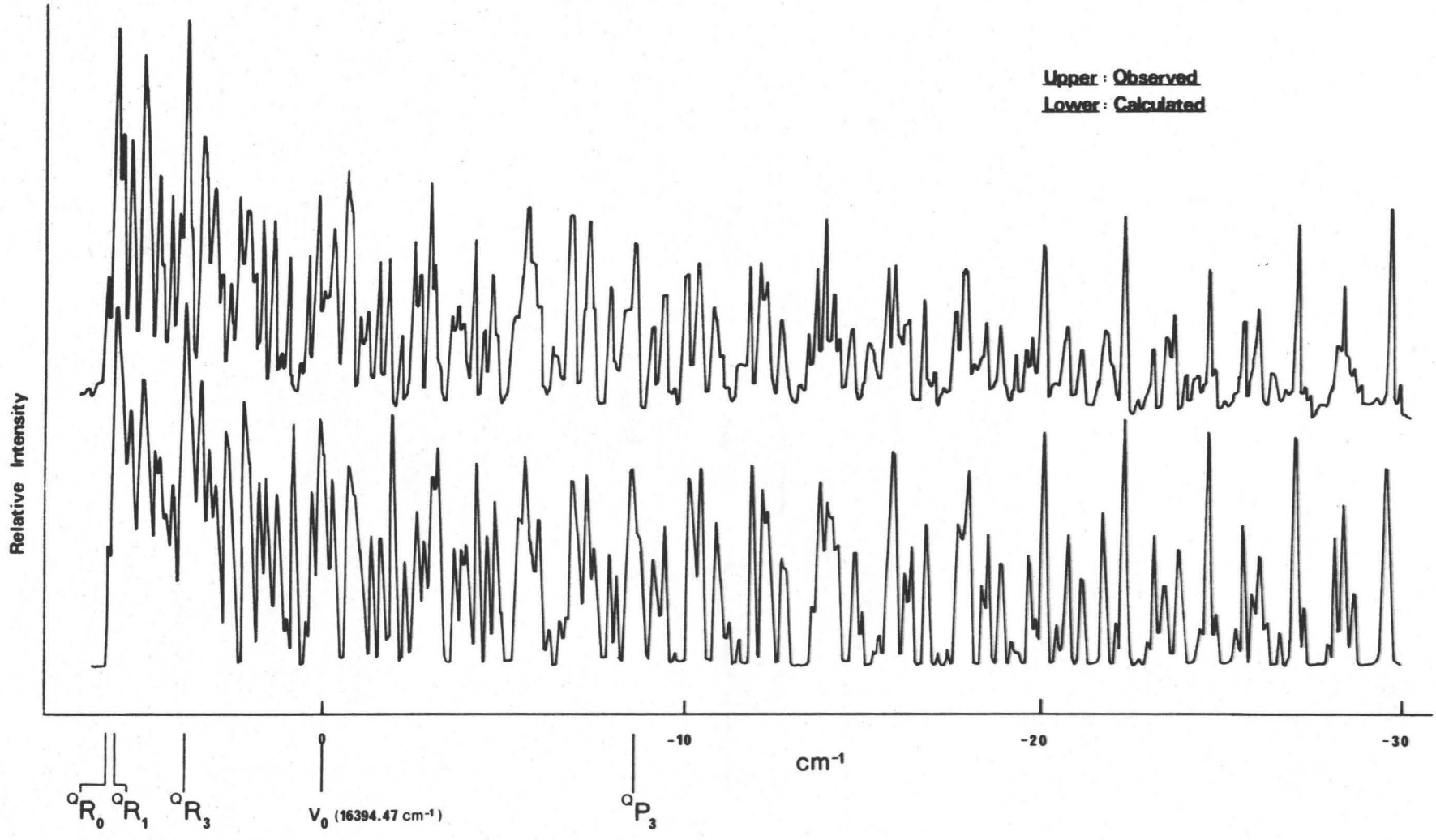

Figure 4.14 **Contours of the Origin band of CH_2S.**

above assignment, the value of ΔA and the theoretical intensities of the heads. An average value of $\Delta\overline{B}$ is obtained from the second differences of the P branch lines. From this value, J_{rev} is estimated at J" = 12. The band heads are, therefore, given the assignment $^{Q}R_{K''_{-1}}(12)$. Then, ν_o and an improved value of A' are obtained from a least squares fit to the band head positions. The J numbering of the P branches ($K_{-1} \geq 3$) is then established from the values of A', $\overline{B}'$ and ν_o. Because of overlap by the singlet-triplet bands, assignment of lines within the P branch region is limited to values of $K''_{-1} \leq 7$ and $J'' \leq 20$.

The improved set of rotational constants, as calculated from a least squares fit of the assignments in the P branch region, is used as a guide in assigning the higher J lines ($J'' \geq 10$) of the $^{Q}R_4$ and $^{Q}R_6$ branches. Because of extensive overlap in this region, reliable J assignments of the remaining R branches are not feasible. Fortunately, assignments are possible up to J" = 29 for the $^{R}R_4$ branch and J" = 27 in the $^{R}R_6$ branch, as these form the strongest branches in the R branch region.

The experimentally resolvable asymmetry split transitions are observed in the higher members ($J'' \geq 12$) of the $^{Q}P_2$ branch. The separate values of B and C derived from these assignments are used as a guide in assigning the other asymmetry split branches of the band system.

A listing of the vacuum wavenumbers and assignments of the 0-0 band of CD_2S is given in Appendix 1. The rotational constants and standard deviation obtained from the least-squares analysis are reported in Table 4-13. The distortion constants of the band may be slightly in error since comparatively few higher J and K_{-1} assignments are possible. The computed contours are found to be remarkably sensitive to small changes in the dis-

tortion constants. Therefore, the agreement between the calculated and observed contours of the 0-0 band of CD_2S is only fair (Figure 4-15).

TABLE 4-13

The CD_2S Origin Band Excited State Constants

$A = 4.7345 \pm 0.0007\ cm^{-1}$	$D_K = 3.05 \times 10^{-4} \pm 1.2 \times 10^{-5}$
$B = 0.45787 \pm 0.00011\ cm^{-1}$	$D_{JK} = 9.6 \times 10^{-6} \pm 1.5 \times 10^{-6}$
$C = 0.41721 \pm 0.00009\ cm^{-1}$	$D_J = 4.78 \times 10^{-7} \pm 7.1 \times 10^{-8}$

$\nu_o = 16483.50 \pm 0.01$

$\sigma = 2.17$

4.10 The Partially Analysed Bands of Thioformaldehyde

4.10.1 The 4_0^2 Band of CH_2S

In Section 3.4.1, it was suggested that the 4_0^2 band is one of three vibronic bands whose origins are grouped together in the 17220 cm^{-1} region. Under high resolution, the type A band at higher energy is seen to contain several $^QR_{K''_{-1}}$ band heads with increasingly large separation to lower wavelengths. This large separation indicates a large change in the A rotational constant on electronic excitation. This is also observed for the $3_0^1 4_0^3$ band. Since transitions to the vibrational levels of the large amplitude inversion mode (ν_4') are expected to give this type of structure to the bands, the band is assigned to the 4_0^2 transition. The head at 17227.03 cm^{-1} shows clear J structure and a good estimate of $\Delta\overline{B}$ is obtained by calculating the second differences. Since J_{rev} is expected at J'' = 10, the band heads, like that of the 0_0^0 band of CH_2S, are composed of the J'' = 9, 10 and 11 transitions. The assignment of the other lines is given in Appendix 1. Since the band is so highly overlapped by the 3_0^1 type A band,

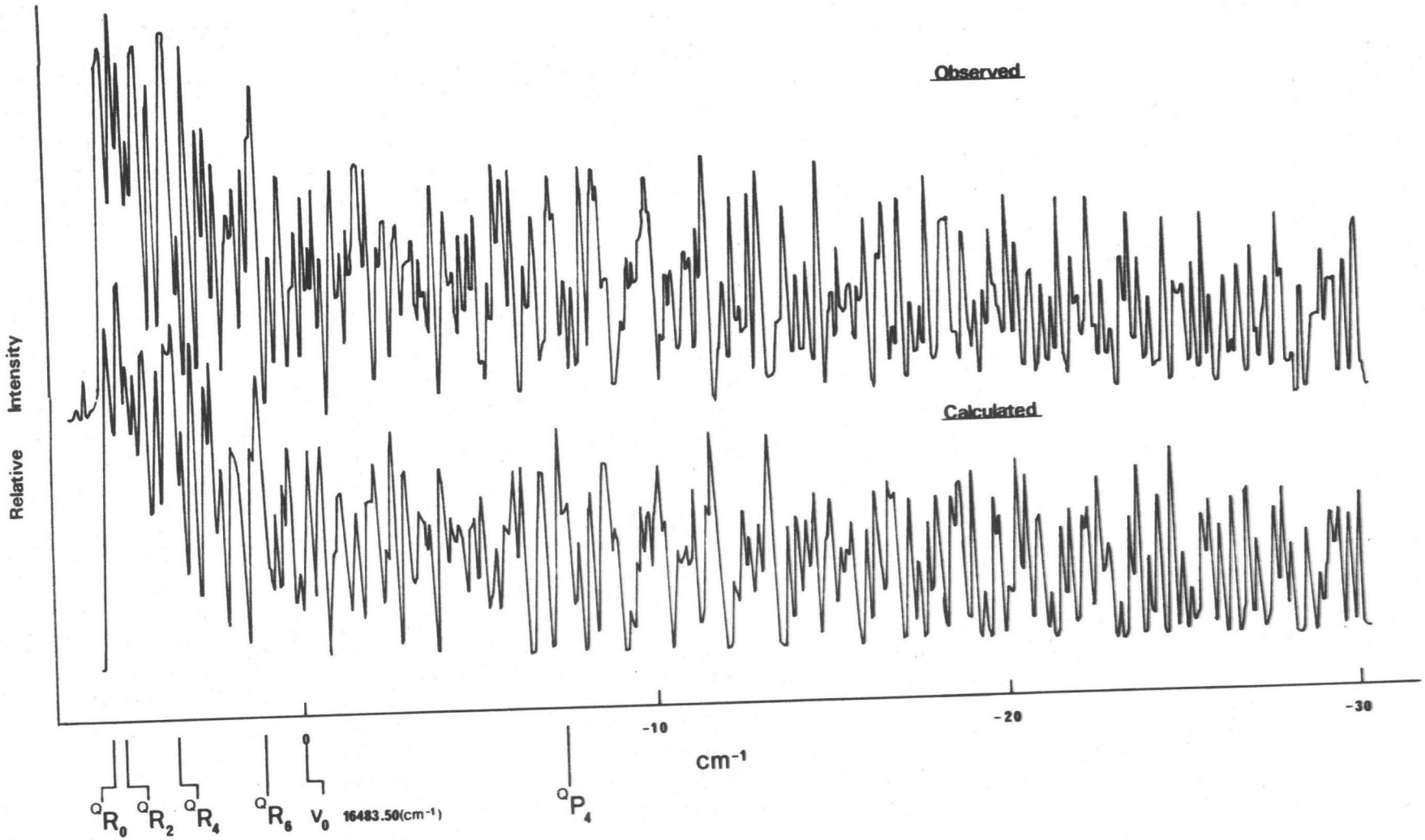

Figure 4.15 Contours of the Origin band of CD_2S.

it is impossible to locate the $^{Q}P_{K''_{-1}}(J)$ and $^{Q}Q_{K''_{-1}}(J)$ transitions and, therefore, the assignments cannot be confirmed by the usual methods. However, a least squares fit of the assignment yields only small residuals. The rotational constants, derived from these assignments, are listed in Table 4-14.

TABLE 4-14

The Rotational Constants of the Partially Analysed Bands of Thioformaldehyde

Band	Molecule	A'	$\overline{B}'$	D_K'	ν_o
4_0^2	CH_2S	8.77	0.523	0.004	17229.4
$2_0^1 4_0^1$	CD_2S	4.660	0.4381	0.0001	17771.3
4_0^5	CD_2S	4.22	0.438	-0.0096	18344.7

4.10.2 The $2_0^1 4_0^1$ Band of CD_2S

A partial rotational analysis of the band at 17771.3 cm^{-1} was attempted so that its polarization could be established and used as an aid in its vibrational assignment. The symmetric top rotational assignments used in the least squares analysis of the band are given in Appendix 1 while the symmetrical top rotational constants of the band are listed in Table 4-14.

Theoretical type B and C band contours were then generated by the computer from the rotational constants calculated from the least squares analysis. Since the values of B and C are not separately known, arbitrary values are chosen with the restriction that their sum equals $2\overline{B}$. The characteristic features of the origin region of the type B and type C bands are used to establish definitely that the band is polarized about the b axis. The band's polarization is consistent with its assignment as $2_0^1 4_0^1$.

4.10.3 The 4_0^5 Band of CD_2S

Like the $3_0^1 4_0^3$ band of CH_2S, the band at 18344.7 cm^{-1} in the CD_2S spectrum shows a relatively strong head at the high frequency end. Because of overlap within this band, only a partial rotational analysis could be made. This yields sufficient information so as to confirm its vibrational assignment as 4_0^5.

The assignments listed in Appendix 1 are used to calculate the symmetric top rotational constants listed in Table 4-14. The K''_{-1} numbering is established from the assignment of the easily identified strong $^RR_0$ band head and the distinctive $^RR_2$ asymmetry split heads. Because of the extensive overlap, the assignment of the J structure is feasible only in the $^RR_6$ and $^QR_4$ branches. A comparison of the observed contour with calculated type B and C band contours establishes that the direction of polarization of this band is along the b-axis, in agreement with its vibrational assignment.

4.11 Perturbation of the Excited State Rotational Levels of CH_2S

Early in the analysis of the 0-0 and $3_0^1 4_0^3$ band of CH_2S, it was discovered that certain energy levels of the excited vibronic state could not be adequately described by the centrifugal-distortion asymmetric rotor energy expressions derived in Section 4.3. The energy expressions must be modified so as to include perturbation interactions between states. The possible types of perturbations which can occur for a C_{2v} molecule are as follows.

4.11.1 Coriolis Coupling

Coriolis forces arise from a coupling of the molecule's rotational motion with the vibrational motion of the molecule's constituent nuclei.

The classical expression for the Coriolis force is given by[25]

$$F_{cor} = 2m(\omega \times t_{x\alpha}) \tag{4-67}$$

where ω is the angular velocity and where $t_{x\alpha}$ is the velocity vector of atom x. The Coriolis force is directed normal to the plane formed by the vectors ω and $t_{x\alpha}$. Interaction of rotation with the normal mode Q_α will excite the normal mode Q_β, if the displacement vectors represented by the normal mode Q_β are along the direction of F_{cor}. Under these conditions, Q_β is excited at vibrational frequency ν_α instead of its normal value of ν_β. If ν_α and ν_β are of similar magnitude, then resonance interaction is expected.

A quantum mechanical treatment of Coriolis coupling requires that the approximate hamiltonian of equation (4-9) be expanded to include the vibrational angular momentum terms, p_g; that is,

$$H = \frac{(P_x - p_x)^2}{2I_x} + \frac{(P_y - p_y)^2}{2I_y} + \frac{(P_z - p_z)^2}{2I_z} + \tfrac{1}{2}\sum_k p_k^2 + V \tag{4-68}$$

or

$$H = H_r^o + H_v + H' \tag{4-69}$$

where the perturbation term H' is given by

$$H' = -\left(\frac{p_x P_x}{I_x} + \frac{p_y P_y}{I_y} + \frac{p_z P_z}{I_z}\right) \tag{4-70}$$

The wavefunctions of the hamiltonian are expressed in terms of product functions of the form $\psi_v \psi_r$. Diagonalization of the vibrational-rotational hamiltonian matrix, which is no longer diagonal in the vibrational quantum numbers v, yields the corrections to the energy levels. The off-diagonal matrix elements are readily deduced from the expression derived for the

perturbation operator and are of the form

$$\langle v;JKM|-\frac{P_g p_g}{I_g}|\ v';JK'M\rangle = (-\frac{1}{I_g})\langle v|p_g|v'\rangle\langle JKM|P_g|JK'M\rangle \qquad (4\text{-}71)$$

Jahn[53] has shown that the vibrational angular momentum operators, p_g, transform as the rotations R_g. Therefore, the integral represented by equation (4-71) will be non-zero if the direct product of the symmetry species of the two interacting vibrational (vibronic) states contains Γ_{R_g}. In this case, the two interacting states are said to be Coriolis coupled about the g axis (g = a, b or c).

Since the integral represented by $\langle JKM|P_g|JK'M\rangle$ is diagonal in J, rotational perturbations can occur only between levels of the same J. P_g transforms as a rotation about the g axis; thus, the integral is non-zero if the direct product of the symmetry designation of ψ_{JKM} and $\psi_{JK'M}$ contains Γ_{R_g}. Therefore, a-axis Coriolis coupling (g = z = a) follows the rotational selection rule $A_1 \leftrightarrow A_2$ and $B_1 \leftrightarrow B_2$, i.e., $\Delta K_{-1}^{INT} = 0$ (with the restriction that interactions between the K = 0 levels of the perturbing states is forbidden). b-Axis and c-axis Coriolis coupling follows the selection rule $\Delta K_{-1}^{INT} = \pm 1$. Furthermore, as indicated in Table 4-14, the off-diagonal matrix elements in the a-axis Coriolis coupling case, $\langle JKM|P_z|JK'M\rangle$. $\langle v|p_g|v'\rangle$ are K_{-1} dependent but J independent (see equation 4-13). The off-diagonal elements in both the b and c axis Coriolis coupling cases are both K_{-1} and J dependent. Thus, a-axis Coriolis coupling is distinguishable from b and c axis Coriolis coupling in that the extent by which the rotational levels are displaced from their unperturbed positions is J independent for a-axis coupling while it is J dependent in b and c-axis coupling cases.

The same rotational selection rules may be reached by considering the full rovibronic selection rules. Since the operators on the left hand side of equation (4-71) both transform as a rotation about the same axis, their product transforms as the A_1 representation. Thus, rotational perturbations can occur only between levels of the same overall rovibronic species. Therefore, if g = z = a, then for a-axis Coriolis coupling, $\Delta K_{-1}^{INT} = 0$ with the restriction that interactions between the K' = 0 levels is forbidden. Similarly, b and c axis Coriolis coupling follows $\Delta K_{-1}^{INT} = 1$, as expected.

4.11.2 Fermi Resonance

The interaction between vibrational levels of the same symmetry is termed Fermi resonance. Perturbations of the rotational levels of these interacting states is possible if the Fermi interaction between the two states is very slight and yet the states are very close together. If the rotational levels of the same J and same overall rovibronic species have very nearly the same energy, in a zeroth order approximation, then resonance interaction is possible. Since the perturbation operator transforms as the A_1 representation, the interacting states follow the selection rules $\Delta J^{INT} = 0$ and $\Delta K_{-1}^{INT} = 0$. These selection rules are identical to those for a-axis Coriolis coupling. The two types of perturbations are, in theory, distinguishable from each other since a-axis Coriolis coupling is K dependent while Fermi resonance is not. In practice, however, it is difficult to distinguish between the two perturbations.

The selection rules for Coriolis and Fermi resonance are summarized in Table 4-15.

TABLE 4-15

The Off-diagonal Matrix Elements for the Coriolis and Fermi Type Interactions

$\Gamma_r^{EV} \times \Gamma_s^{EV}$	Type	Matrix Element	Selection Rules ΔJ^{INT}	ΔK_{-1}^{INT}
A_1	Fermi	W_{12}	0	0
A_2	a-axis Coriolis	$2iA\xi r_s \Omega r_s K^1$	0	0
B_1	b-axis Coriolis	$2iB\xi r_s \Omega r_s \{J(J+1)-K(K\pm1)\}^{\frac{1}{2}}$	0	±1
B_2	c-axis Coriolis	$2iC\xi r_s \Omega r_s \{J(J+1)-K(K\pm1)\}^{\frac{1}{2}}$	0	±1

[1] ξ is the Coriolis coupling parameter defined in reference 56.

Ω is a constant also defined in reference 56.

4.11.3 Singlet-triplet Interactions

Direct interaction between the singlet and triplet A_2 excited states of C_{2v} molecules through the spin-orbit operator, H_{SO}, is symmetry forbidden. However, second order mechanisms such as vibronic spin orbit coupling, $H_{ev} + H_{SO}$, or spin rotation coupling, $H_{or} + H_{SO}$ allow the rovibronic levels of the A_2 excited state to interact. Brand[54] has pointed out that a characteristic feature of carbonyl compounds is the small energy separation between the singlet and triplet A_2 states. This is also the case for thiocarbonyl compounds and leads to a low density of triplet energy levels opposite the lower vibrational levels of the singlet state. A combination of a low density of levels and small matrix elements leads to highly specific interactions, since only a limited number of rotational levels of the singlet and triplet states are sufficiently close in energy that their interaction produces observable effects.

Selection rules for the vibronic spin-orbit operator and the spin-rotation operator have been derived by Stevens and Brand[55] and have been used in the interpretation of the perturbations observed in the $2_0^2 4_0^1$ band of CH_2O[50]. The perturbations observed in this band extend over a very narrow range of J and are J independent. The interactions produced by the spin-rotation coupling operator is also expected to behave in this fashion. Thus, the perturbations observed in the $2_0^2 4_0^1$ band of CH_2O are assigned as this type of singlet-triplet interaction. Since the perturbed lines were shifted and/or broadened on application of a Zeeman field, the presence of a perturbing triplet state is confirmed.

4.11.4 Rotational Perturbations of the Origin Band

In Figure 4-16, the residuals of the individual lines of the $^{Q}R_{3,1}$

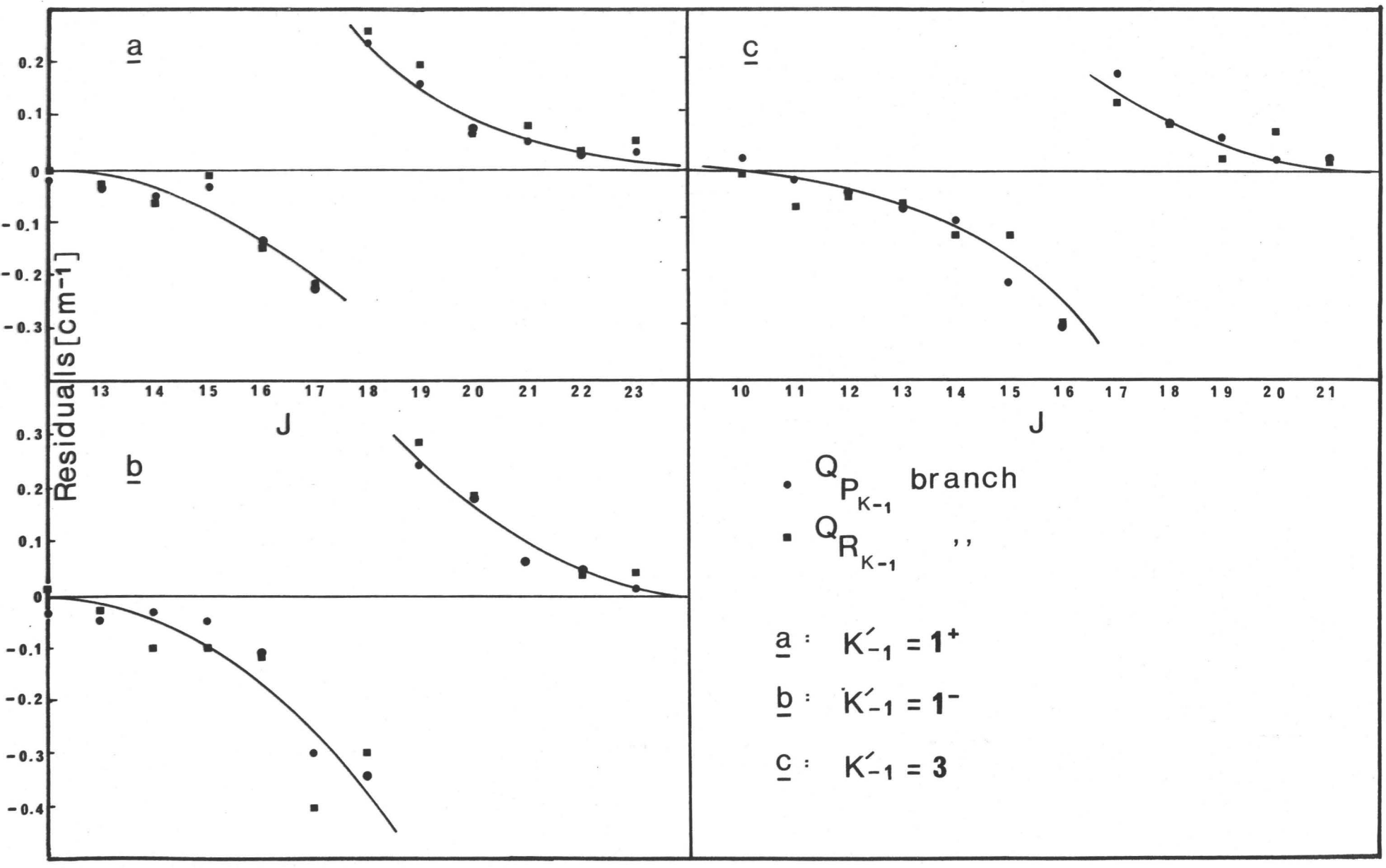

Figure 4-16. Plots of the residuals vs J for lines of the origin band of CH_2S.

and $^{Q}P_{3,1}$ branches of the 0_0^0 band are plotted vs J". In each case, the residuals reach a maximum for a particular value of J and then quickly return to zero. This indicates that the perturbation is of resonance type, that is, it is J independent. Three mechanisms could account for the J independent nature of the perturbation, namely, a-axis Coriolis coupling, Fermi resonance, or singlet-triplet interactions. Coriolis coupling is still possible for the origin band, as a consequence of the zero point vibration. However, the Coriolis and Fermi interactions are very unlikely as the cause of the perturbation of the origin band since the next excited state vibronic level of CH_2S is some 350 cm^{-1} away from the zero point level. Furthermore, in the case of perturbations observed by Suetherham and Innes[50] in the rotational structure of CH_2O, the residuals of individual levels affected by either a-axis Coriolis coupling or Fermi resonance did not show the sharp reversal of sign that is observed for CH_2S. One is tempted, therefore, to conclude that the interaction is of the singlet-triplet type. If a comparison is made between the behaviour of the perturbation present in the 0-0 band of CH_2S with that observed in the $2_0^2 4_0^1$ band of CH_2O, the conclusion gains added support in that a sharp reversal of sign of the residuals is observed for both molecules as J is increased. Actual confirmation of the presence of a perturbing triplet state is not experimentally feasible for CH_2S. Therefore, a conclusive statement as to the type of perturbation present is not possible at this time.

4.11.5 The $3_0^1 4_0^1$ Band of CH_2S

A plot of the individual line residuals vs J" for transitions to the K' = 0 manifold of the $3_0^1 4_0^1$ band of CH_2S is reproduced in Figure 4-17.

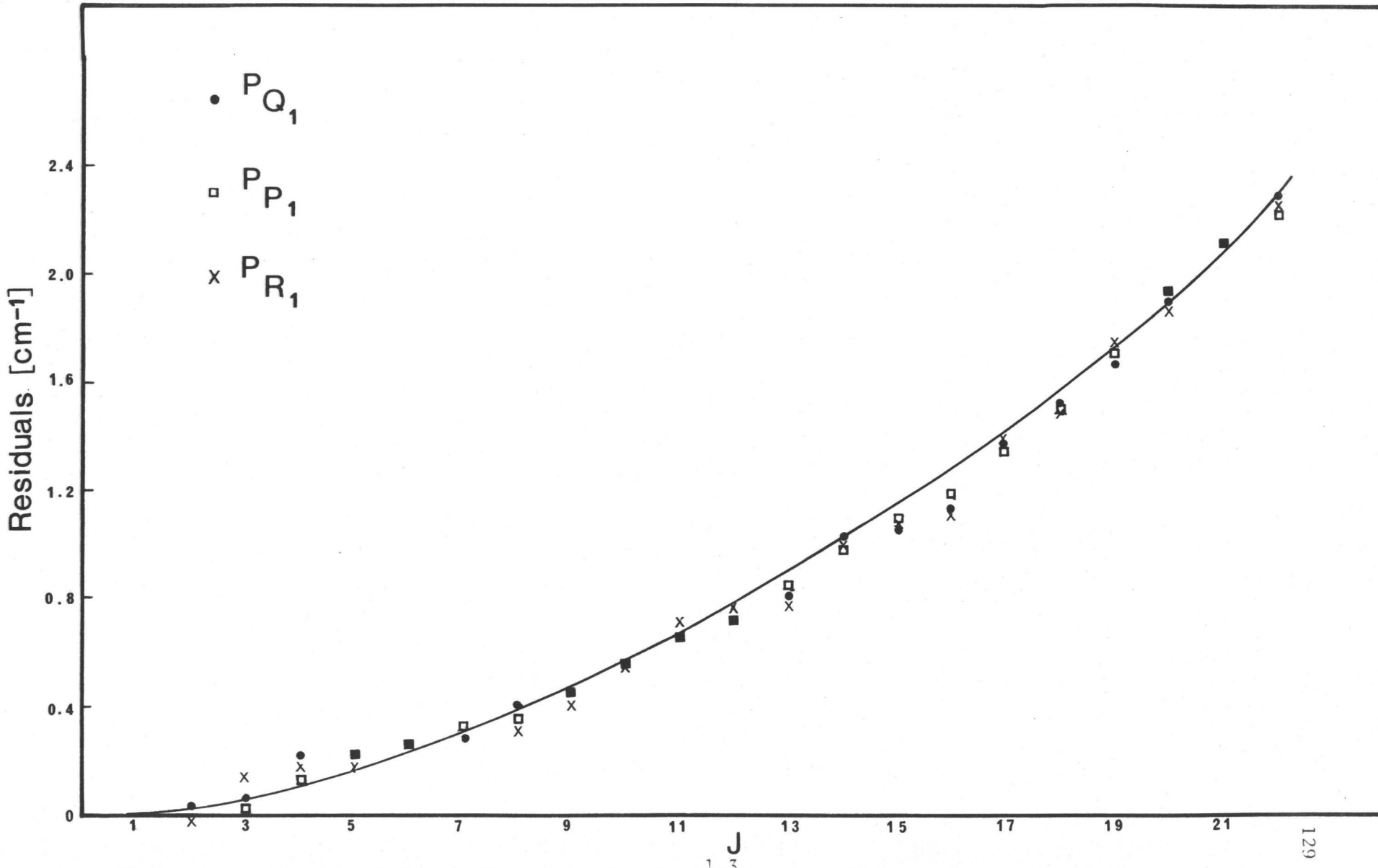

Figure 4-17. A plot of the residual vs J for the $3_0^1 4_0^3$ band of CH_2S.

The residuals are J dependent and, therefore, the perturbation can be assigned as either b or c-axis Coriolis coupling, dependent on whether the interacting state is of A_2 or A_1 vibronic symmetry. The unobserved $\nu_2'\nu_3'$ level, just 14 cm^{-1} below the $\nu_3'3\nu_4'$ level is the state most likely to be the second member of the interacting pair. The energy levels of the excited states of the $3_0^1 4_0^3$ and $2_0^1 3_0^1$ bands are depicted in Figure 4-18. Coriolis interactions between the K' = 0 and, to a lesser extent, the K' = 1 levels of $\nu_3'3\nu_4'$ and the K' = 1 and K' = 0, 2 levels of the perturbing $\nu_2'\nu_3'$ state are energetically favourable.

The overlapped and crowded appearance of the central portion of the band make the identification of the relatively weak transitions to the K' = 1 levels difficult. However, the $^RR_0$ band head can be identified and it is found to be less strongly displaced from its calculated position than levels of equal J in the K'_{-1} = 0 manifold. This observation is in qualitative agreement with that predicted by Figure 4-18.

In conclusion, the perturbation present in the $3_0^1 4_0^3$ band of CH_2S is identified as Coriolis type. It is directed along either the b or c axis. The perturbation is probably between the $\nu_2'\nu_3'$ and $\nu_3'3\nu_4'$ levels. In this case, the interaction would be along the b axis.

4.12 The Geometry of the $^1A_2$ State of Thioformaldehyde

The results of the least squares rotational analysis presented in previous sections have given reliable values for the rotational constants for several vibronic bands of thioformaldehyde. These constants are inversely proportional to the effective moments of inertia (I_o) of the molecule. Thus the geometry of the molecule can, in principle, be determined from these moments of inertia. Ideally, one wishes to determine the

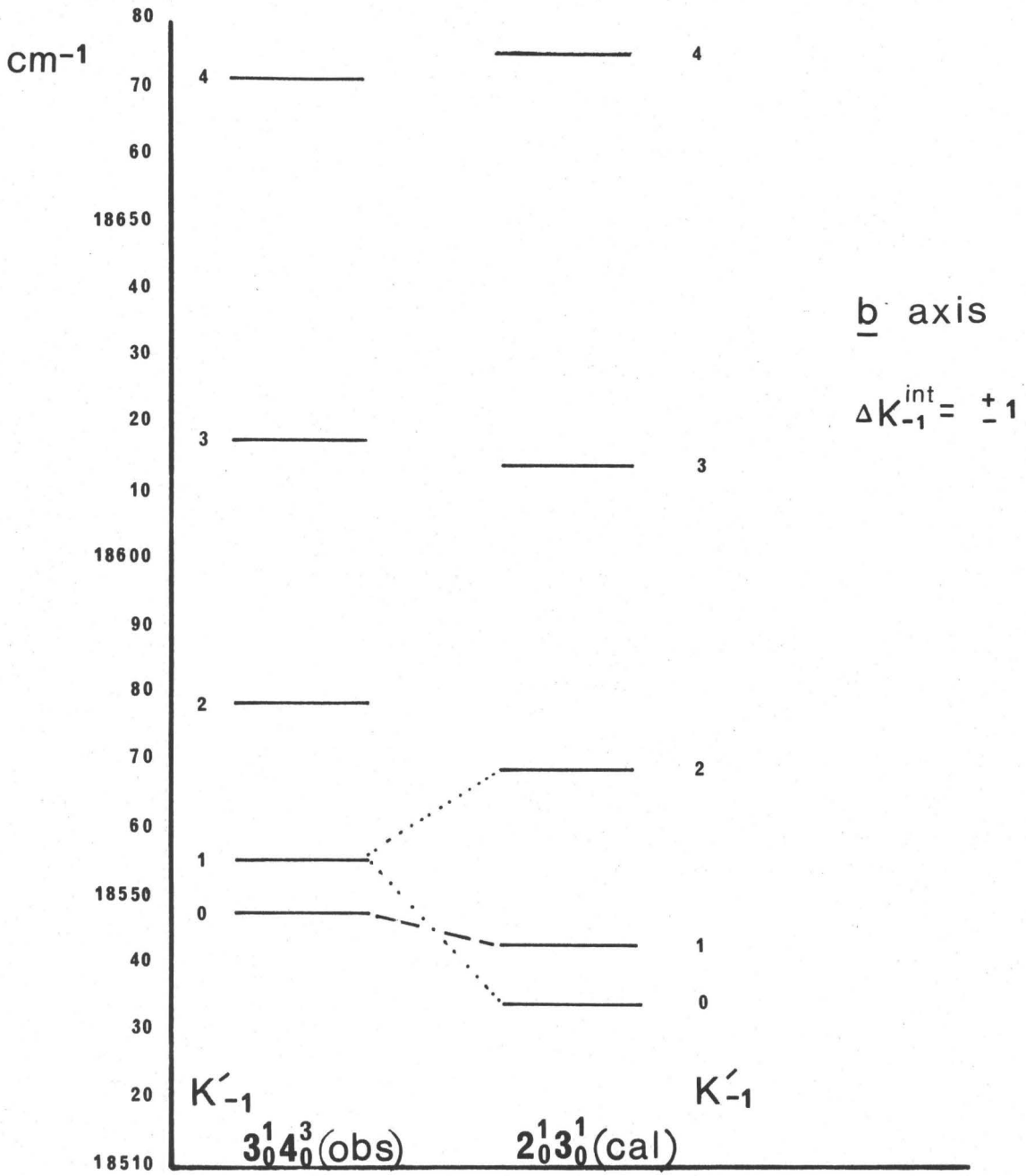

Figure 4-18. The energy levels of the $3_0^1 4_0^3$ and $2_0^1 3_0^1$ bands of CH_2S.

equilibrium geometry for an electronic state, but there are difficulties in calculating this due to the presence of the zero point vibrations. To illustrate these difficulties, we consider the case of the simple diatomic molecule for which the following moments of inertia are defined:

1) The moment of inertia of the equilibrium structure, $I_e = \sum_i m_i r_{ei}^2$. I_e is related to the equilibrium internuclear distance, r_e, which is the value of the bond length at the very bottom of the potential energy well.

2) The moment of inertia of the average structure, $I_{AV} = \sum_i m_i r_{AV}^2 = \sum_i m_i \langle r \rangle^2$. I_{AV} is related to the average of the instantaneous values of r assumed by the molecule during its vibrations, $\langle r \rangle$.

3) The average moment of inertia, $\langle I \rangle = \sum_i m_i \langle r_i^2 \rangle$. The structure determined from the average value of the instantaneous moments of inertia ($\langle r^2 \rangle^{\frac{1}{2}}$) is not simply related to the average structure since $\langle r^2 \rangle \neq \langle r \rangle^2$.

4) The effective moment of inertia $I_o = \sum_i m_i r_{oi}^2$. I_o is proportional to the inverse of the experimentally measured effective rotational constant B_o for the various rotational levels of the molecule. The structure as determined from this quantity is termed the r_o structure.

An insight into the inter-relationship of the various moments of inertia is gained by inspecting equations (4-73) to (4-75). These have been derived by Herschbach and Laurie[57] for the general case of the polyatomic molecule.

$$I_o = \langle I^{-1} \rangle^{-1} + \text{correction terms due to Coriolis coupling} \qquad (4\text{-}73)$$

$$\langle I^{-1} \rangle^{-1} = \langle I \rangle + \text{correction terms due to the expansion of the double inverse} \qquad (4\text{-}74)$$

and

$$\langle I \rangle = I_{STD} + \text{terms due to the harmonic averaging of the moment of inertia} \qquad (4\text{-}75)$$

where I_{STD} is either I_e or I_{AV}. The interested reader is referred to the original paper by Herschbach and Laurie if the equations for the correction terms are desired. Only the case of the diatomic molecule is the observed rotational constant simply related to $\langle I^{-1} \rangle$ since the Coriolis coupling terms vanish. However, even for this case, the relationships between $\langle I^{-1} \rangle^{-1}$, $\langle I \rangle$ and I_{STD} remain complicated.

4.12.1 The r_o Structure

The r_o structure, as determined for a hypothetical rigid molecule of rotational constants A_o, B_o, C_o is neither the average nor the equilibrium structure of the molecule. However, the r_o structure is useful since it is readily calculated and is, in most cases, a reliable estimate of the equilibrium structure.

The method of determining the r_o structure of non-planar molecules such as CH_2S is straightforward. The procedure involves varying, in a least squares routine, arbitrary starting values of the molecular geometrical parameters. The process is continued until the rotational constants, as calculated from the values of these parameters, agree satisfactorily with the observed rotational constants. Since the effective rotational constants are functions of the vibrational states of the molecule, the r_o structure will be different for each vibronic band analysed.

Four geometrical parameters have to be calculated for the excited state of CH_2S, namely, the C-H bond length (r_{CH}), the C=S bond length (r_{CS}), the HCH angle (2β), and the out-of-plane angle (θ). Hence, a minimum of four measured rotational constants is required to determine

TABLE 4-16

The r_o Structural Parameters of the $^1A_2$ State of Thioformaldehyde

	0_0^0	4_0^1
r_{CH}	1.075 ± 0.010 (Å)	1.093 ± 0.013 (Å)
r_{CS}	1.707 ± 0.008 (Å)	1.706 ± 0.008 (Å)
∠HCH	121.6 ± 1.7 (°)	116.8 ± 4.2 (°)
∠out-of-plane	8.9 ± 1.7 (°)	27.8 ± 2.4 (°)

Rotational Constants (cm^{-1})

		Obs.	Cal.	Obs.	Cal.
CH_2S:	A	9.447	9.451	9.060	9.075
	B	.5389	.5369	.5376	.5370
	C	.5091	.5084	.5103	.5105
CD_2S:	A	4.736	4.734	4.620	4.592
	B	.4579	.4573	.4578	.4570
	C	.4172	.4174	.4187	.4194

TABLE 4-17

The r_s Geometry of Thioformaldehyde

	0_0^0	4_0^1
r_{CH}	1.082 ± 0.010 (Å)	1.077 ± 0.010 (Å)
r_{CS}	1.701 ± 0.010 (Å)	1.720 ± 0.010 (Å)
∠HCH	120.0 ± 1.5 (°)	120.8 ± 1.5 (°)
∠out-of-plane	9.7 ± 1.5 (°)	17.7 ± 2 (°)

these parameters. Thus, the rotational constants of the deuterated species must be employed together with the normal isotope in a least squares fit. In doing this, the assumption is made that the r_o values for each isotopically substituted molecule are identical. However, Costain[58] has pointed out that the effective geometrical parameters will be different for each isotopic molecule since the vibrational frequencies of the normal and isotopically substituted molecules are different. Consequently, the r_o structure as determined by this method suffers an additional discrepancy with the equilibrium structure.

Table 4-16 shows the observed and calculated rotational constants, along with the r_o geometrical parameters derived from the 0_0^0 and 4_0^1 bands. The large uncertainties quoted for each of the geometrical parameters may be attributed partially to the inaccuracies inherent in the r_o method.

4.12.2 The r_s Structure

An improvement over the r_o structural determination method has been suggested by Kraitchmann[59]. Isotopic substitution is performed sequentially on each of the atoms of the reference molecule (usually chosen to be normal isotopic molecule). The rotational constants of the reference and isotopically substituted molecules are used in the equation derived by Kraitchmann to give the positions of the isotopically substituted atom with respect to the centre of mass of the reference molecule. If the equilibrium moments of inertia are used in the equations, then the equilibrium structure is calculated. As this is not possible for CH_2S, the effective moments must be used in practice instead of the equilibrium values; however, Costain has shown[58] that the coordinates determined by

this method are closer to the equilibrium values than is the geometry calculated by the r_o method. The geometry calculated by this method is termed the r_s structure.

The equations derived by Kraitchmann are valid only in the case of mono-substitution. Since only spectra of the normal and di-substituted thioformaldehyde were recorded experimentally, the equations must be modified in order to employ the rotational constants of CH_2S and CD_2S.

If the planar inertial dyadic is defined as

$$P = \sum_i m_i r_i r_i - (\sum_i m_i r_i)(\sum_i m_i r_i)/\sum_i m_i \tag{4-76}$$

with P related to the inertial dyadic by

$$P_\alpha = \tfrac{1}{2}(I_\beta + I_\gamma - I_\alpha) \tag{4-77}$$

then the elements of P are of the form

$$P_{xx} = \sum_i m_i x_i^2 - (\sum_i m_i x_i)^2/\sum_i m_i \tag{4-78}$$

and

$$P_{xy} = \sum_i m_i x_i y_i - (\sum_i m_i x_i)(\sum_i m_i y_i)/\sum_i m_i \tag{4-79}$$

If the origin of the molecule fixed coordinate system is chosen to coincide with the centre of mass of the normal (CH_2S) molecule, then only the first term in equations (4-78) and (4-79) are retained since the other terms go to zero. The <u>same</u> coordinate system is used to compute the elements of the planar dyadic (P_α') of the di-deuterated (CD_2S) molecule of mass $M + 2\Delta m$,

$$P_x' = P_x + (\frac{2\Delta m M}{M+2\Delta m}) x_H^2 \tag{4-80}$$

$$= P_x + \mu x_H^2 \tag{4-81}$$

$$P_z' = P_z + \mu z_H^2 \tag{4-82}$$

$$P_y' = P_y + 2\Delta m y_H^2 \tag{4-83}$$

$$= P_y + \mu_y y_H^2 \tag{4-84}$$

$$P_{xy}' = P_{yz}' = 0 \tag{4-85}$$

$$P_{xz}' = \mu x_H z_H \tag{4-86}$$

The secular equation of the substituted molecule in this coordinate system is then

$$\begin{vmatrix} P_x+\mu x_H^2-P' & 0 & \mu x_H z_H \\ 0 & P_y+\mu_y y_H^2-P' & 0 \\ \mu x_H z_H & 0 & P_z+\mu z_H^2-P' \end{vmatrix} = 0 \tag{4-87}$$

The secular equation may be expanded to give a cubic equation in P'.

If, instead, the coordinate system is chosen to coincide with the centre of mass of the isotopically substituted molecule, then the simplified secular equation can be expanded in the form

$$-P'^3 + (P_x' + P_y' + P_z')P'^2 - (P_x'P_y' + P_x'P_z' + P_y'P_z')P' + P_x'P_y'P_z' = 0 \tag{4-88}$$

The coefficients of like powers of P' may be equated to give the non-linear simultaneous equations

$$\mu(x^2 + y^2) + \mu_y y^2 + P_x + P_y + P_z - P_x' - P_y' - P_z' = 0 \tag{4-89}$$

$$\mu x^2(P_y + P_z) + \mu_y y^2(P_x + P_z) + \mu_z^2(P_x + P_y) + \mu_y \cdot \mu \cdot y^2 z^2 + \mu_y \cdot \mu \cdot x^2 y^2 + P_y P_z + P_x P_z + P_x P_y - P_x'P_y' - P_x'P_z' - P_y'P_z' = 0 \tag{4-90}$$

$$\mu P_y P_z x^2 + \mu_y P_x P_z y^2 + \mu P_x P_y z^2 + \mu_y \cdot \mu \cdot P_z x^2 y^2 + \mu_y \cdot \mu \cdot P_x y^2 z^2$$

$$+ P_x P_y P_z - P_x' P_y' P_z' = 0 \qquad (4\text{-}91)$$

These equations may be solved numerically to yield values for the $|x|$, $|y|$ and $|z|$ coordinates of the hydrogen atoms of CH_2S. The symmetry of the molecule fixes the values for the y coordinates of the C and S atoms at zero. The γ (γ = x or z) coordinates of the C and S atoms can be determined by solving suitable pairs of moment equations; for example, $\sum_i m_i \gamma_i = 0$ and $\sum_i m_i (y_i^2 + \gamma_i^2) = I_\beta$ with $\beta \neq y \neq \gamma$. The use of the moment equations introduces a degree of uncertainty in the substitution geometry of thioformaldehyde as different choices of moment equation pairs yield slightly different values for the coordinates of the C and S atoms. Nonetheless, the r_s structure should be an improvement over the r_o structure. The uncertainty in the r_s structure could, in principle, be significantly reduced if full isotopic substitution is performed on the molecule.

The geometry determined from the substitution coordinates of thioformaldehyde in two of its upper vibronic states is presented in Table 4-17. The r_s and r_o structural determination methods yield approximately the same value for the C-H and C=S bond lengths for both vibronic states. Thus, the equilibrium bond lengths should be within 0.01 and 0.02 Å of the values quoted in Tables 4-16 and 4-17, if thioformaldehyde follows the pattern exhibited by most other molecules studied[58]. However, the widely different values for the HCH and out-of-plane angles calculated for the vibrationaless (all $v_i' = 0$) and $v_4' = 1$ levels (as determined from both the r_s and r_o methods) and the large uncertainties associated with these values severely limits the reliability of an estimate of the equil-

ibrium value of these parameters. The values calculated for the out-of-plane angle are in qualitative agreement with the angle calculated from the Coon double-minimum potential (Chapter 3). Therefore, the molecule is probably slightly non-planar at equilibrium in its first excited state. Both the vibrational and rotational data indicate that the equilibrium out-of-plane angle is in the proximity of 15^{o}.

4.13 The Rotational Constants of the ν_4' Vibrational Levels

A theoretical explanation for the large variation observed in both the A rotational constant and in the calculated out-of-plane angle of CH_2O with the number of quanta of the ν_4' vibration excited has been given by Jones and Coon[60]. Since the ν_4' inversion mode of CH_2S is similar to that of CH_2O, the methods developed by these authors are used here to calculate the expectation value of the A' rotational constant of CH_2S in its first four vibrational levels.

If the C-H bond length (r), the C=S bond length (s) and the HCH angle (2β) are assumed to be the same for all vibrational levels and, further, if these parameters are also assumed to remain constant as the molecule executes the large amplitude inversion motion, then $I_o = \langle I^{-1} \rangle^{-1}$ or $A_o = \langle I_a^{-1} \rangle$ since all the correction terms due to Coriolis coupling go to zero (as in the analogous case of a diatomic). Thus, the observed rotational constants are the expectation value of the respective reciprocal moments of inertia, i.e.,

$$A_o = \int_{\theta=0}^{\theta=\theta_{max}} [\, \Phi_v(Q) \,]^2 \, \frac{h}{8\pi^2 c} \, 1/I_a(r,s,\beta;\theta) \, dQ \qquad (4\text{-}92)$$

$\Phi_v(Q)^2$ is the square of the vibrational wavefunction of the Coon double-

minimum potential evaluated at a point Q along the displacement coordinate and θ is the out-of-plane angle. The coordinate Q is related to θ by

$$dQ = [\mu(\theta)]^{\frac{1}{2}} d\theta \tag{4-93}$$

or

$$Q(\theta) = \int_o^{\theta} [\mu(\theta)]^{\frac{1}{2}} r d\theta' \tag{4-94}$$

where $\mu(\theta)$ is the reduced mass and is given by

$$\mu(\theta) = 2M_H \ell(m + \ell n \sin^2)/[n(1 - n) + 2\ell nR \cos\theta + \ell(1 - \ell)R^2] \tag{4-95}$$

and
$$M = M_S + M_C + 2M_H;\ \ell = M_S/M,\ n = 2M_H/M$$
$$m = M_C/M;\ R = r/(s \cos\beta) \tag{4-96}$$

The A_o rotational constant is evaluated (instead of B_o or C_o) since this constant is very sensitive to the effective value of the out-of-plane angle (θ_o).

Figure 4-19 shows how the square of the double-minimum wavefunction of three of the vibrational levels varies with Q_4 or θ. Since the value of the effective out-of-plane angle (θ_o) is indirectly dependent on Φ^2, the variation of θ_o from level to level can be qualitatively understood.

With the aid of equations (4-93) and (4-94), the A rotational constant is evaluated by numerical integration of equation (4-92) over the bending angle (θ). The integration is performed in steps of 0.1 degrees up to the point where $\Phi_v(Q)^2$ is effectively zero. In calculating the A' rotational constant for the 0_0^0, 4_0^1, 4_0^2 and 4_0^3 bands of CH_2S, r_{CS} and r_{CH} are set at the estimated values for the equilibrium bond length (1.705 Å and 1.08 Å respectively) and the H-C-H angle is arbitrarily chosen to be 120^o (an average of the values obtained from the rotational analysis). The excellent

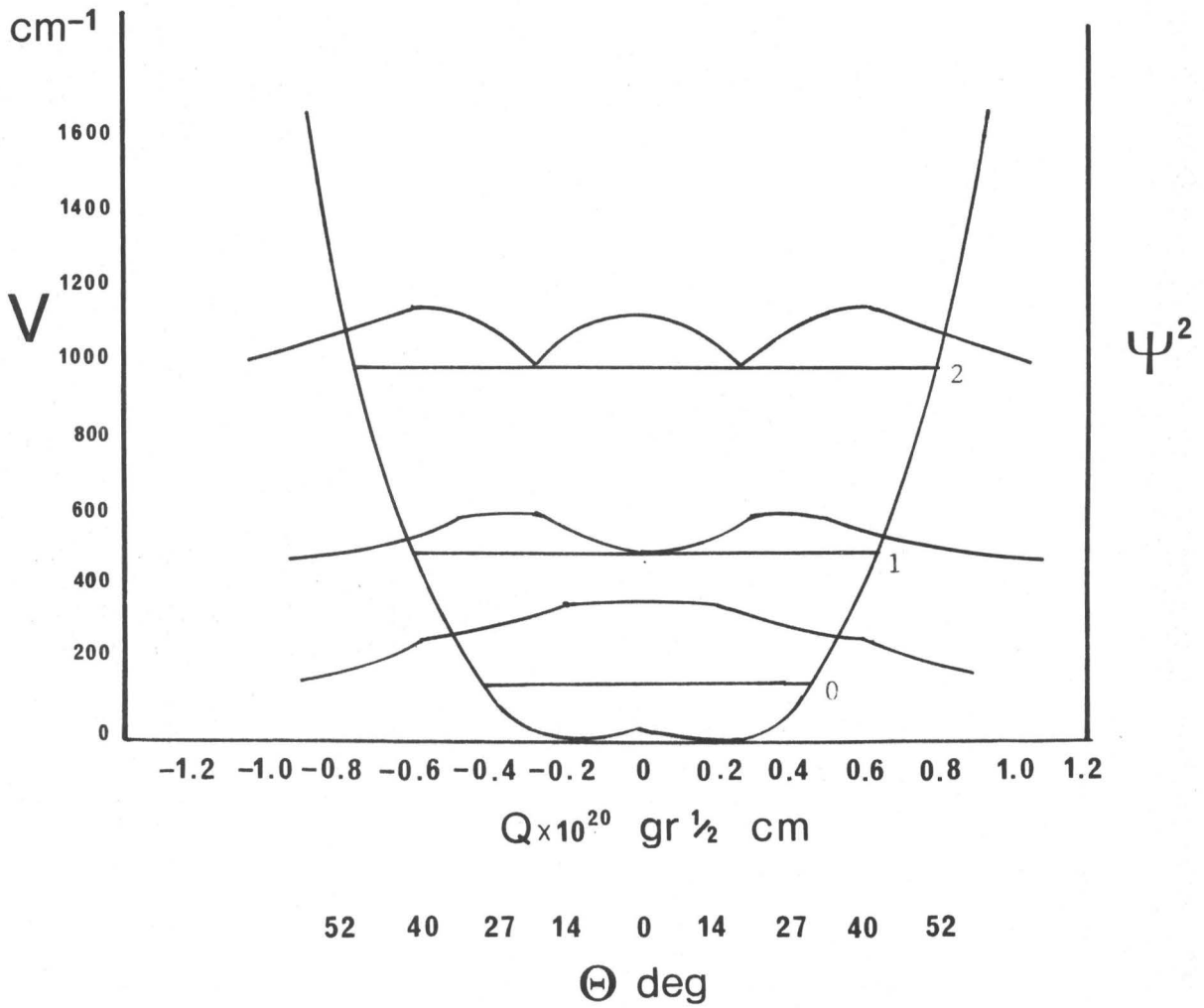

Figure 4-19. A plot of Q and θ vs the square of the double-minimum wavefunction (ψ^2).

qualitative agreement between the calculated and observed values of the A' rotational constant (Figure 4-20) is a further indication that the ν_4' potential is approximately described by a Coon double-minimum potential.

4.14 The Inertial Defect of Slightly Non-planar Molecules

Recall that the planar moment of inertia, P_c, is defined as

$$2P_c^e = I_a^e + I_b^e - I_c^e = 2\sum_i m_i c_i^{e2} \tag{4-97}$$

where I_g^e (g = a, b or c) are the equilibrium moments of inertia of a rigid molecule. Unfortunately, the spectroscopically derived moments of inertia, I_g^o, are those of a non-rigid molecule where the effects of zero point vibrations necessitate that equation (4-97) be modified slightly to

$$2P_c^o = I_a^o + I_b^o - I_c^o = 2\sum_i m_i c_i^e - \Delta_c \tag{4-98}$$

where Δ_c is termed the inertial defect. For the special case of the planar molecule, $2\sum_i m_i c_i^{e2} = 0$, if c represents the out-of-plane coordinate. Thus,

$$\Delta_c = \Delta_P = I_c^o - I_b^o - I_a^o \tag{4-99}$$

for a type I^{ℓ} representation. The planar inertial defect, Δ_P, is now easily calculated from the observed rotational constants. It has been found experimentally, mainly from microwave data, that for virtually all triatomics (which are necessarily planar) and for most other planar polyatomic molecules, the observed planar inertial defect is small and positive. One is therefore tempted to conclude as is often stated in the literature, that an observed positive planar inertial defect for the

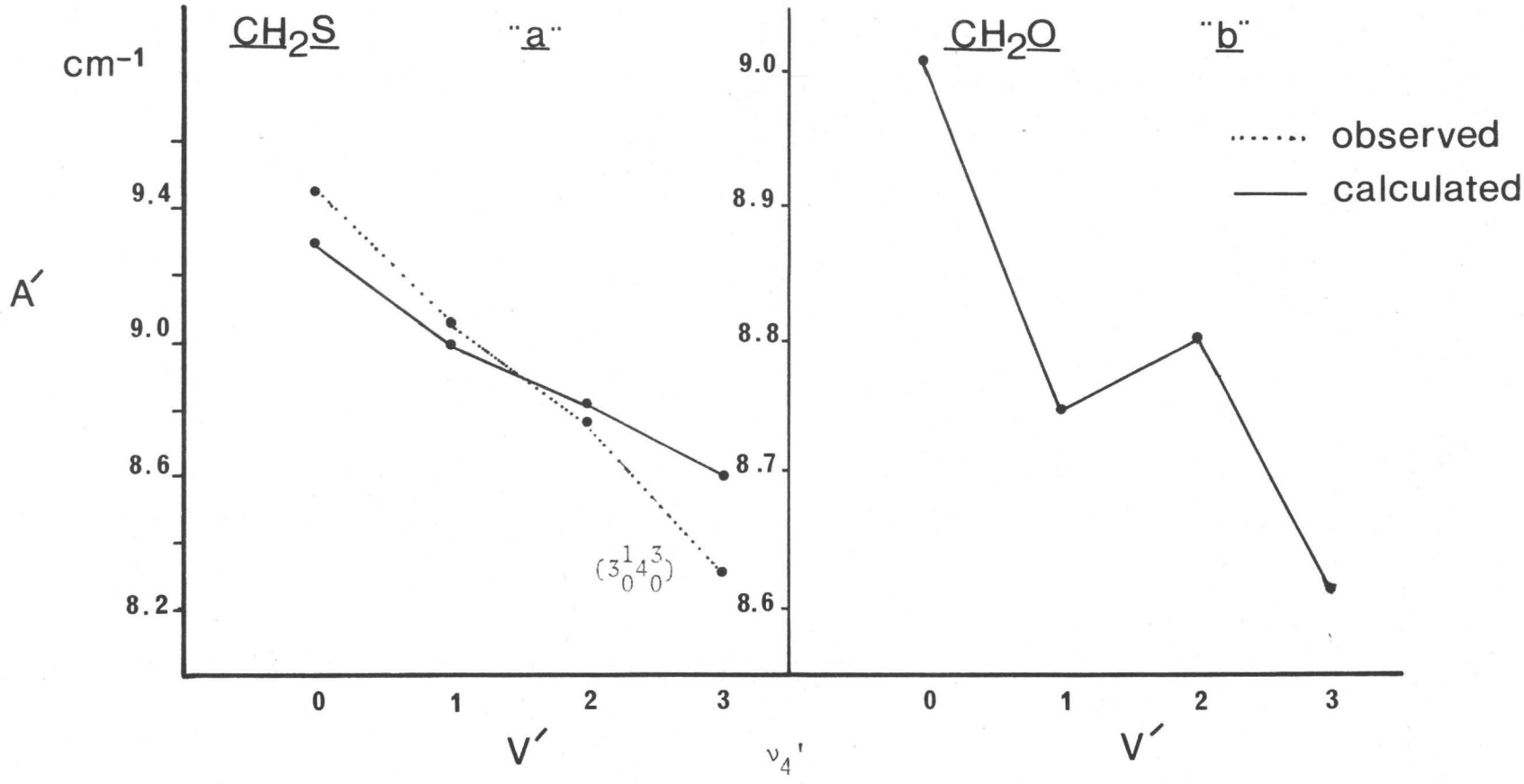

Figure 4-20. (a) A comparison of the observed and calculated values of the A' rotational constant of CH_2S for the 4_0^x (x = 0, 1, 2, 3) bands. The calculated values are obtained from the Coon double minimum function.

(b) The calculated values of the A' rotational constant for a molecule (CH_2O) with a large barrier to inversion.

vibrationaless level (all $v_i = 0$) of a molecule is a strong indication that the molecule is planar. However, slightly non-planar molecules may also exhibit a positive inertial defect. For example, consider the case of the inertial defect of formamide. Earlier investigations of the microwave spectrum of formamide had shown that the inertial defect for the normal and deuterated molecule (H_2NCDO) were positive. A planar structure was then assigned to the molecule. However, in a more recent investigation, Costain and Dowling[61] obtained reliable values for the ground state rotational constants of eight isotopic species of formamide. While the inertial defect of other planar molecules studied previously had been found to increase on deuterium substitution, Δ_p actually decreased on substitution of a heavier isotope for any atom in the NH_2 group. Furthermore, the inertial defect was negative for four of the isotopes studied. The presence of the "inversion" satellite in the microwave spectrum confirmed that the equilibrium structure of the molecule is non-planar in its ground state.

Other anomalies in the behaviour of the inertial defect of different molecules have been reported in the literature. For example, the equilibrium structure of phenol is planar, but because of internal rotation of the OH group, the molecule actually shows a negative planar inertial defect[62]. Azulene is a planar molecule, but it too exhibits a negative Δ_p[63]. Clearly, the observed inertial defect is not a reliable criterion for planarity. The anomalous behaviour of the planar inertial defect may be explained as follows.

Oka and Morino[64] have shown that the inertial defect may be represented as the sum of vibrational, centrifugal and electronic contribu-

tions, i.e.,

$$\Delta_c = \Delta_{vib} + \Delta_{cent} + \Delta_{ele} \tag{4-100}$$

Oka[65] has shown in detailed calculations that the largest term contributing to Δ_c is $\Delta_{c_{vib}}$. As $\Delta_{c_{vib}}$ can be expressed as a sum of terms which involve anharmonic and harmonic contributions, then the expression

$$\Delta_c \simeq \Delta_{c_{vib}} = \Delta_c(har) + \Delta_c(anh) \tag{4-101}$$

is used as the general equation for the inertial defect of any molecule.

In the case of the planar molecule, Herschbach and Laurie[57] have shown that $\Delta_{anh} = 0$ and thus Δ_p may be expressed simply as

$$\Delta_p = \Delta_p(vib) = \Delta_p(har) \tag{4-102}$$

These authors found that $\Delta_p(har)$ is usually positive <u>unless</u> one or more of the out-of-plane vibration modes of the planar molecules is of very low frequency. This observation explains why the inertial defect of virtually all triatomic molecules is positive and why planar azulene, with two low frequency out-of-plane vibrations, exhibits a negative inertial defect.

Consider the non-planar molecule for which the general definition equation (4-98) reduces from

$$-2P_c^o = I_c^o - I_b^o - I_a^o = \Delta_{np} - 2P_c^e \tag{4-103}$$

to

$$-2P_c^o = \Delta_p' = \Delta_{np} - 2P_c^e \tag{4-104}$$

or

$$2\sum_i m_i c_i^{e2} - 2\sum_i m_i c_i^{o2} = 2P_c^e - 2P_c^o = \Delta_{np} \tag{4-105}$$

where Δ_{np} is the inertial defect of the non-planar molecule and where Δ_p' is simply a quantity calculated from the observed rotational constants. In the limit of a planar equilibrium structure, Δ_p' would be termed the planar inertial defect.

Since the form of Δ_{np} is similar to that of Δ_p, the inertial defect of non-planar molecules may take on either positive or negative values. If Δ_{np} is positive and if the molecule is very slightly bent out-of-plane, i.e. $2P_c$ is small, then Δ_p' can take on positive small values. If Δ_p' is positive, then in accordance with equation (4-105), the equilibrium out-of-plane angle (θ_e) would be greater than the value of the effective out-of-plane angle (θ_o) calculated for that particular vibrational state. If Δ_p' is negative, Δ_p' can only take on negative values, and consequently, $\theta_e < \theta_o$.

A reversal of sign of Δ_{np} of CH_2O with the number of ν_4' quanta excited is indicated by the behaviour of θ_o with respect to the fixed value of θ_e[60].

For the $\nu_4' = 0$ and 2 levels, $\theta_o < \theta_e$ and, therefore, $\Delta_{np} > 0$; however, for the $\nu_4' = 1$ and 3 levels, $\theta_o > \theta_e$ and, thus, $\Delta_{np} < 0$.

It is not unreasonable to assume that the same behaviour of Δ_{np} occurs for non-planar CH_2S. In this case, with the aid of Tables 4-16 and 4-18, boundaries can be placed on the values of the equilibrium out-of-plane angle, i.e.,

$$9^o < \theta_e < 28^o \qquad (4\text{-}106)$$

The upper bound is taken from the effective geometry of the molecule in the $\nu_4' = 1$ level and the lower bound is taken from the effective geometry of the vibrationaless level of the excited state.

TABLE 4-18

Summary of the Rotational Constants of the Rotationally Analysed Bands of CH_2S and CD_2S

Band	Molecule	A'	B'	C'	D_K'	D_{JK}'	D_J'	Δ_p' amu Å^2
0_0^0	CH_2S	9.4473	0.53891	0.50910	0.000810	0.0000225	0.000000881	+0.047
0_0^0	CD_2S	4.7356	0.45789	0.41721	0.000305	0.0000096	0.000000478	+0.032
4_0^1	CH_2S	9.0601	0.53763	0.51026	0.000437	0.0000114	0.000000665	-0.179
4_0^1	CD_2S	4.6197	0.45777	0.41872	0.000113	0.0000136	0.000000175	-0.215
$3_0^1 4_0^3$	CH_2S	8.309	0.5294	0.5112	-0.00102	0.0000087	0.00000072	-0.89
5_0^1	CD_2S	4.6886	0.45743	0.41642	0.000170	0.0000139	0.000000267	+0.034

All values are given in cm^{-1}.

The reversal of sign of Δ_p' with the number of quanta of ν_4' excited cannot, alone, be considered proof of the non-planarity of CH_2S. The inertial defect of planar CH_2S is also expected to show a reversal in sign for the higher ν_4' levels (as witnessed for the ν_4'' level of CH_2O). However, this evidence, coupled with that obtained from the vibrational analysis (Chapter 3), along with the observed decrease in the planar inertial defect on deuterium substitution (like non-planar formamide), is considered a strong indication that the molecule is slightly non-planar. The value of the equilibrium out-of-plane angle is specified by equation (4-106).

CHAPTER 5

CONCLUSIONS

The visible electronic absorption spectrum of thioformaldehyde and thioformaldehyde-d_2 has been recorded under high and low resolution. The absorption spectrum which extends from 6100 Å to 4000 Å is assigned to the $^1A_2 \leftarrow {}^1A_1$ electronic transition while the system from 7000 Å to 6100 Å is assigned to the $^3A_2 \leftarrow {}^1A_1$ transition. The vertical electronic transition energies experimentally observed for the singlet-singlet (2.03 e.v.) and singlet-triplet (1.80 e.v.) transitions are in good agreement with the values predicted by ab initio calculations.

A vibrational analysis of the singlet-singlet system has given the excited state vibrational frequencies of all six normal modes of vibration of both CH_2S and CD_2S. Like CH_2O, the energy spacings between quanta of the ν_4' vibrational potential of CH_2S are highly anharmonic. The observed ν_4' vibrational levels are fit to both a quadratic-quartic and a Coon double-minimum potential energy function. The quality of the fit to these potentials is only fair. The vibrational constants obtained from the fit to the quadratic-quartic potential indicate that the molecule is "floppy planar" in the excited state. The fit to the Coon double-minimum potential yields constants which predict a very slightly non-planar excited state with a barrier to inversion of 20 cm^{-1}. A non-planar excited state is predicted from the Walsh diagrams and from ab initio calculations.

A rotational analysis of the 0_0^0 and 4_0^1 bands of CH_2S and CD_2S has been completed. The $3_0^1 4_0^3$ band of CH_2S and the 5_0^1 band of CD_2S have also been rotationally analysed. The type A origin bands of CH_2S and CD_2S are shown to be magnetic dipole allowed. The type B 4_0^1 and $3_0^1 4_0^3$ bands and the type C 5_0^1 band are shown to have polarizations compatible with their vibrational

assignments. A partial rotational/band contour analysis of the 4_0^2 band of CH_2S and the $2_0^1 4_0^1$ and 4_0^5 bands of CD_2S has shown that the polarization of these bands is along the a, b and b axes respectively.

A perturbation in the rotational structure of the 0_0^0 and in the $3_0^1 4_0^3$ bands of CH_2S has been observed. The perturbation within the origin band is suspected to be of the singlet-triplet type while the perturbation within the $3_0^1 4_0^3$ band is assigned as b-axis Coriolis coupling.

The r_o and r_s structural determination methods are used to calculate the geometry of the molecule in the $^1A_2$ state. The values of r_{CH} and r_{CS} are calculated to be 1.08 Å and 1.70 Å respectively and are expected to be within 0.02 Å of their equilibrium values. The observed planar inertial defect (Δ_p') is small and positive for the upper state zero-point level. In addition, Δ_p' is found to decrease on deuterium substitution. The behaviour of Δ_p' with the number of ν_4' quanta excited and the values of the out-of-plane angle (θ) obtained from the r_o structural determination methods are used to show that CH_2S is very slightly non-planar in the excited state. The molecule is bent approximately 15^o out-of-plane.

APPENDIX

CH_2S COMBINATION DIFFERENCES

Upper State			Lower State			Observation	Calculation		Residual	Remarks
J	K_A	K_C	J	K_A	K_C					
1	0	1	0	0	0	34351.4300	34351.4114		0.0186	MHZ
2	1	1	2	1	2	3139.3800	3139.4022		-0.0222	MHZ
2	0	2	1	0	1	68699.5100	68699.3666		0.1434	MHZ
2	1	2	1	1	1	67653.8200	67653.8062		0.0138	MHZ
2	1	1	1	1	0	69746.7200	69746.7216		-0.0016	MHZ
3	1	2	3	1	3	6278.6500	6278.6244	*	0.0256	MHZ
3	0	3	2	0	2	103040.2200	103040.4100		-0.1900	MHZ
3	1	3	2	1	2	101477.6200	101477.7547		-0.1347	MHZ
3	1	2	2	1	1	104617.0400	104616.9769		0.0631	MHZ
3	2	2	2	2	1	103039.9900	103039.8225		0.1675	MHZ
3	2	1	2	2	0	103051.8100	103051.7629		0.0471	MHZ
4	1	3	4	1	4	10463.9700	10463.9576		0.0124	MHZ
4	0	4	3	0	3	137371.0500	137371.0883		-0.0383	MHZ
4	1	4	3	1	3	135297.8100	135298.1655		-0.3555	MHZ
4	1	3	3	1	2	139483.4100	139483.4987		-0.0887	MHZ
4	2	3	3	2	2	137382.0300	137381.9539		0.0761	MHZ
4	2	2	3	2	1	137411.7700	137411.8015		-0.0315	MHZ
4	3	2	3	3	1	137369.1700	137369.2643		-0.0943	MHZ
4	3	1	3	3	0	137369.1700	137369.2961		-0.1261	MHZ
5	1	4	5	1	5	15695.1200	15695.1158		0.0042	MHZ
5	0	5	4	0	4	171687.9000	171687.9528		-0.0528	MHZ
5	1	5	4	1	4	169113.5300	169113.8725		-0.3425	MHZ
5	1	4	4	1	3	174344.8500	174345.0307		-0.1807	MHZ
5	2	4	4	2	3	171720.2300	171720.2493		-0.0193	MHZ
5	2	3	4	2	2	171779.4500	171779.9341		-0.4841	MHZ
5	3	3	4	3	2	171710.9800	171710.8683		0.1017	MHZ
5	3	2	4	3	1	171710.9700	171710.9796		-0.0096	MHZ
5	4	2	4	4	1	171670.6500	171670.6267		0.0233	MHZ
5	4	1	4	4	0	171670.6500	171670.6267		0.0233	MHZ
6	1	5	6	1	6	21971.7100	21971.7020		0.0080	MHZ
7	1	6	7	1	7	29293.2100	29293.1814		0.0286	MHZ
7	0	7	6	0	6	240266.3200	240266.4916		-0.1716	MHZ
7	1	7	6	1	6	236726.7700	236726.5692		0.2008	MHZ
7	2	6	6	2	5	240381.7500	240381.5004		0.2496	MHZ
7	4	4	6	4	3	240331.4300	240331.4633		-0.0333	MHZ
7	4	3	6	4	2	240331.4300	240331.4643		-0.0343	MHZ
7	5	3	6	5	2	240261.3800	240261.1988		0.1812	MHZ
7	5	2	6	5	1	240261.3800	240261.1988		0.1812	MHZ
8	1	7	8	1	8	37658.8300	37658.8500		-0.0200	MHZ
10	1	9	10	1	10	57518.8000	57518.8660		-0.0660	MHZ
11	1	10	11	1	11	69010.6100	69010.6014		0.0086	MHZ
15	2	13	15	2	14	7052.0700	7052.0696		0.0004	MHZ
16	2	14	16	2	15	9050.1600	9050.1477		0.0123	MHZ
17	2	15	17	2	16	11438.5300	11438.5455		-0.0155	MHZ
18	2	16	18	2	17	14261.9000	14261.8891		0.0109	MHZ
19	2	17	19	2	18	17565.9200	17565.9747		-0.0547	MHZ
20	2	18	20	2	19	21397.4400	21397.4026		0.0374	MHZ
21	2	19	21	2	20	25803.1400	25803.1791		-0.0391	MHZ
22	2	20	22	2	21	30830.3500	30830.3932		0.0568	MHZ
23	2	21	23	2	22	36525.3200	36525.2754		0.0446	MHZ

* not included

Upper State			Lower State			Observation	Calculation	Residual	Remarks
J	K_A	K_C	J	K_A	K_C				
24	2	22	24	2	23	42933.8000	42933.7491	0.0509	MHZ
25	2	23	25	2	24	50100.0400	50099.9849	0.0551	MHZ
7	7	1	5	5	1	233.2620	233.1871	0.0749	cm^{-1}
8	7	2	6	5	2	235.5400	235.4696	0.0704	cm^{-1}
9	7	3	7	5	3	237.7580	237.7510	0.0070	cm^{-1}
10	7	4	8	5	4	240.0320	240.0313	0.0007	cm^{-1}
11	7	5	9	5	5	242.3490	242.3105	0.0385	cm^{-1}
12	7	6	10	5	6	244.5790	244.5884	-0.0094	cm^{-1}
13	7	7	11	5	7	246.9290	246.8651	0.0639	cm^{-1}
14	7	8	12	5	8	249.0980	249.1405	-0.0425	cm^{-1}
15	7	9	13	5	9	251.3860	251.4145	-0.0285	cm^{-1}
16	7	10	14	5	10	253.6430	253.6870	-0.0440	cm^{-1}
17	7	11	15	5	11	255.9240	255.9581	-0.0341	cm^{-1}
18	7	12	16	5	12	258.2340	258.2277	0.0063	cm^{-1}
19	7	13	17	5	13	260.4960	260.4957	0.0003	cm^{-1}
20	7	14	18	5	14	262.7380	262.7620	-0.0240	cm^{-1}
21	7	15	19	5	15	265.0080	265.0267	-0.0187	cm^{-1}
22	7	16	20	5	16	267.2570	267.2895	-0.0325	cm^{-1}
23	7	17	21	5	17	269.5580	269.5505	0.0075	cm^{-1}
24	7	18	22	5	18	271.8010	271.8095	-0.0085	cm^{-1}
25	7	19	23	5	19	274.0790	274.0666	0.0124	cm^{-1}
5	5	0	3	3	0	156.3430	156.3740	-0.0310	cm^{-1}
6	5	1	4	3	1	158.6170	158.6614	-0.0444	cm^{-1}
7	5	2	5	3	2	160.8900	160.9479	-0.0579	cm^{-1}
8	5	3	6	3	3	163.3330	163.2337	0.0993	cm^{-1}
9	5	4	7	3	4	165.5380	165.5185	0.0195	cm^{-1}
10	5	5	8	3	5	167.7990	167.8024	-0.0034	cm^{-1}
11	5	6	9	3	6	170.1010	170.0851	0.0159	cm^{-1}
12	5	7	10	3	7	172.3230	172.3667	-0.0437	cm^{-1}
13	5	8	11	3	8	174.6740	174.6469	0.0271	cm^{-1}
14	5	9	12	3	9	176.8930	176.9257	-0.0327	cm^{-1}
15	5	10	13	3	10	179.1450	179.2029	-0.0579	cm^{-1}
16	5	11	14	3	11	181.4440	181.4783	-0.0343	cm^{-1}
17	5	12	15	3	12	183.7540	183.7517	0.0023	cm^{-1}
18	5	13	16	3	13	185.9990	186.0230	-0.0240	cm^{-1}
19	5	14	17	3	14	188.2720	188.2920	-0.0200	cm^{-1}
20	5	15	18	3	15	190.5710	190.5584	0.0126	cm^{-1}
21	5	16	19	3	16	192.8250	192.8219	0.0031	cm^{-1}
22	5	17	20	3	17	195.0810	195.0823	-0.0013	cm^{-1}
23	5	18	21	3	18	197.3260	197.3392	-0.0132	cm^{-1}
24	5	19	22	3	19	199.5900	199.5924	-0.0024	cm^{-1}
9	7	3	9	5	5	218.2450	218.2886	-0.0436	cm^{-1}
10	7	4	10	5	6	218.3190	218.2799	0.0391	cm^{-1}
11	7	5	11	5	7	218.2270	218.2702	-0.0432	cm^{-1}
12	7	6	12	5	8	218.2470	218.2595	-0.0125	cm^{-1}
13	7	7	13	5	9	218.2680	218.2479	0.0201	cm^{-1}
14	7	8	14	5	10	218.3000	218.2352	0.0648	cm^{-1}
15	7	9	15	5	11	218.2760	218.2214	0.0546	cm^{-1}
16	7	10	16	5	12	218.2210	218.2066	0.0144	cm^{-1}
17	7	11	17	5	13	218.2410	218.1907	0.0503	cm^{-1}

CH_2S Combination Differences - continued

Upper State			Lower State			Observation	Calculation	Residual	Remarks
J	K_A	K_C	J	K_A	K_C				
18	7	12	18	5	14	218.1930	218.1735	0.0195	cm^{-1}
20	7	14	20	5	16	218.1440	218.1357	0.0083	cm^{-1}
21	7	15	21	5	17	218.0720	218.1149	-0.0429	cm^{-1}
22	7	16	22	5	18	218.1410	218.0928	0.0482	cm^{-1}
7	7	0	6	5	2	226.3550	226.3176	0.0374	cm^{-1}
8	7	1	7	5	3	227.4810	227.4553	0.0050	cm^{-1}
9	7	2	8	5	4	228.5830	228.5921	-0.0091	cm^{-1}
10	7	3	9	5	5	229.7320	229.7279	0.0041	cm^{-1}
11	7	4	10	5	6	230.8580	230.8625	-0.0045	cm^{-1}
12	7	5	11	5	7	231.9910	231.9961	-0.0051	cm^{-1}
13	7	6	12	5	8	233.1510	233.1285	0.0225	cm^{-1}
14	7	7	13	5	9	234.2760	234.2598	0.0162	cm^{-1}
15	7	8	14	5	10	235.4340	235.3898	0.0442	cm^{-1}
16	7	9	15	5	11	236.5430	236.5186	0.0244	cm^{-1}
17	7	10	16	5	12	237.6710	237.6461	0.0249	cm^{-1}
18	7	11	17	5	13	238.8210	238.7723	0.0487	cm^{-1}
19	7	12	18	5	14	239.9110	239.8970	0.0140	cm^{-1}
20	7	13	19	5	15	240.9290	241.0203	-0.0913	cm^{-1}
21	7	14	20	5	16	242.1280	242.1421	-0.0141	cm^{-1}
22	7	15	21	5	17	243.2770	243.2623	0.0147	cm^{-1}
23	7	16	22	5	18	244.4740	244.3809	0.0931	cm^{-1}
24	7	17	23	5	19	245.4930	245.4979	-0.0049	cm^{-1}
5	5	1	4	3	1	151.8090	151.7919	0.0171	cm^{-1}
6	5	2	5	3	2	152.9030	152.9337	-0.0307	cm^{-1}
7	5	3	6	3	3	154.0090	154.0748	-0.0658	cm^{-1}
8	5	4	7	3	4	155.2080	155.2151	-0.0071	cm^{-1}
9	5	5	8	3	5	156.3510	156.3544	-0.0034	cm^{-1}
10	5	6	9	3	6	157.4730	157.4928	-0.0198	cm^{-1}
11	5	7	10	3	7	158.6110	158.6301	-0.0191	cm^{-1}
12	5	8	11	3	8	159.7460	159.7663	-0.0203	cm^{-1}
13	5	9	12	3	9	160.9030	160.9011	0.0019	cm^{-1}
14	5	10	13	3	10	162.0440	162.0345	0.0095	cm^{-1}
15	5	11	14	3	11	163.1400	163.1662	-0.0262	cm^{-1}
16	5	12	15	3	12	164.2240	164.2963	-0.0723	cm^{-1}
17	5	13	16	3	13	165.4050	165.4243	-0.0193	cm^{-1}
18	5	14	17	3	14	166.5430	166.5502	-0.0072	cm^{-1}
19	5	15	18	3	15	167.6400	167.6738	-0.0338	cm^{-1}
20	5	16	19	3	16	168.8050	168.7947	0.0103	cm^{-1}
21	5	17	20	3	17	169.9550	169.9127	0.0423	cm^{-1}
22	5	18	21	3	18	171.0130	171.0276	-0.0146	cm^{-1}
23	5	19	22	3	19	172.1250	172.1389	-0.0139	cm^{-1}
24	5	20	23	3	20	173.2790	173.2464	0.0326	cm^{-1}
25	5	21	24	3	21	174.3810	174.3496	0.0314	cm^{-1}
5	5	1	4	3	1	151.7540	151.7919	-0.0379	cm^{-1}
6	5	2	5	3	2	152.8950	152.9337	-0.0387	cm^{-1}
7	5	3	6	3	3	154.1920	154.0748	0.1172	cm^{-1}
8	5	4	7	3	4	155.1870	155.2151	-0.0281	cm^{-1}
9	5	5	8	3	5	156.2960	156.3544	-0.0584	cm^{-1}
10	5	6	9	3	6	157.5090	157.4928	0.0162	cm^{-1}
11	5	7	10	3	7	158.5900	158.6301	-0.0401	cm^{-1}

CH_2S Combination Differences - continued

Upper State			Lower State			Observation	Calculation		Residual	Remarks
J	K_A	K_C	J	K_A	K_C					
12	5	8	11	3	8	159.7660	159.7663		-0.0003	cm^{-1}
13	5	9	12	3	9	160.8460	160.9011		-0.0551	cm^{-1}
14	5	10	13	3	10	161.9760	161.0345		-0.0585	cm^{-1}
15	5	11	14	3	11	163.1760	163.1662		0.0098	cm^{-1}
16	5	12	15	3	12	164.3060	164.2963		0.0097	cm^{-1}
17	5	13	16	3	13	165.3860	165.4243		-0.0383	cm^{-1}
18	5	14	17	3	14	166.5140	166.5502		-0.0362	cm^{-1}
19	5	15	18	3	15	167.6700	167.6738		-0.0038	cm^{-1}
20	5	16	19	3	16	168.7870	168.7947		-0.0077	cm^{-1}
21	5	17	20	3	17	169.8390	169.9127		-0.0737	cm^{-1}
22	5	18	21	3	18	171.0320	171.0276		0.0044	cm^{-1}
23	5	19	22	3	19	172.1340	172.1389		-0.0049	cm^{-1}
24	5	20	23	3	20	173.3430	173.2464		0.0966	cm^{-1}
25	5	21	24	3	21	174.3700	174.3496		0.0204	cm^{-1}
10	7	3	9	7	3	11.4940	11.4392		0.0548	cm^{-1}
11	7	4	10	7	4	12.6080	12.5826		0.0254	cm^{-1}
12	7	5	11	7	5	13.7840	13.7259		0.0581	cm^{-1}
13	7	6	12	7	6	14.8710	14.8690		0.0020	cm^{-1}
14	7	7	13	7	7	16.0290	16.0119		0.0171	cm^{-1}
15	7	8	14	7	8	17.1380	17.1547		-0.0167	cm^{-1}
16	7	9	15	7	9	18.3090	18.2972		0.0118	cm^{-1}
17	7	10	16	7	10	19.4710	19.4395		0.0315	cm^{-1}
18	7	11	17	7	11	20.5820	20.5816		0.0004	cm^{-1}
19	7	12	18	7	12	21.7200	21.7235		-0.0035	cm^{-1}
20	7	13	19	7	13	22.8610	22.8650		-0.0040	cm^{-1}
21	7	14	20	7	14	23.9860	24.0064		-0.0204	cm^{-1}
10	6	5	9	6	3	11.3430	11.4439		-0.1009	cm^{-1}
11	6	6	10	6	4	12.4880	12.5878		-0.0998	cm^{-1}
12	6	7	11	6	5	13.5950	13.7316	*	-0.1366	cm^{-1}
13	6	8	12	6	6	14.8570	14.8752		-0.0182	cm^{-1}
14	6	9	13	6	7	15.9590	16.0186		-0.0596	cm^{-1}
15	6	10	14	6	8	17.1070	17.1619		-0.0549	cm^{-1}
16	6	11	15	6	9	18.2570	18.3050		-0.0480	cm^{-1}
17	6	12	16	6	10	19.4280	19.4479		-0.0199	cm^{-1}
18	6	13	17	6	11	20.6000	20.5905		0.0095	cm^{-1}
19	6	14	18	6	12	21.7510	21.7330		0.0180	cm^{-1}
20	6	15	19	6	13	22.7400	22.8752	*	-0.1352	cm^{-1}
21	6	16	20	6	14	23.9430	24.0171		-0.0741	cm^{-1}
22	6	17	21	6	15	25.1430	25.1588		-0.0158	cm^{-1}
24	6	19	23	6	17	27.4930	27.4413		0.0517	cm^{-1}
6	5	1	5	5	1	6.9070	6.8695		0.0375	cm^{-1}
7	5	2	6	5	2	8.0580	8.0142		0.0438	cm^{-1}
8	5	3	7	5	3	9.1750	9.1589		0.0161	cm^{-1}
9	5	4	8	5	4	10.3000	10.3035		-0.0035	cm^{-1}
10	5	5	9	5	5	11.4910	11.4480		0.0430	cm^{-1}
11	5	6	10	5	6	12.5880	12.5923		-0.0043	cm^{-1}
12	5	7	11	5	7	13.7730	13.7366		0.0364	cm^{-1}
13	5	8	12	5	8	14.8220	14.8807		-0.0587	cm^{-1}
14	5	9	13	5	9	15.9520	16.0246		-0.0726	cm^{-1}
15	5	10	14	5	10	17.1000	17.1684		-0.0684	cm^{-1}

CH_2S Combination Differences – continued

Upper State			Lower State			Observation	Calculation	Residual	Remarks
J	K_A	K_C	J	K_A	K_C				
16	5	11	15	5	11	18.2530	18.3120	-0.0590	cm^{-1}
17	5	12	16	5	12	19.4130	19.4555	-0.0425	cm^{-1}
18	5	13	17	5	13	20.5850	20.5987	-0.0137	cm^{-1}
19	5	14	18	5	14	21.8090	21.7418	0.0672	cm^{-1}
20	5	15	19	5	15	22.8800	22.8846	-0.0046	cm^{-1}
21	5	16	20	5	16	23.9800	24.0272	-0.0472	cm^{-1}
22	5	17	21	5	17	25.0840	25.1695	-0.0855	cm^{-1}
23	5	18	22	5	18	26.3080	26.3117	-0.0037	cm^{-1}
24	5	19	23	5	19	27.3860	27.4535	-0.0675	cm^{-1}
25	5	20	24	5	20	28.5250	28.5951	-0.0701	cm^{-1}
5	4	2	4	4	0	5.7420	5.7263	0.0157	cm^{-1}
6	4	3	5	4	1	6.9460	6.8715	0.0745	cm^{-1}
7	4	4	6	4	2	8.0730	8.0166	0.0564	cm^{-1}
8	4	5	7	4	3	9.2020	9.1616	0.0404	cm^{-1}
9	4	6	8	4	4	10.3310	10.3066	0.0244	cm^{-1}
10	4	7	9	4	5	11.4460	11.4515	-0.0055	cm^{-1}
11	4	8	10	4	6	12.5580	12.5963	-0.0383	cm^{-1}
12	4	9	11	4	7	13.8390	13.7410	0.0980	cm^{-1}
13	4	10	12	4	8	14.8630	14.8857	-0.0227	cm^{-1}
14	4	11	13	4	9	15.9900	16.0301	-0.0401	cm^{-1}
15	4	12	14	4	10	17.1130	17.1745	-0.0615	cm^{-1}
16	4	13	15	4	11	18.4040	18.3187	0.0853	cm^{-1}
17	4	14	16	4	12	19.4570	19.4628	-0.0058	cm^{-1}
18	4	15	17	4	13	20.6370	20.6067	0.0303	cm^{-1}
19	4	16	18	4	14	21.7130	21.7505	-0.0375	cm^{-1}
4	3	1	3	3	1	4.5340	4.5821	-0.0481	cm^{-1}
5	3	2	4	3	2	5.7140	5.7277	-0.0137	cm^{-1}
6	3	3	5	3	3	6.8810	6.8732	0.0078	cm^{-1}
7	3	4	6	3	4	8.1220	8.0187	0.1033	cm^{-1}
8	3	5	7	3	5	9.1870	9.1642	0.0228	cm^{-1}
9	3	6	8	3	6	10.3310	10.3097	0.0213	cm^{-1}
10	3	7	9	3	7	11.4900	11.4552	0.0348	cm^{-1}
11	3	8	10	3	8	12.5770	12.6007	-0.0237	cm^{-1}
12	3	9	11	3	9	13.7710	13.7464	0.0246	cm^{-1}
13	3	10	12	3	10	14.8490	14.8921	-0.0431	cm^{-1}
14	3	11	13	3	11	16.0050	16.0380	-0.0330	cm^{-1}
15	3	12	14	3	12	17.2200	17.1842	0.0358	cm^{-1}
16	3	13	15	3	13	18.3490	18.3307	0.0183	cm^{-1}
17	3	14	16	3	14	19.4560	19.4776	-0.0216	cm^{-1}
18	3	15	17	3	15	20.6320	20.6250	0.0070	cm^{-1}
19	3	16	18	3	16	21.7660	21.7732	-0.0072	cm^{-1}
20	3	17	19	3	17	22.8700	22.9223	-0.0523	cm^{-1}
21	3	18	20	3	18	24.0680	24.0724	-0.0044	cm^{-1}
22	3	19	21	3	19	25.2010	25.2239	-0.0229	cm^{-1}
23	3	20	22	3	20	26.3110	26.3770	-0.0660	cm^{-1}
24	3	21	23	3	21	27.5250	27.5321	-0.0071	cm^{-1}
25	3	22	24	3	22	28.6280	28.6895	-0.0615	cm^{-1}
10	7	3	9	7	3	11.4870	11.4392	0.0478	cm^{-1}
11	7	4	10	7	4	12.5390	12.5826	-0.0436	cm^{-1}
12	7	5	11	7	5	13.7640	13.7259	0.0381	cm^{-1}

CH_2S Combination Differences - continued

Upper State			Lower State			Observation	Calculation	Residual	Remarks
J	K_A	K_C	J	K_A	K_C				
13	7	6	12	7	6	14.9040	14.8690	0.0350	cm^{-1}
14	7	7	13	7	7	16.0080	16.0119	-0.0039	cm^{-1}
15	7	8	14	7	8	17.1340	17.1547	-0.0207	cm^{-1}
16	7	9	15	7	9	18.2670	18.2972	-0.0302	cm^{-1}
17	7	10	16	7	10	19.4500	19.4395	0.0105	cm^{-1}
18	7	11	17	7	11	20.5800	20.5816	-0.0016	cm^{-1}
19	7	12	18	7	12	21.7180	21.7235	-0.0055	cm^{-1}
20	7	13	19	7	13	22.8470	22.8650	-0.0180	cm^{-1}
21	7	14	20	7	14	23.9840	24.0064	-0.0224	cm^{-1}
22	7	15	21	7	15	25.2050	25.1474	0.0576	cm^{-1}
23	7	16	22	7	16	26.3330	26.2882	0.0448	cm^{-1}
24	7	17	23	7	17	27.4140	27.4286	-0.0146	cm^{-1}
25	7	18	24	7	18	28.6010	28.5687	0.0323	cm^{-1}
6	5	2	5	5	0	6.8630	6.8695	-0.0065	cm^{-1}
7	5	3	6	5	1	7.9950	8.0142	-0.0192	cm^{-1}
8	5	4	7	5	2	9.1380	9.1589	-0.0209	cm^{-1}
9	5	5	8	5	3	10.3510	10.3035	0.0475	cm^{-1}
10	5	6	9	5	4	11.5030	11.4480	0.0550	cm^{-1}
11	5	7	10	5	5	12.5920	12.5923	-0.0003	cm^{-1}
12	5	8	11	5	6	13.7330	13.7366	-0.0036	cm^{-1}
13	5	9	12	5	7	14.9080	14.8807	0.0273	cm^{-1}
14	5	10	13	5	8	16.0470	16.0246	0.0224	cm^{-1}
15	5	11	14	5	9	17.1690	17.1684	0.0006	cm^{-1}
16	5	12	15	5	10	18.2680	18.3120	-0.0440	cm^{-1}
17	5	13	16	5	11	19.4480	19.4555	-0.0075	cm^{-1}
18	5	14	17	5	12	20.6130	20.5987	0.0143	cm^{-1}
19	5	15	18	5	13	21.7580	21.7418	0.0162	cm^{-1}
20	5	16	19	5	14	22.9010	22.8846	0.0164	cm^{-1}
21	5	17	20	5	15	24.0380	24.0272	0.0108	cm^{-1}
22	5	18	21	5	16	25.2420	25.1695	0.0725	cm^{-1}
23	5	19	22	5	17	26.2940	26.3116	-0.0176	cm^{-1}
24	5	20	23	5	18	27.4560	27.4535	0.0025	cm^{-1}
4	3	2	3	3	0	4.6050	4.5821	0.0229	cm^{-1}
5	3	3	4	3	1	5.7060	5.7277	-0.0217	cm^{-1}
6	3	4	5	3	2	6.8730	6.8731	-0.0001	cm^{-1}
7	3	5	6	3	3	8.0300	8.0186	0.0114	cm^{-1}
8	3	6	7	3	4	9.1260	9.1640	-0.0380	cm^{-1}
9	3	7	8	3	5	10.3350	10.3094	0.0256	cm^{-1}
10	3	8	9	3	6	11.4850	11.4547	0.0303	cm^{-1}
11	3	9	10	3	7	12.5500	12.5999	-0.0499	cm^{-1}
12	3	10	11	3	8	13.7440	13.7450	-0.0010	cm^{-1}
13	3	11	12	3	9	14.8670	14.8898	-0.0228	cm^{-1}
14	3	12	13	3	10	16.0260	16.0344	-0.0084	cm^{-1}
15	3	13	14	3	11	17.1460	17.1787	-0.0327	cm^{-1}
15	3	12	14	3	12	17.1460	17.1842	-0.0382	cm^{-1}
16	3	14	15	3	12	18.2780	18.3226	-0.0446	cm^{-1}
16	3	13	15	3	13	18.3060	18.3307	-0.0247	cm^{-1}
17	3	15	16	3	13	19.4520	19.4660	-0.0140	cm^{-1}
17	3	14	16	3	14	19.4630	19.4776	-0.0146	cm^{-1}
18	3	16	17	3	14	20.6200	20.6087	0.0113	cm^{-1}

Upper State			Lower State			Observation	Calculation	Residual	Remarks
J	K_A	K_C	J	K_A	K_C				
18	3	15	17	3	15	20.5740	20.6250	-0.0510	cm^{-1}
19	3	17	18	3	15	21.7070	21.7506	-0.0436	cm^{-1}
19	3	16	18	3	16	21.8310	21.7732	0.0578	cm^{-1}
20	3	18	19	3	16	22.9110	22.8914	0.0196	cm^{-1}
20	3	17	19	3	17	22.9400	22.9223	0.0177	cm^{-1}
21	3	19	20	3	17	24.1060	24.0311	0.0749	cm^{-1}
21	3	18	20	3	18	24.0480	24.0724	-0.0244	cm^{-1}
22	3	20	21	3	18	25.1920	25.1693	0.0227	cm^{-1}
22	3	19	21	3	19	25.3140	25.2239	0.0901	cm^{-1}
23	3	21	22	3	19	26.3320	26.3058	0.0262	cm^{-1}
23	3	20	22	3	20	26.3940	26.3770	0.0170	cm^{-1}
24	3	22	23	3	20	27.5290	27.4401	0.0889	cm^{-1}
24	3	21	23	3	21	27.4380	27.5321	-0.0941	cm^{-1}
4	4	1	2	2	1	117.6610	117.7073	-0.0463	cm^{-1}
5	4	2	3	2	2	119.9670	119.9966	-0.0296	cm^{-1}
6	4	3	4	2	3	122.2620	122.2855	-0.0235	cm^{-1}
7	4	4	5	2	4	124.5180	124.5741	-0.0561	cm^{-1}
8	4	5	6	2	5	126.8410	126.8625	-0.0215	cm^{-1}
9	4	6	7	2	6	129.0660	129.1509	-0.0849	cm^{-1}
10	4	7	8	2	7	131.4370	131.4393	-0.0023	cm^{-1}
11	4	8	9	2	8	133.7120	133.7280	-0.0160	cm^{-1}
12	4	9	10	2	9	135.9230	136.0171	-0.0941	cm^{-1}
13	4	10	11	2	10	138.2640	138.3069	-0.0429	cm^{-1}
4	4	0	3	2	2	114.2430	114.2702	-0.0272	cm^{-1}
5	4	1	4	2	3	115.4380	115.4140	0.0240	cm^{-1}
6	4	2	5	2	4	116.5550	116.5575	-0.0025	cm^{-1}
7	4	3	6	2	5	117.7360	117.7009	0.0351	cm^{-1}
8	4	4	7	2	6	118.8460	118.8443	0.0017	cm^{-1}
9	4	5	8	2	7	119.9430	119.9878	-0.0448	cm^{-1}
9	7	2	8	5	3	228.5450	228.5921	-0.0471	cm^{-1}
10	7	3	9	5	4	229.8050	229.7279	0.0771	cm^{-1}
11	7	4	10	5	5	230.8150	230.8625	-0.0475	cm^{-1}
12	7	5	11	5	6	232.0250	231.9961	0.0289	cm^{-1}
13	7	6	12	5	7	233.0900	233.1285	-0.0385	cm^{-1}
14	7	7	13	5	8	234.2520	234.2598	-0.0078	cm^{-1}
15	7	8	14	5	9	235.3760	235.3898	-0.0138	cm^{-1}
16	7	9	15	5	10	236.4740	236.5186	-0.0446	cm^{-1}
17	7	10	16	5	11	237.6540	237.6461	0.0079	cm^{-1}
18	7	11	17	5	12	238.7780	238.7723	0.0057	cm^{-1}
19	7	12	18	5	13	239.8910	239.8970	-0.0060	cm^{-1}
20	7	13	19	5	14	241.0240	241.0203	0.0037	cm^{-1}
21	7	14	20	5	15	242.0520	242.1421	-0.0901	cm^{-1}
22	7	15	21	5	16	243.2250	243.2623	-0.0373	cm^{-1}
23	7	16	22	5	17	244.3870	244.3809	0.0061	cm^{-1}
24	7	17	23	5	18	245.4780	245.4979	-0.0199	cm^{-1}
25	7	10	24	5	19	246.6380	246.6131	0.0249	cm^{-1}
3	3	0	1	1	0	78.9510	78.9029	0.0481	cm^{-1}
3	3	1	1	1	1	78.9510	78.9378	0.0132	cm^{-1}
4	3	1	2	1	1	81.1130	81.1585	-0.0455	cm^{-1}
4	3	2	2	1	2	81.2580	81.2632	-0.0052	cm^{-1}

Upper State			Lower State			Observation	Calculation	Residual	Remarks
J	K_A	K_C	J	K_A	K_C				
5	3	2	3	1	2	83.3640	83.3965	-0.0325	cm^{-1}
5	3	3	3	1	3	83.5560	83.6060	-0.0500	cm^{-1}
6	3	3	4	1	3	85.6450	85.6170	0.0280	cm^{-1}
6	3	4	4	1	4	85.9240	85.9661	-0.0421	cm^{-1}
7	3	4	5	1	4	87.8170	87.8202	-0.0032	cm^{-1}
7	3	5	5	1	5	88.4330	88.3437	0.0893	cm^{-1}
8	3	5	6	1	5	89.9430	90.0061	-0.0631	cm^{-1}
8	3	6	6	1	6	90.6800	90.7389	-0.0589	cm^{-1}
9	3	6	7	1	6	92.2150	92.1751	0.0399	cm^{-1}
9	3	7	7	1	7	93.1590	93.1521	0.0069	cm^{-1}
10	3	7	8	1	7	94.2490	94.3275	-0.0785	cm^{-1}
10	3	8	8	1	8	95.5820	95.5833	-0.0013	cm^{-1}
11	3	8	9	1	8	96.3430	96.4635	-0.1250	cm^{-1}
11	3	9	9	1	9	98.0220	98.0330	-0.0110	cm^{-1}
12	3	9	10	1	9	98.5720	98.5835	-0.0115	cm^{-1}
12	3	10	10	1	10	100.5040	100.5012	0.0028	cm^{-1}
13	3	10	11	1	10	100.5890	100.6880	-0.0990	cm^{-1}
13	3	11	11	1	11	102.9660	102.9885	-0.0225	cm^{-1}
14	3	11	12	1	11	102.7320	102.7774	-0.0454	cm^{-1}
14	3	12	12	1	12	105.4490	105.4951	-0.0461	cm^{-1}
15	3	12	13	1	12	104.7390	104.8522	-0.1132	cm^{-1}
15	3	13	13	1	13	108.0440	108.0214	0.0226	cm^{-1}
16	3	13	14	1	13	107.0170	106.9130	0.1040	cm^{-1}
16	3	14	14	1	14	110.5570	110.5677	-0.0107	cm^{-1}
17	3	14	15	1	14	108.9270	108.9604	-0.0334	cm^{-1}
17	3	15	15	1	15	113.1000	113.1346	-0.0346	cm^{-1}
18	3	15	16	1	15	110.9020	110.9952	-0.0932	cm^{-1}
18	3	16	16	1	16	115.7230	115.7223	0.0007	cm^{-1}
19	3	16	17	1	16	112.9650	113.0180	-0.0530	cm^{-1}
19	3	17	17	1	17	118.2910	118.3313	-0.0403	cm^{-1}
20	3	17	18	1	17	115.0470	115.0297	0.0173	cm^{-1}
20	3	18	18	1	18	120.9430	120.9621	-0.0191	cm^{-1}
21	3	18	19	1	18	116.9660	117.0312	-0.0652	cm^{-1}
21	3	19	19	1	19	123.6630	123.6152	0.0478	cm^{-1}
22	3	19	20	1	19	119.0420	119.0234	0.0186	cm^{-1}
22	3	20	20	1	20	126.2670	126.2909	-0.0239	cm^{-1}
3	3	0	3	1	2	72.9980	73.0867	-0.0887	cm^{-1}
3	3	1	3	1	3	73.2440	73.2962	-0.0522	cm^{-1}
4	3	1	4	1	3	72.9870	73.0162	-0.0292	cm^{-1}
4	3	2	4	1	4	73.4220	73.3653	0.0567	cm^{-1}
5	3	2	5	1	4	72.9300	72.9284	0.0016	cm^{-1}
5	3	3	5	1	5	73.4520	73.4519	0.0001	cm^{-1}
6	3	3	6	1	5	72.8080	72.8233	-0.0153	cm^{-1}
6	3	4	6	1	6	73.5140	73.5562	-0.0422	cm^{-1}
7	3	4	7	1	6	72.6880	72.7014	-0.0134	cm^{-1}
7	3	5	7	1	7	73.6740	73.6785	-0.0045	cm^{-1}
8	3	5	8	1	7	72.5850	72.5629	0.0221	cm^{-1}
8	3	6	8	1	8	73.8300	73.8190	0.0110	cm^{-1}
9	3	6	9	1	8	72.3100	72.4080	-0.0980	cm^{-1}
9	3	7	9	1	9	73.8720	73.9779	-0.1059	cm^{-1}

Upper State			Lower State			Observation	Calculation	Residual	Remarks
J	K_A	K_C	J	K_A	K_C				
10	3	7	10	1	9	72.3000	72.2372	0.0628	cm^{-1}
10	3	8	10	1	10	74.1730	74.1555	0.0175	cm^{-1}
11	3	8	11	1	10	72.0640	72.0509	0.0131	cm^{-1}
11	3	9	11	1	11	74.3740	74.3523	0.0217	cm^{-1}
12	3	9	12	1	11	71.8630	71.8495	0.0135	cm^{-1}
12	3	10	12	1	12	74.5010	74.5685	-0.0675	cm^{-1}
13	3	10	13	1	12	71.6430	71.6335	0.0095	cm^{-1}
13	3	11	13	1	13	74.7440	74.8046	-0.0606	cm^{-1}
14	3	11	14	1	13	71.4580	71.4036	0.0544	cm^{-1}
14	3	12	14	1	14	75.0930	75.0609	0.0321	cm^{-1}
15	3	12	15	1	14	71.1290	71.1602	-0.0312	cm^{-1}
15	3	13	15	1	15	75.3850	75.3379	0.0471	cm^{-1}
16	3	13	16	1	15	70.8630	70.9042	-0.0412	cm^{-1}
16	3	14	16	1	16	75.6260	75.6360	-0.0100	cm^{-1}
17	3	14	17	1	16	70.6480	70.6361	0.0119	cm^{-1}
17	3	15	17	1	17	75.9980	75.9557	0.0423	cm^{-1}
18	3	15	18	1	17	70.3260	70.3569	-0.0309	cm^{-1}
18	3	16	18	1	18	76.2610	76.2975	-0.0365	cm^{-1}
19	3	16	19	1	18	70.0480	70.0673	0.0190	cm^{-1}
19	3	17	19	1	19	76.6230	76.6618	-0.0388	cm^{-1}
20	3	17	20	1	19	69.7150	69.7683	-0.0533	cm^{-1}
20	3	18	20	1	20	77.0440	77.0492	-0.0052	cm^{-1}
21	3	18	21	1	20	69.4220	69.4609	-0.0389	cm^{-1}
21	3	19	21	1	21	77.4240	77.4601	-0.0361	cm^{-1}
6	1	6	5	1	4	6.2560	6.2453	0.0107	cm^{-1}
7	1	7	6	1	5	7.1750	7.1635	0.0115	cm^{-1}
8	1	8	7	1	6	8.0460	8.0465	-0.0005	cm^{-1}
9	1	9	8	1	7	8.8790	8.8944	-0.0154	cm^{-1}
10	1	10	9	1	8	9.6870	9.7072	-0.0202	cm^{-1}
11	1	11	10	1	9	10.4820	10.4848	-0.0028	cm^{-1}
12	1	12	11	1	10	11.1970	11.2273	-0.0303	cm^{-1}
13	1	13	12	1	11	11.9040	11.9347	-0.0307	cm^{-1}
14	1	14	13	1	12	12.5720	12.6071	-0.0351	cm^{-1}
15	1	15	14	1	13	13.2650	13.2444	0.0206	cm^{-1}
16	1	16	15	1	14	13.8370	13.8468	-0.0098	cm^{-1}
17	1	17	16	1	15	14.4210	14.4144	0.0066	cm^{-1}
18	1	18	17	1	16	15.0250	14.9473	0.0777	cm^{-1}
19	1	19	18	1	17	15.4450	15.4456	-0.0006	cm^{-1}
20	1	20	19	1	18	15.9150	15.9096	0.0054	cm^{-1}
21	1	21	20	1	19	16.3490	16.3394	0.0096	cm^{-1}
22	1	22	21	1	20	16.7500	16.7352	0.0148	cm^{-1}

CD_2S: GROUND STATE COMBINATION DIFFERENCES

Upper State			Lower State			Observation	Calculation	Residual	Remarks
J	K_A	K_C	J	K_A	K_C				
1	0	1	0	0	0	28400.050	28400.027	0.022	mhz
2	1	2	1	1	1	55390.020	55390.165	-0.145	mhz
2	0	2	1	0	1	56788.780	56788.741	0.038	mhz
2	1	1	1	1	0	58206.900	58207.403	-0.503	mhz
2	2	1	1	0	1	19.502	19.525	-0.023	cm^{-1}
3	2	2	2	0	2	20.471	20.473	-0.002	cm^{-1}
4	2	3	3	0	3	21.343	21.421	-0.078	cm^{-1}
5	2	4	4	0	4	22.335	22.371	-0.036	cm^{-1}
6	2	5	5	0	5	23.450	23.323	0.126	cm^{-1}
7	2	6	6	0	6	24.296	24.280	0.015	cm^{-1}
8	2	7	7	0	7	25.261	25.243	0.017	cm^{-1}
9	2	8	8	0	8	26.247	26.214	0.032	cm^{-1}
10	2	9	9	0	9	27.177	27.196	-0.019	cm^{-1}
11	2	10	10	0	10	28.205	28.190	0.014	cm^{-1}
12	2	11	11	0	11	29.210	29.201	0.009	cm^{-1}
13	2	12	12	0	12	30.227	30.229	-0.002	cm^{-1}
14	2	13	13	0	13	31.274	31.279	-0.005	cm^{-1}
15	2	14	14	0	14	32.339	32.353	-0.014	cm^{-1}
16	2	15	15	0	15	33.461	33.453	0.007	cm^{-1}
17	2	16	16	0	16	34.620	34.583	0.037	cm^{-1}
18	2	17	17	0	17	35.674	35.743	-0.069	cm^{-1}
19	2	18	18	0	18	36.874	36.936	-0.062	cm^{-1}
20	2	19	19	0	19	38.177	38.162	0.014	cm^{-1}
2	2	0	2	0	2	17.531	17.631	-0.100	cm^{-1}
3	2	1	3	0	3	17.625	17.634	-0.009	cm^{-1}
4	2	2	4	0	4	17.662	17.641	0.020	cm^{-1}
5	2	3	5	0	5	17.727	17.655	0.071	cm^{-1}
6	2	4	6	0	6	17.761	17.679	0.081	cm^{-1}
7	2	5	7	0	7	17.693	17.717	-0.024	cm^{-1}
8	2	6	8	0	8	17.795	17.775	0.019	cm^{-1}
9	2	7	9	0	9	17.887	17.856	0.030	cm^{-1}
10	2	8	10	0	10	18.049	17.968	0.080	cm^{-1}
11	2	9	11	0	11	18.132	18.116	0.015	cm^{-1}
12	2	10	12	0	12	18.207	18.307	-0.100	cm^{-1}
13	2	11	13	0	13	18.626	18.546	0.079	cm^{-1}
14	2	12	14	0	14	18.794	18.841	-0.047	cm^{-1}
15	2	13	15	0	15	19.167	19.197	-0.030	cm^{-1}
16	2	14	16	0	16	19.658	19.620	0.037	cm^{-1}
17	2	15	17	0	17	20.124	20.116	0.007	cm^{-1}
18	2	16	18	0	18	20.680	20.688	-0.008	cm^{-1}
19	2	17	19	0	19	21.267	21.341	-0.072	cm^{-1}
6	2	4	5	2	4	5.679	5.708	-0.029	cm^{-1}
6	2	5	5	2	3	5.679	5.668	0.010	cm^{-1}
7	2	5	6	2	5	6.701	6.674	0.026	cm^{-1}
7	2	6	6	2	4	6.701	6.601	0.099	cm^{-1}
8	2	6	7	2	6	7.637	7.651	-0.014	cm^{-1}
8	2	7	7	2	5	7.637	7.526	0.111	cm^{-1}
9	2	7	8	2	7	8.446	8.641 *	-0.195	cm^{-1}
9	2	8	8	2	6	8.446	8.439	0.006	cm^{-1}
10	2	8	9	2	8	9.558	9.646	-0.088	cm^{-1}

CD_2S: Ground State Combination Differences - cont'd.

Upper State			Lower State			Observation	Calculation	Residual	Remarks
J	K_A	K_C	J	K_A	K_C				
10	2	9	9	2	7	9.558	9.339 *	0.218	cm^{-1}
11	2	9	10	2	9	10.707	10.671	0.035	cm^{-1}
11	2	10	10	2	8	10.157	10.222	-0.065	cm^{-1}
12	2	10	11	2	10	11.691	11.718	-0.027	cm^{-1}
12	2	11	11	2	9	11.072	11.084	-0.012	cm^{-1}
13	2	11	12	2	11	12.694	12.792	-0.098	cm^{-1}
13	2	12	12	2	10	11.953	11.922	0.030	cm^{-1}
14	2	12	13	2	12	13.858	13.895	-0.037	cm^{-1}
14	2	13	13	2	11	12.654	12.733	-0.079	cm^{-1}
15	2	13	14	2	13	15.138	15.031	0.105	cm^{-1}
15	2	14	14	2	12	13.547	13.512	0.034	cm^{-1}
16	2	14	15	2	14	16.270	16.203	0.066	cm^{-1}
16	2	15	15	2	13	14.304	14.256	0.047	cm^{-1}
17	2	15	16	2	15	17.479	17.415	0.063	cm^{-1}
17	2	16	16	2	14	14.988	14.962	0.025	cm^{-1}
18	2	16	17	2	16	18.797	18.668	0.128	cm^{-1}
18	2	17	17	2	15	15.568	15.626	-0.058	cm^{-1}
19	2	17	18	2	17	19.899	19.966	-0.067	cm^{-1}
19	2	18	18	2	16	16.151	16.247	-0.096	cm^{-1}
4	4	0	2	2	0	59.524	59.489	0.034	cm^{-1}
4	4	1	2	2	1	59.524	59.489	0.034	cm^{-1}
5	4	1	3	2	1	61.389	61.382	0.007	cm^{-1}
5	4	2	3	2	2	61.389	61.383	0.005	cm^{-1}
6	4	2	4	2	2	63.288	63.272	0.015	cm^{-1}
6	4	3	4	2	3	63.288	63.278	0.009	cm^{-1}
7	4	3	5	2	3	65.140	65.160	-0.020	cm^{-1}
7	4	4	5	2	4	65.140	65.173	-0.033	cm^{-1}
8	4	4	6	2	4	67.075	67.044	0.030	cm^{-1}
8	4	5	6	2	5	67.075	67.070	0.004	cm^{-1}
9	4	5	7	2	5	68.940	68.922	0.017	cm^{-1}
9	4	6	7	2	6	68.940	68.969	-0.029	cm^{-1}
10	4	6	8	2	6	70.741	70.792	-0.051	cm^{-1}
10	4	7	8	2	7	70.925	70.870	0.054	cm^{-1}
11	4	7	9	2	7	72.542	72.652	-0.110	cm^{-1}
11	4	8	9	2	8	72.731	72.775	-0.044	cm^{-1}
12	4	8	10	2	8	74.486	74.499	-0.013	cm^{-1}
12	4	9	10	2	9	74.635	74.684	-0.049	cm^{-1}
13	4	9	11	2	9	76.284	76.333	-0.049	cm^{-1}
13	4	10	11	2	10	76.635	76.597	0.037	cm^{-1}
14	4	10	12	2	10	78.147	78.148	-0.001	cm^{-1}
14	4	11	12	2	11	78.498	78.517	-0.019	cm^{-1}
15	4	11	13	2	11	79.904	79.945	-0.041	cm^{-1}
15	4	12	13	2	12	80.444	80.444	0.000	cm^{-1}
16	4	12	14	2	12	81.729	81.719	0.009	cm^{-1}
16	4	13	14	2	13	82.453	82.380	0.072	cm^{-1}
17	4	13	15	2	13	83.421	83.469	-0.048	cm^{-1}
17	4	14	15	2	14	84.308	84.325	-0.017	cm^{-1}
18	4	14	16	2	14	85.182	85.193	-0.011	cm^{-1}
18	4	15	16	2	15	86.327	86.281	0.045	cm^{-1}
19	4	15	17	2	15	86.896	86.890	0.006	cm^{-1}

CD_2S: Ground State Combination Differences - cont'd.

Upper State			Lower State			Observation	Calculation	Residual	Remarks
J	K_A	K_C	J	K_A	K_C				
19	4	16	17	2	16	88.243	88.249	-0.006	cm^{-1}
5	5	1	4	3	1	75.177	75.174	0.002	cm^{-1}
6	5	2	5	3	2	76.106	76.118	-0.012	cm^{-1}
7	5	3	6	3	3	77.102	77.063	0.039	cm^{-1}
8	5	4	7	3	4	78.047	78.006	0.040	cm^{-1}
9	5	5	8	3	5	78.943	78.947	-0.004	cm^{-1}
10	5	6	9	3	6	79.839	79.888	-0.049	cm^{-1}
11	5	7	10	3	7	80.854	80.826	0.027	cm^{-1}
12	5	8	11	3	8	81.750	81.762	-0.012	cm^{-1}
13	5	9	12	3	9	82.808	82.695	0.112	cm^{-1}
14	5	10	13	3	10	83.697	83.625	0.071	cm^{-1}
15	5	11	14	3	11	84.524	84.550	-0.026	cm^{-1}
16	5	12	15	3	12	85.406	85.470	-0.064	cm^{-1}
17	5	13	16	3	13	86.353	86.384	-0.031	cm^{-1}
18	5	14	17	3	14	87.305	87.291	0.013	cm^{-1}
7	4	3	6	4	3	6.646	6.630	0.015	cm^{-1}
8	4	4	7	4	4	7.600	7.578	0.021	cm^{-1}
9	4	5	8	4	5	8.551	8.526	0.024	cm^{-1}
10	4	6	9	4	6	9.532	9.474	0.057	cm^{-1}
11	4	7	10	4	7	10.472	10.422	0.049	cm^{-1}
12	4	8	11	4	8	11.434	11.371	0.062	cm^{-1}
13	4	9	12	4	9	12.395	12.320	0.074	cm^{-1}
14	4	10	13	4	10	13.190	13.269	-0.079	cm^{-1}
15	4	11	14	4	11	14.210	14.219	-0.009	cm^{-1}
16	4	12	15	4	12	15.114	15.169	-0.055	cm^{-1}
17	4	13	16	4	13	16.114	16.120	-0.006	cm^{-1}
18	4	14	17	4	14	17.054	17.071	-0.017	cm^{-1}
19	4	15	18	4	15	18.061	18.024	0.037	cm^{-1}
7	7	1	6	5	1	112.102	112.117	-0.015	cm^{-1}
8	7	2	7	5	2	113.134	113.060	0.073	cm^{-1}
9	7	3	8	5	3	113.897	114.002	-0.105	cm^{-1}
10	7	4	9	5	4	114.997	114.943	0.053	cm^{-1}
11	7	5	10	5	5	115.942	115.884	0.057	cm^{-1}
12	7	6	11	5	6	116.779	116.823	-0.044	cm^{-1}
13	7	7	12	5	7	117.770	117.762	0.007	cm^{-1}
14	7	8	13	5	8	118.670	118.700	-0.030	cm^{-1}
15	7	9	14	5	9	119.645	119.637	0.008	cm^{-1}
16	7	10	15	5	10	120.667	120.572	0.094	cm^{-1}
17	7	11	16	5	11	121.497	121.506	-0.009	cm^{-1}
18	7	12	17	5	12	122.386	122.439	-0.053	cm^{-1}
19	7	13	18	5	13	123.363	123.370	-0.007	cm^{-1}
20	7	14	19	5	14	124.329	124.299	0.029	cm^{-1}
7	6	2	6	6	0	6.701	6.627	0.073	cm^{-1}
8	6	3	7	6	1	7.498	7.574	-0.076	cm^{-1}
9	6	4	8	6	2	8.537	8.521	0.016	cm^{-1}
10	6	5	9	6	3	9.410	9.468	-0.058	cm^{-1}
11	6	6	10	6	4	10.444	10.415	0.028	cm^{-1}
12	6	7	11	6	5	11.313	11.362	-0.049	cm^{-1}
13	6	8	12	6	6	12.173	12.309	-0.136	cm^{-1}
14	6	9	13	6	7	13.226	13.257	-0.031	cm^{-1}

CD_2S: Ground State Combination Differences - cont'd.

Upper State			Lower State			Observation	Calculation	Residual	Remarks
J	K_A	K_C	J	K_A	K_C				
15	6	10	14	6	8	14.057	14.204	-0.147	cm^{-1}
16	6	11	15	6	9	15.065	15.152	-0.087	cm^{-1}
17	6	12	16	6	10	16.062	16.100	-0.038	cm^{-1}
18	6	13	17	6	11	17.022	17.048	-0.026	cm^{-1}
20	8	12	20	6	14	122.815	122.810	0.004	cm^{-1}
21	8	13	21	6	15	122.862	122.790	0.071	cm^{-1}
22	8	14	22	6	16	122.827	122.769	0.057	cm^{-1}
23	8	15	23	6	17	122.667	122.747	-0.080	cm^{-1}
24	8	16	24	6	18	122.747	122.722	0.024	cm^{-1}
25	8	17	25	6	19	122.744	122.695	0.048	cm^{-1}
26	8	18	26	6	20	122.649	122.666	-0.017	cm^{-1}
27	8	19	27	6	21	122.674	122.635	0.038	cm^{-1}
28	8	20	28	6	22	122.545	122.602	-0.057	cm^{-1}
10	9	1	8	7	1	158.349	158.315	0.033	cm^{-1}
11	9	2	9	7	2	160.242	160.201	0.041	cm^{-1}
12	9	3	10	7	3	162.172	162.085	0.086	cm^{-1}
13	9	4	11	7	4	163.998	163.969	0.028	cm^{-1}
14	9	5	12	7	5	165.815	165.853	-0.038	cm^{-1}
15	9	6	13	7	6	167.806	167.735	0.070	cm^{-1}
16	9	7	14	7	7	169.615	169.617	-0.002	cm^{-1}
17	9	8	15	7	8	171.491	171.497	-0.006	cm^{-1}
18	9	9	16	7	9	173.401	173.377	0.023	cm^{-1}
19	9	10	17	7	10	175.311	175.256	0.054	cm^{-1}
20	9	11	18	7	11	177.137	177.134	0.002	cm^{-1}
10	8	3	9	8	1	9.511	9.461	0.049	cm^{-1}
11	8	4	10	8	2	10.564	10.407	0.156	cm^{-1}
12	8	5	11	8	3	11.344	11.354	-0.010	cm^{-1}
13	8	6	12	8	4	12.230	12.300	-0.070	cm^{-1}
14	8	7	13	8	5	13.289	13.247	0.041	cm^{-1}
15	8	8	14	8	6	14.176	14.193	-0.017	cm^{-1}
16	8	9	15	8	7	15.078	15.140	-0.062	cm^{-1}
17	8	10	16	8	8	16.064	16.086	-0.022	cm^{-1}
18	8	11	17	8	9	17.044	17.033	0.010	cm^{-1}
19	8	12	18	8	10	17.907	17.980	-0.073	cm^{-1}
20	8	13	19	8	11	18.902	18.927	-0.025	cm^{-1}
12	12	0	10	10	0	213.874	213.837	0.036	cm^{-1}
13	12	1	11	10	1	215.685	215.716	-0.031	cm^{-1}
14	12	2	12	10	2	217.560	217.594	-0.034	cm^{-1}
15	12	3	13	10	3	219.523	219.471	0.051	cm^{-1}
16	12	4	14	10	4	221.335	221.347	-0.012	cm^{-1}
17	12	5	15	10	5	223.229	223.222	0.006	cm^{-1}
10	10	0	8	8	0	175.659	175.645	0.013	cm^{-1}
11	10	1	9	8	1	177.552	177.529	0.022	cm^{-1}
12	10	2	10	8	2	179.483	179.412	0.070	cm^{-1}
13	10	3	11	8	3	181.252	181.295	-0.043	cm^{-1}
14	10	4	12	8	4	183.138	183.176	-0.038	cm^{-1}
15	10	5	13	8	5	185.080	185.057	0.022	cm^{-1}
16	10	6	14	8	6	186.920	186.937	-0.017	cm^{-1}
17	10	7	15	8	7	188.774	188.816	-0.042	cm^{-1}
18	10	8	16	8	8	190.705	190.694	0.010	cm^{-1}

CD_2S: Ground State Combination Differences - cont'd.

Upper State			Lower State			Observation	Calculation	Residual	Remarks
J	K_A	K_C	J	K_A	K_C				
19	10	9	17	8	9	192.618	192.571	0.046	cm^{-1}
20	10	10	18	8	10	194.474	194.448	0.025	cm^{-1}
8	8	0	6	6	0	137.178	137.144	0.033	cm^{-1}
9	8	1	7	6	1	139.009	139.032	-0.023	cm^{-1}
10	8	2	8	6	2	140.925	140.920	0.004	cm^{-1}
11	8	3	9	6	3	142.837	142.807	0.030	cm^{-1}
12	8	4	10	6	4	144.739	144.693	0.045	cm^{-1}
13	8	5	11	6	5	146.507	146.578	-0.071	cm^{-1}
14	8	6	12	6	6	148.426	148.463	-0.037	cm^{-1}
15	8	7	13	6	7	150.361	150.347	0.013	cm^{-1}
16	8	8	14	6	8	152.151	152.230	-0.079	cm^{-1}
17	8	9	15	6	9	154.087	154.112	-0.025	cm^{-1}
18	8	10	16	6	10	155.980	155.993	-0.013	cm^{-1}
19	8	11	17	6	11	157.866	157.873	-0.007	cm^{-1}
20	8	12	18	6	12	159.766	159.751	0.014	cm^{-1}
21	8	13	19	6	13	161.629	161.629	0.000	cm^{-1}
22	8	14	20	6	14	163.530	163.505	0.024	cm^{-1}
23	8	15	21	6	15	165.420	165.380	0.039	cm^{-1}
24	8	16	22	6	16	167.271	167.254	0.016	cm^{-1}
25	8	17	23	6	17	169.153	169.125	0.027	cm^{-1}
26	8	18	24	6	18	171.070	170.996	0.074	cm^{-1}
27	8	19	25	6	19	172.861	172.864	-0.003	cm^{-1}
28	8	20	26	6	20	174.704	174.730	-0.026	cm^{-1}
29	8	21	27	6	21	176.628	176.595	0.032	cm^{-1}
6	6	0	4	4	0	98.363	98.402	-0.039	cm^{-1}
7	6	1	5	4	1	100.293	100.294	-0.001	cm^{-1}
8	6	2	6	4	2	102.209	102.185	0.024	cm^{-1}
9	6	3	7	4	3	104.026	104.075	-0.049	cm^{-1}
10	6	4	8	4	4	105.981	105.964	0.016	cm^{-1}
11	6	5	9	4	5	108.041	107.853	0.187	cm^{-1}
12	6	6	10	4	6	109.718	109.741	-0.023	cm^{-1}
13	6	7	11	4	7	111.613	111.628	-0.015	cm^{-1}
14	6	8	12	4	8	113.446	113.514	-0.068	cm^{-1}
15	6	9	13	4	9	115.353	115.398	-0.045	cm^{-1}
16	6	10	14	4	10	117.424	117.281	0.142	cm^{-1}
17	6	11	15	4	11	119.140	119.163	-0.023	cm^{-1}
18	6	12	16	4	12	120.993	121.042	-0.049	cm^{-1}
19	6	13	17	4	13	122.892	122.919	-0.027	cm^{-1}
20	6	14	18	4	14	124.790	124.794	-0.004	cm^{-1}
21	6	15	19	4	15	126.692	126.666	0.025	cm^{-1}
22	6	16	20	4	16	128.478	128.535	-0.057	cm^{-1}
23	6	17	21	4	17	130.379	130.401	-0.022	cm^{-1}
24	6	18	22	4	18	132.275	132.262	0.012	cm^{-1}
25	6	19	23	4	19	134.180	134.119	0.060	cm^{-1}
26	6	20	24	4	20	136.011	135.972	0.038	cm^{-1}
27	6	21	25	4	21	137.875	137.818	0.056	cm^{-1}
28	6	22	26	4	22	139.674	139.659	0.014	cm^{-1}
29	6	23	27	4	23	141.527	141.492	0.034	cm^{-1}
11	10	2	10	10	0	10.477	10.399	0.077	cm^{-1}
11	10	1	10	10	1	10.314	10.399	-0.085	cm^{-1}

Upper State			Lower State			Observation	Calculation	Residual	Remarks
J	K_A	K_C	J	K_A	K_C				
12	10	2	11	10	2	11.320	11.344	-0.024	cm^{-1}
13	10	3	12	10	3	12.314	12.290	0.023	cm^{-1}
14	10	4	13	10	4	13.320	13.235	0.084	cm^{-1}
15	10	5	14	10	5	14.192	14.181	0.010	cm^{-1}
16	10	6	15	10	6	15.174	15.127	0.046	cm^{-1}
17	10	7	16	10	7	16.088	16.072	0.015	cm^{-1}
18	10	8	17	10	8	17.015	17.018	-0.003	cm^{-1}
19	10	9	18	10	9	18.050	17.964	0.085	cm^{-1}
20	10	10	19	10	10	19.037	18.909	0.127	cm^{-1}
10	8	2	9	6	4	132.352	132.399	-0.047	cm^{-1}
11	8	3	10	6	5	133.412	133.338	0.073	cm^{-1}
12	8	4	11	6	6	134.221	134.278	-0.057	cm^{-1}
13	8	5	12	6	7	135.169	135.216	-0.047	cm^{-1}
14	8	6	13	6	8	136.149	136.153	-0.004	cm^{-1}
15	8	7	14	6	9	137.155	137.089	0.065	cm^{-1}
16	8	8	15	6	10	137.884	138.025	-0.141	cm^{-1}
17	8	9	16	6	11	138.976	138.959	0.016	cm^{-1}
18	8	10	17	6	12	139.880	139.892	-0.012	cm^{-1}
19	8	11	18	6	13	140.834	140.824	0.009	cm^{-1}
20	8	12	19	6	14	141.752	141.755	-0.003	cm^{-1}
21	8	13	20	6	15	142.709	142.684	0.024	cm^{-1}
22	8	14	21	6	16	143.626	143.612	0.013	cm^{-1}
23	8	15	22	6	17	144.419	144.538	-0.119	cm^{-1}
24	8	16	23	6	18	145.429	145.462	-0.033	cm^{-1}
25	8	17	24	6	19	146.382	146.385	-0.003	cm^{-1}
26	8	18	25	6	20	147.258	147.306	-0.048	cm^{-1}
27	8	19	26	6	21	148.197	148.225	-0.028	cm^{-1}
28	8	20	27	6	22	149.182	149.141	0.040	cm^{-1}
29	8	21	28	6	23	150.013	150.055	-0.042	cm^{-1}
13	10	4	12	10	2	12.247	12.290	-0.043	cm^{-1}
14	10	5	13	10	3	13.220	13.235	-0.015	cm^{-1}
15	10	6	14	10	4	14.115	14.181	-0.066	cm^{-1}
16	10	7	15	10	5	15.079	15.127	-0.048	cm^{-1}
17	10	8	16	10	6	15.977	16.072	-0.095	cm^{-1}

Upper State			Lower State			Observation	Calculation	Residual	Remarks
J	K_A	K_C	J	K_A	K_C				
2	1	2	1	0	1	16776.208	16776.201	0.006	cm^{-1}
3	1	3	2	0	2	16776.985	16777.012	-0.027	cm^{-1}
4	1	4	3	0	3	16777.702	16777.711	-0.009	cm^{-1}
5	1	5	4	0	4	16778.401	16778.299	0.101	cm^{-1}
6	1	6	5	0	5	16778.685	16778.776	-0.091	cm^{-1}
7	1	7	6	0	6	16779.154	16779.142	0.011	cm^{-1}
8	1	8	7	0	7	16779.383	16779.398	-0.015	cm^{-1}
9	1	9	8	0	8	16779.553	16779.545	0.007	cm^{-1}
10	1	10	9	0	9	16779.553	16779.583	-0.030	cm^{-1}
11	1	11	10	0	10	16779.553	16779.512	0.040	cm^{-1}
12	1	12	11	0	11	16779.383	16779.334	0.048	cm^{-1}
13	1	13	12	0	12	16778.980	16779.049	-0.069	cm^{-1}
14	1	14	13	0	13	16778.685	16778.658	0.026	cm^{-1}
15	1	15	14	0	14	16778.156	16778.163	-0.007	cm^{-1}
16	1	16	15	0	15	16777.525	16777.565	-0.040	cm^{-1}
17	1	17	16	0	16	16776.985	16776.864	0.120	cm^{-1}
18	1	18	17	0	17	16776.062	16776.061	0.000	cm^{-1}
19	1	19	18	0	18	16775.186	16775.159	0.026	cm^{-1}
20	1	20	19	0	19	16774.173	16774.158	0.014	cm^{-1}
1	1	0	1	0	1	16774.174	16774.160	0.013	cm^{-1}
2	1	1	2	0	2	16774.174	16773.992	0.182	cm^{-1}
3	1	2	3	0	3	16773.821	16773.739	0.081	cm^{-1}
4	1	3	4	0	4	16773.344	16773.403	-0.059	cm^{-1}
5	1	4	5	0	5	16773.017	16772.983	0.033	cm^{-1}
6	1	5	6	0	6	16772.482	16772.481	0.001	cm^{-1}
7	1	6	7	0	7	16771.855	16771.895	-0.040	cm^{-1}
8	1	7	8	0	8	16771.288	16771.228	0.059	cm^{-1}
9	1	8	9	0	9	16770.462	16770.480	-0.018	cm^{-1}
10	1	9	10	0	10	16769.641	16769.651	-0.010	cm^{-1}
11	1	10	11	0	11	16768.772	16768.742	0.029	cm^{-1}
12	1	11	12	0	12	16767.644	16767.754	-0.110	cm^{-1}
13	1	12	13	0	13	16766.634	16766.689	-0.055	cm^{-1}
14	1	13	14	0	14	16765.525	16765.546	-0.021	cm^{-1}
15	1	14	15	0	15	16764.360	16764.328	0.032	cm^{-1}
16	1	15	16	0	16	16763.116	16763.034	0.081	cm^{-1}
17	1	16	17	0	17	16761.666	16761.667	-0.001	cm^{-1}
18	1	17	18	0	18	16760.240	16760.228	0.011	cm^{-1}
19	1	18	19	0	19	16758.728	16758.718	0.009	cm^{-1}
20	1	19	20	0	20	16757.051	16757.137	-0.086	cm^{-1}
21	1	20	21	0	21	16755.407	16755.488	-0.081	cm^{-1}
22	1	21	22	0	22	16753.727	16753.771	-0.044	cm^{-1}
23	1	22	23	0	23	16751.937	16751.987	-0.050	cm^{-1}
24	1	23	24	0	24	16750.198	16750.138	0.059	cm^{-1}
2	2	1	1	1	0	16792.731	16792.670	0.061	cm^{-1}
2	2	0	1	1	1	16792.731	16792.705	0.026	cm^{-1}
3	2	2	2	1	1	16793.445	16793.486	-0.041	cm^{-1}
3	2	1	2	1	2	16793.590	16793.591	-0.001	cm^{-1}
4	2	3	3	1	2	16794.171	16794.187	-0.016	cm^{-1}
4	2	2	3	1	3	16794.363	16794.398	-0.035	cm^{-1}
5	2	4	4	1	3	16794.820	16794.773	0.046	cm^{-1}

Upper State			Lower State			Observation	Calculation	Residual	Remarks
J	K_A	K_C	J	K_A	K_C				
5	2	3	4	1	4	16795.099	16795.125	-0.026	cm^{-1}
6	2	5	5	1	4	16795.251	16795.243	0.007	cm^{-1}
6	2	4	5	1	5	16795.867	16795.772	0.094	cm^{-1}
7	2	6	6	1	5	16795.595	16795.598	-0.003	cm^{-1}
7	2	5	6	1	6	16796.332	16796.340	-0.008	cm^{-1}
8	2	7	7	1	6	16795.867	16795.837	0.029	cm^{-1}
8	2	6	7	1	7	16796.811	16796.829	-0.018	cm^{-1}
9	2	8	8	1	7	16795.867	16795.961	-0.094	cm^{-1}
9	2	7	8	1	8	16797.200	16797.241	-0.041	cm^{-1}
10	2	9	9	1	8	16795.867	16795.970	-0.103	cm^{-1}
10	2	8	9	1	9	16797.546	16797.575	-0.029	cm^{-1}
11	2	10	10	1	9	16795.867	16795.863	0.003	cm^{-1}
11	2	9	10	1	10	16797.799	16797.832	-0.033	cm^{-1}
12	2	11	11	1	10	16795.595	16795.642	-0.047	cm^{-1}
12	2	10	11	1	11	16797.972	16798.014	-0.042	cm^{-1}
13	2	12	12	1	11	16795.251	16795.306	-0.055	cm^{-1}
13	2	11	12	1	12	16798.125	16798.120	0.004	cm^{-1}
14	2	13	13	1	12	16794.820	16794.854	-0.034	cm^{-1}
14	2	12	13	1	13	16798.125	16798.153	-0.028	cm^{-1}
15	2	14	14	1	13	16794.363	16794.289	0.073	cm^{-1}
15	2	13	14	1	14	16798.125	16798.112	0.012	cm^{-1}
16	2	15	15	1	14	16793.590	16793.609	-0.019	cm^{-1}
16	2	14	15	1	15	16797.972	16797.999	-0.027	cm^{-1}
17	2	16	16	1	15	16792.731	16792.815	-0.084	cm^{-1}
17	2	15	16	1	16	16797.799	16797.816	-0.017	cm^{-1}
18	2	17	17	1	16	16791.858	16791.907	-0.049	cm^{-1}
18	2	16	17	1	17	16797.546	16797.563	-0.017	cm^{-1}
19	2	18	18	1	17	16790.893	16790.885	0.007	cm^{-1}
19	2	17	18	1	18	16797.200	16797.242	-0.042	cm^{-1}
20	2	19	19	1	18	16789.695	16789.750	-0.055	cm^{-1}
20	2	18	19	1	19	16796.811	16796.853	-0.042	cm^{-1}
21	2	20	20	1	19	16788.452	16788.502	-0.050	cm^{-1}
21	2	19	20	1	20	16796.332	16796.398	-0.066	cm^{-1}
2	2	0	2	1	1	16790.346	16790.343	0.002	cm^{-1}
2	2	1	2	1	2	16790.553	16790.448	0.104	cm^{-1}
3	2	1	3	1	2	16789.935	16789.997	-0.062	cm^{-1}
3	2	2	3	1	3	16790.181	16790.206	-0.025	cm^{-1}
4	2	2	4	1	3	16789.500	16789.536	-0.036	cm^{-1}
4	2	3	4	1	4	16789.935	16789.884	0.050	cm^{-1}
5	2	3	5	1	4	16788.978	16788.960	0.017	cm^{-1}
5	2	4	5	1	5	16789.500	16789.481	0.018	cm^{-1}
6	2	4	6	1	5	16788.272	16788.269	0.002	cm^{-1}
6	2	5	6	1	6	16788.978	16788.999	-0.021	cm^{-1}
7	2	5	7	1	6	16787.466	16787.465	0.000	cm^{-1}
7	2	6	7	1	7	16788.452	16788.435	0.016	cm^{-1}
8	2	6	8	1	7	16786.572	16786.548	0.023	cm^{-1}
8	2	7	8	1	8	16787.817	16787.792	0.024	cm^{-1}
9	2	7	9	1	8	16785.413	16785.518	-0.105	cm^{-1}
9	2	8	9	1	9	16786.975	16787.068	-0.093	cm^{-1}
10	2	8	10	1	9	16784.374	16784.376	-0.002	cm^{-1}

Upper State			Lower State			Observation	Calculation	Residual	Remarks
J	K_A	K_C	J	K_A	K_C				
10	2	9	10	1	10	16786.247	16786.265	-0.018	cm^{-1}
11	2	9	11	1	10	16783.103	16783.123	-0.020	cm^{-1}
11	2	10	11	1	11	16785.413	16785.381	0.031	cm^{-1}
12	2	10	12	1	11	16781.736	16781.760	-0.024	cm^{-1}
12	2	11	12	1	12	16784.374	16784.418	-0.044	cm^{-1}
13	2	11	13	1	12	16780.269	16780.287	-0.018	cm^{-1}
13	2	12	13	1	13	16783.370	16783.376	-0.006	cm^{-1}
14	2	12	14	1	13	16778.685	16778.707	-0.022	cm^{-1}
14	2	13	14	1	14	16782.320	16782.253	0.066	cm^{-1}
15	2	13	15	1	14	16776.985	16777.019	-0.034	cm^{-1}
15	2	14	15	1	15	16781.037	16781.052	-0.015	cm^{-1}
16	2	14	16	1	15	16775.187	16775.225	-0.038	cm^{-1}
16	2	15	16	1	16	16779.752	16779.771	-0.019	cm^{-1}
17	2	15	17	1	16	16773.344	16773.326	0.017	cm^{-1}
17	2	16	17	1	17	16778.401	16778.411	-0.010	cm^{-1}
18	2	16	18	1	17	16771.288	16771.325	-0.037	cm^{-1}
18	2	17	18	1	18	16776.985	16776.972	0.012	cm^{-1}
19	2	17	19	1	18	16769.216	16769.221	-0.005	cm^{-1}
19	2	18	19	1	19	16775.409	16775.455	-0.046	cm^{-1}
20	2	18	20	1	19	16767.010	16767.017	-0.007	cm^{-1}
20	2	19	20	1	20	16773.821	16773.859	-0.038	cm^{-1}
21	2	19	21	1	20	16764.679	16764.714	-0.035	cm^{-1}
21	2	20	21	1	21	16772.148	16772.185	-0.037	cm^{-1}
3	0	3	2	1	2	16759.453	16759.454	-0.001	cm^{-1}
4	0	4	3	1	3	16760.240	16760.260	-0.020	cm^{-1}
5	0	5	4	1	4	16760.967	16760.984	-0.017	cm^{-1}
6	0	6	5	1	5	16761.666	16761.628	0.037	cm^{-1}
7	0	7	6	1	6	16762.294	16762.190	0.103	cm^{-1}
8	0	8	7	1	7	16762.678	16762.669	0.008	cm^{-1}
9	0	9	8	1	8	16763.116	16763.067	0.048	cm^{-1}
10	0	10	9	1	9	16763.364	16763.382	-0.018	cm^{-1}
11	0	11	10	1	10	16763.600	16763.613	-0.013	cm^{-1}
12	0	12	11	1	11	16763.797	16763.761	0.035	cm^{-1}
13	0	13	12	1	12	16763.797	16763.825	-0.028	cm^{-1}
14	0	14	13	1	13	16763.797	16763.803	-0.006	cm^{-1}
15	0	15	14	1	14	16763.797	16763.697	0.099	cm^{-1}
16	0	16	15	1	15	16763.600	16763.504	0.095	cm^{-1}
17	0	17	16	1	16	16763.116	16763.224	-0.108	cm^{-1}
18	0	18	17	1	17	16762.856	16762.857	-0.001	cm^{-1}
19	0	19	18	1	18	16762.515	16762.402	0.113	cm^{-1}
20	0	20	19	1	19	16761.826	16761.857	-0.031	cm^{-1}
21	0	21	20	1	20	16761.182	16761.223	-0.041	cm^{-1}
22	0	22	21	1	21	16760.475	16760.498	-0.023	cm^{-1}
23	0	23	22	1	22	16759.615	16759.681	-0.066	cm^{-1}
24	0	24	23	1	23	16758.725	16758.773	-0.048	cm^{-1}
25	0	25	24	1	24	16757.926	16757.771	0.154	cm^{-1}
5	0	5	5	1	4	16754.847	16754.819	0.027	cm^{-1}
6	0	6	6	1	5	16754.165	16754.125	0.039	cm^{-1}
7	0	7	7	1	6	16753.307	16753.315	-0.008	cm^{-1}
8	0	8	8	1	7	16752.392	16752.388	0.003	cm^{-1}

Upper State			Lower State			Observation	Calculation	Residual	Remarks
J	K_A	K_C	J	K_A	K_C				
9	0	9	9	1	8	16751.350	16751.344	0.005	cm^{-1}
10	0	10	10	1	9	16750.198	16750.183	0.014	cm^{-1}
11	0	11	11	1	10	16748.896	16748.904	-0.008	cm^{-1}
12	0	12	12	1	11	16747.528	16747.507	0.020	cm^{-1}
13	0	13	13	1	12	16745.963	16745.992	-0.029	cm^{-1}
14	0	14	14	1	13	16744.388	16744.358	0.030	cm^{-1}
15	0	15	15	1	14	16742.621	16742.603	0.017	cm^{-1}
16	0	16	16	1	15	16740.771	16740.729	0.041	cm^{-1}
17	0	17	17	1	16	16738.674	16738.735	-0.061	cm^{-1}
18	0	18	18	1	17	16736.577	16736.619	-0.042	cm^{-1}
19	0	19	19	1	18	16734.376	16734.381	-0.005	cm^{-1}
20	0	20	20	1	19	16732.036	16732.021	0.014	cm^{-1}
21	0	21	21	1	20	16729.550	16729.538	0.011	cm^{-1}
22	0	22	22	1	21	16726.932	16726.932	0.000	cm^{-1}
23	0	23	23	1	23	16724.159	16724.203	-0.044	cm^{-1}
24	0	24	24	1	24	16721.337	16721.349	-0.012	cm^{-1}
25	0	25	25	1	24	16718.461	16718.370	0.090	cm^{-1}
1	0	1	2	1	2	16754.165	16754.215	-0.050	cm^{-1}
2	0	2	3	1	3	16752.931	16752.926	0.004	cm^{-1}
3	0	3	4	1	4	16751.536	16751.556	-0.020	cm^{-1}
4	0	4	5	1	5	16760.198	16750.106	0.091	cm^{-1}
5	0	5	6	1	6	16748.591	16748.575	0.016	cm^{-1}
6	0	6	7	1	7	16746.990	16746.963	0.026	cm^{-1}
7	0	7	8	1	8	16745.261	16745.270	-0.009	cm^{-1}
8	0	8	9	1	9	16743.513	16743.495	0.017	cm^{-1}
9	0	9	10	1	10	16741.663	16741.639	0.023	cm^{-1}
10	0	10	11	1	11	16739.716	16739.701	0.014	cm^{-1}
11	0	11	12	1	12	16737.699	16737.681	0.017	cm^{-1}
12	0	12	13	1	13	16735.624	16735.577	0.046	cm^{-1}
13	0	13	14	1	14	16733.391	16733.391	0.000	cm^{-1}
14	0	14	15	1	15	16731.123	16731.120	0.002	cm^{-1}
15	0	15	16	1	16	16728.784	16728.766	0.017	cm^{-1}
16	0	16	17	1	17	16726.350	16726.326	0.023	cm^{-1}
17	0	17	18	1	18	16723.649	16723.800	-0.151	cm^{-1}
18	0	18	19	1	19	16721.132	16721.189	-0.057	cm^{-1}
19	0	19	20	1	20	16718.461	16718.490	-0.029	cm^{-1}
20	0	20	21	1	21	16715.687	16715.704	-0.017	cm^{-1}
21	0	21	22	1	22	16712.800	16712.829	-0.029	cm^{-1}
22	0	22	23	1	23	16709.873	16709.865	0.007	cm^{-1}
23	0	23	24	1	24	16706.769	16706.811	-0.042	cm^{-1}
24	0	24	25	1	25	16703.652	16703.666	-0.014	cm^{-1}
3	3	1	2	2	0	16808.673	16808.731	-0.058	cm^{-1}
3	3	0	2	2	1	16808.673	16808.731	-0.058	cm^{-1}
4	3	2	3	2	1	16809.454	16809.484	-0.030	cm^{-1}
4	3	1	3	2	2	16809.454	16809.484	-0.030	cm^{-1}
5	3	3	4	2	2	16810.108	16810.138	-0.030	cm^{-1}
5	3	2	4	2	3	16810.108	16810.139	-0.031	cm^{-1}
6	3	4	5	2	3	16810.655	16810.693	-0.038	cm^{-1}
6	3	3	5	2	4	16810.655	16810.697	-0.042	cm^{-1}
7	3	5	6	2	4	16811.114	16811.149	-0.035	cm^{-1}

Upper State			Lower State			Observation	Calculation	Residual	Remarks
J	K_A	K_C	J	K_A	K_C				
7	3	4	6	2	5	16811.114	16811.156	-0.042	cm^{-1}
8	3	6	7	2	5	16811.470	16811.506	-0.036	cm^{-1}
8	3	5	7	2	6	16811.470	16811.518	-0.048	cm^{-1}
9	3	7	8	2	6	16811.765	16811.762	0.003	cm^{-1}
9	3	6	8	2	7	16811.765	16811.783	-0.018	cm^{-1}
10	3	8	9	2	7	16811.950	16811.917	0.033	cm^{-1}
10	3	7	9	2	8	16811.950	16811.950	0.000	cm^{-1}
11	3	9	10	2	8	16811.950	16811.970	-0.020	cm^{-1}
11	3	8	10	2	9	16811.950	16812.020	-0.070	cm^{-1}
12	3	10	11	2	9	16811.950	16811.921	0.028	cm^{-1}
12	3	9	11	2	10	16811.950	16811.993	-0.043	cm^{-1}
13	3	11	12	2	10	16811.765	16811.769	-0.004	cm^{-1}
13	3	10	12	2	11	16811.950	16811.869	0.080	cm^{-1}
14	3	12	13	2	11	16811.470	16811.512	-0.042	cm^{-1}
14	3	11	13	2	12	16811.765	16811.650	0.114	cm^{-1}
15	3	13	14	2	12	16811.114	16811.151	-0.037	cm^{-1}
15	3	12	14	2	13	16811.273	16811.334	-0.061	cm^{-1}
16	3	14	15	2	13	16810.655	16810.683	-0.028	cm^{-1}
16	3	13	15	2	14	16810.857	16810.923	-0.066	cm^{-1}
17	3	15	16	2	14	16810.108	16810.108	0.000	cm^{-1}
17	3	14	16	2	15	16810.367	16810.416	-0.049	cm^{-1}
18	3	16	17	2	15	16809.454	16809.425	0.028	cm^{-1}
18	3	15	17	2	16	16809.761	16809.815	-0.054	cm^{-1}
19	3	17	18	2	16	16808.673	16808.633	0.039	cm^{-1}
19	3	16	18	2	17	16809.053	16809.119	-0.066	cm^{-1}
20	3	18	19	2	17	16807.534	16807.730	-0.196	cm^{-1}
20	3	17	19	2	18	16808.303	16808.330	-0.027	cm^{-1}
21	3	19	20	2	18	16806.643	16806.714	-0.071	cm^{-1}
21	3	18	20	2	19	16807.379	16807.447	-0.068	cm^{-1}
22	3	19	21	2	20	16806.398	16806.472	-0.074	cm^{-1}
3	3	1	3	2	2	16805.255	16805.293	-0.038	cm^{-1}
4	3	1	4	2	2	16804.922	16804.900	0.022	cm^{-1}
5	3	2	5	2	3	16804.401	16804.407	-0.006	cm^{-1}
6	3	3	6	2	4	16803.873	16803.816	0.056	cm^{-1}
7	3	4	7	2	5	16803.119	16803.125	-0.006	cm^{-1}
8	3	5	8	2	6	16802.347	16802.333	0.013	cm^{-1}
9	3	6	9	2	7	16801.447	16801.441	0.005	cm^{-1}
10	3	7	10	2	8	16800.442	16800.447	-0.005	cm^{-1}
10	3	8	10	2	9	16800.442	16800.497	-0.055	cm^{-1}
11	3	8	11	2	9	16799.364	16799.351	0.012	cm^{-1}
11	3	9	11	2	10	16799.364	16799.422	-0.058	cm^{-1}
12	3	9	12	2	10	16798.125	16798.152	-0.027	cm^{-1}
12	3	10	12	2	11	16798.125	16798.251	-0.126	cm^{-1}
13	3	10	13	2	11	16796.811	16796.849	-0.038	cm^{-1}
13	3	11	13	2	12	16796.988	16796.984	0.003	cm^{-1}
14	3	11	14	2	12	16795.422	16795.441	-0.019	cm^{-1}
14	3	12	14	2	13	16795.595	16795.621	-0.026	cm^{-1}
15	3	12	15	2	13	16793.914	16793.928	-0.014	cm^{-1}
15	3	13	15	2	14	16794.171	16794.162	0.008	cm^{-1}
16	3	13	16	2	14	16792.282	16792.307	-0.025	cm^{-1}

Upper State			Lower State			Observation	Calculation		Residual	Remarks
J	K_A	K_C	J	K_A	K_C					
16	3	14	16	2	15	16792.541	16792.608		-0.067	cm^{-1}
17	3	14	17	2	15	16790.553	16790.579		-0.026	cm^{-1}
17	3	15	17	2	16	16790.893	16790.959		-0.066	cm^{-1}
18	3	15	18	2	16	16788.715	16788.742		-0.027	cm^{-1}
18	3	16	18	2	17	16789.164	16789.215		-0.051	cm^{-1}
19	3	16	19	2	17	16786.766	16786.795		-0.029	cm^{-1}
19	3	17	19	2	18	16787.466	16787.377		0.088	cm^{-1}
2	1	1	2	2	0	16737.382	16737.376		0.005	cm^{-1}
2	1	2	2	2	1	16737.382	16737.293		0.088	cm^{-1}
3	1	2	3	2	1	16737.066	16737.122		-0.056	cm^{-1}
3	1	3	3	2	2	16736.929	16736.958		-0.029	cm^{-1}
4	1	3	4	2	2	16736.929	16736.784		0.144	cm^{-1}
4	1	4	4	2	3	16736.577	16736.512		0.064	cm^{-1}
5	1	4	5	2	3	16736.577	16736.361	*	0.215	cm^{-1}
5	1	5	5	2	4	16735.909	16735.953		-0.044	cm^{-1}
6	1	5	6	2	4	16735.909	16735.852		0.056	cm^{-1}
6	1	6	6	2	5	16735.287	16735.283		0.003	cm^{-1}
7	1	6	7	2	5	16735.287	16735.257		0.029	cm^{-1}
7	1	7	7	2	6	16734.537	16734.502		0.034	cm^{-1}
8	1	7	8	2	6	16734.537	16734.574		-0.037	cm^{-1}
8	1	8	8	2	7	16733.619	16733.608		0.010	cm^{-1}
9	1	8	9	2	7	16733.867	16733.804		0.062	cm^{-1}
9	1	9	9	2	8	16732.622	16732.603		0.018	cm^{-1}
10	1	9	10	2	8	16732.945	16732.945		0.000	cm^{-1}
10	1	10	10	2	9	16731.510	16731.487		0.022	cm^{-1}
11	1	10	11	2	9	16732.036	16731.996		0.039	cm^{-1}
11	1	11	11	2	10	16730.242	16730.258		-0.016	cm^{-1}
12	1	11	12	2	10	16730.786	16730.956		-0.170	cm^{-1}
12	1	12	12	2	11	16728.981	16728.918		0.062	cm^{-1}
13	1	12	13	2	11	16729.824	16729.824		0.000	cm^{-1}
13	1	13	13	2	12	16727.450	16727.466		-0.016	cm^{-1}
14	1	13	14	2	12	16728.601	16728.599		0.001	cm^{-1}
14	1	14	14	2	13	16725.903	16725.903		0.000	cm^{-1}
15	1	14	15	2	13	16727.271	16727.279		-0.008	cm^{-1}
15	1	15	15	2	14	16724.159	16724.228		-0.069	cm^{-1}
16	1	15	16	2	14	16725.903	16725.863		0.039	cm^{-1}
16	1	16	16	2	15	16722.444	16722.441		0.002	cm^{-1}
17	1	16	17	2	15	16724.357	16724.349		0.007	cm^{-1}
17	1	17	17	2	16	16720.550	16720.543		0.006	cm^{-1}
18	1	17	18	2	16	16722.640	16722.736		-0.096	cm^{-1}
18	1	18	18	2	17	16718.461	16718.533		-0.072	cm^{-1}
19	1	18	19	2	17	16720.913	16721.023		-0.110	cm^{-1}
19	1	19	19	2	18	16716.513	16716.412		0.100	cm^{-1}
20	1	19	20	2	18	16719.156	16719.207		-0.051	cm^{-1}
20	1	20	20	2	19	16714.209	16714.179		0.029	cm^{-1}
21	1	20	21	2	19	16717.312	16717.286		0.025	cm^{-1}
21	1	21	21	2	20	16711.733	16711.835		-0.102	cm^{-1}
4	4	1	3	3	0	16823.386	16823.426		-0.040	cm^{-1}
5	4	2	4	3	1	16824.031	16824.080		-0.049	cm^{-1}
6	4	3	5	3	2	16824.587	16824.636		-0.049	cm^{-1}

Upper State			Lower State			Observation	Calculation	Residual	Remarks
J	K_A	K_C	J	K_A	K_C				
7	4	4	6	3	3	16825.180	16825.094	0.085	cm^{-1}
8	4	5	7	3	4	16825.459	16825.453	0.005	cm^{-1}
9	4	6	8	3	5	16825.706	16825.713	-0.007	cm^{-1}
10	4	7	9	3	6	16825.891	16825.875	0.015	cm^{-1}
11	4	8	10	3	7	16825.891	16825.938	-0.047	cm^{-1}
12	4	9	11	3	8	16825.891	16825.902	-0.011	cm^{-1}
13	4	10	12	3	9	16825.706	16825.767	-0.061	cm^{-1}
14	4	11	13	3	10	16825.459	16825.532	-0.073	cm^{-1}
15	4	12	14	3	11	16825.180	16825.199	-0.019	cm^{-1}
16	4	13	15	3	12	16824.747	16824.766	-0.019	cm^{-1}
17	4	14	16	3	13	16824.180	16824.233	-0.053	cm^{-1}
18	4	15	17	3	14	16823.542	16823.600	-0.058	cm^{-1}
19	4	16	18	3	15	16822.835	16822.867	-0.032	cm^{-1}
20	4	17	19	3	16	16821.981	16822.034	-0.053	cm^{-1}
21	4	18	20	3	17	16821.056	16821.100	-0.044	cm^{-1}
22	4	19	21	3	18	16820.021	16820.064	-0.043	cm^{-1}
23	4	20	22	3	19	16818.852	16818.928	-0.076	cm^{-1}
24	4	21	23	3	20	16817.706	16817.690	0.015	cm^{-1}
25	4	22	24	3	21	16816.272	16816.349	-0.077	cm^{-1}
4	4	0	4	3	1	16818.852	16818.843	0.008	cm^{-1}
5	4	1	5	3	2	16818.317	16818.352	-0.035	cm^{-1}
6	4	2	6	3	3	16817.706	16817.762	-0.056	cm^{-1}
7	4	3	7	3	4	16817.058	16817.073	-0.015	cm^{-1}
8	4	4	8	3	5	16816.272	16816.287	-0.015	cm^{-1}
9	4	5	9	3	6	16815.375	16815.401	-0.026	cm^{-1}
10	4	6	10	3	7	16814.401	16814.417	-0.016	cm^{-1}
11	4	7	11	3	8	16813.314	16813.334	-0.020	cm^{-1}
12	4	8	12	3	9	16812.120	16812.153	-0.033	cm^{-1}
13	4	9	13	3	10	16810.857	16810.872	-0.015	cm^{-1}
14	4	10	14	3	11	16809.454	16809.492	-0.038	cm^{-1}
15	4	11	15	3	12	16807.960	16808.013	-0.053	cm^{-1}
16	4	12	16	3	13	16806.398	16806.434	-0.036	cm^{-1}
17	4	13	17	3	14	16804.724	16804.755	-0.031	cm^{-1}
18	4	14	18	3	15	16802.910	16802.977	-0.067	cm^{-1}
19	4	15	19	3	16	16801.069	16801.098	-0.029	cm^{-1}
20	4	16	20	3	17	16799.111	16799.119	-0.008	cm^{-1}
21	4	17	21	3	18	16796.988	16797.039	-0.051	cm^{-1}
22	4	18	22	3	19	16794.820	16794.858	-0.038	cm^{-1}
23	4	19	23	3	20	16792.541	16792.575	-0.034	cm^{-1}
24	4	20	24	3	21	16790.181	16790.191	-0.010	cm^{-1}
25	4	21	25	3	22	16787.644	16787.705	-0.061	cm^{-1}
3	2	1	3	3	0	16716.937	16716.910	0.026	cm^{-1}
3	2	2	3	3	1	16716.937	16716.910	0.026	cm^{-1}
4	2	2	4	3	1	16716.513	16716.519	-0.006	cm^{-1}
5	2	3	5	3	2	16716.048	16716.029	0.018	cm^{-1}
6	2	4	6	3	3	16715.464	16715.443	0.020	cm^{-1}
7	2	5	7	3	4	16714.778	16714.760	0.018	cm^{-1}
8	2	6	8	3	5	16713.987	16713.979	0.007	cm^{-1}
9	2	7	9	3	6	16713.103	16713.102	0.000	cm^{-1}
10	2	8	10	3	7	16712.074	16712.129	-0.055	cm^{-1}

Upper State			Lower State			Observation	Calculation	Residual	Remarks
J	K_A	K_C	J	K_A	K_C				
11	2	9	11	3	8	16711.039	16711.061	-0.022	cm^{-1}
12	2	10	12	3	9	16709.873	16709.897	-0.024	cm^{-1}
13	2	11	13	3	10	16708.626	16708.638	-0.012	cm^{-1}
13	2	12	13	3	11	16708.626	16708.549	0.076	cm^{-1}
14	2	12	14	3	11	16707.227	16707.285	-0.058	cm^{-1}
14	2	13	14	3	12	16707.227	16707.167	0.059	cm^{-1}
15	2	13	15	3	12	16705.856	16705.837	0.018	cm^{-1}
15	2	14	15	3	13	16705.652	16705.684	-0.032	cm^{-1}
16	2	14	16	3	13	16704.324	16704.297	0.026	cm^{-1}
16	2	15	16	3	14	16704.126	16704.101	0.024	cm^{-1}
17	2	15	17	3	14	16702.696	16702.664	0.031	cm^{-1}
17	2	16	17	3	15	16702.403	16702.416	-0.013	cm^{-1}
18	2	16	18	3	15	16700.962	16700.938	0.023	cm^{-1}
18	2	17	18	3	16	16700.724	16700.631	0.093	cm^{-1}
19	2	17	19	3	16	16699.168	16699.121	0.046	cm^{-1}
19	2	18	19	3	17	16698.786	16698.743	0.042	cm^{-1}
20	2	18	20	3	17	16697.295	16697.213	0.081	cm^{-1}
20	2	19	20	3	18	16696.777	16696.754	0.023	cm^{-1}
21	2	19	21	3	18	16695.257	16695.214	0.042	cm^{-1}
21	2	20	21	3	19	16694.724	16694.662	0.062	cm^{-1}
22	2	20	22	3	19	16693.167	16693.125	0.041	cm^{-1}
22	2	21	22	3	20	16692.519	16692.467	0.051	cm^{-1}
23	2	21	23	3	20	16691.012	16690.946	0.065	cm^{-1}
23	2	22	23	3	21	16690.081	16690.169	-0.088	cm^{-1}
24	2	22	24	3	21	16688.728	16688.678	0.049	cm^{-1}
24	2	23	24	3	22	16687.846	16687.767	0.078	cm^{-1}
25	2	23	25	3	22	16686.415	16686.321	0.093	cm^{-1}
25	2	24	25	3	23	16685.294	16685.261	0.032	cm^{-1}
2	2	1	3	3	0	16713.780	16713.766	0.013	cm^{-1}
3	2	2	4	3	1	16712.332	16712.327	0.005	cm^{-1}
4	2	3	5	3	2	16710.807	16710.789	0.017	cm^{-1}
5	2	4	6	3	3	16709.175	16709.153	0.022	cm^{-1}
6	2	5	7	3	4	16707.434	16707.418	0.015	cm^{-1}
7	2	6	8	3	5	16705.652	16705.585	0.066	cm^{-1}
8	2	7	9	3	6	16703.652	16703.654	-0.002	cm^{-1}
9	2	8	10	3	7	16701.618	16701.623	-0.005	cm^{-1}
10	2	9	11	3	8	16699.524	16699.494	0.030	cm^{-1}
11	2	10	12	3	9	16697.295	16697.265	0.029	cm^{-1}
12	2	11	13	3	10	16695.006	16694.936	0.069	cm^{-1}
12	2	10	13	3	11	16695.006	16695.004	0.002	cm^{-1}
13	2	12	14	3	11	16692.519	16692.508	0.011	cm^{-1}
13	2	11	14	3	12	16692.676	16692.600	0.075	cm^{-1}
14	2	13	15	3	12	16690.081	16689.979	0.101	cm^{-1}
14	2	12	15	3	13	16690.081	16690.102	-0.021	cm^{-1}
15	2	14	16	3	13	16687.346	16687.349	-0.003	cm^{-1}
15	2	13	16	3	14	16687.568	16687.511	0.056	cm^{-1}
16	2	15	17	3	14	16684.663	16684.619	0.044	cm^{-1}
16	2	14	17	3	15	16684.872	16684.827	0.044	cm^{-1}
17	2	16	18	3	15	16681.829	16681.786	0.042	cm^{-1}
17	2	15	18	3	16	16682.076	16682.050	0.025	cm^{-1}

Upper State			Lower State			Observation	Calculation	Residual	Remarks
J	K_A	K_C	J	K_A	K_C				
18	2	17	19	3	16	16678.893	16678.852	0.040	cm^{-1}
18	2	16	19	3	17	16679.255	16679.183	0.071	cm^{-1}
19	2	18	20	3	17	16675.846	16675.815	0.030	cm^{-1}
19	2	17	20	3	18	16676.257	16676.225	0.032	cm^{-1}
20	2	19	21	3	18	16672.729	16672.675	0.053	cm^{-1}
20	2	18	21	3	19	16673.148	16673.176	-0.028	cm^{-1}
21	2	20	22	3	19	16669.410	16679.431	-0.021	cm^{-1}
21	2	19	22	3	20	16670.065	16670.039	0.025	cm^{-1}
22	2	21	23	3	20	16666.125	16666.082	0.042	cm^{-1}
22	2	20	23	3	21	16666.835	16666.813	0.021	cm^{-1}
23	2	22	24	3	21	16662.643	16662.629	0.013	cm^{-1}
23	2	21	24	3	22	16663.483	16663.500	-0.017	cm^{-1}
5	5	0	4	4	1	16836.752	16836.785	-0.033	cm^{-1}
6	5	1	5	4	2	16837.302	16837.341	-0.039	cm^{-1}
7	5	2	6	4	3	16837.829	16837.797	0.031	cm^{-1}
8	5	3	7	4	4	16838.164	16838.155	0.008	cm^{-1}
9	5	4	8	4	5	16838.405	16838.414	-0.009	cm^{-1}
10	5	5	9	4	6	16838.586	16838.575	0.010	cm^{-1}
11	5	6	10	4	7	16838.586	16838.637	-0.051	cm^{-1}
12	5	7	11	4	8	16838.586	16838.600	-0.014	cm^{-1}
13	5	8	12	4	9	16838.405	16838.464	-0.059	cm^{-1}
14	5	9	13	4	10	16838.164	16838.229	-0.065	cm^{-1}
15	5	10	14	4	11	16837.829	16837.896	-0.067	cm^{-1}
16	5	11	15	4	12	16837.489	16837.463	0.025	cm^{-1}
17	5	12	16	4	13	16836.886	16836.931	-0.045	cm^{-1}
18	5	13	17	4	14	16836.299	16836.299	0.000	cm^{-1}
19	5	14	18	4	15	16835.532	16835.569	-0.037	cm^{-1}
20	5	15	19	4	16	16834.677	16834.739	-0.062	cm^{-1}
21	5	16	20	4	17	16833.698	16833.809	-0.111	cm^{-1}
22	5	17	21	4	18	16832.691	16832.780	-0.089	cm^{-1}
23	5	18	22	4	19	16831.544	16831.651	-0.107	cm^{-1}
24	5	19	23	4	20	16830.356	16830.422	-0.066	cm^{-1}
25	5	20	24	4	21	16828.962	16829.093	-0.131	cm^{-1}
5	5	0	5	4	1	16831.010	16831.057	-0.047	cm^{-1}
6	5	1	6	4	2	16830.356	16830.466	-0.110	cm^{-1}
7	5	2	7	4	3	16829.756	16829.777	-0.021	cm^{-1}
8	5	3	8	4	4	16828.962	16828.990	-0.028	cm^{-1}
9	5	4	9	4	5	16828.074	16828.104	-0.030	cm^{-1}
10	5	5	10	4	6	16827.140	16827.119	0.020	cm^{-1}
11	5	6	11	4	7	16826.028	16826.036	-0.008	cm^{-1}
12	5	7	12	4	8	16824.747	16824.853	-0.106	cm^{-1}
13	5	8	13	4	9	16823.542	16823.573	-0.031	cm^{-1}
14	5	9	14	4	10	16822.174	16822.193	-0.019	cm^{-1}
15	5	10	15	4	11	16820.716	16820.714	0.001	cm^{-1}
16	5	11	16	4	12	16819.085	16819.137	-0.052	cm^{-1}
17	5	12	17	4	13	16817.429	16817.470	-0.031	cm^{-1}
18	5	13	18	4	14	16815.662	16815.684	-0.022	cm^{-1}
19	5	14	19	4	15	16813.819	16813.809	0.009	cm^{-1}
20	5	15	20	4	16	16811.765	16811.835	-0.070	cm^{-1}
21	5	16	21	4	17	16809.761	16809.762	-0.001	cm^{-1}

CH_2S: 4_0^1 Band - continued

Upper State			Lower State			Observation	Calculation	Rešidual	Remarks
J	K_A	K_C	J	K_A	K_C				
22	5	17	22	4	18	16807.534	16807.588	-0.054	cm^{-1}
4	3	1	4	4	0	16695.257	16695.213	0.043	cm^{-1}
5	3	2	5	4	1	16694.724	16694.723	0.000	cm^{-1}
6	3	3	6	4	2	16694.129	16694.135	-0.006	cm^{-1}
7	3	4	7	4	3	16693.470	16693.449	0.020	cm^{-1}
8	3	5	8	4	4	16692.676	16692.665	0.010	cm^{-1}
9	3	6	9	4	5	16691.801	16691.782	0.018	cm^{-1}
10	3	7	10	4	6	16690.849	16690.802	0.046	cm^{-1}
11	3	8	11	4	7	16689.769	16689.724	0.044	cm^{-1}
12	3	9	12	4	8	16688.566	16688.548	0.017	cm^{-1}
13	3	10	13	4	9	16687.346	16687.274	0.071	cm^{-1}
14	3	11	14	4	10	16685.924	16685.902	0.021	cm^{-1}
15	3	12	15	4	11	16684.472	16684.432	0.039	cm^{-1}
16	3	13	16	4	12	16682.911	16682.865	0.046	cm^{-1}
17	3	14	17	4	13	16681.234	16681.199	0.034	cm^{-1}
18	3	15	18	4	14	16679.491	16679.436	0.054	cm^{-1}
19	3	16	19	4	15	16677.633	16677.575	0.057	cm^{-1}
20	3	17	20	4	16	16675.666	16675.617	0.048	cm^{-1}
21	3	18	21	4	17	16673.686	16673.561	0.124	cm^{-1}
22	3	19	22	4	18	16671.450	16671.408	0.041	cm^{-1}
23	3	20	23	4	19	16669.186	16669.157	0.028	cm^{-1}
3	3	1	4	4	0	16691.012	16691.023	-0.011	cm^{-1}
4	3	2	5	4	1	16689.484	16689.485	-0.001	cm^{-1}
5	3	3	6	4	2	16687.846	16687.849	-0.003	cm^{-1}
6	3	4	7	4	3	16686.137	16686.115	0.021	cm^{-1}
7	3	5	8	4	4	16684.273	16684.284	-0.011	cm^{-1}
8	3	6	9	4	5	16682.404	16682.354	0.049	cm^{-1}
9	3	7	10	4	6	16680.328	16680.326	0.001	cm^{-1}
10	3	8	11	4	7	16678.233	16678.201	0.031	cm^{-1}
11	3	9	12	4	8	16676.027	16675.977	0.049	cm^{-1}
12	3	10	13	4	9	16673.686	16673.656	0.029	cm^{-1}
13	3	11	14	4	10	16671.202	16671.237	-0.035	cm^{-1}
14	3	12	15	4	11	16668.756	16668.719	0.036	cm^{-1}
15	3	13	16	4	12	16666.125	16666.104	0.020	cm^{-1}
16	3	14	17	4	13	16663.483	16663.391	0.091	cm^{-1}
17	3	15	18	4	14	16660.605	16660.580	0.024	cm^{-1}
18	3	16	19	4	15	16657.729	16657.671	0.057	cm^{-1}
19	3	17	20	4	16	16654.719	16654.664	0.054	cm^{-1}
20	3	18	21	4	17	16651.627	16651.559	0.067	cm^{-1}
21	3	19	22	4	18	16648.411	16648.356	0.054	cm^{-1}
22	3	20	23	4	19	16645.108	16645.055	0.052	cm^{-1}
23	3	21	24	4	20	16641.696	16641.656	0.039	cm^{-1}
6	6	1	5	5	0	16848.870	16848.830	0.039	cm^{-1}
7	6	2	6	5	1	16849.312	16849.286	0.026	cm^{-1}
8	6	3	7	5	2	16849.650	16849.642	0.007	cm^{-1}
9	6	4	8	5	3	16849.881	16849.900	-0.019	cm^{-1}
10	6	5	9	5	4	16850.077	16850.059	0.017	cm^{-1}
11	6	6	10	5	5	16850.077	16850.119	-0.042	cm^{-1}
12	6	7	11	5	6	16850.077	16850.080	-0.003	cm^{-1}
13	6	8	12	5	7	16849.881	16849.942	-0.061	cm^{-1}

Upper State J	K_A	K_C	Lower State J	K_A	K_C	Observation	Calculation	Residual	Remarks
14	6	9	13	5	8	16849.650	16849.705	-0.055	cm^{-1}
15	6	10	14	5	9	16849.312	16849.370	-0.058	cm^{-1}
16	6	11	15	5	10	16848.870	16848.935	-0.065	cm^{-1}
17	6	12	16	5	11	16848.375	16848.401	-0.026	cm^{-1}
18	6	13	17	5	12	16847.725	16847.767	-0.042	cm^{-1}
19	6	14	18	5	13	16846.989	16847.035	-0.046	cm^{-1}
20	6	15	19	5	14	16846.154	16846.203	-0.049	cm^{-1}
21	6	16	20	5	15	16845.200	16845.271	-0.071	cm^{-1}
22	6	17	21	5	16	16844.169	16844.240	-0.071	cm^{-1}
23	6	18	22	5	17	16843.044	16843.110	-0.066	cm^{-1}
24	6	19	23	5	18	16841.787	16841.880	-0.093	cm^{-1}
25	6	20	24	5	19	16840.475	16840.550	-0.075	cm^{-1}
6	6	0	6	5	1	16841.963	16841.957	0.005	cm^{-1}
7	6	1	7	5	2	16841.254	16841.267	-0.013	cm^{-1}
8	6	2	8	5	3	16840.475	16840.478	-0.003	cm^{-1}
9	6	3	9	5	4	16839.581	16839.590	-0.009	cm^{-1}
10	6	4	10	5	5	16838.586	16838.604	-0.018	cm^{-1}
11	6	5	11	5	6	16837.489	16837.519	-0.030	cm^{-1}
12	6	6	12	5	7	16836.299	16836.335	-0.036	cm^{-1}
13	6	7	13	5	8	16835.059	16835.053	0.006	cm^{-1}
14	6	8	14	5	9	16833.698	16833.671	0.026	cm^{-1}
15	6	9	15	5	10	16832.212	16832.191	0.020	cm^{-1}
16	6	10	16	5	11	16830.617	16830.612	0.005	cm^{-1}
17	6	11	17	5	12	16828.962	16828.933	0.028	cm^{-1}
18	6	12	18	5	13	16827.140	16827.156	-0.016	cm^{-1}
19	6	13	19	5	14	16825.180	16825.280	-0.100	cm^{-1}
20	6	14	20	5	15	16823.274	16823.304	-0.030	cm^{-1}
21	6	15	21	5	16	16821.220	16821.229	-0.009	cm^{-1}
22	6	16	22	5	17	16819.085	16819.055	0.029	cm^{-1}
23	6	17	23	5	18	16816.736	16816.782	-0.046	cm^{-1}
24	6	18	24	5	19	16814.401	16814.409	-0.008	cm^{-1}
25	6	19	25	5	20	16811.950	16811.937	0.012	cm^{-1}
5	4	1	5	5	0	16672.277	16672.288	-0.011	cm^{-1}
6	4	2	6	5	1	16671.692	16671.700	-0.008	cm^{-1}
7	4	3	7	5	2	16670.988	16671.013	-0.025	cm^{-1}
8	4	4	8	5	3	16670.272	16670.228	0.044	cm^{-1}
9	4	5	9	5	4	16669.410	16669.344	0.065	cm^{-1}
10	4	6	10	5	5	16668.382	16668.363	0.018	cm^{-1}
11	4	7	11	5	6	16667.301	16667.284	0.017	cm^{-1}
12	4	8	12	5	7	16666.125	16666.106	0.018	cm^{-1}
13	4	9	13	5	8	16664.860	16664.830	0.029	cm^{-1}
14	4	10	14	5	9	16663.483	16683.456	0.026	cm^{-1}
15	4	11	15	5	10	16662.004	16661.984	0.019	cm^{-1}
16	4	12	16	6	11	16660.441	16660.414	0.027	cm^{-1}
17	4	13	17	5	12	16658.794	16658.745	0.048	cm^{-1}
18	4	14	18	5	13	16657.028	16656.978	0.049	cm^{-1}
19	4	15	19	5	14	16655.165	16655.113	0.051	cm^{-1}
20	4	16	20	5	15	16653.194	16653.150	0.043	cm^{-1}
21	4	17	21	5	16	16651.217	16651.089	0.128	cm^{-1}
22	4	18	22	5	17	16648.989	16648.929	0.059	cm^{-1}

Upper State J	K_A	K_C	Lower State J	K_A	K_C	Observation	Calculation	Residual	Remarks
23	4	19	23	5	18	16646.718	16646.671	0.046	cm^{-1}
24	4	20	24	5	19	16644.364	16644.315	0.048	cm^{-1}
4	4	1	5	5	0	16667.043	16667.051	-0.008	cm^{-1}
5	4	2	6	5	1	16665.414	16665.415	-0.001	cm^{-1}
6	4	3	7	5	2	16663.687	16663.680	0.006	cm^{-1}
7	4	4	8	5	3	16661.850	16661.848	0.001	cm^{-1}
8	4	5	9	5	4	16659.921	16659.918	0.002	cm^{-1}
9	4	6	10	5	5	16657.907	16657.890	0.017	cm^{-1}
10	4	7	11	5	6	16655.790	16655.763	0.026	cm^{-1}
11	4	8	12	5	7	16653.568	16653.539	0.028	cm^{-1}
12	4	9	13	5	8	16651.217	16651.216	0.000	cm^{-1}
13	4	10	14	5	9	16648.813	16648.796	0.016	cm^{-1}
14	4	11	15	5	10	16646.314	16646.277	0.036	cm^{-1}
15	4	12	16	5	11	16643.736	16643.661	0.074	cm^{-1}
16	4	13	17	5	12	16640.993	16640.946	0.046	cm^{-1}
17	4	14	18	5	13	16638.181	16638.134	0.046	cm^{-1}
18	4	15	19	5	14	16635.270	16635.223	0.046	cm^{-1}
19	4	16	20	5	15	16632.264	16632.214	0.049	cm^{-1}
20	4	17	21	5	16	16629.156	16629.108	0.047	cm^{-1}
21	4	18	22	5	17	16625.975	16625.903	0.071	cm^{-1}
22	4	19	23	5	18	16622.695	16622.601	0.093	cm^{-1}
23	4	20	24	5	19	16619.262	16619.200	0.061	cm^{-1}
7	7	1	6	6	0	16859.608	16859.591	0.016	cm^{-1}
8	7	1	7	6	2	16859.939	16859.946	-0.007	cm^{-1}
9	7	3	8	6	2	16860.213	16860.202	0.010	cm^{-1}
10	7	3	9	6	4	16860.381	16860.359	0.021	cm^{-1}
11	7	5	10	6	4	16860.381	16860.417	-0.036	cm^{-1}
12	7	5	11	6	6	16860.381	16860.375	0.005	cm^{-1}
13	7	7	12	6	6	16860.213	16860.235	-0.022	cm^{-1}
14	7	7	13	6	8	16859.939	16859.995	-0.056	cm^{-1}
15	7	9	14	6	8	16859.608	16859.657	-0.049	cm^{-1}
16	7	9	15	6	10	16859.179	16859.219	-0.040	cm^{-1}
17	7	11	16	6	10	16858.659	16858.682	-0.023	cm^{-1}
18	7	11	17	6	12	16858.089	16858.045	0.043	cm^{-1}
19	7	13	18	6	12	16857.283	16857.309	-0.026	cm^{-1}
20	7	13	19	6	14	16856.438	16856.474	-0.036	cm^{-1}
21	7	15	20	6	14	16855.487	16855.539	-0.052	cm^{-1}
22	7	15	21	6	16	16854.516	16854.504	0.011	cm^{-1}
10	7	3	10	6	4	16848.870	16848.905	-0.035	cm^{-1}
11	7	4	11	6	5	16847.725	16847.818	-0.093	cm^{-1}
12	7	5	12	6	6	16846.618	16846.632	-0.014	cm^{-1}
13	7	6	13	6	7	16845.356	16845.347	0.008	cm^{-1}
14	7	7	14	6	8	16843.980	16843.963	0.016	cm^{-1}
15	7	8	15	6	9	16842.501	16842.480	0.020	cm^{-1}
16	7	9	16	6	10	16840.922	16840.898	0.023	cm^{-1}
17	7	10	17	6	11	16839.231	16839.217	0.013	cm^{-1}
18	7	11	18	6	12	16837.489	16837.437	0.052	cm^{-1}
19	7	12	19	6	13	16835.532	16835.557	-0.025	cm^{-1}
20	7	13	20	6	14	16833.698	16833.579	0.119	cm^{-1}
21	7	14	21	6	15	16831.544	16831.501	0.042	cm^{-1}

Upper State			Lower State			Observation	Calculation	Residual	Remarks
J	K_A	K_C	J	K_A	K_C				
22	7	15	22	6	16	16829.273	16829.323	-0.050	cm^{-1}
8	8	1	7	7	0	16869.151	16869.108	0.042	cm^{-1}
9	8	2	8	7	1	16869.387	16869.362	0.024	cm^{-1}
10	8	3	9	7	2	16869.584	16869.516	0.067	cm^{-1}
11	8	4	10	7	3	16869.584	16869.572	0.012	cm^{-1}
12	8	5	11	7	4	16869.584	16869.527	0.056	cm^{-1}
13	8	6	12	7	5	16869.387	16869.384	0.002	cm^{-1}
14	8	7	13	7	6	16869.151	16869.141	0.009	cm^{-1}
15	8	8	14	7	7	16868.797	16868.799	-0.002	cm^{-1}
16	8	9	15	7	8	16868.381	16868.357	0.023	cm^{-1}
17	8	10	16	7	9	16867.846	16867.816	0.029	cm^{-1}
18	8	11	17	7	10	16867.200	16867.176	0.023	cm^{-1}
19	8	12	18	7	11	16866.439	16866.436	0.002	cm^{-1}
20	8	13	19	7	12	16865.589	16865.596	-0.007	cm^{-1}
21	8	14	20	7	13	16864.633	16864.656	-0.023	cm^{-1}
22	8	15	21	7	14	16863.604	16863.617	-0.013	cm^{-1}
23	8	16	22	7	15	16862.479	16862.478	0.000	cm^{-1}
24	8	17	23	7	16	16861.231	16861.240	-0.009	cm^{-1}
10	8	2	10	7	3	16858.089	16858.064	0.024	cm^{-1}
11	8	3	11	7	4	16856.976	16856.974	0.001	cm^{-1}
12	8	4	12	7	5	16855.800	16855.785	0.014	cm^{-1}
13	8	5	13	7	6	16854.516	16854.498	0.018	cm^{-1}
14	8	6	14	7	7	16853.122	16853.110	0.011	cm^{-1}
15	8	7	15	7	8	16851.659	16851.624	0.034	cm^{-1}
16	8	8	16	7	9	16850.077	16850.039	0.037	cm^{-1}
17	8	9	17	7	10	16848.375	16848.354	0.020	cm^{-1}
18	8	10	18	7	11	16846.618	16846.570	0.047	cm^{-1}
19	8	11	19	7	12	16844.719	16844.686	0.032	cm^{-1}
20	8	12	20	7	13	16842.728	16842.704	0.023	cm^{-1}
21	8	13	21	7	14	16840.647	16840.622	0.025	cm^{-1}
9	6	3	9	7	2	16621.336	16621.296	0.039	cm^{-1}
10	6	4	10	7	3	16620.267	16620.312	-0.045	cm^{-1}
11	6	5	11	7	4	16619.262	16619.230	0.031	cm^{-1}
12	6	6	12	7	5	16618.052	16618.049	0.002	cm^{-1}
13	6	7	13	7	6	16616.791	16616.770	0.020	cm^{-1}
14	6	8	14	7	7	16615.398	16615.392	0.005	cm^{-1}
15	6	9	15	7	8	16613.936	16613.915	0.020	cm^{-1}
16	6	10	16	7	9	16612.396	16612.340	0.055	cm^{-1}
17	6	11	17	7	10	16610.721	16610.667	0.053	cm^{-1}
18	6	12	18	7	11	16608.947	16608.895	0.051	cm^{-1}
19	6	13	19	7	12	16607.098	16607.025	0.072	cm^{-1}
20	6	14	20	7	13	16605.130	16605.056	0.074	cm^{-1}
21	6	15	21	7	14	16603.148	16602.988	0.159	cm^{-1}
22	6	16	22	7	15	16600.944	16600.822	0.121	cm^{-1}
23	6	17	23	7	16	16598.657	16598.557	0.099	cm^{-1}
24	6	18	24	7	17	16596.309	16596.193	0.115	cm^{-1}
25	6	19	25	7	18	16593.837	16593.731	0.105	cm^{-1}
6	6	1	7	7	0	16615.608	16615.640	-0.032	cm^{-1}
7	6	2	8	7	1	16613.772	16613.807	-0.035	cm^{-1}
8	6	3	9	7	2	16611.892	16611.874	0.017	cm^{-1}

CH_2S: 4_0^1 Band - continued

Upper State			Lower State			Observation	Calculation	Residual	Remarks
J	K_A	K_C	J	K_A	K_C				
9	6	4	10	7	3	16609.849	16609.844	0.004	cm^{-1}
10	6	5	11	7	4	16607.728	16607.715	0.012	cm^{-1}
11	6	6	12	7	5	16605.498	16605.488	0.009	cm^{-1}
12	6	7	13	7	6	16603.148	16603.163	-0.015	cm^{-1}
13	6	8	14	7	7	16600.783	16600.739	0.043	cm^{-1}
14	6	9	15	7	8	16598.264	16598.217	0.046	cm^{-1}
15	6	10	16	7	9	16595.669	16595.597	0.072	cm^{-1}
16	6	11	17	7	10	16592.946	16592.878	0.067	cm^{-1}
17	6	12	18	7	11	16590.141	16590.061	0.079	cm^{-1}
18	6	13	19	7	12	16587.229	16587.146	0.082	cm^{-1}
19	6	14	20	7	13	16584.251	16584.132	0.118	cm^{-1}
20	6	15	21	7	14	16581.146	16581.021	0.124	cm^{-1}
21	6	16	22	7	15	16577.943	16577.811	0.132	cm^{-1}
22	6	17	23	7	16	16574.611	16574.502	0.108	cm^{-1}
23	6	18	24	7	17	16571.243	16571.095	0.147	cm^{-1}
24	6	19	25	7	18	16567.708	16567.590	0.117	cm^{-1}
9	9	0	8	8	1	16877.456	16877.430	0.025	cm^{-1}
10	9	1	9	8	2	16877.631	16877.582	0.048	cm^{-1}
11	9	2	10	8	3	16877.631	16877.634	-0.003	cm^{-1}
12	9	3	11	8	4	16877.631	16877.587	0.043	cm^{-1}
13	9	4	12	8	5	16877.456	16877.440	0.015	cm^{-1}
14	9	5	13	8	6	16877.170	16877.193	-0.023	cm^{-1}
15	9	6	14	8	7	16876.833	16876.847	-0.014	cm^{-1}
10	10	1	9	9	0	16884.634	16884.616	0.017	cm^{-1}
11	10	2	10	9	1	16884.634	16884.665	-0.031	cm^{-1}
12	10	3	11	9	2	16884.634	16884.614	0.019	cm^{-1}
13	10	4	12	9	3	16884.448	16884.463	-0.015	cm^{-1}
14	10	5	13	9	4	16884.195	16884.212	-0.017	cm^{-1}
15	10	6	14	9	5	16883.845	16883.861	-0.016	cm^{-1}
16	10	7	15	9	6	16883.391	16883.411	-0.020	cm^{-1}
17	10	8	16	9	7	16882.869	16882.860	0.008	cm^{-1}
18	10	9	17	9	8	16882.152	16882.210	-0.058	cm^{-1}
19	10	10	18	9	9	16881.410	16881.459	-0.049	cm^{-1}
20	10	11	19	9	10	16880.595	16880.608	-0.013	cm^{-1}
21	10	12	20	9	11	16879.649	16879.657	-0.008	cm^{-1}
22	10	13	21	9	12	16878.558	16878.606	-0.048	cm^{-1}

Upper State			Lower State			Observation	Calculation	Residual	Remarks
J	K_A	K_C	J	K_A	K_C				
2	1	2	1	0	1	16764.565	16764.633	-0.068	cm^{-1}
3	1	3	2	0	2	16765.309	16765.309	0.000	cm^{-1}
4	1	4	3	0	3	16755.856	16765.896	-0.040	cm^{-1}
5	1	5	4	0	4	16766.375	16766.394	-0.019	cm^{-1}
6	1	6	5	0	5	16766.895	16766.804	0.090	cm^{-1}
7	1	7	6	0	6	16767.127	16767.128	-0.001	cm^{-1}
8	1	8	7	0	7	16767.352	16767.368	-0.016	cm^{-1}
9	1	9	8	0	8	16767.562	16767.525	0.036	cm^{-1}
10	1	10	9	0	9	16767.562	16767.602	-0.040	cm^{-1}
11	1	11	10	0	10	16767.562	16767.602	-0.040	cm^{-1}
12	1	12	11	0	11	16767.562	16767.527	0.034	cm^{-1}
13	1	13	12	0	12	16767.352	16767.379	-0.027	cm^{-1}
14	1	14	13	0	13	16767.127	16767.163	-0.036	cm^{-1}
15	1	15	14	0	14	16766.895	16766.881	0.014	cm^{-1}
16	1	16	15	0	15	16766.550	16766.534	0.015	cm^{-1}
17	1	17	16	0	16	16766.156	16766.127	0.028	cm^{-1}
18	1	18	17	0	17	16765.591	16765.662	-0.071	cm^{-1}
19	1	19	18	0	18	16765.121	16765.140	-0.019	cm^{-1}
20	1	20	19	0	19	16765.565	16765.562	0.002	cm^{-1}
21	1	21	20	0	20	16763.932	16763.931	0.000	cm^{-1}
22	1	22	21	0	21	16763.262	16763.247	0.015	cm^{-1}
23	1	23	22	0	22	16762.500	16762.510	-0.010	cm^{-1}
24	1	24	23	0	23	16761.778	16761.720	0.057	cm^{-1}
25	1	25	24	0	24	16760.863	16760.878	-0.015	cm^{-1}
26	1	26	25	0	25	16760.016	16759.983	0.032	cm^{-1}
27	1	27	26	0	26	16759.027	16759.034	-0.007	cm^{-1}
28	1	28	27	0	27	16757.935	16758.031	-0.096	cm^{-1}
29	1	29	28	0	28	16756.938	16756.974	-0.036	cm^{-1}
1	1	0	1	0	1	16762.917	16762.958	-0.041	cm^{-1}
2	1	1	2	0	2	16762.800	16762.856	-0.056	cm^{-1}
3	1	2	3	0	3	16762.688	16762.703	-0.015	cm^{-1}
4	1	3	4	0	4	16762.500	16762.501	-0.001	cm^{-1}
5	1	4	5	0	5	16762.240	16762.251	-0.011	cm^{-1}
6	1	5	6	0	6	16761.985	16761.953	0.031	cm^{-1}
7	1	6	7	0	7	16761.597	16761.611	-0.014	cm^{-1}
8	1	7	8	0	8	16761.240	16761.226	0.013	cm^{-1}
9	1	8	9	0	9	16760.863	16760.800	0.062	cm^{-1}
10	1	9	10	0	10	16760.427	16760.336	0.090	cm^{-1}
11	1	10	11	0	11	16759.832	16759.836	-0.004	cm^{-1}
12	1	11	12	0	12	16759.271	16759.303	-0.032	cm^{-1}
13	1	12	13	0	13	16758.751	16758.740	0.011	cm^{-1}
14	1	13	14	0	14	16758.151	16758.148	0.002	cm^{-1}
15	1	14	15	0	15	16757.518	16757.531	-0.013	cm^{-1}
16	1	15	16	0	16	16756.938	16756.889	0.048	cm^{-1}
17	1	16	17	0	17	16756.226	16756.226	0.000	cm^{-1}
18	1	17	18	0	18	16755.532	16755.541	-0.009	cm^{-1}
19	1	18	19	0	19	16754.827	16754.835	-0.008	cm^{-1}
20	1	19	20	0	20	16754.123	16754.108	0.014	cm^{-1}
21	1	20	21	0	21	16753.331	16753.360	-0.029	cm^{-1}
22	1	21	22	0	22	16752.560	16752.589	-0.029	cm^{-1}

CD_2S: 4_0^1 Band - continued

Upper State			Lower State			Observation	Calculation	Residual	Remarks
J	K_A	K_C	J	K_A	K_C				
23	1	22	23	0	23	16751.776	16751.794	-0.018	cm^{-1}
24	1	23	24	0	24	16750.974	16750.972	0.001	cm^{-1}
25	1	24	25	0	25	16750.152	16750.121	0.031	cm^{-1}
26	1	25	26	0	26	16749.144	16749.237	-0.093	cm^{-1}
27	1	26	27	0	27	16748.288	16748.319	-0.031	cm^{-1}
28	1	27	28	0	28	16747.311	16747.362	-0.051	cm^{-1}
29	1	28	29	0	29	16746.427	16746.362	0.064	cm^{-1}
3	3	1	2	2	0	16781.298	16781.236	0.061	cm^{-1}
3	3	0	2	2	1	16781.298	16781.237	0.060	cm^{-1}
4	3	2	3	2	1	16781.886	16781.899	-0.013	cm^{-1}
4	3	1	3	2	2	16781.886	16781.900	-0.014	cm^{-1}
5	3	3	4	2	2	16782.498	16782.488	0.009	cm^{-1}
5	3	2	4	2	3	16782.498	16782.494	0.003	cm^{-1}
6	3	4	5	2	3	16783.043	16783.004	0.038	cm^{-1}
6	3	3	5	2	4	16783.043	16783.017	0.025	cm^{-1}
7	3	5	6	2	4	16783.469	16783.445	0.023	cm^{-1}
7	3	4	6	2	5	16783.469	16783.472	-0.003	cm^{-1}
8	3	6	7	2	5	16783.835	16783.809	0.025	cm^{-1}
8	3	5	7	2	6	16783.835	16783.857	-0.022	cm^{-1}
9	3	7	8	2	6	16784.040	16784.095	-0.055	cm^{-1}
9	3	6	8	2	7	16784.224	16784.174	0.049	cm^{-1}
10	3	8	9	2	7	16784.224	16784.299	-0.075	cm^{-1}
10	3	7	9	2	8	16784.413	16784.424	-0.011	cm^{-1}
11	3	9	10	2	8	16784.413	16784.421	-0.008	cm^{-1}
11	3	8	10	2	9	16784.563	16784.608	-0.045	cm^{-1}
12	3	10	11	2	9	16784.413	16784.456	-0.043	cm^{-1}
12	3	9	11	2	10	16784.764	16784.727	0.036	cm^{-1}
13	3	11	12	2	10	16784.413	16784.404	0.008	cm^{-1}
13	3	10	12	2	11	16784.767	16784.782	-0.015	cm^{-1}
14	3	12	13	2	11	16784.224	16784.260	-0.036	cm^{-1}
14	3	11	13	2	12	16784.764	16784.775	-0.011	cm^{-1}
15	3	13	14	2	12	16784.040	16784.023	0.016	cm^{-1}
15	3	12	14	2	13	16784.764	16784.707	0.056	cm^{-1}
16	3	14	15	2	13	16783.678	16783.690	-0.014	cm^{-1}
16	3	13	15	2	14	16784.563	16784.579	-0.016	cm^{-1}
17	3	15	16	2	14	16783.268	16783.258	0.009	cm^{-1}
17	3	14	16	2	15	16784.413	16784.394	0.018	cm^{-1}
18	3	16	17	2	15	16782.753	16782.727	0.025	cm^{-1}
19	3	17	18	2	16	16782.135	16782.094	0.041	cm^{-1}
19	3	16	18	2	17	16783.835	16783.861	-0.026	cm^{-1}
20	3	18	19	2	17	16781.298	16781.358	-0.060	cm^{-1}
20	3	17	19	2	18	16783.469	16783.516	-0.047	cm^{-1}
21	3	19	20	2	18	16780.514	16780.518	-0.004	cm^{-1}
21	3	18	20	2	19	16783.043	16783.124	-0.081	cm^{-1}
22	3	20	21	2	19	16779.554	16779.574	-0.020	cm^{-1}
22	3	19	21	2	20	16782.753	16782.685	0.067	cm^{-1}
23	3	21	22	2	20	16778.533	16778.527	0.005	cm^{-1}
23	3	20	22	2	21	16782.135	16782.204	-0.069	cm^{-1}
24	3	22	23	2	21	16777.348	16777.377	-0.029	cm^{-1}
24	3	21	23	2	22	16781.648	16781.684	-0.036	cm^{-1}

Upper State			Lower State			Observation	Calculation		Residual	Remarks
J	K_A	K_C	J	K_A	K_C					
25	3	23	24	2	22	16776.256	16776.125	*	0.130	cm^{-1}
25	3	22	24	2	23	16781.298	16781.126		0.171	cm^{-1}
26	3	24	25	2	23	16774.762	16774.771		-0.009	cm^{-1}
26	3	23	25	2	24	16780.514	16780.536		-0.022	cm^{-1}
27	3	25	26	2	24	16773.344	16773.318		0.025	cm^{-1}
27	3	24	26	2	25	16779.919	16779.916		0.002	cm^{-1}
28	3	26	27	2	25	16771.713	16771.767		-0.054	cm^{-1}
28	3	25	27	2	26	16779.212	16779.269		-0.057	cm^{-1}
29	3	27	28	2	26	16770.163	16770.120		0.042	cm^{-1}
29	3	26	28	2	27	16778.533	16778.599		-0.066	cm^{-1}
3	3	0	3	2	1	16778.366	16778.393		-0.027	cm^{-1}
3	3	1	3	2	2	16778.366	16778.395		-0.029	cm^{-1}
4	3	1	4	2	2	16778.100	16778.106		-0.006	cm^{-1}
4	3	2	4	2	3	16778.100	16778.112		-0.012	cm^{-1}
5	3	2	5	2	3	16777.790	16777.745		0.044	cm^{-1}
5	3	3	5	2	4	16777.790	16777.758		0.031	cm^{-1}
6	3	3	6	2	4	16777.348	16777.309		0.038	cm^{-1}
6	3	4	6	2	5	16777.348	16777.336		0.012	cm^{-1}
7	3	4	7	2	5	16776.837	16776.797		0.039	cm^{-1}
7	3	5	7	2	6	16776.837	16776.844		-0.007	cm^{-1}
8	3	5	8	2	6	16776.256	16776.205		0.050	cm^{-1}
8	3	6	8	2	7	16776.258	16776.283		-0.027	cm^{-1}
9	3	6	9	2	7	16775.639	16775.533		0.105	cm^{-1}
9	3	7	9	2	8	16775.639	16775.655		-0.016	cm^{-1}
10	3	7	10	2	8	16774.762	16774.778		-0.016	cm^{-1}
10	3	8	10	2	9	16774.982	16774.960		0.021	cm^{-1}
11	3	8	11	2	9	16773.916	16773.937		-0.021	cm^{-1}
11	3	9	11	2	10	16774.186	16774.198		-0.012	cm^{-1}
12	3	9	12	2	10	16772.990	16773.009		-0.019	cm^{-1}
12	3	10	12	2	11	16773.344	16773.372		-0.028	cm^{-1}
13	3	10	13	2	11	16771.978	16771.990		-0.012	cm^{-1}
13	3	11	13	2	12	16772.446	16772.481		-0.035	cm^{-1}
14	3	11	14	2	12	16770.838	16770.880		-0.042	cm^{-1}
14	3	12	14	2	13	16771.510	16771.527		-0.017	cm^{-1}
15	3	12	15	2	13	16769.691	16769.676		0.014	cm^{-1}
15	3	13	15	2	14	16770.518	16770.511		0.006	cm^{-1}
16	3	13	16	2	14	16768.341	16768.376		-0.035	cm^{-1}
16	3	14	16	2	15	16769.437	16769.433		0.003	cm^{-1}
17	3	14	17	2	15	16766.895	16766.979		-0.084	cm^{-1}
17	3	15	17	2	16	16768.341	16768.296		0.044	cm^{-1}
18	3	15	18	2	16	16765.591	16765.485		0.105	cm^{-1}
18	3	16	18	2	17	16767.127	16767.100		0.026	cm^{-1}
19	3	16	19	2	17	16763.932	16763.895		0.037	cm^{-1}
19	3	17	19	2	18	16765.856	16765.846		0.009	cm^{-1}
20	3	17	20	2	18	16762.225	16762.207		0.017	cm^{-1}
20	3	18	20	2	19	16764.565	16764.536		0.028	cm^{-1}
21	3	18	21	2	19	16760.427	16760.424		0.002	cm^{-1}
21	3	19	21	2	20	16763.202	16763.170		0.031	cm^{-1}
22	3	19	22	2	20	16758.565	16758.547		0.017	cm^{-1}
22	3	20	22	2	21	16761.778	16761.750		0.027	cm^{-1}

Upper State			Lower State			Observation	Calculation	Residual	Remarks
J	K_A	K_C	J	K_A	K_C				
23	3	20	23	2	21	16756.554	16756.580	-0.026	cm^{-1}
23	3	21	23	2	22	16760.300	16760.277	0.022	cm^{-1}
24	3	21	24	2	22	16754.524	16754.524	0.000	cm^{-1}
24	3	22	24	2	23	16758.741	16758.752	-0.011	cm^{-1}
25	3	22	25	2	23	16752.411	16752.383	0.027	cm^{-1}
25	3	23	25	2	24	16757.199	16757.175	0.023	cm^{-1}
26	3	23	26	2	24	16750.158	16750.161	-0.003	cm^{-1}
26	3	24	26	2	25	16755.535	16755.549	-0.014	cm^{-1}
27	3	24	27	2	25	16747.872	16747.862	0.009	cm^{-1}
27	3	25	27	2	26	16753.884	16753.874	0.009	cm^{-1}
28	3	25	28	2	26	16745.599	16745.491	0.107	cm^{-1}
28	3	26	28	2	27	16752.169	16752.150	0.018	cm^{-1}
2	1	1	2	2	0	16745.269	16745.224	0.044	cm^{-1}
2	1	2	2	2	1	16745.063	16745.107	-0.044	cm^{-1}
3	1	2	3	2	1	16745.063	16745.069	-0.006	cm^{-1}
3	1	3	3	2	2	16744.837	16744.836	0.000	cm^{-1}
4	1	3	4	2	2	16744.838	16744.860	-0.022	cm^{-1}
4	1	4	4	2	3	16744.513	16744.475	0.037	cm^{-1}
5	1	4	5	2	3	16744.513	16744.595	-0.082	cm^{-1}
5	1	5	5	2	4	16744.040	16744.023	0.016	cm^{-1}
6	1	5	6	2	4	16744.224	16744.274	-0.050	cm^{-1}
6	1	6	6	2	5	16743.445	16743.481	-0.036	cm^{-1}
7	1	6	7	2	5	16743.904	16743.893	0.010	cm^{-1}
7	1	7	7	2	6	16742.831	16742.848	-0.017	cm^{-1}
8	1	7	8	2	6	16743.445	16743.451	-0.006	cm^{-1}
8	1	8	8	2	7	16742.091	16742.124	-0.033	cm^{-1}
9	1	8	9	2	7	16742.976	16742.943	0.032	cm^{-1}
9	1	9	9	2	8	16741.315	16741.310	0.004	cm^{-1}
10	1	9	10	2	8	16742.378	16742.367	0.010	cm^{-1}
10	1	10	10	2	9	16740.385	16740.406	-0.021	cm^{-1}
11	1	10	11	2	9	16741.700	16741.719	-0.019	cm^{-1}
11	1	11	11	2	10	16739.357	16739.411	-0.054	cm^{-1}
12	1	11	12	2	10	16741.064	16740.996	0.067	cm^{-1}
12	1	12	12	2	11	16738.352	16738.326	0.025	cm^{-1}
13	1	12	13	2	11	16740.125	16740.193	-0.068	cm^{-1}
13	1	13	13	2	12	16737.125	16737.150	-0.025	cm^{-1}
14	1	13	14	2	12	16739.357	16739.307	0.049	cm^{-1}
14	1	14	14	2	13	16735.853	16735.884	-0.031	cm^{-1}
15	1	14	15	2	13	16738.352	16738.333	0.018	cm^{-1}
15	1	15	15	2	14	16734.556	16734.527	0.028	cm^{-1}
16	1	15	16	2	14	16737.280	16737.269	0.010	cm^{-1}
16	1	16	16	2	15	16733.089	16733.081	0.007	cm^{-1}
17	1	16	17	2	15	16736.102	16736.109	-0.007	cm^{-1}
17	1	17	17	2	16	16731.536	16731.544	-0.008	cm^{-1}
18	1	17	18	2	16	16734.852	16734.852	0.000	cm^{-1}
18	1	18	18	2	17	16729.917	16729.919	-0.002	cm^{-1}
19	1	18	19	2	17	16733.560	16733.494	0.065	cm^{-1}
19	1	19	19	2	18	16728.247	16728.203	0.043	cm^{-1}
20	1	19	20	2	18	16732.075	16732.032	0.042	cm^{-1}
20	1	20	20	2	19	16726.388	16726.399	-0.011	cm^{-1}

Upper State			Lower State			Observation	Calculation	Residual	Remarks
J	K_A	K_C	J	K_A	K_C				
21	1	20	21	2	19	16730.471	16730.464	0.006	cm^{-1}
21	1	21	21	2	20	16724.506	16724.507	-0.001	cm^{-1}
22	1	21	22	2	20	16728.784	16728.788	-0.004	cm^{-1}
22	1	22	22	2	21	16722.535	16722.526	0.008	cm^{-1}
23	1	22	23	2	21	16727.008	16727.002	0.005	cm^{-1}
23	1	23	23	2	22	16720.497	16720.458	0.038	cm^{-1}
24	1	23	24	2	22	16725.137	16725.105	0.031	cm^{-1}
24	1	24	24	2	23	16718.342	16718.303	0.038	cm^{-1}
25	1	24	25	2	23	16723.104	16723.094	0.009	cm^{-1}
25	1	25	25	2	24	16716.056	16716.062	-0.006	cm^{-1}
26	1	25	26	2	24	16720.989	16720.970	0.018	cm^{-1}
26	1	26	26	2	25	16713.593	16713.735	-0.142	cm^{-1}
27	1	26	27	2	25	16718.778	16718.731	0.046	cm^{-1}
27	1	27	27	2	26	16711.349	16711.323	0.025	cm^{-1}
28	1	27	28	2	26	16716.394	16716.377	0.017	cm^{-1}
28	1	28	28	2	27	16708.868	16708.827	0.040	cm^{-1}
29	1	28	29	2	27	16713.986	16713.906	0.079	cm^{-1}
29	1	29	29	2	28	16706.266	16706.248	0.017	cm^{-1}
1	1	1	2	2	0	16743.445	16743.393	0.051	cm^{-1}
1	1	0	2	2	1	16743.445	16743.433	0.012	cm^{-1}
2	1	2	3	2	1	16742.378	16742.264	0.114	cm^{-1}
2	1	1	3	2	2	16742.378	16742.383	-0.005	cm^{-1}
3	1	3	4	2	2	16741.064	16741.042	0.021	cm^{-1}
3	1	2	4	2	3	16741.315	16741.282	0.032	cm^{-1}
4	1	4	5	2	3	16739.713	16739.726	-0.013	cm^{-1}
4	1	3	5	2	4	16740.125	16740.130	-0.005	cm^{-1}
5	1	5	6	2	4	16738.352	16738.315	0.036	cm^{-1}
5	1	4	6	2	5	16738.929	16738.927	0.001	cm^{-1}
6	1	6	7	2	5	16736.783	16736.806	-0.023	cm^{-1}
6	1	5	7	2	6	16737.642	16737.673	-0.031	cm^{-1}
7	1	7	8	2	6	16735.211	16735.196	0.014	cm^{-1}
7	1	6	8	2	7	16736.377	16736.367	0.009	cm^{-1}
8	1	8	9	2	7	16733.560	16733.483	0.076	cm^{-1}
8	1	7	9	2	8	16735.002	16735.011	-0.009	cm^{-1}
9	1	9	10	2	8	16731.680	16731.664	0.016	cm^{-1}
9	1	8	10	2	9	16733.560	16733.604	-0.044	cm^{-1}
10	1	10	11	2	9	16729.714	16729.735	-0.021	cm^{-1}
10	1	9	11	2	10	16732.075	16732.145	-0.070	cm^{-1}
11	1	11	12	2	10	16727.776	16727.692	0.083	cm^{-1}
11	1	10	12	2	11	16730.650	16730.635	0.014	cm^{-1}
12	1	12	13	2	11	16725.512	16725.534	-0.022	cm^{-1}
12	1	11	13	2	12	16728.988	16729.073	-0.085	cm^{-1}
13	1	13	14	2	12	16723.274	16723.255	0.018	cm^{-1}
13	1	12	14	2	13	16727.444	16727.460	-0.016	cm^{-1}
14	1	14	15	2	13	16720.757	16720.853	-0.096	cm^{-1}
14	1	13	15	2	14	16725.828	16725.795	0.032	cm^{-1}
15	1	15	16	2	14	16718.342	16718.324	0.017	cm^{-1}
15	1	14	16	2	15	16723.983	16724.077	-0.094	cm^{-1}
16	1	16	17	2	15	16715.675	16715.666	0.008	cm^{-1}
16	1	15	17	2	16	16722.343	16722.306	0.036	cm^{-1}

Upper State			Lower State			Observation	Calculation		Residual	Remarks
J	K_A	K_C	J	K_A	K_C					
17	1	17	18	2	16	16712.884	16712.876		0.007	cm^{-1}
17	1	16	18	2	17	16720.497	16720.483		0.014	cm^{-1}
18	1	18	19	2	17	16709.947	16709.952		-0.005	cm^{-1}
18	1	17	19	2	18	16718.584	16718.605		-0.021	cm^{-1}
19	1	19	20	2	18	16706.907	16706.894		0.012	cm^{-1}
19	1	18	20	2	19	16716.646	16716.672		-0.026	cm^{-1}
20	1	20	21	2	19	16703.718	16703.700		0.017	cm^{-1}
20	1	19	21	2	20	16714.693	16714.684		0.008	cm^{-1}
21	1	21	22	2	20	16700.407	16700.369		0.037	cm^{-1}
21	1	20	22	2	21	16712.621	16712.640		-0.019	cm^{-1}
22	1	21	23	2	22	16710.564	16710.537		0.026	cm^{-1}
23	1	23	24	2	22	16693.232	16693.298		-0.066	cm^{-1}
23	1	22	24	2	23	16708.375	16708.376		-0.001	cm^{-1}
4	4	1	3	3	0	16789.147	16789.117		0.029	cm^{-1}
5	4	2	4	3	1	16789.697	16789.709		-0.012	cm^{-1}
6	4	3	5	3	2	16790.208	16790.229		-0.021	cm^{-1}
7	4	4	6	3	3	16790.650	16790.677		-0.027	cm^{-1}
8	4	5	7	3	4	16791.128	16791.054		0.073	cm^{-1}
9	4	6	8	3	5	16791.401	16791.359		0.041	cm^{-1}
10	4	7	9	3	6	16791.609	16791.592		0.016	cm^{-1}
11	4	8	10	3	7	16791.798	16791.752		0.045	cm^{-1}
12	4	9	11	3	8	16791.798	16791.839		-0.041	cm^{-1}
13	4	10	12	3	9	16791.798	16791.852		-0.054	cm^{-1}
14	4	11	13	3	10	16791.798	16791.790		0.007	cm^{-1}
15	4	12	14	3	11	16791.609	16791.654		-0.045	cm^{-1}
16	4	13	15	3	12	16791.401	16791.442		-0.041	cm^{-1}
17	4	14	16	3	13	16791.129	16791.152		-0.023	cm^{-1}
18	4	15	17	3	14	16790.835	16790.785		0.049	cm^{-1}
4	4	0	4	3	1	16785.305	16785.328		-0.023	cm^{-1}
5	4	1	5	3	2	16784.971	16784.972		-0.001	cm^{-1}
6	4	2	6	3	3	16784.563	16784.544		0.018	cm^{-1}
7	4	3	7	3	4	16784.040	16784.044		-0.004	cm^{-1}
8	4	4	8	3	5	16783.468	16783.473		-0.005	cm^{-1}
9	4	5	9	3	6	16782.753	16782.829		-0.076	cm^{-1}
10	4	6	10	3	7	16782.135	16782.112		0.023	cm^{-1}
11	4	7	11	3	8	16781.298	16781.321		-0.023	cm^{-1}
12	4	8	12	3	9	16780.514	16780.457		0.056	cm^{-1}
13	4	9	13	3	10	16779.554	16779.519		0.034	cm^{-1}
14	4	10	14	3	11	16778.553	16778.505		0.047	cm^{-1}
15	4	11	15	3	12	16777.348	16777.415		-0.067	cm^{-1}
16	4	12	16	3	13	16776.256	16776.248		0.007	cm^{-1}
17	4	13	17	3	14	16774.992	16775.003		-0.011	cm^{-1}
18	4	15	18	3	16	16773.666	16773.777	*	-0.111	cm^{-1}
19	4	15	19	3	16	16772.290	16772.273		0.017	cm^{-1}
19	4	16	19	3	17	16772.446	16772.408		0.037	cm^{-1}
20	4	16	20	3	17	16770.838	16770.785		0.053	cm^{-1}
20	4	17	20	3	18	16771.030	16770.967		0.063	cm^{-1}
2	2	1	3	3	0	16732.791	16732.836		-0.045	cm^{-1}
2	2	0	3	3	1	16732.791	16732.836		-0.045	cm^{-1}
3	2	2	4	3	1	16731.680	16731.675		0.004	cm^{-1}

Upper State			Lower State			Observation	Calculation	Residual	Remarks
J	K_A	K_C	J	K_A	K_C				
3	2	1	4	3	2	16731.680	16731.677	0.002	cm^{-1}
4	2	3	5	3	2	16730.471	16730.444	0.026	cm^{-1}
4	2	2	5	3	3	16730.471	16730.448	0.022	cm^{-1}
5	2	4	6	3	3	16729.124	16729.140	-0.016	cm^{-1}
5	2	3	6	3	4	16729.124	16729.150	-0.026	cm^{-1}
6	2	5	7	3	4	16727.776	16727.764	0.011	cm^{-1}
6	2	4	7	3	5	16727.776	16727.783	-0.007	cm^{-1}
7	2	6	8	3	5	16726.388	16726.314	0.073	cm^{-1}
7	2	5	8	3	6	16726.388	16726.350	0.037	cm^{-1}
8	2	7	9	3	6	16724.721	16724.791	-0.070	cm^{-1}
8	2	6	9	3	7	16724.891	16724.850	0.040	cm^{-1}
9	2	8	10	3	7	16723.104	16723.193	-0.089	cm^{-1}
9	2	7	10	3	8	16723.274	16723.286	-0.012	cm^{-1}
10	2	9	11	3	8	16721.470	16721.518	-0.048	cm^{-1}
10	2	8	11	3	9	16721.774	16721.658 *	0.115	cm^{-1}
11	2	10	12	3	9	16719.771	16719.767	0.003	cm^{-1}
11	2	9	12	3	10	16719.980	16719.970	0.000	cm^{-1}
12	2	11	13	3	10	16717.903	16717.937	-0.034	cm^{-1}
12	2	10	13	3	11	16718.341	16718.222 *	0.118	cm^{-1}
13	2	12	14	3	11	16716.056	16716.027	0.028	cm^{-1}
13	2	11	14	3	12	16716.394	16716.416	-0.022	cm^{-1}
14	2	13	15	3	12	16713.986	16714.035	-0.049	cm^{-1}
14	2	12	15	3	13	16714.531	16714.555	-0.024	cm^{-1}
5	5	1	4	4	0	16796.449	16796.468	-0.019	cm^{-1}
6	5	2	5	4	1	16796.970	16796.988	-0.018	cm^{-1}
7	5	3	6	4	2	16797.442	16797.436	0.005	cm^{-1}
8	5	4	7	4	3	16797.775	16797.812	-0.037	cm^{-1}
9	5	5	8	4	4	16798.112	16798.118	-0.006	cm^{-1}
10	5	6	9	4	5	16798.535	16798.351	0.183	cm^{-1}
11	5	7	10	4	6	16798.535	16798.513	0.022	cm^{-1}
12	5	8	11	4	7	16798.565	16798.602	-0.037	cm^{-1}
13	5	9	12	4	8	16798.535	16798.619	-0.084	cm^{-1}
14	5	10	13	4	9	16798.535	16798.564	-0.029	cm^{-1}
15	5	11	14	4	10	16798.535	16798.437	0.098	cm^{-1}
16	5	12	15	4	11	16798.202	16798.236	-0.034	cm^{-1}
17	5	13	16	4	12	16797.949	16797.962	-0.013	cm^{-1}
18	5	14	17	4	13	16797.608	16797.615	-0.007	cm^{-1}
19	5	15	18	4	14	16797.194	16797.195	-0.001	cm^{-1}
20	5	16	19	4	15	16796.701	16796.700	0.000	cm^{-1}
21	5	17	20	4	16	16796.141	16796.131	0.009	cm^{-1}
22	5	18	21	4	17	16795.491	16795.486	0.004	cm^{-1}
23	5	19	22	4	18	16794.772	16794.767	0.004	cm^{-1}
24	5	20	23	4	19	16794.015	16793.972	0.043	cm^{-1}
25	5	21	24	4	20	16793.098	16793.100	-0.002	cm^{-1}
26	5	22	25	4	21	16792.188	16792.151	0.037	cm^{-1}
27	5	23	26	4	22	16791.124	16791.124	0.000	cm^{-1}
28	5	24	27	4	23	16790.043	16790.018	0.024	cm^{-1}
29	5	25	28	4	24	16788.862	16788.832	0.029	cm^{-1}
5	5	0	5	4	1	16791.798	16791.732	0.065	cm^{-1}
6	5	1	6	4	2	16791.319	16791.304	0.014	cm^{-1}

Upper State			Lower State			Observation	Calculation	Residual	Remarks
J	K_A	K_C	J	K_A	K_C				
7	5	2	7	4	3	16790.835	16790.805	0.029	cm^{-1}
8	5	3	8	4	4	16790.208	16790.234	-0.026	cm^{-1}
9	5	4	9	4	5	16789.578	16789.591	-0.013	cm^{-1}
10	5	5	10	4	6	16788.862	16788.876	-0.014	cm^{-1}
11	5	6	11	4	7	16788.122	16788.090	0.031	cm^{-1}
12	5	7	12	4	8	16787.240	16787.231	0.009	cm^{-1}
13	5	8	13	4	9	16786.313	16786.299	0.013	cm^{-1}
14	5	9	14	4	10	16785.305	16785.295	0.009	cm^{-1}
15	5	10	15	4	11	16784.225	16784.217	0.007	cm^{-1}
16	5	11	16	4	12	16783.043	16783.067	-0.024	cm^{-1}
17	5	12	17	4	13	16781.886	16781.843	0.042	cm^{-1}
18	5	13	18	4	14	16780.514	16780.545	-0.031	cm^{-1}
19	5	14	19	4	15	16779.212	16779.173	0.038	cm^{-1}
20	5	15	20	4	16	16777.790	16777.727	0.063	cm^{-1}
21	5	16	21	4	17	16776.256	16776.205	0.050	cm^{-1}
22	5	17	22	4	18	16774.610	16774.608	0.001	cm^{-1}
23	5	18	23	4	19	16772.990	16772.934	0.055	cm^{-1}
24	5	19	24	4	20	16771.207	16771.185	0.021	cm^{-1}
25	5	20	25	4	21	16769.437	16769.358	0.079	cm^{-1}
26	5	21	26	4	22	16767.565	16767.452	0.112	cm^{-1}
27	5	22	27	4	23	16765.591	16765.468	0.122	cm^{-1}
4	3	1	4	4	0	16725.137	16725.252	-0.115	cm^{-1}
5	3	2	5	4	1	16724.881	16724.899	-0.018	cm^{-1}
6	3	3	6	4	2	16724.506	16724.474	0.031	cm^{-1}
7	3	4	7	4	3	16723.983	16723.979	0.003	cm^{-1}
8	3	5	8	4	4	16723.417	16723.414	0.002	cm^{-1}
9	3	6	9	4	5	16722.746	16722.778	-0.032	cm^{-1}
10	3	7	10	4	6	16722.071	16722.072	-0.001	cm^{-1}
11	3	8	11	4	7	16721.290	16721.296	-0.006	cm^{-1}
12	3	9	12	4	8	16720.447	16720.450	-0.003	cm^{-1}
13	3	10	13	4	9	16719.563	16719.534	0.028	cm^{-1}
14	3	11	14	4	10	16718.584	16718.549	0.034	cm^{-1}
15	3	12	15	4	11	16717.509	16717.495	0.013	cm^{-1}
16	3	13	16	4	12	16716.394	16716.372	0.021	cm^{-1}
17	3	14	17	4	13	16715.159	16715.181	-0.022	cm^{-1}
18	3	15	18	4	14	16713.986	16713.923	0.062	cm^{-1}
19	3	16	19	4	15	16712.621	16712.597	0.023	cm^{-1}
20	3	17	20	4	16	16711.132	16711.206	-0.074	cm^{-1}
21	3	18	21	4	17	16709.777	16709.749	0.027	cm^{-1}
21	3	19	21	4	18	16709.608	16709.599	0.008	cm^{-1}
22	3	19	22	4	18	16708.129	16708.227	-0.098	cm^{-1}
22	3	20	22	4	19	16708.029	16708.033	-0.004	cm^{-1}
23	3	20	23	4	19	16706.631	16706.642	-0.011	cm^{-1}
23	3	21	23	4	20	16706.426	16706.392	0.033	cm^{-1}
24	3	21	24	4	20	16704.955	16704.995	-0.040	cm^{-1}
24	3	22	24	4	21	16704.774	16704.677	0.096	cm^{-1}
25	3	22	25	4	21	16703.299	16703.285	0.013	cm^{-1}
25	3	23	25	4	22	16702.914	16702.886	0.027	cm^{-1}
26	3	23	26	4	22	16701.523	16701.515	0.007	cm^{-1}
26	3	24	26	4	23	16701.038	16701.019	0.018	cm^{-1}

Upper State			Lower State			Observation	Calculation		Residual	Remarks
J	K_A	K_C	J	K_A	K_C					
27	3	24	27	4	23	16699.697	16699.685		0.011	cm^{-1}
27	3	25	27	4	24	16699.086	16699.076		0.009	cm^{-1}
28	3	25	28	4	24	16697.705	16697.796		-0.091	cm^{-1}
28	3	26	28	4	25	16697.069	16697.055		0.013	cm^{-1}
3	3	1	4	4	0	16721.774	16721.747		0.026	cm^{-1}
4	3	2	5	4	1	16720.497	16720.517		-0.020	cm^{-1}
5	3	3	6	4	2	16719.210	16719.215		-0.005	cm^{-1}
6	3	4	7	4	3	16717.903	16717.843		0.059	cm^{-1}
7	3	5	8	4	4	16716.394	16716.401		-0.007	cm^{-1}
8	3	6	9	4	5	16714.895	16714.887		0.007	cm^{-1}
9	3	7	10	4	6	16713.299	16713.303		-0.004	cm^{-1}
9	3	6	10	4	7	16713.299	16713.304		-0.005	cm^{-1}
10	3	8	11	4	7	16711.682	16711.647		0.034	cm^{-1}
10	3	7	11	4	8	16711.682	16711.649		0.032	cm^{-1}
11	3	9	12	4	8	16709.928	16709.921		0.006	cm^{-1}
11	3	8	12	4	9	16709.929	16709.924		0.004	cm^{-1}
12	3	10	13	4	9	16708.129	16708.123		0.005	cm^{-1}
12	3	9	13	4	10	16708.129	16708.129		0.000	cm^{-1}
13	3	11	14	4	10	16706.266	16706.255		0.010	cm^{-1}
13	3	10	14	4	11	16706.266	16706.265		0.000	cm^{-1}
14	3	12	15	4	11	16704.320	16704.315		0.004	cm^{-1}
14	3	11	15	4	12	16704.320	16704.330		-0.010	cm^{-1}
15	3	13	16	4	12	16702.311	16702.303		0.007	cm^{-1}
15	3	12	16	4	13	16702.311	16702.327		-0.016	cm^{-1}
16	3	14	17	4	13	16700.255	16700.220		0.034	cm^{-1}
16	3	13	17	4	14	16700.255	16700.254		0.000	cm^{-1}
17	3	15	18	4	14	16698.086	16698.065		0.020	cm^{-1}
17	3	14	18	4	15	16698.086	16698.113		-0.027	cm^{-1}
18	3	16	19	4	15	16695.857	16695.837		0.019	cm^{-1}
18	3	15	19	4	16	16695.857	16695.905		-0.048	cm^{-1}
19	3	17	20	4	16	16693.498	16693.536		-0.038	cm^{-1}
19	3	16	20	4	17	16693.600	16693.630		-0.030	cm^{-1}
20	3	18	21	4	17	16691.155	16691.161		-0.006	cm^{-1}
20	3	18	21	4	18	16691.332	16691.170	*	0.162	cm^{-1}
21	3	19	22	4	18	16688.817	16688.712		0.104	cm^{-1}
21	3	18	22	4	19	16688.901	16688.882		0.018	cm^{-1}
22	3	20	23	4	19	16686.169	16686.188		-0.019	cm^{-1}
22	3	19	23	4	20	16686.434	16686.412		0.021	cm^{-1}
23	3	21	24	4	20	16683.574	16683.588		-0.014	cm^{-1}
23	3	20	24	4	21	16683.889	16683.879		0.009	cm^{-1}
24	3	22	25	4	21	16680.903	16680.910		-0.007	cm^{-1}
24	3	21	25	4	22	16681.253	16681.285		-0.032	cm^{-1}
6	6	1	5	5	0	16803.310	16803.290		0.019	cm^{-1}
7	6	2	6	5	1	16803.724	16803.737		-0.013	cm^{-1}
8	6	3	7	5	2	16804.099	16804.113		-0.014	cm^{-1}
9	6	4	8	5	3	16804.345	16804.417		-0.072	cm^{-1}
10	6	5	9	5	4	16804.700	16804.650		0.049	cm^{-1}
11	6	6	10	5	5	16804.845	16804.811		0.033	cm^{-1}
12	6	7	11	5	6	16804.845	16804.900		-0.055	cm^{-1}
13	6	8	12	5	7	16804.845	16804.917		-0.072	cm^{-1}

Upper State			Lower State			Observation	Calculation	Residual	Remarks
J	K_A	K_C	J	K_A	K_C				
14	6	9	13	5	8	16804.845	16804.862	-0.017	cm^{-1}
15	6	10	14	5	9	16804.700	16804.735	-0.035	cm^{-1}
16	6	11	15	5	10	16804.526	16804.535	-0.009	cm^{-1}
17	6	12	16	5	11	16804.290	16804.263	0.026	cm^{-1}
18	6	13	17	5	12	16803.891	16803.918	-0.027	cm^{-1}
19	6	14	18	5	13	16803.495	16803.501	-0.006	cm^{-1}
20	6	15	19	5	14	16803.025	16803.010	0.014	cm^{-1}
21	6	16	20	5	15	16802.438	16802.446	-0.008	cm^{-1}
22	6	17	21	5	16	16801.797	16801.809	-0.012	cm^{-1}
23	6	18	22	5	17	16801.095	16801.098	-0.003	cm^{-1}
24	6	19	23	5	18	16800.264	16800.313	-0.049	cm^{-1}
25	6	20	24	5	19	16799.395	16799.454	-0.059	cm^{-1}
26	6	21	25	5	20	16798.535	16798.521	0.013	cm^{-1}
27	6	22	26	5	21	16797.442	16797.513	-0.071	cm^{-1}
28	6	23	27	5	22	16796.449	16796.430	0.018	cm^{-1}
29	6	24	28	5	23	16795.221	16795.272	-0.051	cm^{-1}
6	6	1	6	5	2	16797.608	16797.608	0.000	cm^{-1}
7	6	2	7	5	3	16797.194	16797.108	0.085	cm^{-1}
8	6	3	8	5	4	16796.499	16796.537	-0.038	cm^{-1}
9	6	4	9	5	5	16795.900	16795.894	0.005	cm^{-1}
10	6	5	10	5	6	16795.221	16795.179	0.041	cm^{-1}
11	6	6	11	5	7	16794.372	16794.392	-0.020	cm^{-1}
12	6	7	12	5	8	16793.537	16793.533	0.003	cm^{-1}
13	6	8	13	5	9	16792.609	16792.602	0.006	cm^{-1}
14	6	9	14	5	10	16791.609	16791.599	0.009	cm^{-1}
15	6	10	15	5	11	16790.553	16790.524	0.029	cm^{-1}
16	6	11	16	5	12	16789.292	16789.375	-0.083	cm^{-1}
17	6	12	17	5	13	16788.122	16788.155	-0.033	cm^{-1}
18	6	13	18	5	14	16786.844	16786.861	-0.017	cm^{-1}
19	6	14	19	5	15	16785.513	16785.494	0.018	cm^{-1}
20	6	15	20	5	16	16784.040	16784.054	-0.014	cm^{-1}
21	6	16	21	5	17	16782.498	16782.540	-0.042	cm^{-1}
22	6	17	22	5	18	16780.968	16780.953	0.014	cm^{-1}
23	6	18	23	5	19	16779.212	16779.292	-0.080	cm^{-1}
24	6	19	24	5	20	16777.556	16777.556	0.000	cm^{-1}
25	6	20	25	5	21	16775.639	16775.747	-0.108	cm^{-1}
26	6	21	26	5	22	16773.916	16773.862	0.053	cm^{-1}
27	6	22	27	5	23	16771.980	16771.903	0.076	cm^{-1}
28	6	23	28	5	24	16769.867	16769.868	-0.001	cm^{-1}
29	6	24	29	5	25	16767.798	16767.759	0.039	cm^{-1}
5	4	1	5	5	0	16714.531	16714.535	-0.004	cm^{-1}
6	4	2	6	5	1	16713.986	16714.110	-0.124	cm^{-1}
7	4	3	7	5	2	16713.593	16713.615	-0.022	cm^{-1}
8	4	4	8	5	3	16713.050	16713.048	0.001	cm^{-1}
9	4	5	9	5	4	16712.500	16712.411	0.088	cm^{-1}
10	4	6	10	5	5	16711.682	16711.704	-0.022	cm^{-1}
11	4	7	11	5	6	16710.938	16710.925	0.012	cm^{-1}
12	4	8	12	5	7	16710.128	16710.076	0.051	cm^{-1}
13	4	9	13	5	8	16709.139	16709.156	-0.017	cm^{-1}
14	4	10	14	5	9	16708.129	16708.165	-0.036	cm^{-1}

Upper State			Lower State			Observation	Calculation	Residual	Remarks
J	K_A	K_C	J	K_A	K_C				
15	4	11	15	5	10	16707.102	16707.104	-0.002	cm^{-1}
16	4	12	16	5	11	16705.993	16705.971	0.021	cm^{-1}
17	4	13	17	5	12	16704.774	16704.768	0.005	cm^{-1}
18	4	14	18	5	13	16703.520	16703.495	0.024	cm^{-1}
19	4	15	19	5	14	16702.131	16702.151	-0.020	cm^{-1}
20	4	16	20	5	15	16700.733	16700.736	-0.003	cm^{-1}
21	4	17	21	5	16	16699.284	16699.251	0.032	cm^{-1}
22	4	18	22	5	17	16697.705	16697.695	0.009	cm^{-1}
23	4	19	23	5	18	16696.065	16696.069	-0.004	cm^{-1}
24	4	20	24	5	19	16694.380	16694.373	0.007	cm^{-1}
25	4	21	25	5	20	16692.697	16692.606	0.090	cm^{-1}
26	4	22	26	5	21	16690.772	16690.770	0.001	cm^{-1}
27	4	23	27	5	22	16688.817	16688.864	-0.047	cm^{-1}
28	4	24	28	5	23	16686.922	16686.889	0.033	cm^{-1}
29	4	25	29	5	24	16684.849	16684.844	0.004	cm^{-1}
4	4	1	5	5	0	16710.128	16710.154	-0.026	cm^{-1}
5	4	2	6	5	1	16708.865	16708.853	0.011	cm^{-1}
6	4	3	7	5	2	16707.461	16707.481	-0.020	cm^{-1}
7	4	4	8	5	3	16705.993	16706.038	-0.045	cm^{-1}
8	4	5	9	5	4	16704.526	16704.525	0.000	cm^{-1}
9	4	6	10	5	5	16702.914	16702.940	-0.026	cm^{-1}
10	4	7	11	5	6	16701.284	16701.285	-0.001	cm^{-1}
11	4	8	12	5	7	16699.548	16699.559	-0.011	cm^{-1}
12	4	9	13	5	8	16697.705	16697.761	-0.056	cm^{-1}
13	4	10	14	5	9	16695.857	16695.893	-0.036	cm^{-1}
14	4	11	15	5	10	16694.029	16693.954	0.074	cm^{-1}
15	4	12	16	5	11	16691.945	16691.944	0.000	cm^{-1}
16	4	13	17	5	12	16689.903	16689.862	0.040	cm^{-1}
17	4	14	18	5	13	16687.687	16687.710	-0.023	cm^{-1}
18	4	15	19	5	14	16685.506	16685.487	0.018	cm^{-1}
19	4	16	20	5	15	16683.182	16683.192	-0.010	cm^{-1}
20	4	17	21	5	16	16680.903	16680.827	0.075	cm^{-1}
21	4	18	22	5	17	16678.388	16678.390	-0.002	cm^{-1}
23	4	20	24	5	19	16673.351	16673.302	0.048	cm^{-1}
24	4	21	25	5	20	16670.641	16670.651	-0.010	cm^{-1}
7	7	0	6	6	1	16809.582	16809.585	-0.003	cm^{-1}
8	7	2	7	6	1	16809.936	16809.960	-0.024	cm^{-1}
9	7	2	8	6	3	16810.286	16810.263	0.022	cm^{-1}
10	7	4	9	6	3	16810.506	16810.494	0.011	cm^{-1}
11	7	4	10	6	5	16810.708	16810.654	0.053	cm^{-1}
12	7	6	11	6	5	16810.708	16810.742	-0.034	cm^{-1}
13	7	6	12	6	7	16810.708	16810.758	-0.050	cm^{-1}
14	7	8	13	6	7	16810.708	16810.701	0.006	cm^{-1}
15	7	8	14	6	9	16810.506	16810.573	-0.067	cm^{-1}
16	7	10	15	6	9	16810.286	16810.372	-0.086	cm^{-1}
17	7	10	16	6	11	16810.077	16810.100	-0.023	cm^{-1}
18	7	12	17	6	11	16809.726	16809.754	-0.028	cm^{-1}
19	7	12	18	6	13	16809.343	16809.336	0.006	cm^{-1}
20	7	14	19	6	13	16808.840	16808.846	-0.006	cm^{-1}
21	7	15	20	6	14	16808.279	16808.282	-0.003	cm^{-1}

Upper State J	K_A	K_C	Lower State J	K_A	K_C	Observation	Calculation	Residual	Remarks
22	7	16	21	6	15	16807.643	16807.646	-0.003	cm^{-1}
23	7	17	22	6	16	16806.916	16806.936	-0.020	cm^{-1}
24	7	18	23	6	17	16806.144	16806.154	-0.010	cm^{-1}
25	7	19	24	6	18	16805.286	16805.297	-0.011	cm^{-1}
26	7	20	25	6	19	16804.345	16804.367	-0.022	cm^{-1}
27	7	21	26	6	20	16803.310	16803.363	-0.053	cm^{-1}
28	7	22	27	6	21	16802.276	16802.285	-0.009	cm^{-1}
29	7	23	28	6	22	16801.096	16801.133	-0.037	cm^{-1}
7	7	0	7	6	1	16803.025	16802.958	0.066	cm^{-1}
8	7	1	8	6	2	16802.438	16802.386	0.051	cm^{-1}
9	7	2	9	6	3	16801.746	16801.742	0.003	cm^{-1}
10	7	3	10	6	4	16801.096	16801.026	0.069	cm^{-1}
11	7	4	11	6	5	16800.264	16800.239	0.024	cm^{-1}
12	7	5	12	6	6	16799.395	16799.379	0.015	cm^{-1}
13	7	6	13	6	7	16798.535	16798.448	0.086	cm^{-1}
14	7	7	14	6	8	16797.442	16797.444	-0.002	cm^{-1}
15	7	8	15	6	9	16796.449	16796.368	0.080	cm^{-1}
16	7	9	16	6	10	16795.221	16795.220	0.000	cm^{-1}
17	7	10	17	6	11	16794.015	16793.999	0.015	cm^{-1}
18	7	11	18	6	12	16792.704	16792.706	-0.002	cm^{-1}
19	7	12	19	6	13	16791.319	16791.340	-0.021	cm^{-1}
20	7	13	20	6	14	16789.903	16789.901	0.001	cm^{-1}
21	7	14	21	6	15	16788.428	16788.389	0.038	cm^{-1}
22	7	15	22	6	16	16786.844	16786.804	0.039	cm^{-1}
23	7	16	23	6	17	16785.165	16785.145	0.019	cm^{-1}
24	7	17	24	6	18	16783.469	16783.413	0.055	cm^{-1}
25	7	18	25	6	19	16791.648	16781.607	0.040	cm^{-1}
26	7	19	26	6	20	16779.736	16779.728	0.007	cm^{-1}
27	7	20	27	6	21	16777.790	16777.774	0.015	cm^{-1}
28	7	21	28	6	22	16775.639	16775.746	-0.107	cm^{-1}
6	5	1	6	6	0	16703.299	16703.320	-0.021	cm^{-1}
7	5	2	7	6	1	16702.914	16702.825	0.088	cm^{-1}
8	5	3	8	6	2	16702.311	16702.258	0.052	cm^{-1}
9	5	4	9	6	3	16701.523	16701.621	-0.098	cm^{-1}
10	5	5	10	6	4	16700.902	16700.913	-0.011	cm^{-1}
11	5	6	11	6	5	16700.079	16700.133	-0.054	cm^{-1}
12	5	7	12	6	6	16699.284	16699.283	0.000	cm^{-1}
13	5	8	13	6	7	16698.365	16698.362	0.002	cm^{-1}
14	5	9	14	6	8	16697.380	16697.370	0.009	cm^{-1}
15	5	10	15	6	9	16696.287	16696.307	-0.020	cm^{-1}
16	5	11	16	6	10	16695.233	16695.173	0.059	cm^{-1}
17	5	12	17	6	11	16694.029	16693.968	0.060	cm^{-1}
18	5	13	18	6	12	16692.697	16692.692	0.004	cm^{-1}
19	5	14	19	6	13	16691.332	16691.345	-0.013	cm^{-1}
20	5	15	20	6	14	16689.903	16689.927	-0.024	cm^{-1}
21	5	16	21	6	15	16688.484	16688.437	0.046	cm^{-1}
22	5	17	22	6	16	16686.922	16686.877	0.044	cm^{-1}
23	5	18	23	6	17	16685.226	16685.245	-0.019	cm^{-1}
24	5	19	24	6	18	16683.574	16683.542	0.031	cm^{-1}
25	5	20	25	6	19	16681.772	16681.767	0.004	cm^{-1}

Upper State			Lower State			Observation	Calculation	Residual	Remarks
J	K_A	K_C	J	K_A	K_C				
26	5	21	26	6	20	16679.923	16679.922	0.001	cm^{-1}
27	5	22	27	6	21	16678.008	16678.004	0.003	cm^{-1}
28	5	23	28	6	22	16675.999	16676.016	-0.017	cm^{-1}
29	5	24	29	6	23	16673.939	16673.956	-0.017	cm^{-1}
5	5	1	6	6	0	16698.086	16698.065	0.020	cm^{-1}
6	5	2	7	6	1	16696.677	16696.693	-0.016	cm^{-1}
7	5	3	8	6	2	16695.233	16695.251	-0.018	cm^{-1}
8	5	4	9	6	3	16693.749	16693.737	0.011	cm^{-1}
9	5	5	10	6	4	16692.131	16692.153	-0.022	cm^{-1}
10	5	6	11	6	5	16690.494	16690.497	-0.003	cm^{-1}
11	5	7	12	6	6	16688.817	16688.771	0.045	cm^{-1}
12	5	8	13	6	7	16686.922	16686.974	-0.052	cm^{-1}
13	5	9	14	6	8	16685.099	16685.105	-0.006	cm^{-1}
14	5	10	15	6	9	16683.182	16683.165	0.016	cm^{-1}
15	5	11	16	6	10	16681.111	16681.155	-0.044	cm^{-1}
16	5	12	17	6	11	16679.062	16679.073	-0.011	cm^{-1}
17	5	13	18	6	12	16676.956	16676.920	0.035	cm^{-1}
18	5	14	19	6	13	16674.716	16674.696	0.019	cm^{-1}
19	5	15	20	6	14	16692.404	16672.400	0.003	cm^{-1}
20	5	16	21	6	15	16670.013	16670.033	-0.020	cm^{-1}
21	5	17	22	6	16	16667.663	16667.595	0.067	cm^{-1}
22	5	18	23	6	17	16665.112	16665.085	0.026	cm^{-1}
23	5	19	24	6	18	16662.497	16662.504	-0.007	cm^{-1}
24	5	20	25	6	19	16659.835	16659.852	-0.017	cm^{-1}
25	5	21	26	6	20	16657.087	16657.127	-0.040	cm^{-1}
26	5	22	27	6	21	16654.313	16654.332	-0.019	cm^{-1}
27	5	23	28	6	22	16651.450	16651.464	-0.014	cm^{-1}
28	5	24	29	6	23	16648.516	16648.525	-0.009	cm^{-1}
8	8	1	7	7	0	16815.335	16815.358	-0.023	cm^{-1}
9	8	2	8	7	1	16815.650	16815.660	-0.010	cm^{-1}
10	8	3	9	7	2	16815.928	16815.890	0.037	cm^{-1}
11	8	4	10	7	3	16816.130	16816.048	0.082	cm^{-1}
12	8	5	11	7	4	16816.130	16816.134	-0.004	cm^{-1}
13	8	6	12	7	5	16816.130	16816.148	-0.018	cm^{-1}
14	8	7	13	7	6	16816.130	16816.090	0.040	cm^{-1}
15	8	8	14	7	7	16815.928	16815.959	-0.031	cm^{-1}
16	8	9	15	7	8	16815.710	16815.757	-0.047	cm^{-1}
17	8	10	16	7	9	16815.470	16815.482	-0.012	cm^{-1}
18	8	11	17	7	10	16815.129	16815.135	-0.006	cm^{-1}
19	8	12	18	7	11	16814.629	16814.716	-0.087	cm^{-1}
20	8	13	19	7	12	16814.199	16814.224	-0.025	cm^{-1}
21	8	14	20	7	13	16813.653	16813.659	-0.006	cm^{-1}
22	8	15	21	7	14	16812.996	16813.021	-0.025	cm^{-1}
23	8	16	22	7	15	16812.306	16812.310	-0.004	cm^{-1}
24	8	17	23	7	16	16811.564	16811.526	0.037	cm^{-1}
25	8	18	24	7	17	16810.708	16810.669	0.038	cm^{-1}
26	8	19	25	7	18	16809.726	16809.739	-0.013	cm^{-1}
27	8	20	26	7	19	16808.840	16808.735	0.104	cm^{-1}
28	8	21	27	7	20	16807.643	16807.658	-0.015	cm^{-1}
29	8	22	28	7	21	16806.450	16806.506	-0.056	cm^{-1}

Upper State			Lower State			Observation	Calculation	Residual	Remarks
J	K_A	K_C	J	K_A	K_C				
8	8	1	8	7	2	16807.785	16807.787	-0.002	cm^{-1}
9	8	2	9	7	3	16807.132	16807.142	-0.010	cm^{-1}
10	8	3	10	7	4	16806.450	16806.425	0.024	cm^{-1}
11	8	4	11	7	5	16805.578	16805.636	-0.058	cm^{-1}
12	8	5	12	7	6	16804.845	16804.775	0.069	cm^{-1}
13	8	6	13	7	7	16803.891	16803.842	0.048	cm^{-1}
14	8	7	14	7	8	16802.844	16802.837	0.006	cm^{-1}
15	8	8	15	7	9	16801.749	16801.760	-0.011	cm^{-1}
16	8	9	16	7	10	16800.591	16800.611	-0.020	cm^{-1}
17	8	10	17	7	11	16799.395	16799.389	0.005	cm^{-1}
18	8	11	18	7	12	16798.112	16798.094	0.017	cm^{-1}
19	8	12	19	7	13	16796.702	16796.727	-0.025	cm^{-1}
20	8	13	20	7	14	16795.221	16795.288	-0.067	cm^{-1}
21	8	14	21	7	15	16793.767	16793.775	-0.008	cm^{-1}
22	8	15	22	7	16	16792.188	16792.190	-0.002	cm^{-1}
23	8	16	23	7	17	16790.553	16790.531	0.021	cm^{-1}
24	8	17	24	7	18	16788.862	16788.799	0.062	cm^{-1}
25	8	18	25	7	19	16787.026	16786.994	0.031	cm^{-1}
26	8	19	26	7	20	16785.165	16785.115	0.049	cm^{-1}
7	6	1	7	7	0	16691.598	16691.620	-0.022	cm^{-1}
8	6	2	8	7	1	16690.990	16691.053	-0.063	cm^{-1}
9	6	3	9	7	2	16690.494	16690.415	0.078	cm^{-1}
10	6	4	10	7	3	16689.691	16689.706	-0.015	cm^{-1}
11	6	5	11	7	4	16688.901	16688.927	-0.026	cm^{-1}
12	6	6	12	7	5	16688.035	16688.076	-0.041	cm^{-1}
13	6	7	13	7	6	16687.181	16687.154	0.026	cm^{-1}
14	6	8	14	7	7	16686.187	16686.161	0.025	cm^{-1}
15	6	9	15	7	8	16685.089	16685.098	-0.009	cm^{-1}
16	6	10	16	7	9	16683.889	16683.963	-0.074	cm^{-1}
17	6	11	17	7	10	16682.742	16682.756	-0.014	cm^{-1}
18	6	12	18	7	11	16681.434	16681.479	-0.045	cm^{-1}
19	6	13	19	7	12	16680.085	16680.130	-0.045	cm^{-1}
20	6	14	20	7	13	16678.677	16678.711	-0.034	cm^{-1}
21	6	15	21	7	14	16677.296	16677.219	0.076	cm^{-1}
22	6	16	22	7	15	16675.579	16675.657	-0.078	cm^{-1}
23	6	17	23	7	16	16673.939	16674.023	-0.084	cm^{-1}
24	6	18	24	7	17	16672.404	16672.317	0.086	cm^{-1}
6	6	1	7	7	0	16685.506	16685.490	0.015	cm^{-1}
7	6	2	8	7	1	16684.060	16684.048	0.011	cm^{-1}
8	6	3	9	7	2	16682.552	16682.534	0.017	cm^{-1}
9	6	4	10	7	3	16680.903	16680.950	-0.047	cm^{-1}
10	6	5	11	7	4	16679.279	16679.295	-0.016	cm^{-1}
11	6	6	12	7	5	16677.593	16677.568	0.024	cm^{-1}
12	6	7	13	7	6	16675.767	16675.771	-0.004	cm^{-1}
13	6	8	14	7	7	16673.939	16673.902	0.036	cm^{-1}
14	6	9	15	7	8	16671.964	16671.962	0.001	cm^{-1}
15	6	10	16	7	9	16669.879	16669.951	-0.072	cm^{-1}
16	6	11	17	7	10	16667.895	16667.869	0.025	cm^{-1}
17	6	12	18	7	11	16665.736	16665.715	0.020	cm^{-1}
18	6	13	19	7	12	16663.491	16663.491	0.000	cm^{-1}

Upper State			Lower State			Observation	Calculation	Residual	Remarks
J	K_A	K_C	J	K_A	K_C				
19	6	14	20	7	13	16661.184	16661.195	-0.011	cm^{-1}
20	6	15	21	7	14	16658.904	16658.827	0.076	cm^{-1}
21	6	16	22	7	15	16656.366	16656.388	-0.022	cm^{-1}
22	6	17	23	7	16	16653.958	16653.877	0.080	cm^{-1}
23	6	18	24	7	17	16651.253	16651.295	-0.042	cm^{-1}
24	6	19	25	7	18	16648.675	16648.641	0.033	cm^{-1}
25	6	20	26	7	19	16645.897	16645.916	-0.019	cm^{-1}
26	6	21	27	7	20	16643.099	16643.119	-0.020	cm^{-1}
27	6	22	28	7	21	16640.208	16640.249	-0.041	cm^{-1}
28	6	23	29	7	22	16637.242	16637.308	-0.066	cm^{-1}
9	9	0	8	8	1	16820.656	16820.613	0.042	cm^{-1}
10	9	2	9	8	1	16820.885	16820.841	0.043	cm^{-1}
11	9	2	10	8	3	16821.070	16820.997	0.072	cm^{-1}
12	9	4	11	8	3	16821.070	16821.081	-0.011	cm^{-1}
13	9	4	12	8	5	16821.070	16821.093	-0.023	cm^{-1}
14	9	6	13	8	5	16821.070	16821.033	0.036	cm^{-1}
15	9	6	14	8	7	16820.885	16820.901	-0.016	cm^{-1}
16	9	8	15	8	7	16820.656	16820.696	-0.040	cm^{-1}
17	9	8	16	8	9	16820.409	16820.419	-0.010	cm^{-1}
18	9	10	17	8	9	16820.069	16820.069	0.000	cm^{-1}
19	9	10	18	8	11	16819.656	16819.647	0.008	cm^{-1}
20	9	12	19	8	11	16819.166	16819.152	0.013	cm^{-1}
21	9	13	20	8	12	16818.590	16818.585	0.004	cm^{-1}
22	9	14	21	8	13	16817.950	16817.945	0.004	cm^{-1}
23	9	15	22	8	14	16817.218	16817.232	-0.014	cm^{-1}
24	9	16	23	8	15	16816.421	16816.445	-0.024	cm^{-1}
25	9	17	24	8	16	16815.651	16815.586	0.064	cm^{-1}
26	9	18	25	8	17	16814.692	16814.654	0.038	cm^{-1}
27	9	19	26	8	18	16813.653	16813.648	0.004	cm^{-1}
28	9	20	27	8	19	16812.554	16812.568	-0.014	cm^{-1}
10	9	1	10	8	2	16811.374	16811.380	-0.006	cm^{-1}
11	9	3	11	8	3	16810.506	16810.590	-0.084	cm^{-1}
12	9	3	12	8	4	16809.726	16809.727	-0.001	cm^{-1}
13	9	4	13	8	5	16808.840	16808.793	0.046	cm^{-1}
14	9	5	14	8	6	16807.781	16807.786	-0.005	cm^{-1}
15	9	6	15	8	7	16806.709	16806.707	0.001	cm^{-1}
16	9	7	16	8	8	16805.578	16805.556	0.022	cm^{-1}
17	9	8	17	8	9	16804.345	16804.332	0.012	cm^{-1}
18	9	9	18	8	10	16803.025	16803.036	-0.011	cm^{-1}
19	9	10	19	8	11	16801.749	16801.667	0.081	cm^{-1}
20	9	11	20	8	12	16800.264	16800.225	0.038	cm^{-1}
21	9	12	21	8	13	16798.778	16798.711	0.066	cm^{-1}
22	9	13	22	8	14	16797.194	16797.123	0.070	cm^{-1}
23	9	14	23	8	15	16795.491	16795.463	0.027	cm^{-1}
24	9	15	24	8	16	16793.769	16793.730	0.038	cm^{-1}
25	9	16	25	8	17	16791.960	16791.923	0.036	cm^{-1}
26	9	17	26	8	18	16790.043	16790.043	0.000	cm^{-1}
10	7	3	10	8	2	16678.154	16678.095	0.058	cm^{-1}
11	7	4	11	8	3	16677.296	16677.315	-0.019	cm^{-1}
12	7	5	12	8	4	16676.487	16676.464	0.022	cm^{-1}

Upper State			Lower State			Observation	Calculation	Residual	Remarks
J	K_A	K_C	J	K_A	K_C				
13	7	6	13	8	5	16675.539	16675.541	-0.002	cm^{-1}
14	7	7	14	8	6	16674.559	16674.548	0.010	cm^{-1}
15	7	8	15	8	7	16673.351	16673.483	-0.132	cm^{-1}
16	7	9	16	8	8	16672.404	16672.347	0.056	cm^{-1}
17	7	10	17	8	9	16671.101	16671.140	-0.039	cm^{-1}
18	7	11	18	8	10	16669.876	16669.862	0.014	cm^{-1}
19	7	12	19	8	11	16668.513	16668.512	0.000	cm^{-1}
20	7	13	20	8	12	16667.088	16667.091	-0.003	cm^{-1}
21	7	14	21	8	13	16665.567	16665.598	-0.031	cm^{-1}
22	7	15	22	8	14	16664.017	16664.034	-0.017	cm^{-1}
23	7	16	23	8	15	16662.497	16662.398	0.098	cm^{-1}
24	7	17	24	8	16	16660.715	16660.691	0.023	cm^{-1}
25	7	18	25	8	17	16658.904	16658.912	-0.008	cm^{-1}
26	7	19	26	8	18	16657.087	16657.061	0.025	cm^{-1}
27	7	20	27	8	19	16655.116	16655.138	-0.022	cm^{-1}
28	7	21	28	8	20	16653.094	16653.144	-0.050	cm^{-1}
29	7	22	29	8	21	16651.083	16651.077	0.005	cm^{-1}
7	7	1	8	8	0	16672.404	16672.441	-0.037	cm^{-1}
8	7	2	9	8	1	16670.927	16670.928	-0.001	cm^{-1}
9	7	3	10	8	2	16669.361	16669.343	0.017	cm^{-1}
10	7	4	11	8	3	16667.669	16667.687	-0.018	cm^{-1}
11	7	5	12	8	4	16665.969	16665.961	0.007	cm^{-1}
12	7	6	13	8	5	16664.204	16664.163	0.040	cm^{-1}
13	7	7	14	8	6	16662.282	16662.294	-0.012	cm^{-1}
14	7	8	15	8	7	16660.347	16660.354	-0.007	cm^{-1}
15	7	9	16	8	8	16658.355	16658.343	0.011	cm^{-1}
16	7	10	17	8	9	16656.199	16656.260	-0.061	cm^{-1}
17	7	11	18	8	10	16654.097	16654.106	-0.009	cm^{-1}
18	7	12	19	8	11	16651.860	16651.881	-0.021	cm^{-1}
19	7	13	20	8	12	16649.577	16649.584	-0.007	cm^{-1}
20	7	14	21	8	13	16647.210	16647.216	-0.006	cm^{-1}
21	7	15	22	8	14	16644.749	16644.777	-0.028	cm^{-1}
22	7	16	23	8	15	16642.223	16642.265	-0.042	cm^{-1}
23	7	17	24	8	16	16639.645	16639.682	-0.037	cm^{-1}
24	7	18	25	8	17	16636.991	16637.028	-0.037	cm^{-1}
25	7	19	26	8	18	16634.269	16634.301	-0.032	cm^{-1}
26	7	20	27	8	19	16631.484	16631.503	-0.019	cm^{-1}
27	7	21	28	8	20	16628.606	16628.632	-0.026	cm^{-1}
28	7	22	29	8	21	16625.648	16625.690	-0.042	cm^{-1}
10	10	1	9	9	0	16825.377	16825.357	0.019	cm^{-1}
11	10	1	10	9	2	16825.562	16825.511	0.050	cm^{-1}
12	10	3	11	9	2	16825.562	16825.593	-0.031	cm^{-1}
13	10	3	12	9	4	16825.562	16825.602	-0.040	cm^{-1}
14	10	5	13	9	4	16825.562	16825.539	0.022	cm^{-1}
15	10	5	14	9	6	16825.377	16825.404	-0.027	cm^{-1}
16	10	7	15	9	6	16825.183	16825.197	-0.014	cm^{-1}
17	10	7	16	9	8	16824.942	16824.917	0.024	cm^{-1}
18	10	9	17	9	8	16824.580	16824.564	0.015	cm^{-1}
19	10	9	18	9	10	16824.131	16824.139	-0.008	cm^{-1}
20	10	11	19	9	10	16823.651	16823.641	0.009	cm^{-1}

Upper State			Lower State			Observation	Calculation		Residual	Remarks
J	K_A	K_C	J	K_A	K_C					
21	10	12	20	9	11	16823.153	16823.070		0.082	cm^{-1}
22	10	13	21	9	12	16822.407	16822.427		-0.020	cm^{-1}
23	10	14	22	9	13	16821.737	16821.710		0.026	cm^{-1}
24	10	15	23	9	14	16820.855	16820.921		-0.066	cm^{-1}
25	10	16	24	9	15	16820.069	16820.058		0.010	cm^{-1}
26	10	17	25	9	16	16819.166	16819.122		0.043	cm^{-1}
27	10	18	26	9	17	16818.093	16818.113		-0.020	cm^{-1}
9	8	1	9	9	0	16666.764	16666.802		-0.038	cm^{-1}
10	8	2	10	9	1	16666.105	16666.092		0.012	cm^{-1}
11	8	3	11	9	2	16665.336	16665.311		0.024	cm^{-1}
12	8	4	12	9	3	16664.500	16664.459		0.040	cm^{-1}
13	8	5	13	9	4	16663.491	16663.536		-0.045	cm^{-1}
14	8	6	14	9	5	16662.497	16663.542		-0.045	cm^{-1}
15	8	7	15	9	6	16661.522	16661.476		0.045	cm^{-1}
16	8	8	16	9	7	16660.347	16660.339		0.007	cm^{-1}
17	8	9	17	9	8	16659.113	16659.131		-0.018	cm^{-1}
18	8	10	18	9	9	16657.851	16657.851		0.000	cm^{-1}
19	8	11	19	9	10	16656.509	16656.500		0.008	cm^{-1}
20	8	12	20	9	11	16655.116	16655.078		0.038	cm^{-1}
21	8	13	21	9	12	16653.647	16653.584		0.063	cm^{-1}
22	8	14	22	9	13	16652.132	16652.018	*	0.113	cm^{-1}
23	8	15	23	9	14	16650.315	16650.381		-0.066	cm^{-1}
24	8	16	24	9	15	16648.675	16648.672		0.003	cm^{-1}
8	8	1	9	9	0	16658.904	16658.929		-0.025	cm^{-1}
9	8	2	10	9	1	16657.302	16657.344		-0.042	cm^{-1}
10	8	3	11	9	2	16655.686	16655.689		-0.003	cm^{-1}
11	8	4	12	9	3	16653.958	16653.962		-0.004	cm^{-1}
12	8	5	13	9	4	16652.132	16652.164		-0.032	cm^{-1}
13	8	6	14	9	5	16650.315	16650.294		0.020	cm^{-1}
14	8	7	15	9	6	16648.324	16648.354		-0.030	cm^{-1}
15	8	8	16	9	7	16646.313	16646.342		-0.029	cm^{-1}
16	8	9	17	9	8	16644.219	16644.259		-0.040	cm^{-1}
17	8	10	18	9	9	16642.069	16642.105		-0.036	cm^{-1}
18	8	11	19	9	10	16639.818	16639.879		-0.061	cm^{-1}
19	8	12	20	9	11	16637.555	16637.581		-0.026	cm^{-1}
20	8	13	21	9	12	16635.190	16635.212		-0.022	cm^{-1}
21	8	14	22	9	13	16632.731	16632.772		-0.041	cm^{-1}
22	8	15	23	9	14	16630.217	16630.260		-0.043	cm^{-1}
23	8	16	24	9	15	16627.637	16627.676		-0.039	cm^{-1}
25	8	18	26	9	17	16622.275	16622.293		-0.018	cm^{-1}
26	8	19	27	9	18	16619.535	16619.493		0.041	cm^{-1}
11	11	0	10	10	1	16829.643	16829.597		0.045	cm^{-1}
12	11	2	11	10	1	16829.643	16829.676		-0.033	cm^{-1}
13	11	2	12	10	3	16829.643	16829.683		-0.040	cm^{-1}
14	11	4	13	10	3	16829.643	16829.617		0.025	cm^{-1}
15	11	4	14	10	5	16829.450	16829.479		-0.029	cm^{-1}
16	11	6	15	10	5	16829.278	16829.268		0.009	cm^{-1}
17	11	6	16	10	7	16828.973	16828.985		-0.012	cm^{-1}
18	11	8	17	10	7	16828.636	16828.629		0.006	cm^{-1}
19	11	9	18	10	9	16828.213	16828.200		0.012	cm^{-1}

Upper State			Lower State			Observation	Calculation		Residual	Remarks
J	K_A	K_C	J	K_A	K_C					
20	11	10	19	10	9	16827.716	16827.699		0.016	cm^{-1}
21	11	11	20	10	10	16827.125	16827.124		0.000	cm^{-1}
22	11	12	21	10	11	16826.483	16826.477		0.005	cm^{-1}
23	11	13	22	10	12	16825.764	16825.756		0.007	cm^{-1}
24	11	14	23	10	13	16824.942	16824.963		-0.021	cm^{-1}
25	11	15	24	10	14	16824.131	16824.096		0.034	cm^{-1}
26	11	16	25	10	15	16823.153	16823.156		-0.003	cm^{-1}
27	11	17	26	10	16	16822.192	16822.142		0.049	cm^{-1}
28	11	18	27	10	17	16821.070	16821.055		0.014	cm^{-1}
10	9	1	10	10	0	16653.647	16653.711		-0.064	cm^{-1}
11	9	2	11	10	1	16652.907	16652.930		-0.023	cm^{-1}
12	9	3	12	10	2	16652.132	16652.077		0.055	cm^{-1}
13	9	4	13	10	3	16651.252	16651.152		0.099	cm^{-1}
14	9	5	14	10	4	16650.182	16650.157		0.024	cm^{-1}
15	9	6	15	10	5	16649.139	16649.090		0.048	cm^{-1}
16	9	7	16	10	6	16647.970	16647.952		0.017	cm^{-1}
17	9	8	17	10	7	16646.719	16646.742		-0.023	cm^{-1}
18	9	9	18	10	8	16645.501	16645.461		0.039	cm^{-1}
19	9	10	19	10	9	16644.116	16644.109		0.006	cm^{-1}
20	9	11	20	10	10	16642.738	16642.685		0.052	cm^{-1}
21	9	12	21	10	11	16641.162	16641.189		-0.027	cm^{-1}
22	9	13	22	10	12	16639.645	16639.622		0.022	cm^{-1}
23	9	14	23	10	13	16637.932	16637.983		-0.051	cm^{-1}
24	9	15	24	10	14	16636.297	16636.272		0.024	cm^{-1}
25	9	16	25	10	15	16634.491	16634.489		0.001	cm^{-1}
26	9	17	26	10	16	16632.731	16632.634		0.096	cm^{-1}
27	9	18	27	10	17	16630.755	16630.708		0.046	cm^{-1}
28	9	19	28	10	18	16628.823	16628.709	*	0.113	cm^{-1}
29	9	20	29	10	19	16626.623	16626.638		-0.015	cm^{-1}
9	9	1	10	10	0	16644.997	16644.968		0.028	cm^{-1}
10	9	2	11	10	1	16643.333	16643.312		0.020	cm^{-1}
11	9	3	12	10	2	16641.587	16641.585		0.001	cm^{-1}
12	9	4	13	10	3	16639.818	16639.786		0.031	cm^{-1}
13	9	5	14	10	4	16637.932	16637.916		0.015	cm^{-1}
14	9	6	15	10	5	16635.990	16635.975		0.014	cm^{-1}
15	9	7	16	10	6	16633.965	16633.963		0.001	cm^{-1}
16	9	8	17	10	7	16631.882	16631.879		0.002	cm^{-1}
17	9	9	18	10	8	16629.704	16629.724		-0.020	cm^{-1}
18	9	10	19	10	9	16627.451	16627.497		-0.046	cm^{-1}
19	9	11	20	10	10	16625.182	16625.199		-0.017	cm^{-1}
20	9	12	21	10	11	16622.812	16622.829		-0.017	cm^{-1}
21	9	13	22	10	12	16620.351	16620.388		-0.037	cm^{-1}
22	9	14	23	10	13	16617.821	16617.874		-0.053	cm^{-1}
23	9	15	24	10	14	16615.282	16615.289		-0.007	cm^{-1}
24	9	16	25	10	15	16612.578	16612.633		-0.055	cm^{-1}
25	9	17	26	10	16	16609.842	16609.904		-0.062	cm^{-1}
26	9	18	27	10	17	16607.049	16607.103		-0.054	cm^{-1}
12	12	0	11	11	1	16833.326	16833.341		-0.015	cm^{-1}
13	12	2	12	11	1	16833.326	16833.345		-0.019	cm^{-1}
14	12	2	13	11	3	16833.326	16833.276		0.049	cm^{-1}

Upper State			Lower State			Observation	Calculation	Residual	Remarks
J	K_A	K_C	J	K_A	K_C				
15	12	4	14	11	3	16833.118	16833.135	-0.017	cm^{-1}
16	12	4	15	11	5	16832.895	16832.920	-0.025	cm^{-1}
18	12	6	17	11	7	16832.286	16832.274	0.011	cm^{-1}
19	12	8	18	11	7	16831.824	16831.841	-0.017	cm^{-1}
20	12	8	19	11	9	16831.337	16831.335	0.001	cm^{-1}
17	12	6	16	11	5	16832.611	16832.633	-0.022	cm^{-1}
13	13	1	12	12	0	16836.550	16836.599	-0.049	cm^{-1}
14	13	1	13	12	2	16836.550	16836.527	0.022	cm^{-1}
15	13	3	14	12	2	16836.344	16836.382	-0.038	cm^{-1}
16	13	3	15	12	4	16836.147	16836.164	-0.017	cm^{-1}
17	13	5	16	12	4	16835.867	16835.874	-0.007	cm^{-1}
18	13	5	17	12	6	16835.503	16835.510	-0.007	cm^{-1}
19	13	7	18	12	6	16835.071	16835.073	-0.002	cm^{-1}
20	13	7	19	12	8	16834.575	16834.563	0.011	cm^{-1}
21	13	9	20	12	8	16833.972	16833.979	-0.007	cm^{-1}
22	13	10	21	12	9	16833.326	16833.323	0.002	cm^{-1}
23	13	11	22	12	10	16832.611	16832.593	0.017	cm^{-1}
24	13	12	23	12	11	16831.824	16831.789	0.034	cm^{-1}
11	11	1	12	12	0	16615.769	16615.759	0.009	cm^{-1}
12	11	2	13	12	1	16613.958	16613.959	-0.001	cm^{-1}
13	11	3	14	12	2	16612.083	16612.088	-0.005	cm^{-1}
14	11	4	15	12	3	16610.120	16610.145	-0.025	cm^{-1}
15	11	5	16	12	4	16608.105	16608.131	-0.026	cm^{-1}
16	11	6	17	12	5	16606.049	16606.046	0.003	cm^{-1}

CH_2S: $3_0^1 4_0^3$ BAND

Upper State			Lower State			Observation	Calculation	Residual	Remarks
J	K_A	K_C	J	K_A	K_C				
2	2	1	1	1	0	18572.108	18572.142	-0.034	cm^{-1}
2	2	0	1	1	1	18572.108	18572.177	-0.069	cm^{-1}
3	2	2	2	1	1	18572.949	18572.937	0.011	cm^{-1}
3	2	1	2	1	2	18572.949	18573.042	-0.093	cm^{-1}
4	2	3	3	1	2	18573.447	18573.609	-0.062	cm^{-1}
4	2	2	3	1	3	18573.763	18573.819	-0.056	cm^{-1}
5	2	4	4	1	3	18574.119	18574.159	-0.040	cm^{-1}
5	2	3	4	1	4	18574.517	18574.509	0.007	cm^{-1}
6	2	5	5	1	4	18574.517	18574.586	-0.069	cm^{-1}
6	2	4	5	1	5	18575.081	18575.112	-0.031	cm^{-1}
7	2	6	6	1	5	18574.773	18574.890	-0.117	cm^{-1}
7	2	5	6	1	6	18575.612	18575.628	-0.016	cm^{-1}
8	2	7	7	1	6	18575.081	18575.072	0.008	cm^{-1}
8	2	6	7	1	7	18575.991	18576.057	-0.066	cm^{-1}
9	2	8	8	1	7	18575.081	18575.132	-0.051	cm^{-1}
9	2	7	8	1	8	18576.334	18576.400	-0.066	cm^{-1}
10	2	9	9	1	8	18575.081	18575.069	0.011	cm^{-1}
10	2	8	9	1	9	18576.600	18576.657	-0.057	cm^{-1}
11	2	10	10	1	9	18574.776	18574.884	-0.108	cm^{-1}
11	2	9	10	1	10	18576.860	18576.828	0.031	cm^{-1}
12	2	11	11	1	10	18574.517	18574.577	-0.060	cm^{-1}
12	2	10	11	1	11	18576.860	18576.915	-0.055	cm^{-1}
13	2	12	12	1	11	18574.119	18574.149	-0.030	cm^{-1}
13	2	11	12	1	12	18576.860	18576.917	-0.057	cm^{-1}
14	2	13	13	1	12	18573.547	18573.599	-0.052	cm^{-1}
14	2	12	13	1	13	18576.860	18576.835	0.024	cm^{-1}
15	2	14	14	1	13	18572.949	18572.927	0.021	cm^{-1}
15	2	13	14	1	14	18576.600	18576.669	-0.069	cm^{-1}
16	2	15	15	1	14	18572.108	18572.135	-0.027	cm^{-1}
16	2	14	15	1	15	18576.334	18576.421	-0.087	cm^{-1}
17	2	16	16	1	15	18571.204	18571.222	-0.018	cm^{-1}
17	2	15	16	1	16	18575.991	18576.091	-0.100	cm^{-1}
18	2	17	17	1	16	18570.182	18570.188	-0.006	cm^{-1}
18	2	16	17	1	17	18575.612	18575.680	-0.068	cm^{-1}
19	2	18	18	1	17	18568.951	18569.034	-0.083	cm^{-1}
19	2	17	18	1	18	18575.081	18575.188	-0.107	cm^{-1}
20	2	19	19	1	18	18567.636	18567.761	-0.125	cm^{-1}
20	2	18	19	1	19	18574.517	18574.617	-0.100	cm^{-1}
2	2	0	2	1	1	18569.773	18569.815	-0.042	cm^{-1}
2	2	1	2	1	2	18570.003	18569.920	0.082	cm^{-1}
3	2	1	3	1	2	18569.382	18569.447	-0.065	cm^{-1}
3	2	2	3	1	3	18569.773	18569.657	0.115	cm^{-1}
4	2	2	4	1	3	18568.951	18568.957	-0.006	cm^{-1}
4	2	3	4	1	4	18569.283	18569.306	-0.023	cm^{-1}
5	2	3	5	1	4	18568.382	18568.344	0.037	cm^{-1}
5	2	4	5	1	5	18568.951	18568.867	0.083	cm^{-1}
6	2	4	6	1	5	18567.636	18567.610	0.025	cm^{-1}
6	2	5	6	1	6	18568.382	18568.341	0.040	cm^{-1}
7	2	5	7	1	6	18566.712	18566.753	-0.041	cm^{-1}
7	2	6	7	1	7	18567.636	18567.728	-0.092	cm^{-1}

Upper State			Lower State			Observation	Calculation	Residual	Remarks
J	K_A	K_C	J	K_A	K_C				
8	2	6	8	1	7	18565.756	18565.776	-0.020	cm^{-1}
8	2	7	8	1	8	18567.022	18567.027	-0.005	cm^{-1}
9	2	7	9	1	8	18564.542	18564.677	-0.135	cm^{-1}
9	2	8	9	1	9	18566.203	18566.239	-0.036	cm^{-1}
10	2	8	10	1	9	18563.350	18563.458	-0.108	cm^{-1}
10	2	9	10	1	10	18565.353	18565.364	-0.011	cm^{-1}
11	2	9	11	1	10	18562.135	18562.119	0.015	cm^{-1}
11	2	10	11	1	11	18564.355	18564.402	-0.047	cm^{-1}
12	2	10	12	1	11	18560.631	18560.661	-0.030	cm^{-1}
12	2	11	12	1	12	18563.350	18563.354	-0.004	cm^{-1}
13	2	11	13	1	12	18559.052	18559.084	-0.032	cm^{-1}
13	2	12	13	1	13	18562.135	18562.219	-0.084	cm^{-1}
14	2	12	14	1	13	18557.412	18557.389	0.022	cm^{-1}
14	2	13	14	1	14	18560.961	18560.998	-0.037	cm^{-1}
15	2	13	15	1	14	18555.553	18555.576	-0.023	cm^{-1}
15	2	14	15	1	15	18559.699	18558.590	0.008	cm^{-1}
16	2	14	16	1	15	18553.578	18553.647	-0.069	cm^{-1}
16	2	15	16	1	16	18558.261	18558.297	-0.036	cm^{-1}
17	2	15	17	1	16	18551.568	18551.602	-0.034	cm^{-1}
17	2	16	17	1	17	18556.827	18556.818	0.008	cm^{-1}
18	2	16	18	1	17	18549.441	18549.442	-0.001	cm^{-1}
18	2	17	18	1	18	18555.244	18555.254	-0.010	cm^{-1}
19	2	17	19	1	18	18547.181	18547.168	0.012	cm^{-1}
19	2	18	19	1	19	18553.578	18553.604	-0.026	cm^{-1}
20	2	18	20	1	19	18544.881	18544.781	0.099	cm^{-1}
20	2	19	20	1	20	18551.887	18551.870	0.016	cm^{-1}
21	2	19	21	1	20	18542.281	18542.282	-0.002	cm^{-1}
21	2	20	21	1	21	18550.070	18550.050	0.019	cm^{-1}
20	2	20	22	1	21	18539.682	18539.673	0.008	cm^{-1}
22	2	21	22	1	22	18548.162	18548.147	0.014	cm^{-1}
23	2	21	23	1	22	18536.941	18536.954	-0.013	cm^{-1}
23	2	22	23	1	23	18546.203	18546.159	0.043	cm^{-1}
24	2	22	24	1	23	18534.190	18534.126	0.063	cm^{-1}
24	2	23	24	1	24	18544.149	18544.087	0.061	cm^{-1}
25	2	23	25	1	24	18531.291	18531.192	0.098	cm^{-1}
25	2	24	25	1	25	18542.010	18541.931	0.078	cm^{-1}
26	2	24	26	1	25	18528.199	18528.152	0.047	cm^{-1}
26	2	25	26	1	26	18539.682	18539.692	-0.010	cm^{-1}
27	2	26	27	1	27	18537.405	18537.369	0.035	cm^{-1}
28	2	27	28	1	28	18535.089	18534.964	0.124	cm^{-1}
5	2	3	6	1	6	18562.135	18562.099	0.035	cm^{-1}
5	2	4	6	1	5	18561.377	18561.365	0.011	cm^{-1}
6	2	4	7	1	7	18560.423	18560.447	-0.024	cm^{-1}
6	2	5	7	1	6	18559.405	18559.466	-0.061	cm^{-1}
7	2	5	8	1	8	18558.798	18558.708	0.089	cm^{-1}
7	2	6	8	1	7	18557.412	18557.446	-0.034	cm^{-1}
8	2	6	9	1	9	18556.827	18556.883	-0.056	cm^{-1}
8	2	7	9	1	8	18555.244	18555.304	-0.060	cm^{-1}
9	2	7	10	1	10	18555.050	18554.972	0.078	cm^{-1}
10	2	8	11	1	11	18552.998	18552.976	0.021	cm^{-1}

Upper State			Lower State			Observation	Calculation		Residual	Remarks
J	K_A	K_C	J	K_A	K_C					
10	2	9	11	1	10	18550.6190	18550.655		-0.036	cm^{-1}
11	2	9	12	1	12	18550.918	18550.896		0.021	cm^{-1}
11	2	10	12	1	11	18548.162	18548.149		0.012	cm^{-1}
12	2	10	13	1	13	18548.680	18548.731		-0.051	cm^{-1}
12	2	11	13	1	12	18545.550	18545.521		0.028	cm^{-1}
13	2	11	14	1	14	18546.490	18546.483		0.006	cm^{-1}
13	2	12	14	1	13	18542.711	18542.773		-0.062	cm^{-1}
14	2	12	15	1	15	18544.149	18544.152		-0.003	cm^{-1}
14	2	13	15	1	14	18539.902	18539.904		-0.002	cm^{-1}
15	2	13	16	1	16	18541.676	18541.738		-0.062	cm^{-1}
15	2	14	16	1	15	18536.941	18536.916		0.024	cm^{-1}
16	2	14	17	1	17	18539.231	18539.243		-0.012	cm^{-1}
16	2	15	17	1	16	18533.935	18533.807		0.127	cm^{-1}
17	2	15	18	1	18	18536.627	18536.667		-0.040	cm^{-1}
17	2	16	18	1	17	18530.557	18530.580		-0.023	cm^{-1}
18	2	16	19	1	19	18533.935	18534.012		-0.077	cm^{-1}
18	2	17	19	1	18	18527.262	18527.233		0.028	cm^{-1}
19	2	17	20	1	20	18531.291	18531.277		0.013	cm^{-1}
19	2	18	20	1	19	18523.813	18523.768		0.044	cm^{-1}
2	0	2	1	1	1	18541.000	18541.004	*	-0.004	cm^{-1}
3	0	3	2	1	2	18541.676	18541.869	*	-0.193	cm^{-1}
4	0	4	3	1	3	18542.455	18542.647	*	-0.192	cm^{-1}
5	0	5	4	1	4	18543.141	18543.336	*	-0.195	cm^{-1}
6	0	6	5	1	5	18543.660	18543.937	*	-0.277	cm^{-1}
7	0	7	6	1	6	18544.149	18544.450	*	-0.301	cm^{-1}
8	0	8	7	1	7	18544.550	18544.875	*	-0.325	cm^{-1}
9	0	9	8	1	8	18544.800	18545.211	*	-0.411	cm^{-1}
10	0	10	9	1	9	18544.881	18545.459	*	-0.578	cm^{-1}
11	0	11	10	1	10	18544.881	18545.618	*	-0.737	cm^{-1}
12	0	12	11	1	11	18544.881	18545.689	*	-0.808	cm^{-1}
13	0	13	12	1	12	18544.881	18545.670	*	-0.789	cm^{-1}
14	0	14	13	1	13	18544.601	18545.563	*	-0.962	cm^{-1}
15	0	15	14	1	14	18544.249	18545.366	*	-1.117	cm^{-1}
16	0	16	15	1	15	18543.856	18545.080	*	-1.224	cm^{-1}
17	0	17	16	1	16	18543.309	18544.704	*	-1.395	cm^{-1}
18	0	18	17	1	17	18542.711	18544.238	*	-1.527	cm^{-1}
19	0	19	18	1	18	18542.010	18543.681	*	-1.671	cm^{-1}
20	0	20	19	1	19	18541.148	18543.035	*	-1.887	cm^{-1}
21	0	21	20	1	20	18540.176	18542.297	*	-2.121	cm^{-1}
22	0	22	21	1	21	18539.231	18541.469	*	-2.238	cm^{-1}
1	0	1	1	1	0	18538.827	18538.888	*	-0.061	cm^{-1}
2	0	2	2	1	1	18538.586	18538.643	*	-0.057	cm^{-1}
3	0	3	3	1	3	18538.185	18538.275	*	-0.090	cm^{-1}
5	0	5	5	1	4	18536.941	18537.171	*	-0.230	cm^{-1}
6	0	6	6	1	5	18536.189	18536.434	*	-0.245	cm^{-1}
7	0	7	7	1	6	18535.227	18535.575	*	-0.348	cm^{-1}
8	0	8	8	1	7	18534.190	18534.593	*	-0.403	cm^{-1}
9	0	9	9	1	8	18533.033	18533.488	*	-0.455	cm^{-1}
10	0	10	10	1	9	18531.723	18532.261	*	-0.538	cm^{-1}
11	0	11	11	1	10	18530.250	18530.910	*	-0.660	cm^{-1}

Upper State			Lower State			Observation	Calculation	Residual	Remarks
J	K_A	K_C	J	K_A	K_C				
12	0	12	12	1	11	18528.700	18529.435 *	-0.735	cm^{-1}
14	0	14	14	1	13	18525.122	18526.117 *	-0.995	cm^{-1}
15	0	15	15	1	14	18523.209	18524.273 *	-1.064	cm^{-1}
16	0	16	16	1	15	18521.182	18522.305 *	-1.123	cm^{-1}
17	0	17	17	1	16	18518.851	18520.214 *	-1.363	cm^{-1}
18	0	18	18	1	17	18516.529	18517.999 *	-1.470	cm^{-1}
18	0	18	18	1	17	18516.529	18517.999 *	-1.470	cm^{-1}
19	0	19	19	1	18	18513.984	18515.661 *	-1.677	cm^{-1}
20	0	20	20	1	19	18511.296	18513.199 *	-1.903	cm^{-1}
21	0	21	21	1	20	18508.514	18510.613 *	-2.099	cm^{-1}
22	0	22	22	1	21	18505.687	18507.904 *	-2.217	cm^{-1}
23	0	23	23	1	22	18502.595	18505.071 *	-2.476	cm^{-1}
1	0	1	2	1	2	18536.399	18536.666 *	-0.267	cm^{-1}
2	0	2	3	1	3	18535.086	18535.363 *	-0.277	cm^{-1}
3	0	3	4	1	4	18533.935	18533.971 *	-0.036	cm^{-1}
4	0	4	5	1	5	18532.315	18532.492 *	-0.177	cm^{-1}
5	0	5	6	1	6	18530.704	18530.926 *	-0.222	cm^{-1}
6	0	6	7	1	7	18529.024	18529.272 *	-0.248	cm^{-1}
7	0	7	8	1	8	18527.222	18527.530 *	-0.308	cm^{-1}
8	0	8	9	1	9	18525.337	18525.701 *	-0.364	cm^{-1}
9	0	9	10	1	10	18523.329	18523.783 *	-0.454	cm^{-1}
10	0	10	11	1	11	18521.182	18521.779 *	-0.597	cm^{-1}
11	0	11	12	1	12	18519.020	18519.686 *	-0.666	cm^{-1}
12	0	12	13	1	13	18516.779	18517.505 *	-0.726	cm^{-1}
13	0	13	14	1	14	18514.207	18515.237 *	-1.030	cm^{-1}
14	0	14	15	1	15	18511.859	18512.880 *	-1.021	cm^{-1}
15	0	15	16	1	16	18509.331	18510.435 *	-1.104	cm^{-1}
16	0	16	17	1	17	18506.693	18507.902 *	-1.209	cm^{-1}
17	0	17	18	1	18	18503.919	18505.280 *	-1.361	cm^{-1}
18	0	18	19	1	19	18501.042	18502.569 *	-1.527	cm^{-1}
19	0	19	20	1	20	18498.056	18499.770 *	-1.714	cm^{-1}
20	0	20	21	1	21	18494.985	18496.881 *	-1.896	cm^{-1}
21	0	21	22	1	22	18491.803	18493.903 *	-2.100	cm^{-1}
22	0	22	23	1	23	18488.600	18490.836 *	-2.236	cm^{-1}
3	3	1	2	2	0	18584.577	18584.541	0.035	cm^{-1}
4	3	2	3	2	1	18585.248	18585.265	-0.017	cm^{-1}
5	3	3	4	2	2	18585.926	18585.883	0.042	cm^{-1}
6	3	4	5	2	3	18586.353	18586.395	-0.042	cm^{-1}
7	3	5	6	2	4	18586.778	18586.801	-0.023	cm^{-1}
8	3	6	7	2	5	18587.104	18587.099	0.004	cm^{-1}
9	3	7	8	2	6	18587.328	18587.290	0.037	cm^{-1}
10	3	8	9	2	7	18587.328	18587.372	-0.044	cm^{-1}
11	3	9	10	2	8	18587.328	18587.345	-0.017	cm^{-1}
12	3	10	11	2	9	18587.328	18587.208	0.119	cm^{-1}
13	3	11	12	2	10	18586.939	18586.961	-0.022	cm^{-1}
4	3	1	4	2	2	18580.775	18580.681	0.093	cm^{-1}
5	3	2	5	2	3	18580.159	18580.153	0.005	cm^{-1}
6	3	3	6	2	4	18579.569	18579.518	0.050	cm^{-1}
7	3	4	7	2	5	18578.799	18578.776	0.022	cm^{-1}
8	3	5	8	2	6	18578.077	18577.927	0.149	cm^{-1}

CH_2S: $3_0^1 4_0^3$ Band - continued

Upper State			Lower State			Observation	Calculation	Residual	Remarks
J	K_A	K_C	J	K_A	K_C				
9	3	6	9	2	7	18577.074	18576.969	0.104	cm^{-1}
10	3	7	10	2	8	18575.991	18575.902	0.088	cm^{-1}
11	3	8	11	2	9	18574.773	18574.726	0.046	cm^{-1}
12	3	9	12	2	10	18573.547	18573.439	0.107	cm^{-1}
13	3	10	13	2	11	18572.108	18572.040	0.067	cm^{-1}
4	4	1	3	3	0	18594.262	18594.234	0.027	cm^{-1}
5	4	2	4	3	1	18594.924	18594.852	0.071	cm^{-1}
6	4	3	5	3	2	18595.386	18595.365	0.020	cm^{-1}
7	4	4	6	3	3	18595.724	18595.773	-0.049	cm^{-1}
8	4	5	7	3	4	18596.060	18596.074	-0.014	cm^{-1}
9	4	6	8	3	5	18596.318	18596.269	0.048	cm^{-1}
10	4	7	9	3	6	18596.318	18596.359	-0.041	cm^{-1}
11	4	8	10	3	7	18596.318	18596.342	-0.024	cm^{-1}
12	4	9	11	3	8	18596.318	18596.219	0.098	cm^{-1}
13	4	10	12	3	9	18596.060	18595.990	0.069	cm^{-1}
14	4	11	13	3	10	18595.724	18595.654	0.069	cm^{-1}
15	4	12	14	3	11	18595.201	18595.211	-0.010	cm^{-1}
16	4	13	15	3	12	18594.652	18594.661	-0.009	cm^{-1}
17	4	14	16	3	13	18593.991	18594.004	-0.013	cm^{-1}
18	4	15	17	3	14	18593.202	18593.239	-0.037	cm^{-1}
19	4	16	18	3	15	18592.335	18592.365	-0.030	cm^{-1}
20	4	17	19	3	16	18591.381	18591.384	-0.003	cm^{-1}
21	4	18	20	3	17	18590.362	18590.294	0.067	cm^{-1}
22	4	19	21	3	18	18589.099	18589.095	0.003	cm^{-1}
23	4	20	22	3	19	18587.764	18587.787	-0.023	cm^{-1}
24	4	21	23	3	20	18586.363	18586.369	-0.006	cm^{-1}
25	4	22	24	3	21	18584.772	18584.840	-0.068	cm^{-1}
26	4	23	25	3	22	18583.150	18583.200	-0.057	cm^{-1}
27	4	24	26	3	23	18581.397	18581.449	-0.052	cm^{-1}
28	4	25	27	3	24	18579.569	18579.586	-0.017	cm^{-1}
29	4	26	28	3	25	18577.574	18577.610	-0.036	cm^{-1}
4	4	1	4	3	2	18589.703	18589.651	0.051	cm^{-1}
5	4	2	5	3	3	18589.099	18589.124	-0.025	cm^{-1}
6	4	3	6	3	4	18588.516	18588.491	0.024	cm^{-1}
7	4	4	7	3	5	18587.764	18587.752	0.011	cm^{-1}
8	4	5	8	3	6	18586.939	18586.908	0.030	cm^{-1}
9	4	6	9	3	7	18585.926	18585.958	-0.032	cm^{-1}
10	4	7	10	3	8	18584.954	18584.902	0.051	cm^{-1}
11	4	8	11	3	9	18583.772	18583.740	0.031	cm^{-1}
12	4	9	12	3	10	18582.481	18582.471	0.009	cm^{-1}
13	4	10	13	3	11	18581.098	18581.097	0.000	cm^{-1}
14	4	11	14	3	12	18579.569	18579.616	-0.047	cm^{-1}
15	4	12	15	3	13	18578.077	18578.028	0.048	cm^{-1}
16	4	13	16	3	14	18576.334	18576.334	0.000	cm^{-1}
17	4	14	17	3	15	18574.517	18574.533	-0.016	cm^{-1}
18	4	15	18	3	16	18572.593	18572.625	-0.032	cm^{-1}
19	4	16	19	3	17	18570.573	18570.610	-0.037	cm^{-1}
20	4	17	20	3	18	18568.382	18568.488	-0.106	cm^{-1}
21	4	18	21	3	19	18566.203	18566.258	-0.055	cm^{-1}
22	4	19	22	3	20	18563.859	18563.920	-0.061	cm^{-1}

Upper State			Lower State			Observation	Calculation	Residual	Remarks
J	K_A	K_C	J	K_A	K_C				
23	4	20	23	3	21	18561.377	18561.475	-0.098	cm^{-1}
24	4	21	24	3	22	18558.798	18558.922	-0.124	cm^{-1}
25	4	22	25	3	23	18556.150	18556.262	-0.112	cm^{-1}
26	4	23	26	3	24	18553.345	18553.493	-0.148	cm^{-1}
27	4	24	27	3	25	18550.619	18550.616	0.002	cm^{-1}
3	2	1	3	3	0	18496.455	18496.360	0.094	cm^{-1}
3	2	2	3	3	1	18496.455	18496.360	0.094	cm^{-1}
4	2	2	4	3	1	18495.920	18495.940	-0.020	cm^{-1}
4	2	3	4	3	2	18495.920	18495.939	-0.019	cm^{-1}
5	2	3	5	3	2	18495.450	18495.414	0.035	cm^{-1}
5	2	4	5	3	3	18495.450	18495.413	0.036	cm^{-1}
6	2	4	6	3	3	18494.760	18494.783	-0.023	cm^{-1}
6	2	5	6	3	4	18494.760	18494.781	-0.021	cm^{-1}
7	2	5	7	3	4	18494.098	18494.048	0.050	cm^{-1}
7	2	6	7	3	5	18494.098	18494.044	0.053	cm^{-1}
8	2	6	8	3	5	18493.223	18493.207	0.015	cm^{-1}
9	2	7	8	3	6	18493.223	18493.200	0.022	cm^{-1}
9	2	7	9	3	6	18492.262	18492.262	0.000	cm^{-1}
9	2	8	9	3	7	18492.262	18492.251	0.010	cm^{-1}
10	2	8	10	3	7	18491.264	18491.212	0.051	cm^{-1}
10	2	9	10	3	8	18491.264	18491.196	0.067	cm^{-1}
11	2	9	11	3	8	18490.022	18490.057	-0.035	cm^{-1}
11	2	10	11	3	9	18490.022	18490.035	-0.013	cm^{-1}
12	2	10	12	3	9	18488.803	18488.798	0.004	cm^{-1}
12	2	11	12	3	10	18488.803	18488.767	0.035	cm^{-1}
13	2	11	13	3	10	18487.448	18487.434	0.013	cm^{-1}
13	2	12	13	3	11	18487.448	18487.393	0.055	cm^{-1}
14	2	12	14	3	11	18485.979	18485.967	0.011	cm^{-1}
14	2	13	14	3	12	18485.979	18485.911	0.067	cm^{-1}
15	2	13	15	3	12	18484.437	18484.395	0.041	cm^{-1}
15	2	14	15	3	13	18484.437	18484.323	0.113	cm^{-1}
16	2	14	16	3	13	18482.682	18482.719	-0.037	cm^{-1}
16	2	15	16	3	14	18482.682	18482.627	0.054	cm^{-1}
17	2	15	17	3	14	18480.926	18480.939	-0.013	cm^{-1}
17	2	16	17	3	15	18480.926	18480.823	-0.102	cm^{-1}
18	2	16	18	3	15	18479.160	18479.055	0.104	cm^{-1}
18	2	17	18	3	16	18479.012	18478.912	0.099	cm^{-1}
19	2	17	19	3	16	18477.184	18477.068	0.115	cm^{-1}
19	2	18	19	3	17	18476.954	18476.892	0.061	cm^{-1}
20	2	18	20	3	17	18475.052	18474.977	0.074	cm^{-1}
20	2	19	20	3	18	18484.710	18474.764	-0.054	cm^{-1}
2	2	0	3	3	1	18493.223	18493.239	-0.016	cm^{-1}
3	2	1	4	3	2	18491.803	18491.777	0.025	cm^{-1}
4	2	2	5	3	3	18490.240	18490.211	0.029	cm^{-1}
5	2	3	6	3	4	18488.515	18488.539	-0.024	cm^{-1}

Upper State			Lower State			Observation	Calculation	Residual	Remarks
J	K_A	K_C	J	K_A	K_C				
6	2	4	7	3	5	18486.729	18486.763	-0.034	cm^{-1}
7	2	5	8	3	6	18484.877	18484.882	-0.005	cm^{-1}
8	2	6	9	3	7	18482.894	18482.895	-0.001	cm^{-1}
9	2	7	10	3	8	18480.926	18480.804	0.121	cm^{-1}
10	2	8	11	3	9	18478.586	18478.609	-0.023	cm^{-1}
11	2	9	12	3	10	18476.353	18476.309	-0.043	cm^{-1}
12	2	10	13	3	11	18473.906	18473.905	0.000	cm^{-1}
13	2	12	14	3	11	18471.452	18471.349	0.103	cm^{-1}
13	2	11	14	3	12	18471.452	18471.394	0.058	cm^{-1}
5	5	1	4	4	0	18601.413	18601.373	0.039	cm^{-1}
6	5	2	5	4	1	18601.907	18601.885	0.021	cm^{-1}
7	5	3	6	4	2	18602.229	18602.292	-0.063	cm^{-1}
8	5	4	7	4	3	18602.612	18602.593	0.018	cm^{-1}
9	5	5	8	4	4	18602.825	18602.788	0.036	cm^{-1}
10	5	6	9	4	5	18602.825	18602.877	-0.052	cm^{-1}
11	5	7	10	4	6	18602.825	18602.860	-0.035	cm^{-1}
12	5	8	11	4	7	18602.825	18602.737	0.087	cm^{-1}
13	5	9	12	4	8	18602.612	18602.508	0.104	cm^{-1}
14	5	10	13	4	9	18602.229	18602.172	0.056	cm^{-1}
15	5	11	14	4	10	18601.745	18601.730	0.014	cm^{-1}
16	5	12	15	4	11	18601.103	18601.182	-0.079	cm^{-1}
17	5	13	16	4	12	18600.423	18600.526	-0.103	cm^{-1}
18	5	14	17	4	13	18599.875	18599.765	0.110	cm^{-1}
19	5	15	18	4	14	18598.897	18598.896	0.000	cm^{-1}
20	5	16	19	4	15	18597.922	18597.920	0.001	cm^{-1}
6	6	1	5	5	0	18606.030	18606.137	-0.107	cm^{-1}
7	6	2	6	5	1	18606.477	18606.543	-0.066	cm^{-1}
8	6	3	7	5	2	18606.768	18606.843	-0.075	cm^{-1}
9	6	4	8	5	3	18607.049	18607.037	0.011	cm^{-1}
10	6	5	9	5	4	18607.049	18607.125	-0.076	cm^{-1}
11	6	6	10	5	5	18607.049	18607.107	-0.058	cm^{-1}
12	6	7	11	5	6	18607.049	18606.983	0.065	cm^{-1}
13	6	8	12	5	7	18606.768	18606.752	0.015	cm^{-1}
14	6	9	13	5	8	18606.477	18606.416	0.060	cm^{-1}
15	6	10	14	5	9	18606.030	18605.973	0.056	cm^{-1}
16	6	11	15	5	10	18605.434	18605.424	0.010	cm^{-1}
17	6	12	16	5	11	18604.713	18604.768	-0.055	cm^{-1}
18	6	13	17	5	12	18603.990	18604.005	-0.015	cm^{-1}
19	6	14	18	5	13	18603.116	18603.136	-0.020	cm^{-1}
20	6	15	19	5	14	18602.229	18602.160	0.069	cm^{-1}
21	6	16	20	5	15	18601.104	18601.076	0.027	cm^{-1}
22	6	17	21	5	16	18599.875	18599.886	-0.011	cm^{-1}
23	6	18	22	5	17	18598.559	18598.589	-0.030	cm^{-1}
24	6	19	23	5	18	18597.215	18597.184	0.030	cm^{-1}
25	6	20	24	5	19	18595.724	18595.671	0.052	cm^{-1}
6	6	1	6	5	2	18599.197	18599.264	-0.067	cm^{-1}
7	6	2	7	5	3	18598.559	18598.524	0.034	cm^{-1}
8	6	3	8	5	4	18597.600	18597.679	-0.079	cm^{-1}
9	6	4	9	5	5	18596.744	18596.727	0.016	cm^{-1}
10	6	6	10	5	6	18595.724	18595.670	0.053	cm^{-1}

CH_2S: $3_0^1 4_0^3$ Band - continued

Upper State			Lower State			Observation	Calculation	Residual	Remarks
J	K_A	K_C	J	K_A	K_C				
11	6	6	11	5	7	18594.442	18594.507	-0.065	cm^{-1}
12	6	7	12	5	8	18593.200	18593.238	-0.038	cm^{-1}
13	6	8	13	5	9	18591.842	18591.863	-0.021	cm^{-1}
14	6	9	14	5	10	18590.362	18590.382	-0.020	cm^{-1}
15	6	10	15	5	11	18588.787	18588.794	-0.007	cm^{-1}
16	6	11	16	5	12	18587.104	18587.100	0.003	cm^{-1}
17	6	12	17	5	13	18585.386	18585.300	0.085	cm^{-1}
18	6	13	18	5	14	18583.408	18583.394	0.013	cm^{-1}
19	6	14	19	5	15	18581.394	18581.381	0.013	cm^{-1}
20	6	15	20	5	16	18579.272	18579.261	0.010	cm^{-1}
21	6	16	21	5	17	18577.074	18577.034	0.039	cm^{-1}
22	6	17	22	5	18	18574.773	18574.701	0.071	cm^{-1}
23	6	18	23	5	19	18572.274	18572.260	0.013	cm^{-1}
24	6	19	24	5	20	18569.773	18569.713	0.059	cm^{-1}
11	7	5	10	6	4	18608.892	18609.309 *	-0.417	cm^{-1}

Upper State			Lower State			Observation	Calculation	Residual	Remarks
J	K_A	K_C	J	K_A	K_C				
4	1	3	3	0	3	18815.851	18815.865	-0.014	cm^{-1}
5	1	4	4	0	4	18816.616	18816.550	0.065	cm^{-1}
6	1	5	5	0	5	18817.191	18817.184	0.006	cm^{-1}
7	1	6	6	0	6	18817.793	18817.769	0.023	cm^{-1}
8	1	7	7	0	7	18818.319	18818.307	0.011	cm^{-1}
9	1	8	8	0	8	18818.833	18818.799	0.033	cm^{-1}
10	1	9	9	0	9	18819.236	18819.248	-0.012	cm^{-1}
11	1	10	10	0	10	18819.714	18819.656	0.058	cm^{-1}
12	1	11	11	0	11	18819.995	18820.024	-0.029	cm^{-1}
13	1	12	12	0	12	18820.397	18820.356	0.040	cm^{-1}
14	1	13	13	0	13	18820.663	18820.654	0.008	cm^{-1}
15	1	14	14	0	14	18820.876	18820.920	-0.044	cm^{-1}
16	1	15	15	0	15	18821.130	18821.156	-0.026	cm^{-1}
17	1	16	16	0	16	18821.436	18821.364	0.071	cm^{-1}
18	1	17	17	0	17	18821.600	18821.544	0.055	cm^{-1}
19	1	18	18	0	18	18821.703	18821.698	0.004	cm^{-1}
20	1	19	19	0	19	18821.850	18821.825	0.024	cm^{-1}
21	1	20	20	0	20	18821.934	18821.925	0.008	cm^{-1}
22	1	21	21	0	21	18821.934	18821.997	-0.063	cm^{-1}
23	1	22	22	0	22	18821.934	18822.040	-0.106	cm^{-1}
24	1	23	23	0	23	18821.934	18822.050	-0.116	cm^{-1}
25	1	24	24	0	24	18821.934	18822.026	-0.092	cm^{-1}
26	1	25	25	0	25	18821.934	18821.965	-0.031	cm^{-1}
27	1	26	26	0	26	18821.934	18821.863	0.071	cm^{-1}
3	1	3	3	0	3	18812.047	18812.042	0.004	cm^{-1}
4	1	4	4	0	4	18811.703	18811.669	0.033	cm^{-1}
5	1	5	5	0	5	18811.208	18811.206	0.002	cm^{-1}
6	1	6	6	0	6	18810.629	18810.652	-0.023	cm^{-1}
7	1	7	7	0	7	18809.996	18810.011	-0.015	cm^{-1}
8	1	8	8	0	8	18809.301	18809.284	0.016	cm^{-1}
9	1	9	9	0	9	18808.502	18808.474	0.027	cm^{-1}
10	1	10	10	0	10	18807.563	18807.583	-0.020	cm^{-1}
11	1	11	11	0	11	18806.619	18806.614	0.004	cm^{-1}
12	1	12	12	0	12	18805.594	18805.569	0.024	cm^{-1}
13	1	13	13	0	13	18804.465	18804.452	0.012	cm^{-1}
14	1	14	14	0	14	18803.256	18803.265	-0.009	cm^{-1}
15	1	15	15	0	15	18802.044	18802.011	0.032	cm^{-1}
16	1	16	16	0	16	18800.681	18800.693	-0.012	cm^{-1}
17	1	17	17	0	17	18799.369	18799.312	0.056	cm^{-1}
18	1	18	18	0	18	18797.854	18797.871	-0.017	cm^{-1}
19	1	19	19	0	19	18796.363	18796.370	-0.007	cm^{-1}
20	1	20	20	0	20	18794.834	18794.812	0.021	cm^{-1}
21	1	21	21	0	21	18793.241	18793.197	0.043	cm^{-1}
22	1	22	22	0	22	18791.527	18791.525	0.001	cm^{-1}
23	1	23	23	0	23	18789.800	18789.796	0.003	cm^{-1}
24	1	24	24	0	24	18788.004	18788.010	-0.006	cm^{-1}
25	1	25	25	0	25	18786.139	18786.167	-0.028	cm^{-1}
26	1	26	26	0	26	18784.261	18784.265	-0.004	cm^{-1}
27	1	27	27	0	27	18782.307	18782.305	0.001	cm^{-1}
28	1	28	28	0	28	18780.251	18780.285	-0.034	cm^{-1}

Upper State			Lower State			Observation	Calculation		Residual	Remarks
J	K_A	K_C	J	K_A	K_C					
29	1	29	29	0	29	18778.260	18778.204		0.055	cm^{-1}
30	1	30	30	0	30	18776.083	18776.062		0.020	cm^{-1}
3	3	0	2	2	0	18831.338	18831.373		-0.035	cm^{-1}
3	3	1	2	2	1	18831.338	18831.373		-0.035	cm^{-1}
4	3	1	3	2	1	18832.034	18832.025		0.008	cm^{-1}
4	3	2	3	2	2	18832.034	18832.027		0.007	cm^{-1}
5	3	2	4	2	2	18832.658	18832.601		0.056	cm^{-1}
5	3	3	4	2	3	18832.658	18832.607		0.050	cm^{-1}
6	3	3	5	2	3	18833.080	18833.101		-0.021	cm^{-1}
6	3	3	5	2	3	18833.080	18833.101		-0.021	cm^{-1}
6	3	4	5	2	4	18833.080	18833.114		-0.034	cm^{-1}
7	3	4	6	2	4	18833.540	18833.524		0.015	cm^{-1}
7	3	5	6	2	5	18833.540	18833.550		-0.010	cm^{-1}
8	3	5	7	2	5	18833.934	18833.867		0.066	cm^{-1}
8	3	6	7	2	6	18833.934	18833.914		0.019	cm^{-1}
9	3	6	8	2	6	18834.094	18834.130		-0.036	cm^{-1}
9	3	7	8	2	7	18834.094	18834.207		-0.113	cm^{-1}
10	3	7	9	2	7	18834.362	18834.309		0.052	cm^{-1}
10	3	8	9	2	8	18834.362	18834.430		-0.068	cm^{-1}
11	3	8	10	2	8	18834.362	18834.404		-0.042	cm^{-1}
11	3	9	10	2	9	18834.628	18834.584		0.043	cm^{-1}
12	3	9	11	2	9	18834.362	18834.410		-0.048	cm^{-1}
12	3	10	11	2	10	18834.628	18834.669		-0.041	cm^{-1}
13	3	10	12	2	10	18834.362	18834.328		0.034	cm^{-1}
13	3	11	12	2	11	18834.628	18834.686		-0.058	cm^{-1}
14	3	11	13	2	11	18834.090	18834.153		-0.063	cm^{-1}
14	3	12	13	2	12	18834.628	18834.637		-0.009	cm^{-1}
15	3	12	14	2	12	18833.934	18833.885		0.049	cm^{-1}
15	3	13	14	2	13	18834.628	18834.521		0.106	cm^{-1}
16	3	13	15	2	13	18833.540	18833.521		0.019	cm^{-1}
16	3	14	15	2	14	18834.362	18834.341		0.020	cm^{-1}
17	3	14	16	2	14	18833.080	18833.060		0.019	cm^{-1}
17	3	15	16	2	15	18834.095	18834.098		-0.003	cm^{-1}
18	3	15	17	2	15	18832.482	18832.501		-0.019	cm^{-1}
18	3	16	17	2	16	18833.961	18833.791		0.169	cm^{-1}
19	3	16	18	2	16	18831.806	18831.844		-0.038	cm^{-1}
19	3	17	18	2	17	18833.377	18833.423		-0.046	cm^{-1}
20	3	17	19	2	17	18831.083	18831.089		-0.006	cm^{-1}
20	3	18	19	2	18	18833.080	18832.995		0.084	cm^{-1}
21	3	18	20	2	18	18830.184	18830.236		-0.052	cm^{-1}
21	3	19	20	2	19	18832.486	18832.507		-0.021	cm^{-1}
22	3	19	21	2	19	18829.241	18829.288		-0.047	cm^{-1}
22	3	20	21	2	20	18832.034	18831.960		0.073	cm^{-1}
23	3	20	22	2	20	18828.217	18828.246		-0.029	cm^{-1}
23	3	21	22	2	21	18831.338	18831.356		-0.018	cm^{-1}
24	3	21	23	2	21	18827.146	18827.113		0.032	cm^{-1}
24	3	22	23	2	22	18830.565	18830.695	*	-0.130	cm^{-1}
25	3	22	24	2	22	18825.922	18825.893		0.028	cm^{-1}
25	3	23	24	2	23	18829.933	18829.979		-0.046	cm^{-1}
26	3	23	25	2	23	18824.574	18824.588		-0.014	cm^{-1}

Upper State			Lower State			Observation	Calculation	Residual	Remarks
J	K_A	K_C	J	K_A	K_C				
26	3	24	25	2	24	18829.241	18829.208	0.032	cm^{-1}
5	3	2	5	2	4	18827.810	18827.872	-0.062	cm^{-1}
5	3	3	5	2	3	18827.810	18827.858	-0.048	cm^{-1}
6	3	3	6	2	5	18827.401	18827.433	-0.032	cm^{-1}
6	3	4	6	2	4	18827.461	18827.407	0.054	cm^{-1}
7	3	4	7	2	6	18826.839	18826.923	-0.084	cm^{-1}
7	3	5	7	2	5	18826.839	18826.875	-0.036	cm^{-1}
8	3	5	8	2	7	18826.297	18826.342	-0.045	cm^{-1}
8	3	6	8	2	6	18826.297	18826.262	0.034	cm^{-1}
9	3	6	9	2	8	18825.648	18825.690	-0.042	cm^{-1}
9	3	7	9	2	7	18825.648	18825.566	0.081	cm^{-1}
10	3	7	10	2	9	18824.953	18824.970	-0.017	cm^{-1}
10	3	8	10	2	8	18824.774	18824.783	-0.009	cm^{-1}
11	3	8	11	2	10	18824.205	18824.181	0.023	cm^{-1}
11	3	9	11	2	9	18823.921	18823.912	0.008	cm^{-1}
12	3	9	12	2	11	18823.290	18823.326	-0.036	cm^{-1}
12	3	10	12	2	10	18822.937	18822.950	-0.013	cm^{-1}
13	3	10	13	2	12	18822.409	18822.405	0.003	cm^{-1}
13	3	11	13	2	11	18821.934	18821.894	0.039	cm^{-1}
14	3	11	14	2	13	18821.436	18821.420	0.015	cm^{-1}
14	3	12	14	2	12	18820.770	18820.742	0.027	cm^{-1}
15	3	12	15	2	14	18820.387	18820.372	0.014	cm^{-1}
15	3	13	15	2	13	18819.490	18819.490	0.000	cm^{-1}
16	3	13	16	2	15	18819.236	18819.264	-0.028	cm^{-1}
16	3	14	16	2	14	18818.092	18818.138	-0.046	cm^{-1}
17	3	14	17	2	16	18818.092	18818.097	-0.005	cm^{-1}
17	3	15	17	2	15	18816.616	18816.683	-0.067	cm^{-1}
18	3	15	18	2	17	18816.914	18816.874	0.039	cm^{-1}
18	3	16	18	2	16	18815.170	18815.123	0.046	cm^{-1}
19	3	16	19	2	18	18815.655	18815.596	0.058	cm^{-1}
19	3	17	19	2	17	18813.478	18813.458	0.019	cm^{-1}
20	3	17	20	2	19	18814.270	18814.266	0.003	cm^{-1}
20	3	18	20	2	18	18811.703	18811.686	0.016	cm^{-1}
21	3	18	21	2	20	18812.880	18812.888	-0.008	cm^{-1}
21	3	19	21	2	19	18809.776	18809.808	-0.032	cm^{-1}
22	3	19	22	2	21	18811.407	18811.463	-0.056	cm^{-1}
22	3	20	22	2	20	18807.827	18807.823	0.003	cm^{-1}
23	3	20	23	2	22	18809.996	18809.995	0.000	cm^{-1}
23	3	21	23	2	21	18805.594	18805.732	-0.138	cm^{-1}
24	3	21	24	2	23	18808.509	18808.487	0.021	cm^{-1}
24	3	22	24	2	22	18803.582	18803.536	0.045	cm^{-1}
25	3	22	25	2	24	18806.952	18806.942	0.009	cm^{-1}
25	1	24	26	2	24	18746.809	18746.837	-0.028	cm^{-1}
5	1	5	5	2	3	18793.520	18793.550	-0.030	cm^{-1}
5	1	4	5	2	4	18794.050	18794.179	-0.119	cm^{-1}
6	1	6	6	2	4	18792.995	18792.973	0.021	cm^{-1}
6	1	5	6	2	5	18793.883	18793.860	0.022	cm^{-1}
7	1	7	7	2	5	18792.353	18792.293	0.059	cm^{-1}
7	1	6	7	2	6	18793.520	18793.489	0.030	cm^{-1}
8	1	8	8	2	6	18791.527	18791.509	0.017	cm^{-1}

Upper State			Lower State			Observation	Calculation	Residual	Remarks
J	K_A	K_C	J	K_A	K_C				
8	1	7	8	2	7	18792.995	18793.063	-0.068	cm^{-1}
9	1	9	9	2	7	18790.653	18790.617	0.035	cm^{-1}
9	1	8	9	2	8	18792.600	18792.585	0.015	cm^{-1}
10	1	10	10	2	8	18789.603	18789.614	-0.011	cm^{-1}
10	1	9	10	2	9	18792.037	18792.052	-0.015	cm^{-1}
11	1	11	11	2	9	18788.526	18788.497	0.028	cm^{-1}
11	1	10	11	2	10	18791.527	18791.465	0.061	cm^{-1}
12	1	12	12	2	10	18787.177	18787.262	-0.085	cm^{-1}
12	1	11	12	2	11	18790.852	18790.823	0.028	cm^{-1}
13	1	13	13	2	11	18785.827	18785.906	-0.079	cm^{-1}
13	1	12	13	2	12	18790.108	18790.127	-0.019	cm^{-1}
14	1	14	14	2	12	18784.423	18784.424	-0.001	cm^{-1}
14	1	13	14	2	13	18789.339	18789.375	-0.036	cm^{-1}
15	1	15	15	2	13	18782.865	18782.814	0.050	cm^{-1}
15	1	14	15	2	14	18788.526	18788.567	-0.041	cm^{-1}
16	1	16	16	2	14	18781.003	18781.072	-0.069	cm^{-1}
16	1	15	16	2	15	18787.684	18787.703	-0.019	cm^{-1}
17	1	17	17	2	15	18779.223	18779.196	0.026	cm^{-1}
17	1	16	17	2	16	18786.762	18786.781	-0.019	cm^{-1}
18	1	18	18	2	16	18777.147	18777.183	-0.036	cm^{-1}
18	1	17	18	2	17	18785.827	18785.801	0.025	cm^{-1}
19	1	19	19	2	17	18775.023	18775.030	-0.007	cm^{-1}
19	1	18	19	2	18	18784.718	18784.762	-0.044	cm^{-1}
20	1	20	20	2	18	18772.816	18772.737	0.078	cm^{-1}
20	1	19	20	2	19	18783.638	18783.663	-0.025	cm^{-1}
21	1	21	21	2	19	18770.348	18770.302	0.045	cm^{-1}
21	1	20	21	2	20	18782.467	18782.501	-0.034	cm^{-1}
22	1	22	22	2	20	18767.685	18767.725	-0.040	cm^{-1}
22	1	21	22	2	21	18781.280	18781.277	0.002	cm^{-1}
23	1	23	23	2	21	18764.929	18765.006	-0.077	cm^{-1}
23	1	22	23	2	22	18779.954	18779.989	-0.035	cm^{-1}
24	1	24	24	2	22	18762.205	18762.145	0.059	cm^{-1}
24	1	23	24	2	23	18778.622	18778.634	-0.012	cm^{-1}
25	1	24	25	2	24	18777.147	18777.211	-0.064	cm^{-1}
26	1	25	26	2	25	18775.648	18775.717	-0.069	cm^{-1}
27	1	26	27	2	26	18774.076	18774.152	-0.076	cm^{-1}
28	1	27	28	2	27	18772.441	18772.513	-0.072	cm^{-1}
29	1	28	29	2	28	18770.721	18770.797	-0.076	cm^{-1}
1	1	0	2	2	0	18792.995	18793.026	-0.031	cm^{-1}
1	1	1	2	2	1	18792.995	18792.985	0.009	cm^{-1}
2	1	1	3	2	1	18792.037	18791.971	0.065	cm^{-1}
2	1	2	3	2	2	18792.037	18791.850	0.186	cm^{-1}
3	1	2	4	2	2	18790.852	18790.861	-0.009	cm^{-1}
3	1	3	4	2	3	18790.653	18790.621	0.031	cm^{-1}
4	1	3	5	2	3	18789.800	18789.695	0.104	cm^{-1}
4	1	4	5	2	4	18789.339	18789.298	0.040	cm^{-1}
5	1	4	6	2	4	18788.526	18788.471	0.054	cm^{-1}
5	1	5	6	2	5	18787.831	18787.882	-0.051	cm^{-1}

Upper State			Lower State			Observation	Calculation	Residual	Remarks
J	K_A	K_C	J	K_A	K_C				
6	1	5	7	2	5	18787.177	18787.185	-0.008	cm^{-1}
6	1	6	7	2	6	18786.335	18786.372	-0.037	cm^{-1}
7	1	6	8	2	6	18785.827	18785.837	-0.010	cm^{-1}
7	1	7	8	2	7	18784.718	18784.768	-0.050	cm^{-1}
8	1	7	9	2	7	18784.432	18784.422	0.009	cm^{-1}
8	1	8	9	2	8	18783.092	18783.070	0.021	cm^{-1}
9	1	8	10	2	8	18782.865	18782.938	-0.073	cm^{-1}
9	1	9	10	2	9	18781.280	18781.278	0.001	cm^{-1}
10	1	9	11	2	9	18781.280	18781.380	-0.100	cm^{-1}
10	1	10	11	2	10	18779.413	18779.392	0.020	cm^{-1}
11	1	10	12	2	10	18779.748	18779.746	0.001	cm^{-1}
11	1	11	12	2	11	18777.340	18777.413	-0.073	cm^{-1}
12	1	11	13	2	11	18777.997	18778.031	-0.034	cm^{-1}
12	1	12	13	2	12	18775.383	18775.340	0.042	cm^{-1}
13	1	12	14	2	12	18776.282	18776.232	0.049	cm^{-1}
13	1	13	14	2	13	18773.197	18773.173	0.023	cm^{-1}
14	1	13	15	2	13	18774.332	18774.344	-0.012	cm^{-1}
14	1	14	15	2	14	18770.721	18770.912	-0.191	cm^{-1}
15	1	14	16	2	14	18772.442	18772.364	0.077	cm^{-1}
15	1	15	16	2	15	18768.550	18768.558	-0.008	cm^{-1}
16	1	15	17	2	15	18770.348	18770.288	0.059	cm^{-1}
16	1	16	17	2	16	18766.129	18766.110	0.018	cm^{-1}
17	1	16	18	2	16	18768.145	18768.113	0.031	cm^{-1}
17	1	17	18	2	17	18763.609	18763.569	0.039	cm^{-1}
18	1	17	19	2	17	18765.846	18765.836	0.009	cm^{-1}
18	1	18	19	2	18	18760.985	18760.935	0.049	cm^{-1}
19	1	18	20	2	18	18763.609	18763.453	0.155	cm^{-1}
19	1	19	20	2	19	18758.053	18758.208	-0.155	cm^{-1}
20	1	19	21	2	19	18760.998	18760.964	0.033	cm^{-1}
20	1	20	21	2	20	18755.366	18755.389	-0.023	cm^{-1}
21	1	20	22	2	20	18758.529	18758.364	0.164	cm^{-1}
21	1	21	22	2	21	18752.466	18752.477	-0.011	cm^{-1}
22	1	21	23	2	21	18755.757	18755.654	0.102	cm^{-1}
22	1	22	23	2	22	18749.353	18749.474	-0.121	cm^{-1}
23	1	22	24	2	22	18752.771	18752.830	-0.059	cm^{-1}
23	1	23	24	2	23	18746.443	18746.380	0.062	cm^{-1}
24	1	23	25	2	23	18750.015	18749.891	0.123	cm^{-1}
24	1	24	25	2	24	18743.266	18743.195	0.070	cm^{-1}
25	1	24	26	2	24	18746.809	18746.837	-0.028	cm^{-1}
25	1	25	26	2	25	18739.846	18739.920	-0.074	cm^{-1}
26	1	25	27	2	25	18743.769	18743.666	0.102	cm^{-1}
26	1	26	27	2	26	18736.566	18736.555	0.010	cm^{-1}
27	1	26	28	2	26	18740.398	18740.376	0.021	cm^{-1}
27	1	27	28	2	27	18733.044	18733.102	-0.058	cm^{-1}
28	1	27	29	2	27	18737.021	18736.968	0.052	cm^{-1}
29	1	28	30	2	28	18733.516	18733.440	0.075	cm^{-1}
4	4	0	3	3	0	18839.736	18839.725	0.010	cm^{-1}
5	4	1	4	3	1	18840.288	18840.303	-0.015	cm^{-1}
6	4	2	5	3	2	18840.755	18840.808	-0.053	cm^{-1}
7	4	3	6	3	3	18841.379	18841.238	0.140	cm^{-1}

CD_2S: 5_0^1 Band - continued

Upper State			Lower State			Observation	Calculation	Residual	Remarks
J	K_A	K_C	J	K_A	K_C				
8	4	4	7	3	4	18841.500	18841.593	-0.093	cm^{-1}
9	4	5	8	3	5	18841.922	18841.875	0.047	cm^{-1}
10	4	6	9	3	6	18842.195	18842.081	0.114	cm^{-1}
11	4	7	10	3	7	18842.195	18842.211	-0.016	cm^{-1}
12	4	8	11	3	8	18842.195	18842.266	-0.071	cm^{-1}
13	4	9	12	3	9	18842.195	18842.245	-0.050	cm^{-1}
14	4	10	13	3	10	18842.195	18842.146	0.048	cm^{-1}
15	4	11	14	3	11	18841.922	18841.970	-0.048	cm^{-1}
16	4	12	15	3	12	18841.700	18841.716	-0.016	cm^{-1}
17	4	13	16	3	13	18841.379	18841.381	-0.002	cm^{-1}
18	4	14	17	3	14	18841.002	18840.966	0.035	cm^{-1}
19	4	15	18	3	15	18840.573	18840.369	0.103	cm^{-1}
20	4	16	19	3	16	18840.007	18839.889	0.117	cm^{-1}
21	4	17	20	3	17	18839.189	18839.224	-0.035	cm^{-1}
22	4	18	21	3	18	18838.643	18838.473	0.169	cm^{-1}
23	4	19	22	3	19	18837.574	18837.633	-0.059	cm^{-1}
6	4	2	6	3	4	18835.128	18835.123	0.004	cm^{-1}
7	4	3	7	3	5	18834.628	18834.605	0.022	cm^{-1}
8	4	4	8	3	6	18833.934	18834.013	-0.079	cm^{-1}
9	4	5	9	3	7	18833.377	18833.346	0.031	cm^{-1}
10	4	6	10	3	8	18832.658	18832.604	0.054	cm^{-1}
11	4	7	11	3	9	18831.803	18831.787	0.016	cm^{-1}
12	4	8	12	3	10	18830.876	18830.894	-0.018	cm^{-1}
13	4	9	13	3	11	18829.933	18829.927	0.005	cm^{-1}
14	4	10	14	3	12	18828.822	18828.884	-0.062	cm^{-1}
15	4	11	15	3	13	18827.810	18827.766	0.044	cm^{-1}
16	4	12	16	3	14	18826.535	18826.572	-0.037	cm^{-1}
17	4	13	17	3	15	18825.230	18825.303	-0.073	cm^{-1}
5	5	0	4	4	0	18847.698	18847.674	0.023	cm^{-1}
6	5	1	5	4	1	18848.213	18848.177	0.035	cm^{-1}
7	5	3	6	4	2	18848.592	18848.607	-0.015	cm^{-1}
8	5	3	7	4	3	18848.985	18848.963	0.022	cm^{-1}
9	5	4	8	4	4	18849.280	18849.244	0.035	cm^{-1}
10	5	5	9	4	5	18849.500	18849.450	0.049	cm^{-1}
11	5	6	10	4	6	18849.579	18849.583	-0.004	cm^{-1}
12	5	7	11	4	7	18849.579	18849.640	-0.061	cm^{-1}
13	5	8	12	4	8	18849.579	18849.622	-0.043	cm^{-1}
14	5	9	13	4	9	18849.500	18849.530	-0.030	cm^{-1}
15	5	10	14	4	10	18849.280	18849.362	-0.082	cm^{-1}
16	5	11	15	4	11	18849.050	18849.118	-0.068	cm^{-1}
17	5	12	16	4	12	18848.789	18848.798	-0.009	cm^{-1}
18	5	13	17	4	13	18848.408	18848.402	0.005	cm^{-1}
19	5	14	18	4	14	18847.915	18847.930	-0.015	cm^{-1}
20	5	15	19	4	15	18847.330	18847.381	-0.051	cm^{-1}
21	5	16	20	4	16	18846.718	18846.754	-0.036	cm^{-1}
22	5	17	21	4	17	18846.044	18846.049	-0.005	cm^{-1}
23	5	18	22	4	18	18845.279	18845.267	0.011	cm^{-1}
24	5	19	23	4	19	18844.393	18844.405	-0.012	cm^{-1}
25	5	20	24	4	20	18843.462	18843.464	-0.002	cm^{-1}
26	5	21	25	4	21	18842.467	18842.443	0.023	cm^{-1}

Upper State			Lower State			Observation	Calculation	Residual	Remarks
J	K_A	K_C	J	K_A	K_C				
27	5	22	26	4	22	18841.379	18841.341	0.037	cm^{-1}
28	5	23	27	4	23	18840.228	18840.157	0.070	cm^{-1}
5	5	0	5	4	2	18842.936	18842.938	-0.002	cm^{-1}
6	5	1	6	4	3	18842.467	18842.494	-0.027	cm^{-1}
7	5	2	7	4	4	18841.922	18841.976	-0.054	cm^{-1}
8	5	3	8	4	5	18841.379	18841.384	-0.005	cm^{-1}
9	5	4	9	4	6	18840.755	18840.717	0.037	cm^{-1}
10	5	5	10	4	7	18840.007	18839.976	0.030	cm^{-1}
11	5	6	11	4	8	18839.189	18839.160	0.028	cm^{-1}
12	5	7	12	4	9	18838.295	18838.269	0.026	cm^{-1}
13	5	8	13	4	10	18837.263	18837.302	-0.039	cm^{-1}
14	5	9	14	4	11	18836.264	18836.260	0.003	cm^{-1}
15	5	10	15	4	12	18835.128	18835.143	-0.015	cm^{-1}
16	5	11	16	4	13	18833.934	18833.950	-0.016	cm^{-1}
17	5	12	17	4	14	18832.658	18832.680	-0.022	cm^{-1}
18	5	13	18	4	15	18831.338	18831.335	0.002	cm^{-1}
19	5	14	19	4	16	18829.933	18829.912	0.020	cm^{-1}
20	5	15	20	4	17	18828.429	18828.413	0.015	cm^{-1}
21	5	16	21	4	18	18826.839	18826.837	0.001	cm^{-1}
22	5	17	22	4	19	18825.230	18825.183	0.046	cm^{-1}
23	5	18	23	4	20	18823.477	18823.451	0.025	cm^{-1}
24	5	19	24	4	21	18821.703	18821.642	0.060	cm^{-1}
25	5	20	25	4	22	18819.714	18819.754	-0.040	cm^{-1}
26	5	21	26	4	23	18817.793	18817.789	0.003	cm^{-1}
27	5	22	27	4	24	18815.655	18815.745	-0.090	cm^{-1}
28	5	23	28	4	25	18813.478	18813.622 *	-0.144	cm^{-1}
29	5	24	29	4	26	18811.407	18811.421	-0.014	cm^{-1}
4	3	2	4	4	0	18775.383	18775.378	0.004	cm^{-1}
5	3	3	5	4	1	18775.023	18775.012	0.010	cm^{-1}
6	3	4	6	4	2	18774.569	18774.571	-0.002	cm^{-1}
7	3	5	7	4	3	18774.076	18774.058	0.017	cm^{-1}
8	3	6	8	4	4	18773.480	18773.471	0.008	cm^{-1}
9	3	7	9	4	5	18772.816	18772.811	0.004	cm^{-1}
10	3	8	10	4	6	18772.079	18772.078	0.000	cm^{-1}
11	3	9	11	4	7	18771.311	18771.271	0.039	cm^{-1}
12	3	10	12	4	8	18770.348	18770.391	-0.043	cm^{-1}
13	3	11	13	4	9	18769.379	18769.437	-0.058	cm^{-1}
14	3	12	14	4	10	18768.409	18768.410	-0.001	cm^{-1}
15	3	13	15	4	11	18767.320	18767.309	0.010	cm^{-1}
16	3	14	16	4	12	18766.129	18766.134	-0.005	cm^{-1}
17	3	15	17	4	13	18764.929	18764.885	0.044	cm^{-1}
18	3	16	18	4	14	18763.609	18763.560	0.048	cm^{-1}
19	3	17	19	4	15	18762.208	18762.160	0.047	cm^{-1}
20	3	18	20	4	16	18760.764	18760.685	0.078	cm^{-1}
21	3	19	21	4	17	18759.093	18759.132	-0.039	cm^{-1}
21	3	18	21	4	18	18759.317	18759.317	0.000	cm^{-1}
22	3	20	22	4	18	18757.460	18757.503	-0.043	cm^{-1}
22	3	19	22	4	19	18757.703	18757.746	-0.043	cm^{-1}
23	3	21	23	4	19	18755.757	18755.794	-0.037	cm^{-1}
23	3	20	23	4	20	18756.189	18756.110	0.078	cm^{-1}

CD_2S: 5_0^1 Band - continued

Upper State			Lower State			Observation	Calculation		Residual	Remarks
J	K_A	K_C	J	K_A	K_C					
24	3	22	24	4	20	18753.989	18754.006		-0.017	cm^{-1}
24	3	21	24	4	21	18754.678	18754.412		0.265	cm^{-1}
25	3	23	25	4	21	18752.206	18752.138		0.067	cm^{-1}
25	3	22	25	4	22	18752.771	18752.653		0.117	cm^{-1}
26	3	24	26	4	22	18750.015	18750.187		-0.172	cm^{-1}
26	3	23	26	4	23	18750.818	18750.835		-0.017	cm^{-1}
27	3	25	27	4	23	18748.171	18748.153		0.018	cm^{-1}
27	3	24	27	4	24	18748.891	18748.959		-0.068	cm^{-1}
28	3	26	28	4	24	18746.032	18746.032		0.000	cm^{-1}
28	3	25	28	4	25	18747.007	18747.028		-0.021	cm^{-1}
29	3	27	29	4	25	18743.769	18743.825		-0.056	cm^{-1}
29	3	26	29	4	26	18745.083	18745.043		0.039	cm^{-1}
30	3	28	30	4	26	18741.599	18741.527		0.071	cm^{-1}
30	3	27	30	4	27	18742.992	18743.006		-0.014	cm^{-1}
3	3	0	4	4	0	18771.882	18771.884		-0.002	cm^{-1}
4	3	1	5	4	1	18770.721	18770.643		0.077	cm^{-1}
5	3	2	6	4	2	18769.379	18769.328		0.050	cm^{-1}
6	3	3	7	4	3	18767.923	18767.941		-0.018	cm^{-1}
7	3	4	8	4	4	18766.476	18766.480		-0.004	cm^{-1}
8	3	5	9	4	5	18764.929	18764.945		-0.016	cm^{-1}
9	3	6	10	4	6	18763.284	18763.338		-0.054	cm^{-1}
10	3	7	11	4	7	18761.607	18761.657		-0.050	cm^{-1}
11	3	8	12	4	8	18759.877	18759.904		-0.027	cm^{-1}
12	3	9	13	4	9	18758.053	18758.077		-0.024	cm^{-1}
13	3	10	14	4	10	18756.189	18756.179		0.009	cm^{-1}
14	3	11	15	4	11	18754.199	18754.208		-0.009	cm^{-1}
15	3	12	16	4	12	18752.206	18752.165		0.040	cm^{-1}
16	3	13	17	4	13	18750.015	18750.051		-0.036	cm^{-1}
17	3	14	18	4	14	18747.875	18747.866		0.008	cm^{-1}
18	3	15	19	4	15	18745.548	18745.611		-0.063	cm^{-1}
19	3	16	20	4	16	18743.266	18743.286		-0.020	cm^{-1}
19	3	17	20	4	17	18743.266	18743.193		0.072	cm^{-1}
20	3	17	21	4	17	18740.909	18740.892		0.016	cm^{-1}
20	3	18	21	4	18	18740.909	18740.767	*	0.141	cm^{-1}
21	3	18	22	4	18	18738.470	18738.430		0.039	cm^{-1}
21	3	19	22	4	19	18738.268	18738.266		0.002	cm^{-1}
22	3	19	23	4	19	18735.896	18735.901		-0.005	cm^{-1}
22	3	20	23	4	20	18735.706	18735.687		0.018	cm^{-1}
23	3	20	24	4	20	18733.322	18733.306		0.015	cm^{-1}
23	3	21	24	4	21	18733.044	18733.031		0.012	cm^{-1}
24	3	21	25	4	21	18730.665	18730.646		0.018	cm^{-1}
24	3	22	25	4	22	18730.273	18730.297		-0.024	cm^{-1}
25	3	22	26	4	22	18727.942	18727.922		0.019	cm^{-1}
25	3	23	26	4	23	18727.533	18727.484		0.048	cm^{-1}
26	3	23	27	4	23	18725.236	18725.134		0.101	cm^{-1}
26	3	24	27	4	24	18724.642	18724.591		0.050	cm^{-1}
27	3	24	28	4	24	18722.285	18722.285		0.000	cm^{-1}
27	3	25	28	4	25	18721.599	18721.618		-0.019	cm^{-1}
28	3	25	29	4	25	18719.471	18719.374		0.096	cm^{-1}
28	3	26	29	4	26	18718.609	18718.563		0.045	cm^{-1}

CD_2S: 5_0^1 Band - continued

Upper State			Lower State			Observation	Calculation	Residual	Remarks
J	K_A	K_C	J	K_A	K_C				
29	3	26	30	4	26	18716.439	18716.403	0.035	cm^{-1}
29	3	27	30	4	27	18715.417	18715.426	-0.009	cm^{-1}
6	6	0	5	5	0	18855.167	18855.214	-0.047	cm^{-1}
7	6	1	6	5	1	18855.656	18855.643	0.012	cm^{-1}
8	6	2	7	5	2	18855.976	18855.997	-0.021	cm^{-1}
9	6	3	8	5	3	18856.273	18856.278	-0.005	cm^{-1}
10	6	4	9	5	5	18856.400	18856.483	-0.083	cm^{-1}
11	6	5	10	5	5	18856.636	18856.615	0.020	cm^{-1}
12	6	6	11	5	6	18856.636	18856.671	-0.035	cm^{-1}
13	6	7	12	5	7	18856.636	18856.653	-0.017	cm^{-1}
14	6	8	13	5	8	18856.500	18856.561	-0.061	cm^{-1}
15	6	9	14	5	9	18856.273	18856.393	-0.120	cm^{-1}
16	6	10	15	5	10	18856.273	18856.150	0.123	cm^{-1}
17	6	11	16	5	11	18855.800	18855.831	-0.031	cm^{-1}
18	6	12	17	5	12	18855.400	18855.437	-0.037	cm^{-1}
19	6	13	18	5	13	18854.986	18854.967	0.018	cm^{-1}
20	6	14	19	5	14	18854.469	18854.422	0.047	cm^{-1}
21	6	15	20	5	15	18853.732	18853.800	-0.068	cm^{-1}
22	6	16	21	5	16	18853.107	18853.101	0.005	cm^{-1}
23	6	17	22	5	17	18852.290	18852.326	-0.036	cm^{-1}
9	6	3	9	5	5	18847.698	18847.754	-0.056	cm^{-1}
10	6	4	10	5	6	18847.011	18847.012	-0.001	cm^{-1}
11	6	5	11	5	7	18846.217	18846.196	0.020	cm^{-1}
12	6	6	12	5	8	18845.276	18845.305	-0.029	cm^{-1}
13	6	7	13	5	9	18844.393	18844.339	0.053	cm^{-1}
14	6	8	14	5	10	18843.298	18843.298	0.000	cm^{-1}
15	6	9	15	5	11	18842.195	18842.182	0.012	cm^{-1}
16	6	10	16	5	12	18841.002	18840.990	0.011	cm^{-1}
17	6	11	17	5	13	18839.738	18839.723	0.014	cm^{-1}
18	6	12	18	5	14	18838.295	18838.380	-0.085	cm^{-1}
19	6	13	19	5	15	18836.956	18836.961	-0.005	cm^{-1}
7	4	4	7	5	2	18764.108	18764.175	-0.067	cm^{-1}
8	4	5	8	5	3	18763.609	18763.587	0.021	cm^{-1}
9	4	6	9	5	4	18762.934	18762.927	0.007	cm^{-1}
10	4	7	10	5	5	18762.208	18762.192	0.015	cm^{-1}
11	4	8	11	5	6	18761.429	18761.385	0.043	cm^{-1}
12	4	9	12	5	7	18760.518	18760.503	0.014	cm^{-1}
13	4	10	13	5	8	18759.536	18759.549	-0.013	cm^{-1}
14	4	11	14	5	9	18758.529	18758.521	0.007	cm^{-1}
15	4	12	15	5	10	18757.460	18757.419	0.040	cm^{-1}
16	4	13	16	5	11	18756.189	18756.244	-0.055	cm^{-1}
17	4	14	17	5	12	18755.056	18754.995	0.060	cm^{-1}
18	4	15	18	5	13	18753.697	18753.673	0.023	cm^{-1}
19	4	16	19	5	14	18752.206	18752.277	-0.071	cm^{-1}
20	4	17	20	5	15	18750.818	18750.808	0.009	cm^{-1}
21	4	18	21	5	16	18749.353	18749.264	0.088	cm^{-1}
22	4	19	22	5	17	18747.626	18747.647	-0.021	cm^{-1}
23	4	20	23	5	18	18746.032	18745.956	0.075	cm^{-1}
4	4	0	5	5	0	18760.764	18760.762	0.001	cm^{-1}
5	4	1	6	5	1	18759.370	18759.447	-0.077	cm^{-1}

Upper State			Lower State			Observation	Calculation	Residual	Remarks
J	K_A	K_C	J	K_A	K_C				
6	4	2	7	5	2	18758.053	18758.060	-0.007	cm^{-1}
7	4	3	8	5	3	18756.680	18756.599	0.081	cm^{-1}
8	4	4	9	5	4	18755.056	18755.064	-0.008	cm^{-1}
9	4	5	10	5	5	18753.430	18753.456	-0.026	cm^{-1}
10	4	6	11	5	6	18751.742	18751.774	-0.032	cm^{-1}
11	4	7	12	5	7	18750.015	18750.018	-0.003	cm^{-1}
12	4	8	13	5	8	18748.171	18748.189	-0.018	cm^{-1}
13	4	9	14	5	9	18746.248	18746.286	-0.038	cm^{-1}
14	4	10	15	5	10	18744.320	18744.310	0.009	cm^{-1}
15	4	11	16	5	11	18742.065	18742.260	-0.195	cm^{-1}
16	4	12	17	5	12	18740.121	18740.136	-0.015	cm^{-1}
17	4	13	18	5	13	18737.980	18737.939	0.040	cm^{-1}
18	4	14	19	5	14	18735.706	18735.668	0.037	cm^{-1}
19	4	15	20	5	15	18733.322	18733.324	-0.002	cm^{-1}
20	4	16	21	5	16	18730.889	18730.905	-0.016	cm^{-1}
21	4	17	22	5	17	18728.383	18728.414	-0.031	cm^{-1}
22	4	18	23	5	18	18725.842	18725.848	-0.006	cm^{-1}
23	4	19	24	5	19	18723.188	18723.210	-0.022	cm^{-1}
24	4	20	25	5	20	18720.442	18720.498	-0.056	cm^{-1}
25	4	21	26	5	21	18717.655	18717.713	-0.058	cm^{-1}
7	7	0	6	6	0	18862.345	18862.342	0.002	cm^{-1}
8	7	1	7	6	1	18862.726	18862.695	0.030	cm^{-1}
9	7	2	8	6	2	18863.007	18862.974	0.032	cm^{-1}
10	7	3	9	6	3	18863.200	18863.178	0.021	cm^{-1}
11	7	4	10	6	4	18863.324	18863.308	0.015	cm^{-1}
12	7	5	11	6	5	18863.324	18863.363	-0.039	cm^{-1}
13	7	6	12	6	6	18863.324	18863.344	-0.020	cm^{-1}
14	7	7	13	6	7	18863.234	18863.249	-0.015	cm^{-1}
15	7	8	14	6	8	18863.007	18863.080	-0.073	cm^{-1}
16	7	9	15	6	9	18862.831	18862.836	-0.005	cm^{-1}
17	7	10	16	6	10	18862.519	18862.516	0.002	cm^{-1}
18	7	11	17	6	11	18862.137	18862.121	0.015	cm^{-1}
19	7	12	18	6	12	18861.652	18861.651	0.000	cm^{-1}
20	7	13	19	6	13	18861.167	18861.105	0.061	cm^{-1}
21	7	14	20	6	14	18860.450	18860.483	-0.033	cm^{-1}
22	7	15	21	6	15	18859.746	18859.785	-0.039	cm^{-1}
23	7	16	22	6	16	18858.982	18859.010	-0.028	cm^{-1}
24	7	17	23	6	17	18858.148	18858.160	-0.012	cm^{-1}
25	7	18	24	6	18	18857.207	18857.232	-0.025	cm^{-1}
26	7	19	25	6	19	18856.273	18856.228	0.044	cm^{-1}
27	7	20	26	6	20	18855.167	18855.146	0.020	cm^{-1}
28	7	21	27	6	21	18853.980	18853.988	-0.008	cm^{-1}
29	7	22	28	6	22	18852.718	18852.751	-0.033	cm^{-1}
30	7	23	29	6	23	18851.429	18851.437	-0.008	cm^{-1}
8	7	1	8	6	3	18855.167	18855.121	0.045	cm^{-1}
9	7	2	9	6	4	18854.469	18854.453	0.015	cm^{-1}
10	7	3	10	6	5	18853.732	18853.710	0.021	cm^{-1}
11	7	4	11	6	6	18852.932	18852.893	0.038	cm^{-1}
12	7	5	12	6	7	18851.996	18852.001	-0.005	cm^{-1}
13	7	6	13	6	8	18851.053	18851.034	0.018	cm^{-1}

Upper State			Lower State			Observation	Calculation		Residual	Remarks
J	K_A	K_C	J	K_A	K_C					
14	7	7	14	6	9	18850.002	18849.992		0.009	cm^{-1}
15	7	8	15	6	10	18848.789	18848.875		-0.086	cm^{-1}
16	7	9	16	6	11	18847.698	18847.683		0.014	cm^{-1}
17	7	10	17	6	12	18846.437	18846.416		0.020	cm^{-1}
18	7	11	18	6	13	18845.059	18845.073		-0.014	cm^{-1}
19	7	12	19	6	14	18843.643	18843.654		-0.011	cm^{-1}
20	7	13	20	6	15	18842.195	18842.160		0.034	cm^{-1}
21	7	14	21	6	16	18840.573	18840.589		-0.016	cm^{-1}
22	7	15	22	6	17	18838.935	18838.942		-0.007	cm^{-1}
23	7	16	23	6	18	18837.263	18837.219		0.043	cm^{-1}
24	7	17	24	6	19	18835.450	18835.419		0.030	cm^{-1}
25	7	18	25	6	20	18833.540	18833.542		-0.002	cm^{-1}
26	7	19	26	6	21	18831.585	18831.589		-0.004	cm^{-1}
27	7	20	27	6	22	18829.526	18829.557		-0.031	cm^{-1}
28	7	21	28	6	23	18827.461	18827.448		0.012	cm^{-1}
6	5	2	6	6	0	18754.675	18754.510		0.164	cm^{-1}
7	5	3	7	6	1	18753.989	18753.996		-0.007	cm^{-1}
8	5	4	8	6	2	18753.430	18753.408		0.021	cm^{-1}
9	5	5	9	6	3	18752.771	18752.747		0.023	cm^{-1}
10	5	6	10	6	4	18752.206	18752.012	*	0.193	cm^{-1}
11	5	7	11	6	5	18751.216	18751.203		0.012	cm^{-1}
12	5	8	12	6	6	18750.319	18750.321		-0.002	cm^{-1}
13	5	9	13	6	7	18749.353	18749.365		-0.012	cm^{-1}
14	5	10	14	6	8	18748.392	18748.336		0.055	cm^{-1}
15	5	11	15	6	9	18747.225	18747.232		-0.007	cm^{-1}
16	5	12	16	6	10	18746.032	18746.055		-0.023	cm^{-1}
17	5	13	17	6	11	18744.850	18744.804		0.045	cm^{-1}
18	5	14	18	6	12	18743.482	18743.479		0.002	cm^{-1}
19	5	15	19	6	13	18742.065	18742.080		-0.015	cm^{-1}
20	5	16	20	6	14	18740.590	18740.608		-0.018	cm^{-1}
21	5	17	21	6	15	18739.184	18739.061		0.122	cm^{-1}
22	5	18	22	6	16	18737.426	18737.440		-0.014	cm^{-1}
23	5	19	23	6	17	18735.706	18735.744		-0.038	cm^{-1}
24	5	20	24	6	18	18733.922	18733.975		-0.053	cm^{-1}
25	5	21	25	6	19	18732.096	18732.131		-0.035	cm^{-1}
26	5	22	26	6	20	18730.273	18730.212		0.060	cm^{-1}
27	5	23	27	6	21	18728.187	18728.219		-0.032	cm^{-1}
28	5	24	28	6	22	18726.116	18726.152		-0.036	cm^{-1}
29	5	25	29	6	23	18724.023	18724.010		0.012	cm^{-1}
30	5	26	30	6	24	18721.722	18721.793		-0.071	cm^{-1}
5	5	0	6	6	0	18749.353	18749.271		0.081	cm^{-1}
6	5	1	7	6	1	18747.874	18747.883		-0.009	cm^{-1}
7	5	2	8	6	3	18746.443	18746.422		0.020	cm^{-1}
8	5	3	9	6	3	18744.850	18744.887		-0.037	cm^{-1}
9	5	4	10	6	4	18743.266	18743.279		-0.013	cm^{-1}
10	5	5	11	6	5	18741.599	18741.597		0.001	cm^{-1}
11	5	6	12	6	6	18739.846	18739.841		0.004	cm^{-1}
12	5	7	13	6	7	18737.980	18738.011		-0.031	cm^{-1}
13	5	8	14	6	8	18736.135	18736.108		0.026	cm^{-1}
14	5	9	15	6	9	18734.120	18734.131		-0.011	cm^{-1}

Upper State			Lower State			Observation	Calculation	Residual	Remarks
J	K_A	K_C	J	K_A	K_C				
15	5	10	16	6	10	18732.096	18732.080	0.015	cm^{-1}
16	5	11	17	6	11	18729.975	18729.955	0.019	cm^{-1}
17	5	12	18	6	12	18727.747	18727.756	-0.009	cm^{-1}
18	5	13	19	6	13	18725.437	18725.483	-0.046	cm^{-1}
19	5	14	20	6	14	18723.188	18723.135	0.052	cm^{-1}
20	5	15	21	6	15	18720.756	18720.714	0.041	cm^{-1}
21	5	16	22	6	16	18718.266	18718.218	0.047	cm^{-1}
22	5	17	23	6	17	18715.666	18715.648	0.017	cm^{-1}
23	5	18	24	6	18	18712.952	18713.004	-0.052	cm^{-1}
24	5	19	25	6	19	18710.274	18710.285	-0.011	cm^{-1}
25	5	20	26	6	20	18707.564	18707.492	0.071	cm^{-1}
26	5	21	27	6	21	18704.631	18704.624	0.006	cm^{-1}
27	5	22	28	6	22	18701.676	18701.681	-0.005	cm^{-1}
28	5	23	29	6	23	18698.613	18698.664	-0.051	cm^{-1}
29	8	24	30	6	24	18695.573	18695.572	0.000	cm^{-1}
8	8	0	7	7	0	18869.089	18869.051	0.037	cm^{-1}
9	8	1	8	7	1	18869.355	18869.328	0.026	cm^{-1}
10	8	2	9	7	2	18869.549	18869.531	0.017	cm^{-1}
11	8	3	10	7	3	18869.709	18869.659	0.049	cm^{-1}
12	8	4	11	7	4	18869.709	18869.712	-0.003	cm^{-1}
13	8	5	12	7	5	18869.709	18869.691	0.017	cm^{-1}
14	8	6	13	7	6	18869.549	18869.594	-0.045	cm^{-1}
15	8	7	14	7	7	18869.355	18869.423	-0.068	cm^{-1}
16	8	8	15	7	8	18869.088	18869.177	-0.089	cm^{-1}
17	8	9	16	7	9	18868.821	18868.855	-0.034	cm^{-1}
18	8	10	17	7	10	18868.486	18868.458	0.027	cm^{-1}
19	8	11	18	7	11	18867.983	18867.985	-0.002	cm^{-1}
20	8	12	19	7	12	18867.406	18867.437	-0.031	cm^{-1}
21	8	13	20	7	13	18866.816	18866.813	0.002	cm^{-1}
22	8	14	21	7	14	18866.084	18866.114	-0.030	cm^{-1}
23	8	15	22	7	15	18865.322	18865.338	-0.016	cm^{-1}
24	8	16	23	7	16	18864.412	18864.485	-0.073	cm^{-1}
6	6	0	7	7	0	18737.426	18737.415	0.010	cm^{-1}
7	6	1	8	7	1	18735.896	18735.954	-0.058	cm^{-1}
8	6	2	9	7	2	18734.383	18734.419	-0.036	cm^{-1}
9	6	3	10	7	3	18732.789	18732.810	-0.021	cm^{-1}
10	6	4	11	7	4	18731.158	18731.128	0.029	cm^{-1}
11	6	5	12	7	5	18729.358	18729.372	-0.014	cm^{-1}
12	6	6	13	7	6	18727.533	18727.542	-0.009	cm^{-1}
13	6	7	14	7	7	18725.661	18725.639	0.022	cm^{-1}
14	6	8	15	7	8	18723.678	18723.661	0.016	cm^{-1}
15	6	9	16	7	9	18721.599	18721.609	-0.010	cm^{-1}
16	6	10	17	7	10	18719.471	18719.484	-0.013	cm^{-1}
17	6	11	18	7	11	18717.201	18717.284	-0.083	cm^{-1}
18	6	12	19	7	12	18714.949	18715.010	-0.061	cm^{-1}
19	6	13	20	7	13	18712.671	18712.661	0.009	cm^{-1}
20	6	14	21	7	14	18710.274	18710.239	0.035	cm^{-1}
21	6	15	22	7	15	18707.564	18707.741	-0.177	cm^{-1}
22	6	16	23	7	16	18705.185	18705.170	0.014	cm^{-1}
23	6	17	24	7	17	18702.450	18702.523	-0.072	cm^{-1}

Upper State			Lower State			Observation	Calculation	Residual	Remarks
J	K_A	K_C	J	K_A	K_C				
24	6	18	25	7	18	18699.832	18699.802	0.029	cm^{-1}
25	6	19	26	7	19	18697.025	18697.006	0.018	cm^{-1}
10	9	1	9	8	1	18875.561	18875.537	0.023	cm^{-1}
11	9	2	10	8	2	18875.701	18875.663	0.037	cm^{-1}
12	9	3	11	8	3	18875.701	18875.714	-0.013	cm^{-1}
13	9	4	12	8	4	18875.702	18875.690	0.011	cm^{-1}
14	9	5	13	8	5	18875.561	18875.591	-0.030	cm^{-1}
15	9	6	14	8	6	18875.359	18875.418	-0.059	cm^{-1}
16	9	7	15	8	7	18875.151	18875.168	-0.017	cm^{-1}
17	9	8	16	8	8	18874.849	18874.844	0.004	cm^{-1}
18	9	9	17	8	9	18874.457	18874.444	0.012	cm^{-1}
19	9	10	18	8	10	18874.026	18873.969	0.056	cm^{-1}
20	9	11	19	8	11	18873.392	18873.418	-0.026	cm^{-1}
21	9	12	20	8	12	18872.784	18872.791	-0.007	cm^{-1}
22	9	13	21	8	13	18872.079	18872.088	-0.009	cm^{-1}
23	9	14	22	8	14	18871.368	18871.310	0.058	cm^{-1}
24	9	15	23	8	15	18870.417	18870.454	-0.037	cm^{-1}
25	9	16	24	8	16	18869.549	18869.523	0.025	cm^{-1}
26	9	17	25	8	17	18868.486	18868.515	-0.029	cm^{-1}
27	9	18	26	8	18	18867.406	18867.430	-0.024	cm^{-1}
28	9	19	27	8	19	18866.362	18866.268	0.093	cm^{-1}
29	9	20	28	8	20	18864.995	18865.029	-0.034	cm^{-1}
30	9	21	29	8	21	18863.718	18863.713	0.004	cm^{-1}
8	7	2	8	8	0	18732.096	18732.178	-0.082	cm^{-1}
9	7	3	9	8	1	18731.565	18731.515	0.049	cm^{-1}
10	7	4	10	8	2	18730.665	18730.779	-0.114	cm^{-1}
11	7	5	11	8	3	18729.975	18729.969	0.005	cm^{-1}
12	7	6	12	8	4	18729.124	18729.085	0.038	cm^{-1}
13	7	7	13	8	5	18728.187	18728.128	0.059	cm^{-1}
14	7	8	14	8	6	18727.082	18727.096	-0.014	cm^{-1}
15	7	9	15	8	7	18726.116	18725.990	0.125	cm^{-1}
16	7	10	16	8	8	18724.864	18724.811	0.053	cm^{-1}
17	7	11	17	8	9	18723.678	18723.557	0.120	cm^{-1}
18	7	12	18	8	10	18722.285	18722.229	0.056	cm^{-1}
19	7	13	19	8	11	18720.756	18720.826	-0.070	cm^{-1}
20	7	14	20	8	12	18719.471	18719.349	0.121	cm^{-1}
21	7	15	21	8	13	18717.655	18717.798	-0.143	cm^{-1}
22	7	16	22	8	14	18716.127	18716.172	-0.045	cm^{-1}
23	7	17	23	8	15	18714.471	18714.472	-0.001	cm^{-1}
24	7	18	24	8	16	18712.671	18712.697	-0.026	cm^{-1}
25	7	19	25	8	17	18710.877	18710.847	0.029	cm^{-1}
26	7	20	26	8	18	18708.950	18708.922	0.028	cm^{-1}
27	7	21	27	8	19	18706.955	18706.921	0.033	cm^{-1}
28	7	22	28	8	20	18704.854	18704.846	0.007	cm^{-1}
29	7	23	29	8	21	18702.699	18702.695	0.003	cm^{-1}
30	7	24	30	8	22	18700.469	18700.469	0.000	cm^{-1}
7	7	0	8	8	0	18725.236	18725.197	0.038	cm^{-1}
8	7	1	9	8	1	18723.678	18723.662	0.015	cm^{-1}
9	7	2	10	8	2	18722.072	18722.054	0.018	cm^{-1}
10	7	3	11	8	3	18720.442	18720.371	0.070	cm^{-1}

Upper State			Lower State			Observation	Calculation	Residual	Remarks
J	K_A	K_C	J	K_A	K_C				
11	7	4	12	8	4	18718.606	18718.615	-0.009	cm^{-1}
12	7	5	13	8	5	18716.792	18716.785	0.007	cm^{-1}
13	7	6	14	8	6	18714.949	18714.880	0.068	cm^{-1}
14	7	7	15	8	7	18712.952	18712.902	0.049	cm^{-1}
15	7	8	16	8	8	18710.877	18710.850	0.026	cm^{-1}
16	7	9	17	8	9	18708.706	18708.724	-0.018	cm^{-1}
17	7	10	18	8	10	18706.550	18706.523	0.026	cm^{-1}
18	7	11	19	8	11	18704.240	18704.248	-0.008	cm^{-1}
19	7	12	20	8	12	18701.918	18701.899	0.018	cm^{-1}
20	7	13	21	8	13	18699.476	18699.475	0.000	cm^{-1}
21	7	14	22	8	14	18697.025	18696.977	0.047	cm^{-1}
22	7	15	23	8	15	18694.455	18694.404	0.050	cm^{-1}
23	7	16	24	8	16	18691.785	18691.756	0.028	cm^{-1}
24	7	17	25	8	17	18689.069	18689.034	0.034	cm^{-1}
25	7	18	26	8	18	18686.345	18686.236	0.108	cm^{-1}
26	7	19	27	8	19	18683.389	18683.363	0.025	cm^{-1}
27	7	20	28	8	20	18680.340	18680.416	-0.076	cm^{-1}
28	7	21	29	8	21	18677.376	18677.392	-0.016	cm^{-1}
29	7	22	30	8	22	18674.306	18674.294	0.011	cm^{-1}
11	10	1	10	9	1	18881.293	18881.316	-0.023	cm^{-1}
11	11	0	10	10	0	18886.636	18886.614	0.021	cm^{-1}
12	12	0	11	11	0	18891.581	18891.596	-0.015	cm^{-1}
13	13	0	12	12	0	18896.100	18896.131	-0.031	cm^{-1}

Upper State			Lower State			Observation	Calculation		Residual	Remarks
J	K_A	K_C	J	K_A	K_C					
10	0	10	9	0	9	16400.592	16400.541		0.050	cm^{-1}
11	0	11	10	0	10	16400.592	16400.609		-0.017	cm^{-1}
12	0	12	11	0	11	16400.592	16400.579		0.012	cm^{-1}
2	1	1	1	1	0	16396.250	16396.264		-0.014	cm^{-1}
2	1	2	1	1	1	16396.250	16396.210		0.039	cm^{-1}
3	1	2	2	1	1	16397.158	16397.126		0.031	cm^{-1}
3	1	3	2	1	2	16397.158	16397.052		0.105	cm^{-1}
4	1	3	3	1	2	16397.824	16397.887		-0.063	cm^{-1}
4	1	4	3	1	3	16397.824	16397.799		0.024	cm^{-1}
5	1	4	4	1	3	16398.601	16398.548		0.052	cm^{-1}
5	1	5	4	1	4	16398.401	16398.450		-0.049	cm^{-1}
6	1	5	5	1	4	16399.191	16399.108		0.082	cm^{-1}
6	1	6	5	1	5	16399.038	16399.006		0.031	cm^{-1}
7	1	6	6	1	5	16399.604	16399.568		0.035	cm^{-1}
7	1	7	6	1	6	16399.428	16399.467		-0.039	cm^{-1}
8	1	7	7	1	6	16399.888	16399.926		-0.038	cm^{-1}
8	1	8	7	1	7	16399.888	16399.832		0.055	cm^{-1}
9	1	8	8	1	7	16400.152	16400.184		-0.032	cm^{-1}
9	1	9	8	1	8	16400.152	16400.101		0.050	cm^{-1}
10	1	9	9	1	8	16400.357	16400.342		0.015	cm^{-1}
10	1	10	9	1	9	16400.357	16400.275		0.082	cm^{-1}
11	1	10	10	1	9	16400.357	16400.398		-0.041	cm^{-1}
11	1	11	10	1	10	16400.357	16400.352		0.004	cm^{-1}
12	1	11	11	1	10	16400.357	16400.353		0.003	cm^{-1}
12	1	12	11	1	11	16400.357	16400.335		0.021	cm^{-1}
13	1	12	12	1	11	16400.152	16400.208		-0.056	cm^{-1}
13	1	13	12	1	12	16400.152	16400.221		-0.069	cm^{-1}
14	1	13	13	1	12	16399.888	16399.962		-0.074	cm^{-1}
14	1	14	13	1	13	16399.888	16400.012		-0.124	cm^{-1}
15	1	15	14	1	14	16399.604	16399.706		-0.102	cm^{-1}
15	1	14	14	1	13	16399.604	16399.614		-0.010	cm^{-1}
16	1	16	15	1	15	16399.198	16399.305	*	-0.107	cm^{-1}
16	1	15	15	1	14	16399.038	16399.166	*	-0.128	cm^{-1}
17	1	17	16	1	16	16398.401	16398.808	*	-0.407	cm^{-1}
17	1	16	16	1	15	16398.401	16398.617	*	-0.216	cm^{-1}
18	1	18	17	1	17	16397.905	16398.315	*	-0.310	cm^{-1}
18	1	17	17	1	16	16398.236	16397.967	*	0.268	cm^{-1}
19	1	19	18	1	18	16397.824	16397.526	*	0.297	cm^{-1}
19	1	18	18	1	17	16397.407	16397.215	*	0.191	cm^{-1}
20	1	20	19	1	19	16396.925	16396.741	*	0.183	cm^{-1}
20	1	19	19	1	18	16396.451	16396.363		0.087	cm^{-1}
21	1	21	20	1	20	16395.938	16395.859		0.078	cm^{-1}
21	1	20	20	1	19	16395.499	16395.410		0.089	cm^{-1}
22	1	22	21	1	21	16394.946	16394.882		0.063	cm^{-1}
22	1	21	21	1	20	16394.259	16394.355		-0.096	cm^{-1}
23	1	23	22	1	22	16393.871	16393.808		0.062	cm^{-1}
23	1	22	22	1	21	16393.263	16393.199		0.063	cm^{-1}
24	1	24	23	1	23	16392.642	16392.638		0.003	cm^{-1}
24	1	23	23	1	22	16391.959	16391.943		0.015	cm^{-1}
25	1	25	24	1	24	16391.382	16391.371		0.010	cm^{-1}

Upper State			Lower State			Observation	Calculation		Residual	Remarks
J	K_A	K_C	J	K_A	K_C					
25	1	24	24	1	23	16390.584	16390.585		-0.001	cm^{-1}
26	1	26	25	1	25	16389.998	16390.008		-0.010	cm^{-1}
26	1	25	25	1	24	16389.157	16389.126		0.030	cm^{-1}
27	1	27	26	1	26	16388.606	16388.548		0.057	cm^{-1}
27	1	26	26	1	25	16387.490	16387.566		-0.076	cm^{-1}
28	1	28	27	1	27	16386.921	16386.992		-0.071	cm^{-1}
28	1	27	27	1	26	16385.989	16385.905		0.083	cm^{-1}
29	1	29	28	1	28	16385.270	16385.338		-0.068	cm^{-1}
29	1	28	28	1	27	16384.014	16384.144		-0.130	cm^{-1}
2	1	1	3	1	2	16390.584	16390.448		0.135	cm^{-1}
2	1	2	3	1	3	16390.584	16390.568		0.015	cm^{-1}
3	1	2	4	1	3	16388.933	16388.983		-0.050	cm^{-1}
3	1	3	4	1	4	16389.157	16389.154		0.002	cm^{-1}
4	1	3	5	1	4	16387.490	16387.419		0.070	cm^{-1}
4	1	4	5	1	5	16387.625	16387.645		-0.020	cm^{-1}
5	1	4	6	1	5	16385.707	16385.754		-0.047	cm^{-1}
5	1	5	6	1	6	16385.989	16386.041		-0.052	cm^{-1}
6	1	5	7	1	6	16384.014	16383.989		0.024	cm^{-1}
6	1	6	7	1	7	16384.360	16384.341		0.018	cm^{-1}
7	1	6	8	1	7	16382.110	16382.124		-0.014	cm^{-1}
7	1	7	8	1	8	16382.587	16382.547		0.039	cm^{-1}
8	1	7	9	1	8	16380.176	16380.158		0.017	cm^{-1}
8	1	8	9	1	9	16380.680	16380.658		0.022	cm^{-1}
9	1	8	10	1	9	16378.079	16378.093		-0.014	cm^{-1}
9	1	9	10	1	10	16378.668	16378.673		-0.005	cm^{-1}
10	1	9	11	1	10	16375.924	16375.928		-0.004	cm^{-1}
10	1	10	11	1	11	16376.577	16376.594		-0.017	cm^{-1}
11	1	10	12	1	11	16373.650	16373.662		-0.012	cm^{-1}
11	1	11	12	1	12	16374.386	16374.420		-0.034	cm^{-1}
12	1	11	13	1	12	16371.273	16371.297		-0.024	cm^{-1}
12	1	12	13	1	13	16372.106	16372.151		-0.045	cm^{-1}
13	1	12	14	1	13	16368.796	16368.832		-0.036	cm^{-1}
13	1	13	14	1	14	16369.751	16369.787		-0.036	cm^{-1}
14	1	13	15	1	14	16366.209	16366.267		-0.058	cm^{-1}
14	1	14	15	1	15	16367.295	16367.329		-0.034	cm^{-1}
15	1	14	16	1	15	16363.571	16363.603		-0.032	cm^{-1}
15	1	15	16	1	16	16364.724	16364.775		-0.051	cm^{-1}
16	1	15	17	1	16	16360.701	16360.839	*	-0.138	cm^{-1}
16	1	16	17	1	17	16362.013	16362.127	*	-0.114	cm^{-1}
17	1	16	18	1	17	16357.741	16357.975	*	-0.234	cm^{-1}
17	1	17	18	1	18	16359.076	16359.384	*	-0.308	cm^{-1}
18	1	17	19	1	18	16355.245	16355.012	*	0.232	cm^{-1}
18	1	18	19	1	19	16356.206	16356.547	*	-0.341	cm^{-1}
19	1	18	20	1	19	16352.119	16351.950	*	0.168	cm^{-1}
19	1	19	20	1	20	16353.864	16353.614	*	0.249	cm^{-1}
20	1	19	21	1	20	16348.870	16348.788	*	0.081	cm^{-1}
20	1	20	21	1	21	16350.775	16350.587	*	0.187	cm^{-1}
21	1	20	22	1	21	16345.585	16345.527		0.057	cm^{-1}
21	1	21	22	1	22	16347.526	16347.466		0.059	cm^{-1}
22	1	21	23	1	22	16342.203	16342.167		0.035	cm^{-1}

Upper State			Lower State			Observation	Calculation	Residual	Remarks
J	K_A	K_C	J	K_A	K_C				
22	1	22	23	1	23	16344.304	16344.249	0.054	cm^{-1}
23	1	23	24	1	23	16338.727	16338.708	0.018	cm^{-1}
23	1	23	24	1	24	16340.956	16340.938	0.017	cm^{-1}
24	1	23	25	1	24	16335.159	16335.150	0.008	cm^{-1}
24	1	24	25	1	25	16337.500	16337.532	-0.032	cm^{-1}
25	1	24	26	1	25	16331.453	16331.494	-0.041	cm^{-1}
25	1	25	26	1	26	16334.007	16334.031	-0.024	cm^{-1}
26	1	25	27	1	26	16327.757	16327.739	0.017	cm^{-1}
26	1	26	27	1	27	16330.312	16330.435	-0.123	cm^{-1}
27	1	26	28	1	27	16323.852	16323.886	-0.034	cm^{-1}
27	1	27	28	1	28	16326.757	16326.744	0.012	cm^{-1}
28	1	27	29	1	28	16319.884	16319.935	-0.051	cm^{-1}
28	1	28	29	1	29	16322.939	16322.958	-0.019	cm^{-1}
29	1	28	30	1	29	16315.837	16315.886	-0.049	cm^{-1}
29	1	29	30	1	30	16319.138	16319.077	0.060	cm^{-1}
4	2	3	3	2	2	16397.158	16397.140	0.017	cm^{-1}
5	2	4	4	2	3	16397.824	16397.796	0.027	cm^{-1}
6	2	5	5	2	4	16398.401	16398.353	0.047	cm^{-1}
7	2	6	6	2	5	16398.810	16398.813	-0.003	cm^{-1}
8	2	7	7	2	6	16399.191	16399.174	0.017	cm^{-1}
9	2	8	8	2	7	16399.428	16399.436	-0.008	cm^{-1}
10	2	9	9	2	8	16399.604	16399.600	0.003	cm^{-1}
11	2	10	10	2	9	16399.604	16399.666	-0.062	cm^{-1}
12	2	11	11	2	10	16399.603	16399.634	-0.031	cm^{-1}
13	2	12	12	2	11	16399.428	16399.503	-0.075	cm^{-1}
14	2	13	13	2	12	16399.191	16399.273	-0.082	cm^{-1}
2	2	0	3	2	1	16389.769	16389.806	-0.037	cm^{-1}
3	2	1	4	2	2	16388.392	16388.365	0.026	cm^{-1}
4	2	2	5	2	3	16386.921	16386.827	0.094	cm^{-1}
5	2	3	6	2	4	16385.270	16385.189	0.080	cm^{-1}
6	2	4	7	2	5	16383.451	16383.453	-0.002	cm^{-1}
7	2	5	8	2	6	16381.675	16381.618	0.056	cm^{-1}
8	2	6	9	2	7	16379.695	16379.684	0.010	cm^{-1}
9	2	7	10	2	8	16377.666	16377.650	0.015	cm^{-1}
10	2	8	11	2	9	16375.535	16375.516	0.018	cm^{-1}
11	2	9	12	2	10	16373.314	16373.282	0.031	cm^{-1}
12	2	10	13	2	11	16370.936	16370.947	-0.011	cm^{-1}
12	2	11	13	2	12	16370.936	16371.009	-0.073	cm^{-1}
13	2	11	14	2	12	16368.560	16368.512	0.047	cm^{-1}
13	2	12	14	2	13	16368.560	16368.591	-0.031	cm^{-1}
14	2	12	15	2	13	16365.885	16365.975	-0.090	cm^{-1}
14	2	13	15	2	14	16366.043	16366.076	-0.033	cm^{-1}
15	2	13	16	2	14	16363.381	16363.337	0.044	cm^{-1}
15	2	14	16	2	15	16363.571	16363.463	0.107	cm^{-1}
19	2	17	20	2	18	16351.819	16351.759	0.059	cm^{-1}
19	2	18	20	2	19	16352.119	16352.035	0.083	cm^{-1}
20	2	18	21	2	19	16348.667	16348.606	0.060	cm^{-1}
20	2	19	21	2	20	16348.870	16348.934	-0.064	cm^{-1}
21	2	19	22	2	20	16345.409	16345.350	0.058	cm^{-1}
21	2	20	22	2	21	16345.761	16345.735	0.025	cm^{-1}

Upper State			Lower State			Observation	Calculation		Residual	Remarks
J	K_A	K_C	J	K_A	K_C					
22	2	20	23	2	21	16342.034	16341.989		0.044	cm^{-1}
22	2	21	23	2	22	16342.468	16342.438		0.029	cm^{-1}
4	3	1	3	3	0	16395.938	16395.970		-0.032	cm^{-1}
5	3	2	4	3	1	16396.692	16396.625		0.066	cm^{-1}
6	3	3	5	3	2	16397.158	16397.181		-0.023	cm^{-1}
7	3	4	6	3	3	16397.628	16397.639		-0.011	cm^{-1}
8	3	5	7	3	4	16397.965	16397.999		-0.034	cm^{-1}
9	3	6	8	3	5	16398.236	16398.260		-0.024	cm^{-1}
10	3	7	9	3	6	16398.401	16398.422		-0.021	cm^{-1}
11	3	8	10	3	7	16398.401	16398.486		-0.085	cm^{-1}
12	3	9	11	3	8	16398.401	16398.451		-0.050	cm^{-1}
13	3	10	12	3	9	16398.236	16398.317	*	-0.081	cm^{-1}
14	3	11	13	3	10	16397.965	16398.084	*	-0.119	cm^{-1}
15	3	12	14	3	11	16397.628	16397.752	*	-0.124	cm^{-1}
16	3	13	15	3	12	16396.925	16397.320	*	-0.395	cm^{-1}
17	3	14	16	3	13	16396.925	16396.789	*	0.135	cm^{-1}
18	3	15	17	3	14	16396.250	16396.159	*	0.091	cm^{-1}
19	3	16	18	3	15	16395.499	16395.428		0.070	cm^{-1}
20	3	17	19	3	16	16394.686	16394.597		0.088	cm^{-1}
21	3	18	20	3	17	16393.705	16393.667		0.038	cm^{-1}
22	3	19	21	3	18	16392.642	16392.635		0.006	cm^{-1}
23	3	20	23	3	19	16391.539	16391.503		0.035	cm^{-1}
24	3	21	23	3	20	16390.277	16390.270		0.006	cm^{-1}
25	3	22	24	3	21	16388.922	16388.936		-0.014	cm^{-1}
26	3	23	25	3	22	16387.490	16387.500		-0.010	cm^{-1}
27	3	24	26	3	23	16385.989	16385.962		0.026	cm^{-1}
28	3	25	27	3	24	16384.360	16384.323		0.036	cm^{-1}
29	3	26	28	3	25	16382.587	16382.580		0.006	cm^{-1}
3	3	0	3	3	1	16391.797	16391.780		0.016	cm^{-1}
4	3	1	4	3	2	16391.382	16391.387		-0.005	cm^{-1}
5	3	2	5	3	3	16390.921	16390.896		0.024	cm^{-1}
6	3	3	6	3	4	16390.277	16390.307		-0.030	cm^{-1}
7	3	4	7	3	5	16389.595	16389.619		-0.024	cm^{-1}
8	3	5	8	3	6	16388.791	16388.833		-0.042	cm^{-1}
9	3	6	9	3	7	16387.922	16387.948		-0.026	cm^{-1}
10	3	7	10	3	8	16386.921	16386.965		-0.044	cm^{-1}
4	3	1	5	3	2	16385.709	16385.658		0.050	cm^{-1}
5	3	2	6	3	3	16384.014	16384.021		-0.007	cm^{-1}
6	3	3	7	3	4	16382.318	16382.286		0.031	cm^{-1}
7	3	4	8	3	5	16380.431	16380.453		-0.022	cm^{-1}
8	3	5	9	3	6	16378.478	16378.521		-0.043	cm^{-1}
9	3	6	10	3	7	16376.457	16376.491		-0.034	cm^{-1}
10	3	7	11	3	8	16374.386	16374.362		0.023	cm^{-1}
11	3	8	12	3	9	16372.106	16372.134		-0.028	cm^{-1}
12	3	9	13	3	10	16369.751	16369.808		-0.057	cm^{-1}
13	3	10	14	3	11	16367.295	16367.382	*	-0.087	cm^{-1}
14	3	11	15	3	12	16364.724	16364.858	*	-0.134	cm^{-1}
15	3	12	16	3	13	16362.013	16362.234	*	-0.221	cm^{-1}
15	3	12	16	3	13	16362.013	16362.234	*	-0.221	cm^{-1}
16	3	13	17	3	14	16359.201	16259.511	*	-0.310	cm^{-1}

Upper State			Lower State			Observation	Calculation	Residual	Remarks
J	K_A	K_C	J	K_A	K_C				
17	3	14	18	3	15	16356.875	16356.689 *	0.185	cm^{-1}
18	3	15	19	3	16	16353.864	16353.767 *	0.096	cm^{-1}
19	3	16	20	3	17	16350.775	16350.745	0.030	cm^{-1}
20	3	17	21	3	18	16347.662	16347.622	0.039	cm^{-1}
21	3	18	22	3	19	16344.440	16344.400	0.040	cm^{-1}
22	3	19	23	3	20	16341.113	16341.076	0.036	cm^{-1}
23	3	20	24	3	21	16337.669	16337.652	0.016	cm^{-1}
24	3	21	25	3	22	16334.140	16334.126	0.013	cm^{-1}
25	3	22	26	3	23	16330.513	16330.499	0.013	cm^{-1}
26	3	23	27	3	24	16326.757	16326.770	-0.013	cm^{-1}
27	3	24	28	3	25	16322.939	16322.939	0.000	cm^{-1}
28	3	25	29	3	26	16318.992	16319.005	-0.013	cm^{-1}
29	3	26	30	3	27	16315.013	16314.968	0.044	cm^{-1}
5	4	1	4	4	0	16394.946	16394.986	-0.040	cm^{-1}
6	4	2	5	4	1	16395.499	16395.541	-0.042	cm^{-1}
7	4	3	6	4	2	16395.938	16395.997	-0.059	cm^{-1}
8	4	4	7	4	3	16396.250	16396.354	-0.104	cm^{-1}
9	4	5	8	4	4	16396.692	16396.613	0.078	cm^{-1}
10	4	6	9	4	5	16396.925	16396.773	0.151	cm^{-1}
11	4	7	10	4	6	16396.925	16396.834	0.091	cm^{-1}
12	4	8	11	4	7	16396.925	16396.795	0.129	cm^{-1}
13	4	9	12	4	8	16396.692	16396.658	0.033	cm^{-1}
14	4	10	13	4	9	16396.451	16396.421	0.029	cm^{-1}
15	4	11	14	4	10	16395.938	16396.086	-0.148	cm^{-1}
16	4	12	15	4	11	16395.705	16395.650	0.054	cm^{-1}
17	4	13	16	4	12	16395.143	16395.115	0.027	cm^{-1}
18	4	14	17	4	13	16394.511	16394.480	0.030	cm^{-1}
19	4	15	18	4	14	16393.705	16393.746	-0.041	cm^{-1}
20	4	16	19	4	15	16392.933	16392.911	0.021	cm^{-1}
21	4	17	20	4	16	16391.959	16391.976	-0.017	cm^{-1}
22	4	18	21	4	17	16390.921	16390.941	-0.020	cm^{-1}
23	4	19	22	4	18	16389.769	16389.805	-0.036	cm^{-1}
6	4	2	7	4	3	16380.680	16380.647	0.032	cm^{-1}
7	4	3	8	4	4	16378.791	16378.812	-0.021	cm^{-1}
8	4	4	9	4	5	16376.790	16376.879	-0.089	cm^{-1}
9	4	5	10	4	6	16374.820	16374.846	-0.026	cm^{-1}
10	4	6	11	4	7	16372.677	16372.716	-0.039	cm^{-1}
11	4	7	12	4	8	16370.409	16370.486	-0.077	cm^{-1}
12	4	8	13	4	9	16368.026	16368.158	-0.132	cm^{-1}
13	4	9	14	4	10	16365.693	16365.730	-0.037	cm^{-1}
14	4	10	15	4	11	16363.204	16363.204	0.000	cm^{-1}
15	4	11	16	4	12	16360.701	16360.578	0.122	cm^{-1}
16	4	12	17	4	13	16357.743	16357.854	-0.111	cm^{-1}
17	4	13	18	4	14	16355.057	16355.030	0.027	cm^{-1}
18	4	14	19	4	15	16352.119	16352.106	0.012	cm^{-1}
19	4	15	20	4	16	16349.065	16349.083	-0.018	cm^{-1}
20	4	16	21	4	17	16345.961	16345.960	0.000	cm^{-1}
21	4	17	22	4	18	16342.757	16342.737	0.019	cm^{-1}
22	4	18	23	4	19	16339.450	16339.415	0.034	cm^{-1}
23	4	19	24	4	20	16335.997	16335.992	0.004	cm^{-1}

Upper State			Lower State			Observation	Calculation	Residual	Remarks
J	K_A	K_C	J	K_A	K_C				
24	4	20	25	4	21	16332.464	16332.468	-0.004	cm^{-1}
25	4	21	26	4	22	16328.857	16328.844	0.012	cm^{-1}
26	4	22	27	4	23	16325.149	16325.120	0.028	cm^{-1}
27	4	23	28	4	24	16321.313	16321.294	0.018	cm^{-1}
28	4	24	29	4	25	16317.363	16317.367	-0.004	cm^{-1}
29	4	25	30	4	26	16313.270	16313.339	-0.069	cm^{-1}
6	5	2	5	5	1	16393.469	16393.435	0.034	cm^{-1}
7	5	3	6	5	2	16393.871	16393.888	-0.017	cm^{-1}
8	5	4	7	5	3	16394.259	16394.243	0.015	cm^{-1}
9	5	5	8	5	4	16394.511	16394.498	0.012	cm^{-1}
10	5	6	9	5	5	16394.686	16394.655	0.030	cm^{-1}
11	5	7	10	5	6	16394.686	16394.712	-0.026	cm^{-1}
12	5	8	11	5	7	16394.686	16394.670	0.016	cm^{-1}
13	5	9	12	5	8	16394.511	16394.528	-0.017	cm^{-1}
14	5	10	13	5	9	16394.259	16394.287	-0.028	cm^{-1}
15	5	11	14	5	10	16393.871	16393.946	-0.075	cm^{-1}
16	5	12	15	5	11	16393.469	16393.505	-0.036	cm^{-1}
17	5	13	16	5	12	16392.933	16392.964	-0.031	cm^{-1}
18	5	14	17	5	13	16392.297	16392.324	-0.027	cm^{-1}
19	5	15	18	5	14	16391.539	16391.583	-0.044	cm^{-1}
20	5	16	19	5	15	16390.751	16390.742	0.009	cm^{-1}
21	5	17	20	5	16	16389.769	16389.800	-0.031	cm^{-1}
22	5	18	21	5	17	16388.606	16388.758	-0.152	cm^{-1}
23	5	19	22	5	18	16387.626	16387.615	0.010	cm^{-1}
24	5	20	23	5	19	16386.441	16386.371	0.069	cm^{-1}
25	5	21	24	5	20	16384.934	16385.025	-0.091	cm^{-1}
5	5	0	5	5	1	16387.193	16387.154	0.038	cm^{-1}
6	5	1	6	5	2	16386.441	16386.561	-0.120	cm^{-1}
7	5	2	7	5	3	16385.887	16385.869	0.017	cm^{-1}
8	5	3	8	5	4	16384.931	16385.079	-0.148	cm^{-1}
5	5	0	6	5	1	16380.431	16380.280	0.150	cm^{-1}
6	5	1	7	5	2	16378.688	16378.542	0.145	cm^{-1}
7	5	2	8	5	3	16376.790	16376.705	0.084	cm^{-1}
8	5	3	9	5	4	16374.830	16374.769	0.060	cm^{-1}
9	5	4	10	5	5	16372.677	16372.734	-0.057	cm^{-1}
10	5	5	11	5	6	16370.698	16370.600	0.097	cm^{-1}
11	5	6	12	5	7	16368.402	16368.367	0.034	cm^{-1}
12	5	7	13	5	8	16366.047	16366.035	0.011	cm^{-1}
13	5	8	14	5	9	16363.571	16363.604	-0.033	cm^{-1}
14	5	9	15	5	10	16361.051	16361.073	-0.022	cm^{-1}
15	5	10	16	5	11	16358.422	16358.444	-0.022	cm^{-1}
16	5	11	17	5	12	16355.721	16355.714	0.006	cm^{-1}
17	5	12	18	5	13	16352.879	16352.886	-0.007	cm^{-1}
18	5	13	19	5	14	16349.917	16349.957	-0.040	cm^{-1}
19	5	14	20	5	15	16346.900	16346.929	-0.029	cm^{-1}
20	5	16	21	5	17	16343.782	16343.801	-0.019	cm^{-1}
21	5	17	22	5	18	16340.555	16340.573	-0.018	cm^{-1}
22	5	18	23	5	19	16337.227	16337.245	-0.018	cm^{-1}
23	5	19	24	5	20	16333.820	16333.816	0.003	cm^{-1}
24	5	20	25	5	21	16330.312	16330.287	0.024	cm^{-1}

Upper State			Lower State			Observation	Calculation	Residual	Remarks
J	K_A	K_C	J	K_A	K_C				
25	5	21	26	5	22	16326.757	16326.657	0.099	cm^{-1}
26	5	22	27	5	23	16322.939	16322.927	0.011	cm^{-1}
27	5	23	28	5	24	16319.138	16319.095	0.042	cm^{-1}
28	5	24	29	5	25	16315.205	16315.163	0.041	cm^{-1}

Upper State			Lower State			Observation	Calculation	Residual	Remarks
J	K_A	K_C	J	K_A	K_C				
11	0	11	10	0	10	16489.168	16489.128	0.039	cm^{-1}
12	0	12	11	0	11	16489.168	16489.206	-0.038	cm^{-1}
13	0	13	12	0	12	16489.168	16489.213	-0.045	cm^{-1}
14	0	14	13	0	13	16489.168	16489.149	0.018	cm^{-1}
1	0	1	2	0	2	16481.506	16481.537	-0.031	cm^{-1}
2	0	2	3	0	3	16480.437	16480.447	-0.010	cm^{-1}
3	0	3	4	0	4	16479.309	16479.285	0.023	cm^{-1}
4	0	4	5	0	5	16478.077	16478.054	0.023	cm^{-1}
5	0	5	6	0	6	16476.787	16476.752	0.034	cm^{-1}
6	0	6	7	0	7	16475.417	16475.382	0.034	cm^{-1}
7	0	7	8	0	8	16473.951	16473.943	0.007	cm^{-1}
8	0	8	9	0	9	16472.470	16472.438	0.031	cm^{-1}
9	0	9	10	0	10	16470.873	16470.866	0.006	cm^{-1}
10	0	10	11	0	11	16469.230	16469.228	0.001	cm^{-1}
11	0	11	12	0	12	16467.539	16467.525	0.013	cm^{-1}
12	0	12	13	0	13	16465.760	16465.759	0.000	cm^{-1}
13	0	13	14	0	14	16463.942	16463.929	0.013	cm^{-1}
14	0	14	15	0	15	16462.045	16462.035	0.009	cm^{-1}
15	0	15	16	0	16	16460.090	16460.079	0.010	cm^{-1}
16	0	16	17	0	17	16458.084	16458.060	0.024	cm^{-1}
17	0	17	18	0	18	16455.983	16455.977	0.005	cm^{-1}
18	0	18	19	0	19	16453.815	16453.832	-0.017	cm^{-1}
19	0	19	20	0	20	16451.659	16451.623	0.035	cm^{-1}
5	1	4	6	1	5	16476.304	16476.441	-0.137	cm^{-1}
5	1	5	6	1	6	16476.787	16476.817	-0.030	cm^{-1}
6	1	5	7	1	6	16475.083	16475.020	0.062	cm^{-1}
6	1	6	7	1	7	16475.417	16475.481	-0.064	cm^{-1}
7	1	6	8	1	7	16473.455	16473.525	-0.070	cm^{-1}
7	1	7	8	1	8	16474.098	16474.077	0.020	cm^{-1}
8	1	7	9	1	8	16471.910	16471.955	-0.045	cm^{-1}
8	1	8	9	1	9	16472.470	16472.604	-0.134	cm^{-1}
9	1	8	10	1	9	16470.328	16470.312	0.015	cm^{-1}
9	1	9	10	1	10	16471.088	16471.064	0.023	cm^{-1}
10	1	9	11	1	10	16468.636	16468.595	0.041	cm^{-1}
10	1	10	11	1	11	16469.529	16469.456	0.073	cm^{-1}
11	1	10	12	1	11	16466.759	16466.804	-0.045	cm^{-1}
11	1	11	12	1	12	16467.773	16467.779	-0.006	cm^{-1}
12	1	11	13	1	12	16464.927	16464.940	-0.013	cm^{-1}
12	1	12	13	1	13	16466.044	16466.035	0.008	cm^{-1}
13	1	12	14	1	13	16462.989	16463.004	-0.015	cm^{-1}
13	1	13	14	1	14	16464.191	16464.224	-0.033	cm^{-1}
14	1	13	15	1	14	16461.005	16460.995	0.009	cm^{-1}
14	1	14	15	1	15	16462.326	16462.345	-0.019	cm^{-1}
15	1	14	16	1	15	16458.883	16458.915	-0.032	cm^{-1}
15	1	15	16	1	16	16460.405	16460.399	0.006	cm^{-1}
16	1	15	17	1	16	16456.638	16456.764	-0.126	cm^{-1}
16	1	16	17	1	17	16458.345	16458.385	-0.040	cm^{-1}
17	1	16	18	1	17	16454.450	16454.542	-0.092	cm^{-1}
17	1	17	18	1	18	16456.280	16456.303	-0.023	cm^{-1}
18	1	18	19	1	19	16454.109	16454.154	-0.045	cm^{-1}

Upper State			Lower State			Observation	Calculation	Residual	Remarks
J	K_A	K_C	J	K_A	K_C				
2	2	0	3	2	1	16480.004	16480.000	0.003	cm^{-1}
2	2	1	3	2	2	16480.004	16480.001	0.002	cm^{-1}
3	2	1	4	2	2	16478.837	16478.834	0.003	cm^{-1}
3	2	2	4	2	3	16478.837	16478.838	-0.001	cm^{-1}
4	2	2	5	2	3	16477.634	16477.593	0.040	cm^{-1}
4	2	3	5	2	4	16477.634	16477.602	0.031	cm^{-1}
5	2	3	6	2	4	16476.304	16476.278	0.025	cm^{-1}
5	2	4	6	2	5	16476.304	16476.295	0.009	cm^{-1}
6	2	4	7	2	5	16474.914	16474.888	0.025	cm^{-1}
6	2	5	7	2	6	16474.914	16474.915	-0.001	cm^{-1}
7	2	5	8	5	6	16473.410	16473.422	-0.012	cm^{-1}
7	2	6	8	2	7	16473.410	16473.464	-0.054	cm^{-1}
8	2	6	9	2	7	16471.916	16471.879	0.036	cm^{-1}
8	2	7	9	2	8	16471.916	16471.942	-0.026	cm^{-1}
9	2	7	10	2	8	16470.328	16470.258	0.069	cm^{-1}
9	2	8	10	2	9	16470.328	16470.347	-0.019	cm^{-1}
10	2	8	11	2	9	16468.636	16468.558	0.077	cm^{-1}
10	2	9	11	2	10	16468.636	16468.682	-0.046	cm^{-1}
11	2	9	12	2	10	16466.759	16466.780	-0.021	cm^{-1}
11	2	10	12	2	11	16466.977	16466.945	0.032	cm^{-1}
12	2	10	13	2	11	16464.927	16464.921	0.005	cm^{-1}
12	2	11	13	2	12	16465.103	16465.136	-0.033	cm^{-1}
13	2	11	14	2	12	16462.989	16462.982	0.007	cm^{-1}
13	2	12	14	2	13	16463.266	16463.257	0.008	cm^{-1}
14	2	12	15	2	13	16461.005	16460.961	0.043	cm^{-1}
14	2	13	15	2	14	16461.305	16461.306	-0.001	cm^{-1}
15	2	13	16	2	14	16458.883	16458.860	0.023	cm^{-1}
15	2	14	16	2	15	16459.295	16459.285	0.009	cm^{-1}
16	2	14	17	2	15	16456.738	16456.677	0.061	cm^{-1}
16	2	15	17	2	16	16457.213	16457.193	0.019	cm^{-1}
17	2	15	18	2	16	16454.450	16454.412	0.037	cm^{-1}
17	2	16	18	2	17	16455.037	16455.030	0.006	cm^{-1}
18	2	17	19	2	18	16452.800	16452.797	0.002	cm^{-1}
11	3	8	10	3	7	16488.156	16488.146	0.009	cm^{-1}
4	3	1	5	3	2	16477.040	16477.039	0.000	cm^{-1}
5	3	2	6	3	3	16475.698	16475.730	-0.032	cm^{-1}
6	3	3	7	3	4	16474.299	16474.347	-0.048	cm^{-1}
7	3	4	8	3	5	16472.855	16472.892	-0.037	cm^{-1}
8	3	5	9	3	6	16471.318	16471.363	-0.045	cm^{-1}
9	3	6	10	3	7	16469.737	16469.761	-0.024	cm^{-1}
10	3	7	11	3	8	16468.077	16468.085	-0.008	cm^{-1}
11	3	8	12	3	9	16466.331	16466.334	-0.003	cm^{-1}
12	3	9	13	3	10	16464.536	16464.509	0.026	cm^{-1}
13	3	10	14	3	11	16462.641	16462.608	0.032	cm^{-1}
14	3	11	15	3	12	16460.630	16460.632	-0.002	cm^{-1}
15	3	12	16	3	13	16458.595	16458.580	0.014	cm^{-1}
16	3	13	17	3	14	16456.467	16456.451	0.015	cm^{-1}
17	3	14	18	3	15	16454.254	16454.244	0.009	cm^{-1}
18	3	15	19	3	16	16452.001	16451.959	0.041	cm^{-1}
11	4	7	10	4	6	16487.277	16487.346	-0.069	cm^{-1}

Upper State			Lower State			Observation	Calculation	Residual	Remarks
J	K_A	K_C	J	K_A	K_C				
16	4	12	15	4	11	16486.947	16487.001	-0.054	cm^{-1}
17	4	13	16	4	12	16486.687	16486.710	-0.023	cm^{-1}
18	4	14	17	4	13	16486.320	16486.345	-0.025	cm^{-1}
19	4	15	18	4	14	16485.895	16485.906	-0.011	cm^{-1}
20	4	16	19	4	15	16485.333	16485.392	-0.059	cm^{-1}
21	4	17	20	4	16	16484.886	16484.802	0.083	cm^{-1}
22	4	18	21	4	17	16484.075	16484.137	-0.062	cm^{-1}
23	4	19	22	4	18	16483.367	16483.396	-0.029	cm^{-1}
24	4	20	23	4	19	16482.511	16482.579	-0.068	cm^{-1}
25	4	21	24	4	20	16481.679	16481.685	-0.006	cm^{-1}
26	4	22	25	4	21	16480.727	16480.713	0.013	cm^{-1}
27	4	23	26	4	22	16479.629	16479.664	-0.035	cm^{-1}
28	4	24	27	4	23	16478.585	16478.537	0.047	cm^{-1}
29	4	25	28	4	24	16477.389	16477.331	0.057	cm^{-1}
30	4	26	29	4	25	16476.154	16476.045	0.108	cm^{-1}
4	4	1	4	4	0	16481.030	16480.978	0.051	cm^{-1}
5	4	2	5	4	1	16480.727	16480.617	0.109	cm^{-1}
6	4	3	6	4	2	16480.004	16480.183	-0.179	cm^{-1}
7	4	4	7	4	3	16479.629	16479.677	-0.048	cm^{-1}
8	4	5	8	4	4	16479.053	16479.098	-0.045	cm^{-1}
4	4	0	5	4	1	16476.154	16476.243	-0.089	cm^{-1}
5	4	1	6	4	2	16474.914	16474.934	-0.020	cm^{-1}
6	4	2	7	4	3	16473.566	16473.553	0.012	cm^{-1}
7	4	3	8	4	4	16472.122	16472.099	0.022	cm^{-1}
8	4	4	9	4	5	16470.578	16470.572	0.005	cm^{-1}
9	4	5	10	4	6	16468.951	16468.972	-0.021	cm^{-1}
10	4	6	11	4	7	16467.309	16467.299	0.009	cm^{-1}
11	4	7	12	4	8	16465.565	16465.553	0.011	cm^{-1}
12	4	8	13	4	9	16463.749	16463.733	0.015	cm^{-1}
13	4	9	14	4	10	16461.849	16461.839	0.009	cm^{-1}
14	4	10	15	4	11	16459.863	16459.871	-0.008	cm^{-1}
15	4	11	16	4	12	16457.814	16457.829	-0.015	cm^{-1}
16	4	12	17	4	13	16455.709	16455.712	-0.003	cm^{-1}
17	4	13	18	4	14	16453.480	16453.521	-0.041	cm^{-1}
18	4	14	19	4	15	16451.257	16451.253	0.003	cm^{-1}
19	4	15	20	4	16	16448.887	16448.911	-0.024	cm^{-1}
11	5	6	10	5	5	16486.320	16486.300	0.019	cm^{-1}
5	5	0	6	5	1	16473.951	16473.890	0.060	cm^{-1}
6	5	1	7	5	2	16472.470	16472.510	-0.040	cm^{-1}
7	5	2	8	5	3	16471.088	16471.057	0.030	cm^{-1}
8	5	3	9	5	4	16469.579	16469.531	0.047	cm^{-1}
9	5	4	10	5	5	16467.773	16467.932	-0.159	cm^{-1}
10	5	5	11	5	6	16466.331	16466.261	0.069	cm^{-1}
11	5	6	12	5	7	16464.536	16464.516	0.019	cm^{-1}
12	5	7	13	5	8	16462.641	16462.698	-0.057	cm^{-1}
13	5	8	14	5	9	16460.810	16460.807	0.002	cm^{-1}
14	5	9	15	5	10	16458.883	16458.842	0.040	cm^{-1}
15	5	10	16	5	11	16456.759	16456.803	-0.044	cm^{-1}
16	5	11	17	5	12	16454.602	16454.690	-0.088	cm^{-1}
11	6	5	10	6	4	16484.886	16484.991	-0.105	cm^{-1}

Upper State			Lower State			Observation	Calculation		Residual	Remarks
J	K_A	K_C	J	K_A	K_C					
12	6	6	11	6	5	16485.079	16485.069		0.009	cm^{-1}
13	6	7	12	6	6	16485.079	16485.074		0.004	cm^{-1}
14	6	8	13	6	7	16485.079	16485.006		0.072	cm^{-1}
15	6	9	14	6	8	16484.886	16484.865		0.020	cm^{-1}
16	6	10	15	6	9	16484.712	16484.650		0.061	cm^{-1}
17	6	11	16	6	10	16484.380	16484.361		0.018	cm^{-1}
18	6	12	17	6	11	16484.075	16483.998		0.076	cm^{-1}
19	6	13	18	6	12	16483.578	16483.562		0.016	cm^{-1}
20	6	14	19	6	13	16483.053	16483.050		0.002	cm^{-1}
21	6	15	20	6	14	16482.511	16482.464		0.046	cm^{-1}
22	6	16	21	6	15	16481.825	16481.804		0.020	cm^{-1}
23	6	17	22	6	16	16481.030	16481.068		-0.038	cm^{-1}
24	6	18	23	6	17	16480.241	16480.256		-0.015	cm^{-1}
25	6	19	24	6	18	16479.309	16479.369		-0.060	cm^{-1}
26	6	20	25	6	19	16478.419	16478.405		0.013	cm^{-1}
27	6	21	26	6	20	16477.289	16477.365		-0.076	cm^{-1}
28	6	22	27	6	21	16476.154	16476.248		-0.094	cm^{-1}
6	6	1	6	6	0	16477.875	16477.830		0.044	cm^{-1}
7	6	2	7	6	1	16477.389	16477.325		0.064	cm^{-1}
8	6	3	8	6	2	16476.787	16476.747		0.039	cm^{-1}
9	6	4	9	6	3	16476.154	16476.096		0.057	cm^{-1}
6	6	0	7	6	1	16471.088	16471.204		-0.116	cm^{-1}
7	6	1	8	6	2	16469.797	16469.751		0.045	cm^{-1}
8	6	2	9	6	3	16468.299	16468.227		0.072	cm^{-1}
9	6	3	10	6	4	16466.542	16466.629		-0.087	cm^{-1}
10	6	4	11	6	5	16464.927	16464.959		-0.032	cm^{-1}
11	6	5	12	6	6	16463.266	16463.215		0.050	cm^{-1}
12	6	6	13	6	7	16461.463	16461.399		0.063	cm^{-1}
13	6	7	14	6	8	16459.598	16459.509		0.088	cm^{-1}
14	6	8	15	6	9	16457.613	16457.546		0.066	cm^{-1}
15	6	9	16	6	10	16455.566	16455.510		0.056	cm^{-1}
16	6	10	17	6	11	16453.486	16453.399		0.086	cm^{-1}
11	7	4	10	7	3	16483.367	16483.400		-0.033	cm^{-1}
7	7	0	8	7	1	16468.077	16468.165		-0.088	cm^{-1}
8	7	1	9	7	2	16466.542	16466.641		-0.099	cm^{-1}
9	7	2	10	7	3	16465.103	16465.044		0.058	cm^{-1}
10	7	3	11	7	4	16463.266	16463.375		-0.109	cm^{-1}
11	7	4	12	7	5	16461.630	16461.633		-0.003	cm^{-1}
12	7	5	13	7	6	16459.810	16459.818		-0.008	cm^{-1}
13	7	6	14	7	7	16457.814	16457.930		-0.116	cm^{-1}
14	7	7	15	7	8	16455.983	16455.968		0.014	cm^{-1}
15	7	8	16	7	9	16454.109	16453.934	*	0.175	cm^{-1}
9	8	2	9	8	1	16472.470	16472.616		-0.146	cm^{-1}
8	8	1	8	8	0	16473.174	16473.265		-0.091	cm^{-1}
10	8	3	10	8	2	16471.910	16471.894		0.015	cm^{-1}
10	8	2	11	8	3	16461.463	16461.488		-0.025	cm^{-1}
11	8	3	12	8	4	16459.763	16459.747		0.015	cm^{-1}
12	8	4	13	8	5	16457.990	16457.934		0.056	cm^{-1}
13	8	5	14	8	6	16456.104	16456.047		0.056	cm^{-1}
14	8	6	15	8	7	16454.109	16454.087		0.021	cm^{-1}

CH_2S: 4_0^2 BAND

Upper State			Lower State			Observation	Calculation	Residual	Remarks
J	K_A	K_C	J	K_A	K_C				
11	0	9	10	0	10	17225.44	17225.42	0.02	cm^{-1}
11	1	10	10	1	9	17234.65	17234.67	-0.02	cm^{-1}
11	1	11	10	1	10	17234.37	17234.39	-0.02	cm^{-1}
11	2	9	10	2	8	17231.81	17231.80	0.01	cm^{-1}
11	3	8	10	3	7	17227.03	17227.06	-0.03	cm^{-1}
12	3	9	11	3	8	17227.03	17227.00	0.03	cm^{-1}
13	3	10	12	3	9	17226.84	17226.85	-0.01	cm^{-1}
14	3	11	13	3	10	17226.60	17226.59	0.01	cm^{-1}
15	3	12	14	3	11	17226.24	17226.24	0.00	cm^{-1}
16	3	13	15	3	12	17225.79	17225.78	0.01	cm^{-1}
17	3	14	16	3	13	17225.23	17225.22	0.01	cm^{-1}
18	3	15	17	3	14	17224.55	17224.55	0.00	cm^{-1}
19	3	16	18	3	15	17223.79	17223.79	0.00	cm^{-1}
20	3	17	19	3	16	17222.91	17222.93	-0.02	cm^{-1}

CD_2S: $2_0^1 4_0^1$ BAND

Upper State			Lower State			Observation	Calculation	Residual	Remarks
J	K_A	K_C	J	K_A	K_C				
5	5	1	4	4	0	17809.964	17809.948	0.015	cm^{-1}
6	5	2	5	4	1	17810.472	17810.462	0.009	cm^{-1}
7	5	3	6	4	2	17810.952	17810.903	0.048	cm^{-1}
8	5	4	7	4	3	17811.255	17811.272	-0.017	cm^{-1}
9	5	5	8	4	4	17811.567	17811.568	-0.001	cm^{-1}
10	5	6	9	4	5	17811.774	17811.791	-0.017	cm^{-1}
11	5	7	10	4	6	17811.978	17811.941	0.036	cm^{-1}
13	5	9	12	4	8	17811.978	17812.019	-0.041	cm^{-1}
14	5	10	13	4	9	17811.978	17811.948	0.029	cm^{-1}
15	5	11	14	4	10	17811.774	17811.802	-0.028	cm^{-1}
16	5	12	15	4	11	17811.564	17811.581	-0.017	cm^{-1}
17	5	13	16	4	12	17811.255	17811.285	-0.030	cm^{-1}
18	5	14	17	4	13	17810.952	17810.913	0.038	cm^{-1}
19	5	15	18	4	14	17810.472	17810.465	0.006	cm^{-1}
20	5	16	19	4	15	17809.964	17809.940	0.023	cm^{-1}
12	5	8	11	4	7	17811.978	17812.017	-0.039	cm^{-1}
12	6	7	11	5	6	17818.736	17818.772	-0.036	cm^{-1}
12	8	5	11	7	4	17831.174	17831.145	0.028	cm^{-1}
12	9	4	11	8	3	17836.801	17836.770	0.030	cm^{-1}
12	10	3	11	9	2	17841.964	17842.026	-0.062	cm^{-1}
12	11	2	11	10	1	17846.943	17846.919	0.023	cm^{-1}

CD_2S: 4_0^5 BAND

Upper State			Lower State			Observation	Calculation	Residual	Remarks
J	K_A	K_C	J	K_A	K_C				
11	5	7	10	4	6	18375.108	18375.044	0.064	cm^{-1}
12	5	8	11	4	7	18375.108	18375.036	-0.032	cm^{-1}
13	5	9	12	4	8	18375.108	18375.156	-0.048	cm^{-1}
14	5	10	13	4	9	18375.108	18375.104	0.004	cm^{-1}
15	5	11	14	4	10	18375.000	18374.977	0.022	cm^{-1}
16	5	12	15	4	11	18374.816	18374.778	0.037	cm^{-1}
17	5	13	16	4	12	18374.581	18374.505	0.076	cm^{-1}
18	5	14	17	4	13	18374.128	18374.157	-0.029	cm^{-1}
19	5	15	18	4	14	18373.718	18373.735	-0.017	cm^{-1}
20	5	16	19	4	15	18373.237	18373.237	0.000	cm^{-1}
11	6	6	10	5	5	18377.727	18377.644	0.083	cm^{-1}
12	6	7	11	5	6	18377.841	18377.738	0.102	cm^{-1}
13	6	8	12	5	7	18377.841	18377.761	0.079	cm^{-1}
14	6	9	13	5	8	18377.727	18377.711	0.015	cm^{-1}
15	6	10	14	5	9	18377.572	18377.590	-0.018	cm^{-1}
16	6	11	15	5	10	18377.348	18377.396	-0.048	cm^{-1}
17	6	12	16	5	11	18377.128	18377.129	-0.001	cm^{-1}
18	6	13	17	5	12	18376.903	18376.790	-0.112	cm^{-1}
19	6	14	18	5	13	18376.330	18376.377	-0.047	cm^{-1}
11	7	5	10	6	4	18379.454	18379.448	0.006	cm^{-1}
12	7	6	11	6	5	18379.454	18379.544	-0.089	cm^{-1}
13	7	7	12	6	6	18379.454	18379.568	-0.114	cm^{-1}
14	7	8	13	6	7	18379.454	18379.520	-0.066	cm^{-1}
15	7	9	14	6	8	18379.366	18379.401	-0.035	cm^{-1}
16	7	10	15	6	9	18379.182	18379.209	-0.027	cm^{-1}
17	7	11	16	6	10	18378.925	18378.946	-0.021	cm^{-1}
18	7	12	17	6	11	18378.595	18378.611	-0.016	cm^{-1}
19	7	13	18	6	12	18378.218	18378.203	0.014	cm^{-1}
12	4	9	11	3	8	18371.507	18371.584	-0.077	cm^{-1}
12	8	5	11	7	4	18380.782	18380.726	0.056	cm^{-1}
12	9	4	11	8	3	18381.523	18381.483	0.039	cm^{-1}
12	11	2	11	10	1	18382.650	18382.655	-0.005	cm^{-1}

BIBLIOGRAPHY

1. Y. Beers, G. P. Klein, W. H. Kirchhoff and D. R. Johnson, J. Mol. Spectrosc. 44, 553 (1972).

2. M. W. Sinclair, J. C. Ribes, N. Fourikis, R. D. Brown and P. D. Godfrey, Int. Astron. Union Circ. No. 3262, Nov. 1971.

3. D. R. Johnson and F. X. Powell, Science 169, 679 (1970).

4. D. R. Johnson, F. X. Powell and W. H. Kirchhoff, J. Mol. Spectrosc. 39, 136 (1971).

5. J. W. C. Johns and W. B. Olson, J. Mol. Spectrosc. 39, 479 (1971).

6. M. E. Jacox and D. E. Milligan, J. Mol. Spectrosc. 58, 142 (1975).

7. A. B. Callear, J. Connor and D. R. Dickson, Nature 221, 1238 (1969).

8. K. J. Rosengren, Acta Chemica Scand. 16, 2284 (1962).

9. G. Herzberg, "Electronic Spectra of Polyatomic Molecules", D. Van Nostrand Reinhold Company, New York (1966).

10. G. W. King, "Spectroscopy and Molecular Structure", Holt, Rinehart and Winston, Inc., New York (1964).

11. M. D. Harmony, "Introduction to Molecular Energies and Spectra", Holt, Rinehart and Winston, Inc., New York (1972).

12. I. N. Levine, "Quantum Chemistry", Vol. 1, Allyn and Bacon, Boston (1970).

13. P. J. Bruna, S. D. Peyerimhoff and R. J. Buenker, Chem. Phys. 3, 35 (1974).

14. A. D. Walsh, J. Chem. Soc. 2260 (1953).

15. H. Suzuki, "Electronic Absorption Spectra and Geometry of Organic Molecules", Academic Press, New York (1967).

16. G. W. King, J. Sci. Instru. 35, 11 (1958).

17. H. M. Crosswhite, J. Res. Nat. Bur. Stand. - A. Phys. and Chem. 79A, 17 (1975).

18. B. Edlén, J. Opt. Soc. Amer. 43, 339 (1953).

19. H. C. Longuet-Higgins, Mol. Phys. 6, 445 (1963).

20. G. W. King, R. M. Hainer and P. C. Cross, J. Chem. Phys. 11, 27 (1943).

21. J. C. D. Brand and J. K. G. Watson, J. Mol. Spectrosc. 10, 166 (1963).

22. J. H. Callomon and K. K. Innes, J. Mol. Spectrosc. 10, 166 (1963).

23. V. A. Job, V. Sethuraman and K. K. Innes, J. Mol. Spectrosc. 30, 365 (1969).

24. (a) R. M. Badger, J. Chem. Phys. 2, 128 (1934).
(b) Ibid, J. Chem. Phys. 3, 710 (1935).

25. G. Herzberg, "Infrared and Raman Spectra of Polyatomic Molecules", D. Van Nostrand Co., New York (1945).

26. O. Redlich, Z. Physik. Chem. B. 28, 371 (1935).

27. W. R. Angus, C. R. Bailey, J. B. Hale, C. K. Ingold, A. H. Leckie, C. G. Raisin, J. W. Thompson and C. L. Wilson, J. Chem. Soc. 971 (1936).

28. J. E. Wollrab, "Rotational Spectra and Molecular Structure", Academic Press, New York (1967).

29. J. B. Coon, N. W. Naugle and R. D. McKenzie, J. Mol. Spectrosc. 20, 107 (1966).

30. (a) S. I. Chan and D. Stelman, J. Mol. Spectrosc. 10, 278 (1963).
(b) S. I. Chan, D. Stelman and L. E. Thompson, J. Chem. Phys. 41, 2828 (1964).

31. S. I. Chan, T. R. Borgers, J. W. Russell, H. L. Strauss and W. D. Gwinn, J. Chem. Phys. 44, 1103 (1966).

32. J. Laane, J. Chem. Phys. 50, 776 (1969).

33. D. C. Moule and Ch. V. S. Ramachandra Rao, J. Mol. Spectrosc. 45, 120 (1973).

34. J. Laane and R. C. Lord, J. Chem. Phys. 47, 4941 (1967).

35. (a) E. B. Wilson, Jr. and J. B. Howard, J. Chem. Phys. 4, 260 (1936).
(b) E. B. Wilson, Jr., J. Chem. Phys. 4, 313 (1936).
(c) E. B. Wilson, Jr., J. Chem. Phys. 5, 617 (1937).

36. H. C. Allen, Jr. and P. C. Cross, "Molecular Vib-Rotors", John Wiley and Sons, Inc., New York (1963).

37. E. B. Wilson, Jr., J. C. Decius and P. C. Cross, "Molecular Vibrations", McGraw-Hill, New York (1955).

38. D. M. Dennison, Rev. Mod. Phys. 3, 280 (1931).

39. J. T. Hougen, J. Chem. Phys. 37, 1433 (1962).

40. O. M. Jordahl, Phys. Rev. 45, 87 (1934).

41. H. C. Allen, Jr. and W. B. Olson, J. Chem. Phys. 37, 212 (1962).

42. J. K. G. Watson, J. Chem. Phys. 48, 4517 (1968).

43. W. H. Kirchhoff, J. Mol. Spectrosc. 41, 333 (1972).

44. R. Mecke, Z. Physik. 81, 313 (1933).

45. J. M. Hollas, "Specialist Periodical Reports: Molecular Spectroscopy", Vol. 1, The Chemical Society, p. 62.

46. K. G. Kidd and G. W. King, J. Mol. Spectrosc. 40, 461 (1971).

47. R. M. Lees, J. Mol. Spectrosc. 33, 124 (1970).

48. R. A. Sawyer, "Experimental Spectroscopy", Dover, New York (1963).

49. J. E. Parkin, J. Mol. Spectrosc. 15, 483 (1965).

50. V. Sethuraman, V. A. Job and K. K. Innes, J. Mol. Spectrosc. 33, 189 (1970).

51. J. A. Pople and J. W. Sidman, J. Chem. Phys. 27, 1270 (1957).

52. J. W. Sidman, Chem. Revs. 58, 689 (1958).

53. H. A. Jahn, Phys. Rev. 56, 680 (1939).

54. (a) J. C. D. Brand and C. G. Stevens, J. Chem. Phys. 58, 3331 (1973).
(b) J. C. D. Brand, W. H. Chan and D. S. Liu, J. Mol. Spectrosc. 50, 310 (1974).

55. C. G. Stevens and J. C. Brand, J. Chem. Phys. 58, 3324 (1973).

56. I. M. Mills, Pure and Appl. Chem. 11, 325 (1965).

57. (a) D. R. Herschbach and V. W. Laurie, J. Chem. Phys. 37, 1668 (1962).
(b) V. W. Laurie and D. R. Herschbach, J. Chem. Phys. 37, 1687 (1962).
(c) D. R. Herschbach and V. W. Laurie, J. Chem. Phys. 40, 3142 (1964).

58. C. C. Costain, J. Chem. Phys. 29, 864 (1958).

59. J. Kraitchman, Am. J. Phys. 21, 17 (1953).

60. V. T. Jones and J. B. Coon, J. Mol. Spectrosc. 31, 137 (1969).

61. C. C. Costain and J. M. Dowling, J. Chem. Phys. 32, 158 (1960).

62. T. Kojima, J. Phys. Soc. Jap. 15, 286 (1960).

63. A. J. McHugh and I. G. Ross, Aust. J. Chem. 22, 1 (1969).

64. T. Oka and Y. Morino, J. Mol. Spectrosc. 6, 472 (1961).

65. T. Oka and Y. Morino, J. Mol. Spectrosc. 11, 349 (1963).

66. R. C. Meatherall, Ph.D. Thesis, McMaster University, Hamilton, Ontario, Canada, p. 84 (1974).